

University of Bath



PHD

Synthesis And Catalytic Reactivity Of Ruthenium And Rhodium N-Alkyl Substituted N-Heterocyclic Carbene Complexes

Bramananthan, Nicola

Award date:
2014

Awarding institution:
University of Bath

[Link to publication](#)

General rights

Copyright and moral rights for the publications made accessible in the public portal are retained by the authors and/or other copyright owners and it is a condition of accessing publications that users recognise and abide by the legal requirements associated with these rights.

- Users may download and print one copy of any publication from the public portal for the purpose of private study or research.
- You may not further distribute the material or use it for any profit-making activity or commercial gain
- You may freely distribute the URL identifying the publication in the public portal ?

Take down policy

If you believe that this document breaches copyright please contact us providing details, and we will remove access to the work immediately and investigate your claim.

SYNTHESIS AND CATALYTIC REACTIVITY OF RUTHENIUM AND RHODIUM N-ALKYL SUBSTITUTED N-HETEROCYCLIC CARBENE COMPLEXES

Nicola Bramanathan

A thesis submitted for the degree of Doctor of Philosophy



UNIVERSITY OF
BATH

University of Bath
Department of Chemistry

September 2014

Attention is drawn to the fact that copyright of this thesis rests with the author. A copy of this thesis has been supplied on condition that anyone who consults it is understood to recognise that its copyright rests with the author and that they must not copy it or use material from it except as permitted by law or with the consent of the author.

This thesis may be made available for consultation within the University Library and may be photocopied or lent to other libraries for the purpose of consultation.

CONTENTS

ACKNOWLEDGEMENTS	5
ABSTRACT	6
ABBREVIATIONS – SPECTROSCOPIC	8
ABBREVIATIONS – UNITS	8
ABBREVIATIONS – CHEMICAL	9
CHAPTER 1:	
1.1 N-heterocyclic carbenes (NHCs)	10
1.2 Non-innocent behaviour of NHCs: C-H bond activation	14
1.3 Earliest example of C-H activation	15
1.4 N-aryl and N-alkyl substituents in C-H activation	16
1.5 C-H activation of NHCs in Rh, Ir and Ru complexes	18
1.6 C-C and C-H bond activations reactions in NHCs	23
1.7 C-H activation of NHCs in early and late transition metals	24
1.8 Metal induced C-N bond activation reaction of NHCs	25
1.9 Reversing C-H activation	26
1.10 Catalysis with C-H activated NHC metal complexes	27
1.11 Thesis synopsis	31
CHAPTER 2:	
2.1 Ruthenium hydride NHC complexes	37
2.2 Synthesis of Ru(ⁱ Pr ₂ Me ₂ ')(ⁱ Pr ₂ Me ₂) ₂ Cl	40
2.3 Synthesis of Ru(^t Bu')(PPh ₃) ₂ Cl	43
2.4 Reactivity of Ru(DMSO) ₄ Cl ₂ towards NHCs	46
2.5 Synthesis of Ru(IEt ₂ Me ₂ ')(DMSO) ₃ Cl	47
2.6 Reactivity of Ru(IEt ₂ Me ₂ ')(DMSO) ₃ Cl	50
2.7 Reactivity of Ru(IEt ₂ Me ₂ ')(DMSO) ₃ Cl towards PPh ₃ : Synthesis of Ru(IEt ₂ Me ₂ ')(PPh ₃) ₂ Cl	56
2.8 Attempts to prepare Ru(IEt ₂ Me ₂ ')(PPh ₃) ₂ Cl using an alternative route	59
2.9 Chapter summary	62
2.10 Experimental	
2.10.1 General Methods	63

2.10.2 Synthesis of $\text{I}^t\text{Pr}_2\text{Me}_2=\text{S}$	63
2.10.3 Synthesis of $\text{I}^t\text{Pr}_2\text{Me}_2$	63
2.10.4 Synthesis of IEt_2Me_2	63
2.10.5 Synthesis I^tBu_2	64
2.10.6 Synthesis of $\text{Ru}(\text{PPh}_3)_3\text{Cl}_2$	64
2.10.7 Synthesis of $\text{Ru}(\text{DMSO})_4\text{Cl}_2$	64
2.10.8 Synthesis of $\text{Ru}(\text{I}^t\text{Pr}_2\text{Me}_2)(\text{I}^t\text{Pr}_2\text{Me}_2)_2\text{Cl}$ (2.9)	64
2.10.9 Synthesis of $\text{Ru}(\text{I}^t\text{Bu}_2)(\text{PPh}_3)_2\text{Cl}$ (2.10a/b)	65
2.10.10 Synthesis of $\text{Ru}(\text{IEt}_2\text{Me}_2)(\text{DMSO})_3\text{Cl}$ (2.12)	65
2.10.11 Synthesis of $\text{Ru}(\text{IEt}_2\text{Me}_2)(\text{CO})_3\text{Cl}$ (2.13)	66
2.10.12 Synthesis of $\text{Ru}(\text{IEt}_2\text{Me}_2)(\text{PPh}_3)_2\text{Cl}$ (2.15)	66
2.10.13 Synthesis of $\text{Ru}(\text{IEt}_2\text{Me}_2)_4\text{Cl}_2$ (2.16)	67

CHAPTER 3:

3.1 Coordination of amine- and phosphine- boranes to metal centres	70
3.2 Dehydrocoupling of amine and phosphine boranes	75
3.3 Coordination and dehydrocoupling of amine and phosphine boranes by $\text{Ru}(\text{P-P})\text{L}$ derivatives	77
3.4 Reactivity of $[\text{Ru}(\text{NHC})_4\text{H}]^+$ with H_2	78
3.5 Reactivity of $[\text{Ru}(\text{NHC})_4\text{H}]^+$ with amine boranes	79
3.6 Catalytic dehydrogenation and transfer hydrogenation with amine boranes	81
3.7 Optimisation of Ru catalysed transfer hydrogenation of ketones by amine boranes	83
3.8 Optimised temperature for catalytic transfer hydrogenation of acetophenone to 1-phenyl ethanol	85
3.9 Influence of NHC and solvent on transfer hydrogenation	86
3.10 Transfer hydrogenation of nitriles	86
3.11 Transfer hydrogenation of alkynes and alkenes	88
3.12 Comment on catalytic activity of other reported examples employing amine boranes	95
3.13 Chapter summary	98
3.14 Experimental	
3.14.1 General Methods	99

3.14.2 Synthesis of 1,3,4,5-tetramethylimidazole-2-ylidene (IMe ₄)	99
3.14.3 Synthesis of [Ru(IMe ₄) ₄ H][BAR ^F ₄]	99
3.14.4 General procedure for transfer hydrogenation of ketones and alkenes	99
3.14.5 General procedure for transfer hydrogenation of nitriles	99
3.14.6 General procedure for transfer hydrogenation of alkynes	100
3.14.7 Isolation of hydrochloride amine salts	100

CHAPTER 4:

4.1 Ring expanded N-heterocyclic carbenes (RE-NHCs)	105
4.2 Synthesis of RE-NHCs	105
4.3 Group 8 and 9 transition metal complexes bearing RE-NHCs	107
4.4 Group 10 and 11 transition metal complexes bearing RE-NHCs	111
4.5 RE-NHCs with small N-substituents	116
4.6 Preparation of the salts [6-MeH]PF ₆ and [6-EtH]PF ₆	117
4.7 Generating the free carbenes 6-Me and 6-Et	117
4.8 Reactions with ruthenium precursors with 6-Me/6-Et	119
4.9 Synthesis of Rh(6-Me)(PPh ₃) ₂ H	122
4.10 Synthesis of Rh(6-Et)(PPh ₃) ₂ H	124
4.11 Reaction of Rh(PPh ₃) ₃ (CO)H with NHCs	127
4.12 Preparation of the bifluoride complexes; Rh(6-NHC)(PPh ₃) ₂ (FHF)	131
4.13 Synthesis of Rh(6-Me)(PPh ₃) ₂ (FHF)	131
4.14 Synthesis of Rh(6-Et)(PPh ₃) ₂ (FHF)	135
4.15 Comment on the formation of Rh FHF complexes	139
4.16 Intermolecular and intramolecular exchange of the bifluoride complexes	140
4.17 Synthesis of Rh(6-Me)(PPh ₃) ₂ F	143
4.18 Synthesis of Rh(6-Et)(PPh ₃) ₂ F	145
4.19 Reactivity of Rh(6-NHC)(PPh ₃) ₂ F	148
4.20 Reaction with Me ₃ SiCF ₃	150
4.21 Chapter summary	152
4.22 Experimental	
4.22.1 General Methods	153

4.22.2 Synthesis of [6-MeH]PF ₆	153
4.22.3 Synthesis of [6-EtH]PF ₆	153
4.22.4 Synthesis of Ru(6-Me')(PPh ₃) ₂ (CO)H (4.35)	154
4.22.5 Synthesis of Rh(6-Me)(PPh ₃) ₂ H (4.36)	154
4.22.6 Synthesis of Rh(6-Et)(PPh ₃) ₂ H (4.37)	155
4.22.7 Synthesis of Rh(PPh ₃) ₂ (CO) ₂ Rh(PPh ₃)(6-Et) (4.38)	155
4.22.8 Synthesis of Rh(6-Me)(PPh ₃) ₂ (FHF) (4.42)	156
4.22.9 Synthesis of Rh(6-Et)(PPh ₃) ₂ (FHF) (4.43)	156
4.22.10 Synthesis of Rh(6-Me)(PPh ₃) ₂ F (4.48)	157
4.22.11 Synthesis of Rh(6-Et)(PPh ₃) ₂ F (4.49)	157
4.22.12 Synthesis of Rh(6- ⁱ Pr)(PPh ₃) ₂ Cl (4.50)	158
4.22.13 Synthesis of Rh(6-Et)(PPh ₃) ₂ Cl (4.51)	158
4.22.14 Synthesis of Rh(6- ⁱ Pr)(PPh ₃)(CO)F (4.54)	159
4.22.15 Synthesis of Rh(6- ⁱ Pr)(PPh ₃) ₂ (CF ₃) (4.58)	159
APPENDIX 1: X-ray crystal structure of Rh(6- ⁱ Pr)(PPh ₃) ₂ Cl (4.48)	165
APPENDIX 2: ³¹ P { ¹ H} NMR spectrum for 4.48	166
APPENDIX 3: X-ray crystal structure of Rh(6-Et)(PPh ₃) ₂ Cl (4.49)	167
APPENDIX 4: ³¹ P { ¹ H} NMR spectrum for 4.49	168

ACKNOWLEDGEMENTS

I would like to express my gratitude to my project supervisor Prof. Mike Whittlesey for his excellent advice, support, helpful assistance and guidance throughout my PhD. I have been very fortunate to work under his supervision and would like to thank him again for giving me the opportunity to carry out this research project in his group.

I would also like to thank Dr John Lowe for helping me with NMR spectroscopy and Dr. Mary Mahon for solving my crystal structures.

Thanks must also go to my lab mates Dr. Mike Page, Dr. Charlie Ellul, Dr. Araminta Ledger and Dr. Tom Martin and who showed me around the lab when I first started and for helping me get started with my PhD. I would also like to thank the present members of the Whittlesey group, Caroline Davies, Rebecca Poulten, Lee Collins, Mateusz Cybulski and Dr Ian Riddlestone for helping me throughout my PhD and for making it an enjoyable and memorable experience.

Finally I would like to thank my parents and sister for their continuing love, support and encouragement. They have always been there for me, thank you again, I have finally finished! 😊

ABSTRACT

This thesis describes the synthesis and stoichiometric/catalytic reactivity of Ru and Rh N-alkyl substituted N-heterocyclic carbene complexes. In an effort to make new $\text{Ru}(\text{NHC})_x$ ($x = 1-4$) complexes, a range of Ru halide precursors, including $\text{Ru}(\text{DMSO})_4\text{Cl}_2$ and $\text{Ru}(\text{PPh}_3)_3\text{Cl}_2$, were combined with N-alkyl substituted carbenes. Treatment of $\text{Ru}(\text{PPh}_3)_3\text{Cl}_2$ with $^i\text{Pr}_2\text{Me}_2$ or ^iBu resulted in C-H activation of the NHCs to form $\text{Ru}(^i\text{Pr}_2\text{Me}_2)_2(^i\text{Pr}_2\text{Me}_2')\text{Cl}$ and $\text{Ru}(^i\text{Bu}')(\text{PPh}_3)_2\text{Cl}$ respectively. C-H activation also took place with $\text{Ru}(\text{DMSO})_4\text{Cl}_2$ and IEt_2Me_2 to give $\text{Ru}(\text{IEt}_2\text{Me}_2')(\text{DMSO})_3\text{Cl}$. This underwent substitution with ^{13}CO to afford the tricarbonyl complex $\text{Ru}(\text{IEt}_2\text{Me}_2')(\text{CO})_3\text{Cl}$, and with PPh_3 to give the bis-phosphine species $\text{Ru}(\text{IEt}_2\text{Me}_2')(\text{PPh}_3)_2\text{Cl}$. Attempts to generate $\text{Ru}(\text{IEt}_2\text{Me}_2')(\text{PPh}_3)_2\text{Cl}$ by an alternative reaction of IEt_2Me_2 with $\text{Ru}(\text{PPh}_3)_3\text{Cl}_2$ proved successful with two equiv. of carbene, although with four equiv. of NHC, the dichloride complex $\text{Ru}(\text{IEt}_2\text{Me}_2)_4\text{Cl}_2$ was produced.

Upon turning to $\text{Ru}(\text{PPh}_3)_3\text{HCl}$, our group observed that the non-metallated tetrakiscarbene species $[\text{Ru}(\text{NHC})_4\text{H}]^+$ are formed instead where alkyl = Me, Et and ^iPr . The reactivity of these species towards a range of amine boranes were investigated. $[\text{Ru}(\text{IME}_4)_4\text{H}]^+$ was able to catalyse the dehydrogenation of $\text{H}_3\text{B}\cdot\text{NMe}_2\text{H}$ to form the dimeric species $[\text{H}_2\text{B}\cdot\text{NMe}_2]_2$ and also catalytically hydrogenate a series of organic substrates such as ketones, nitriles, alkynes and alkenes at 323 K.

Treatment of $\text{Rh}(\text{PPh}_3)_4\text{H}$ with the six-membered ring NHCs 6-Me and 6-Et afforded the rhodium mono-carbene hydride complexes $\text{Rh}(6\text{-NHC})(\text{PPh}_3)_2\text{H}$, in each case as a mixture of cis- and trans-phosphine isomers. Treatment of $\text{Rh}(\text{PPh}_3)_3(\text{CO})\text{H}$ with 6-Et did not afford a hydride complex but instead gave the CO bridged dimer $\text{Rh}(\text{PPh}_3)_2(\text{CO})_2\text{Rh}(\text{PPh}_3)(6\text{-Et})$. Reaction of $\text{Rh}(6\text{-Me})(\text{PPh}_3)_2\text{H}$ with $\text{Et}_3\text{N}\cdot 3\text{HF}$ gave only the trans-isomer of the bifluoride complex $\text{Rh}(6\text{-Me})(\text{PPh}_3)_2(\text{FHF})$, whereas the 6-Et hydride precursor gave $\text{Rh}(6\text{-Et})(\text{PPh}_3)_2(\text{FHF})$ as a mixture of cis- and trans-phosphine isomers. ^{19}F NMR Magnetization transfer and chemical exchange experiments revealed intra- and intermolecular F exchange in both of these bifluoride compounds. Treatment of 6- $\text{Rh}(\text{NHC})(\text{PPh}_3)_2\text{H}$ (NHC= 6-Me, 6-Et,

6-ⁱPr) with $\text{CF}_3\text{CF}=\text{CF}_2$ gave the corresponding fluoride complexes $\text{Rh}(6\text{-NHC})(\text{PPh}_3)_2\text{F}$. The 6-ⁱPr derivative reacted slowly with H_2 to partially reform $\text{Rh}(6\text{-}^i\text{Pr})(\text{PPh}_3)_2\text{H}$, but rapidly with CO to give $\text{Rh}(6\text{-}^i\text{Pr})(\text{PPh}_3)(\text{CO})\text{F}$ and $\text{Rh}(\text{PPh}_3)_2(\text{CO})\text{F}$, and also with Me_3SiCF_3 to form $\text{Rh}(6\text{-}^i\text{Pr})(\text{PPh}_3)_2(\text{CF}_3)$.

ABBREVIATIONS -- SPECTROSCOPIC

br	broad
COSY	correlation spectroscopy
d	doublet
dd	doublet of doublets
δ	NMR chemical shift
HSQC	Heteronuclear single quantum coherence
IR	Infrared
$^xJ_{YZ}$	Coupling constant of Y to Z across x bonds
m	multiplet
NMR	Nuclear magnetic resonance
q	quartet
quint	quintet
s	singlet
sept	septet
t	triplet
$\nu(XY)$	IR shift of XY bond
vt	virtual triplet

ABBREVIATIONS -- UNITS

atm.	Atmosphere
cm^{-1}	Wavenumber
equiv.	Equivalents
g	Gram
h	Hour(s)
Hz	Hertz
K	Kelvin
mg	Milligram
MHz	MegaHertz
min	Minute(s)
mL	Millilitre
mmol	Millimole

ppm	Parts per million
Å	Angström
µL	microlitre

ABBREVIATIONS -- CHEMICAL

Arphos	Ph ₂ PCH ₂ CH ₂ CH ₂ AsPh ₂
BAr ₄ ^F	B(3,5-C ₆ H ₃ (CF ₃) ₂) ₄
COD	1,5-cyclooctadiene
COE	cyclooctene
dppf	1,1-bis(diphenylphosphino)ferrocene
dppe	1,2-bis(diphenylphosphino)ethane
lAd	1,3-diadamantylimidazol-2-ylidene
lCy	1,3-bis(cyclohexyl)-imidazol-2-ylidene
lEt ₂ Me ₂	1,3-diethyl-4,5-dimethylimidazol-2-ylidene
l ⁱ Pr ₂ Me ₂	1,3-diisopropyl-4,5-dimethyl-imidazol-2-ylidene
lMes	1,3-bis(2,4,6-trimethylphenyl)imidazol-2-ylidene
l ^t Bu	1,3-di- <i>tert</i> -butylimidazol-2-ylidene
lEt ₂	1,3-diethyl-imidazol-2-ylidene
l ⁿ Pr ₂	1,3-di- <i>n</i> -propylimidazol-2-ylidene
l ⁿ Bu	1,3-di- <i>n</i> -butylimidazol-2-ylidene
lMe ₄	1,3,4,5-tetramethylimidazol-2-ylidene
l ⁱ Pr	1,3-diisopropyl-imidazol-2-ylidene
l ⁱ PrMe	1-isopropyl-3-methyl-imidazol-2-ylidene
lSiMes	1,3-bis(2,4,6-trimethylphenyl)imidazol-2-ylidene
Xanthphos	4,5-bis(diphenylphosphino)-9,9-dimethylxanthene
6-Mes	1,3-bis(2,4,6-trimethylphenyl)-3,4,5,6-tetrahydropyrimidin-2-ylidene
6- ⁱ Pr	1,3-bis(2-propyl)-3,4,5,6-tetrahydropyrimidin-2-ylidene
%V _{Bur}	Percent buried volume

1. INTRODUCTION

1.1 N-HETEROCYCLIC CARBENES (NHCs)

NHCs are a class of nucleophilic singlet state carbenes where the carbenic carbon is part of an N-based heterocyclic ring containing between four and eight ring atoms. The nitrogen atoms contain substituents such as aryl or alkyl groups.¹ In the case of five-membered ring systems, the C-C bond in the backbone can either be saturated or unsaturated. Larger 6-8 membered ring carbenes are all saturated (Figure 1.1).

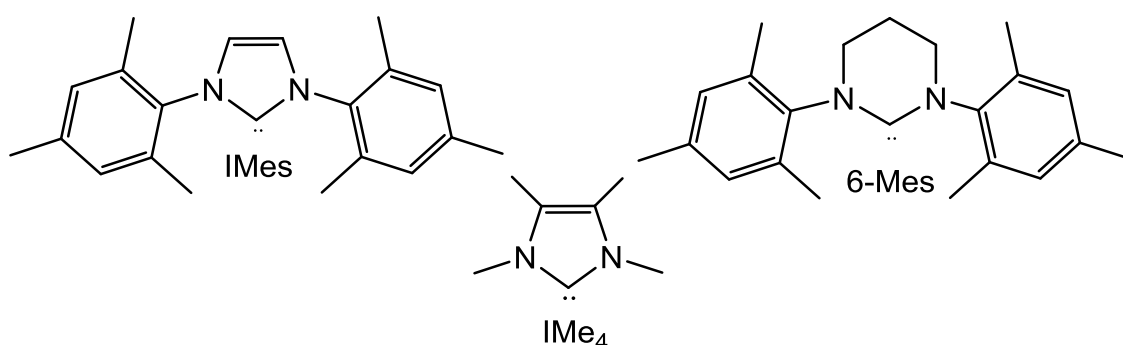
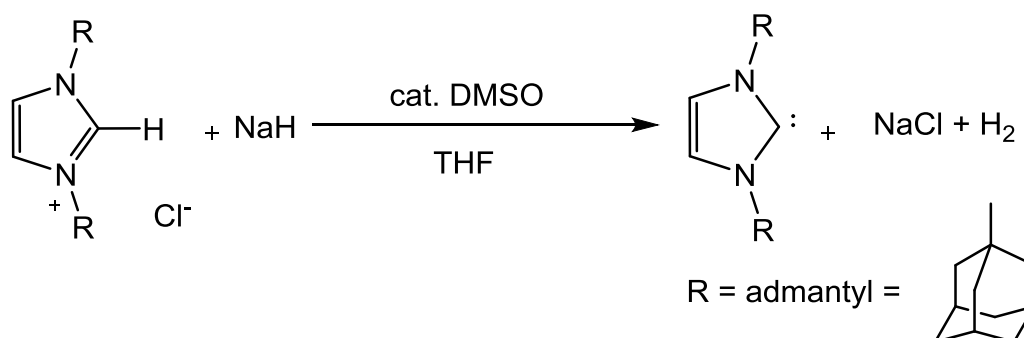


Figure 1.1: Selection of five and six membered ring NHCs

Early work trapping in-situ generated NHCs started in the 1960's by Öfele and Wanzlick, but the real breakthrough came from Ardeungo and co-workers upon isolating the free N-adamantyl substituted carbene, IAd (Scheme 1.1).²



Scheme 1.1: Isolation of the first free NHC

The first stable N-heterocyclic carbene (NHC) was only isolated in 1991.² Since then NHCs have been used widely as alternative ligands to phosphines in organometallic catalysis, because (a) NHCs can form very stable bonds with a range of transition metals and (b) they have readily tuneable stereoelectronic properties.³

The bonding to transition metals shows some similarities to a Fischer type interaction, since the carbene has two π donor substituents. However π -donation from the nitrogen lone pairs into the empty p_{π} orbital on the carbenic carbon stabilises the carbene (Figure 1.2).

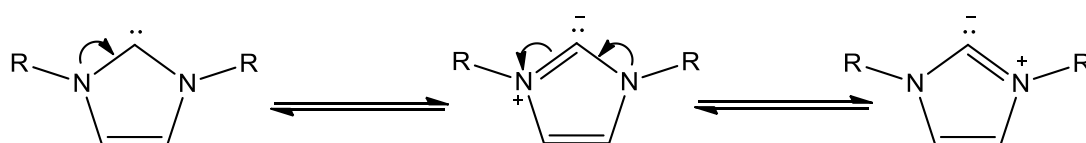


Figure 1.2: σ - electron withdrawing and π - electron donating heteroatoms stabilise singlet carbenes

Soon after, Hermann and co-workers identified the use of NHCs as supporting ligands in homogeneous catalysis.⁴⁻⁶ Due to their strong σ -electron donating properties they form strong NHC-metal bonds.⁷ The Tolman electronic parameters for common NHCs show they are better donors than even the most donating phosphines.⁸

In order to measure the steric bulk of NHCs, an early phosphine-like model was proposed by Nolan which utilized Tolman's classification of sterics.^{9,10} However, this first model highlighted the need for an improved metric parameter for steric bulk for this ligand family as this representation proved to be quite simple.^{9,10} Soon after Nolan and co-workers expressed the steric bulk of the carbene in terms of $\% V_{bur}$.^{11,12} This parameter described the volume occupied by a particular NHC ligand in a sphere over a 3 Å radius. This value was derived from DFT calculations positioning the carbenic carbon 2 Å from a ruthenium centre, and was approximately the distance from the N atoms to the position of the normalised metal atom (Figure 1.3).¹¹ The main advantages of this model was that $\% V_{bur}$ could also be applied to phosphine ligands allowing a more direct comparison between NHC and PR_3 groups.¹¹

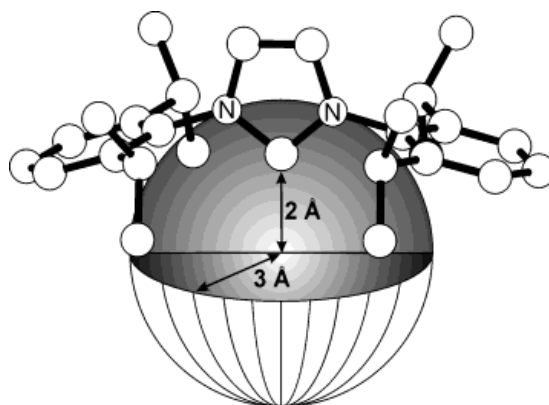


Figure 1.3: Steric parameter determination ($\%V_{bur}$) of NHC ligands

NHCs are known typically for their excellent σ -electron donating properties. However, work on NHC complexes^{13,14} has shown that with both electron rich and electron poor metal centres, NHCs have the ability to either stabilise an electron rich metal as an acceptor via $d \rightarrow \pi^*$ back donation or can contribute electron density to an electron poor system via $\pi \rightarrow d$ donation. These features may help to enhance the thermal stability of the metal-NHC bond in catalytic systems over their phosphine containing analogues.

Many established catalytic systems have benefited from the introduction of NHC ligands. In particular, the increased donor ability of NHC ligands enhanced the catalytic activity of the ruthenium-based Grubbs alkene metathesis catalyst, $[\text{Ru}(=\text{CHPh})(\text{PCy}_3)_2\text{Cl}_2]$, in one of the most well-known examples of modern catalyst design (Figure 1.4).^{10,15,16}

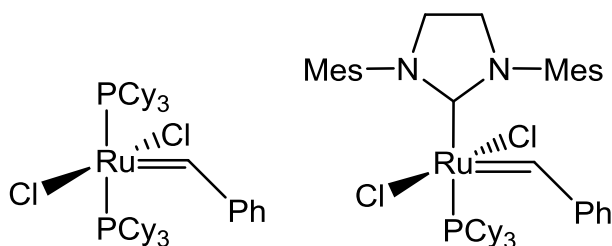


Figure 1.4: 1st generation and 2nd generation metathesis catalysts

Modifications to Crabtree's hydrogenation catalyst¹⁷ provided another example of the benefits of NHC incorporation to the thermal stability of a complex, Nolan et al conducted catalytic hydrogenations of alkenes with Crabtree's catalyst, $[\text{Ir}(\text{cod})(\text{py})(\text{PCy}_3)]\text{PF}_6$, and the NHC derivative,

$[\text{Ir}(\text{SIMes})(\text{cod})(\text{py})]\text{PF}_6$ (Figure 1.5).¹⁸ Reaction at room temperature of 1-methyl-1-cyclohexene under H_2 gave moderate yields of the corresponding alkanes with both catalysts. However, increasing the temperature to 323 K led to a significant increase in activity of the SIMes substituted complex, achieving 100 % conversion to methylcyclohexane in only 7 h. In contrast, Crabtree's catalyst was deactivated at this temperature.

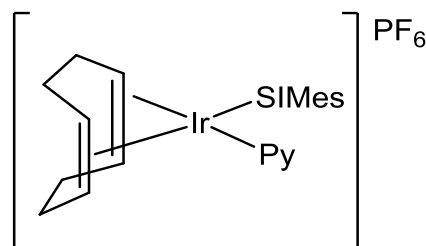
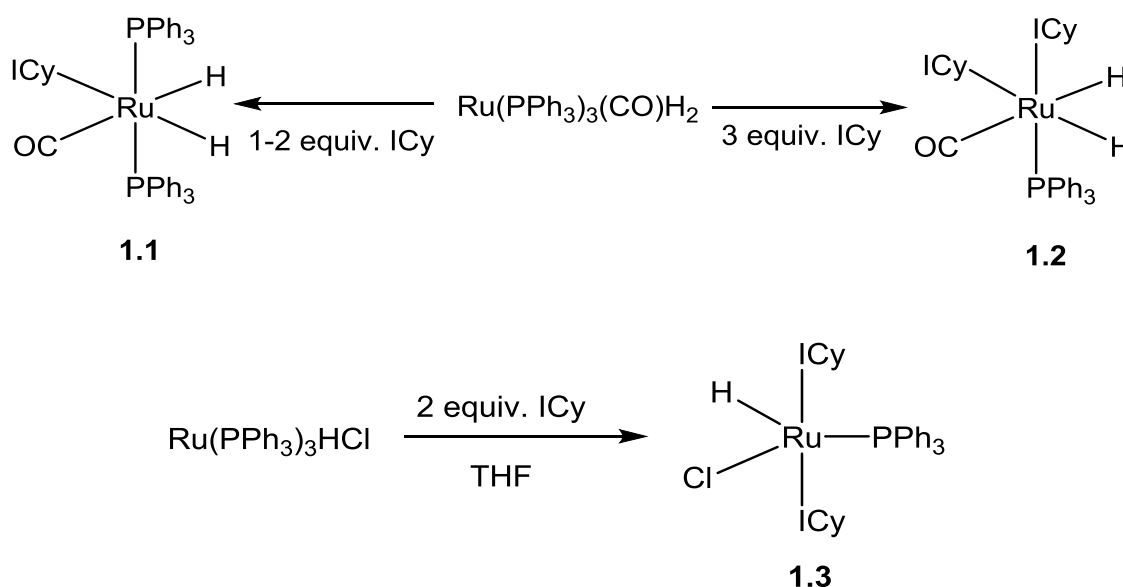


Figure 1.5: Structure of $[\text{Ir}(\text{SIMes})(\text{cod})(\text{py})]\text{PF}_6$

There are now many examples of metal hydride complexes in which one or more phosphine ligands have been replaced by NHCs.¹⁹⁻³² Our group reported the substitution of one or two PPh_3 ligands in $\text{Ru}(\text{PPh}_3)_3(\text{CO})\text{H}_2$ and $\text{Ru}(\text{PPh}_3)_3\text{HCl}$ by the alkyl substituted NHC ICy, which allowed the isolation and full characterization of the 16- and 18-electron mono- and bis-ICy complexes **1.1-1.3** (Scheme 1.2).³³



Scheme 1.2: Reactivity of ruthenium hydride precursors towards NHCs

activation compared to phosphines, as the C-H bond is three bonds from the metal in the latter but four bonds away in an NHC, necessarily placing it closer to the metal centre (Figure 1.6).⁴⁰ N-groups containing bulky substituents are more likely to undergo C-H activation, which will also be favoured by the formation of five-membered rings. N-Me substituted NHCs are unlikely to undergo C-H activation due to the strain of the resulting four membered ring product.

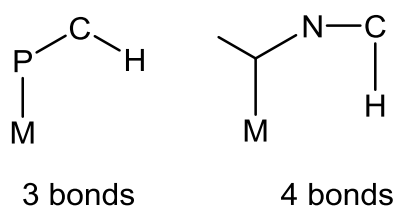
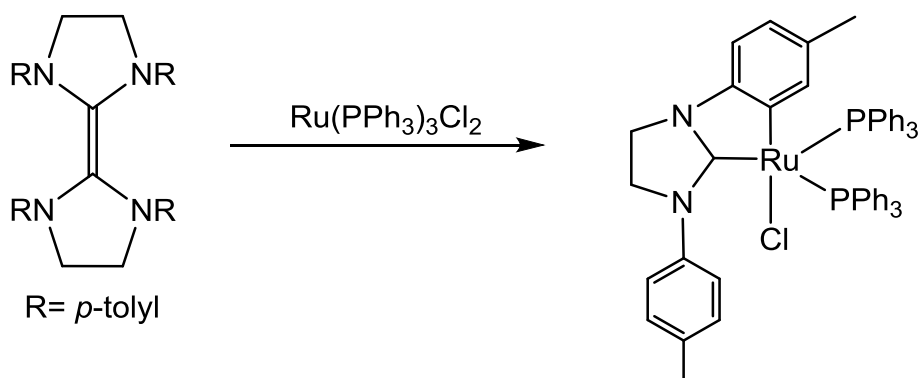


Figure 1.6: C-H activation; M-NHC vs M-PR₃

1.3 Early examples of C-H activation

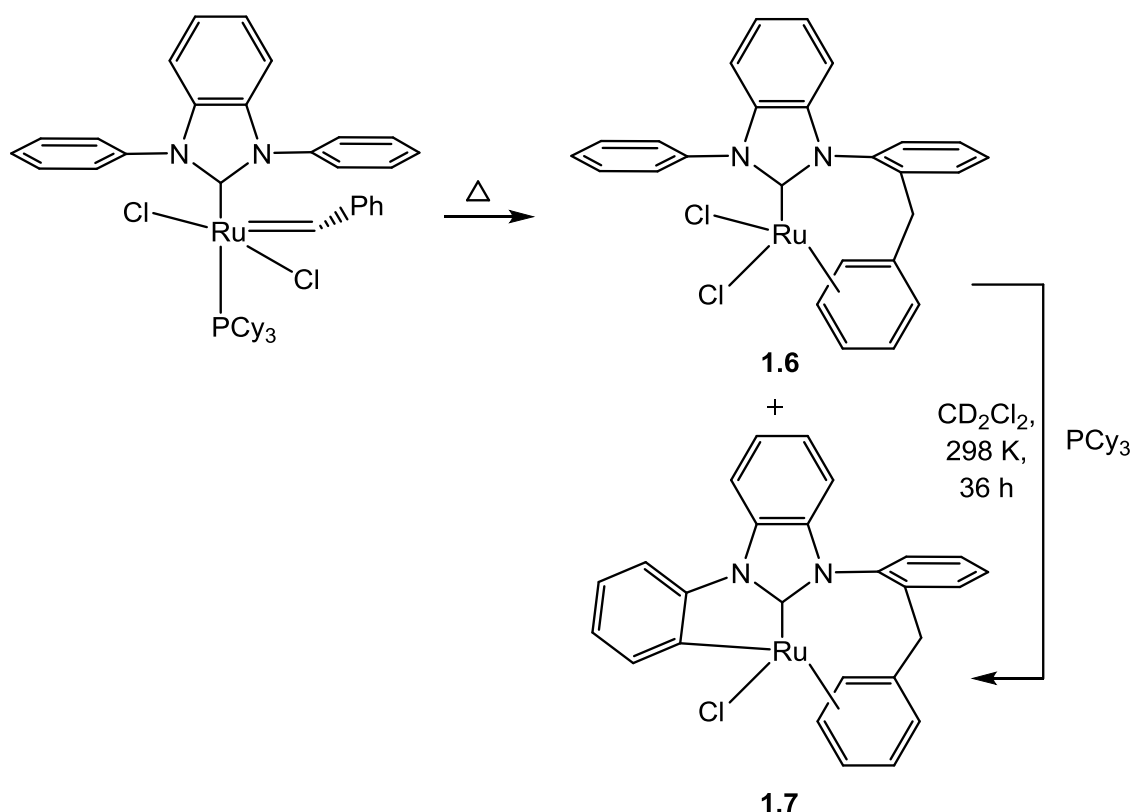
Lappert and co-workers reported the first example of C-H activation in aryl substituted NHC complexes in 1977.⁴¹ The 16e⁻ complex Ru(PPh₃)₃Cl₂ was refluxed with a carbene dimer (an enetetramine) containing N-*p*-tolyl substituents to afford a complex with a metallated N-aryl arm (Scheme 1.4).



Scheme 1.4: First example of C-H activation in aryl substituted NHC complexes

Grubbs and co-workers reported a double C-H activation of an alkene metathesis catalyst, in which a Ru benzylidene carbon atom was inserted into an *ortho* C-H bond of one of the N-phenyl rings of an N,N'-diphenylbenzimidazol-2-ylidene (biph) ligand (Scheme 1.5).⁴² The Ru centre

further inserted into another ortho C-H bond of the other N-phenyl ring of the biph ligand to give a new Ru-C bond. The formation of a five-membered metallacycle causes the planes of the phenyl groups of the biph ligands to be perpendicular to each other. The PCy₃ eliminated in the formation of **1.6** acts as a base in assisting the C-H activation by receiving the HCl eliminated from **1.6** to generate [HPCy₃⁺]Cl and **1.7**.



Scheme 1.5: Thermal decomposition of a ruthenium alkene metathesis catalyst, resulting in double C-H activation

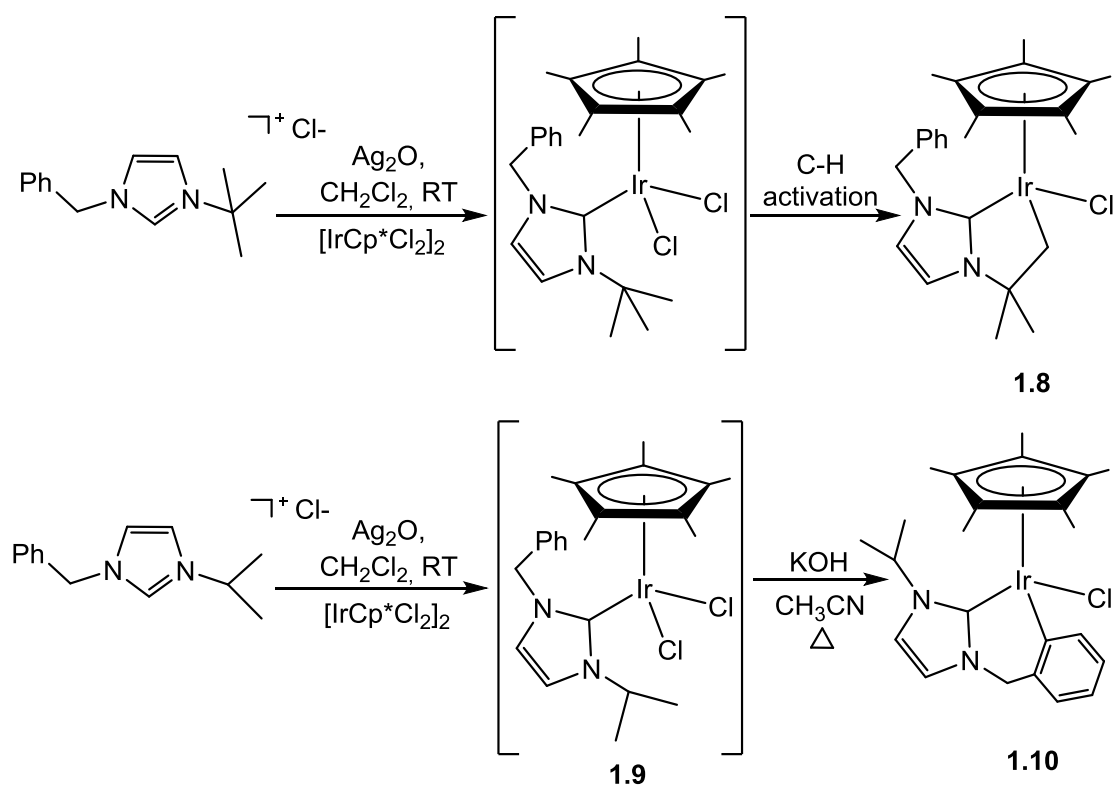
1.4 N-aryl and N-alkyl substituents in C-H activation

It is more difficult to induce C-H activation in N-alkyl substituted NHCs than in N-aryl substituted derivatives. Although alkyl C-H bonds are weaker and easier to cleave, the M-C bonds formed in the resulting activated products are weaker for M-alkyl than M-aryl.⁴³ Previous reports⁴⁴⁻⁴⁶ have shown that C-H activation of N-aryl substituents is preferred over N-alkyl, because an aryl system donates more π -bonding to a metal centre than an N-alkyl group which makes it more favourable to C-H activation. Phenyl and mesityl substituents on the nitrogen have a higher tendency to undergo C-H

activation, since the steric bulk keeps the C-H bonds closer to the metal centre.⁴⁶

Morris et al reported the synthesis of Ru(SiMes')(PPh₃)₂H (' refers to an activated NHC ligand) and Ru(IMes')(PPh₃)₂H both resulting from cyclometallation of a C-H bond. They also tried to induce C-H activation with I^tBu, but failed to do so. Instead they formed a reactive "Ru(I^tBu)(PPh₃)₂" species which could not be isolated, but which reacted with H₂ to afford two isomers of Ru(I^tBu)(PPh₃)₂H₂, both of which contained agostic C-H interactions to the I^tBu ligands.⁴⁴

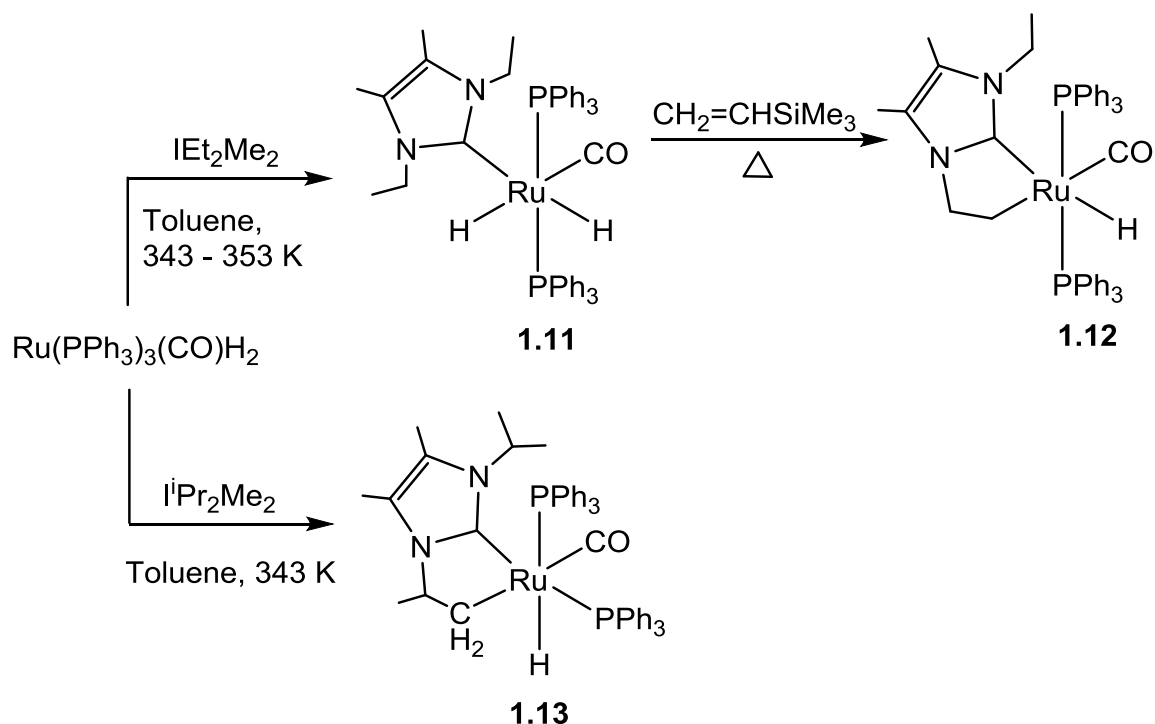
Peris and co-workers synthesised NHCs which contained both aryl and alkyl N-substituents in the form of 1-benzyl-3-*tert*-butylimidazol-2-ylidene and 1-benzyl-3-isopropylimidazol-2-ylidene. These were then reacted with [IrCp*Cl₂]₂ to see which group would activate (Scheme 1.6). Aryl activation although favoured thermodynamically, would give a less stable six-membered ring product than made upon activation of an N-alkyl group which yields a more favourable five-membered ring. When they reacted 1-benzyl-3-*tert*-butylimidazol-2-ylidene with [IrCp*Cl₂]₂, the resulting product **1.8** was formed via aliphatic C-H activation with no evidence of the aromatic C-H activated product, but when 1-benzyl-3-isopropylimidazol-2-ylidene was used, aromatic C-H activation was preferred affording **1.10**, although this required the addition of a strong base as the intermediate containing the non-metalated species **1.9** was stable. They concluded that steric hindrance from the type of imidazolyidene ligand used played an important part in determining the pathway of C-H activation.⁴⁵



Scheme 1.6: Alkyl and aryl C-H activation of NHCs in a Cp*Ir derived fragment

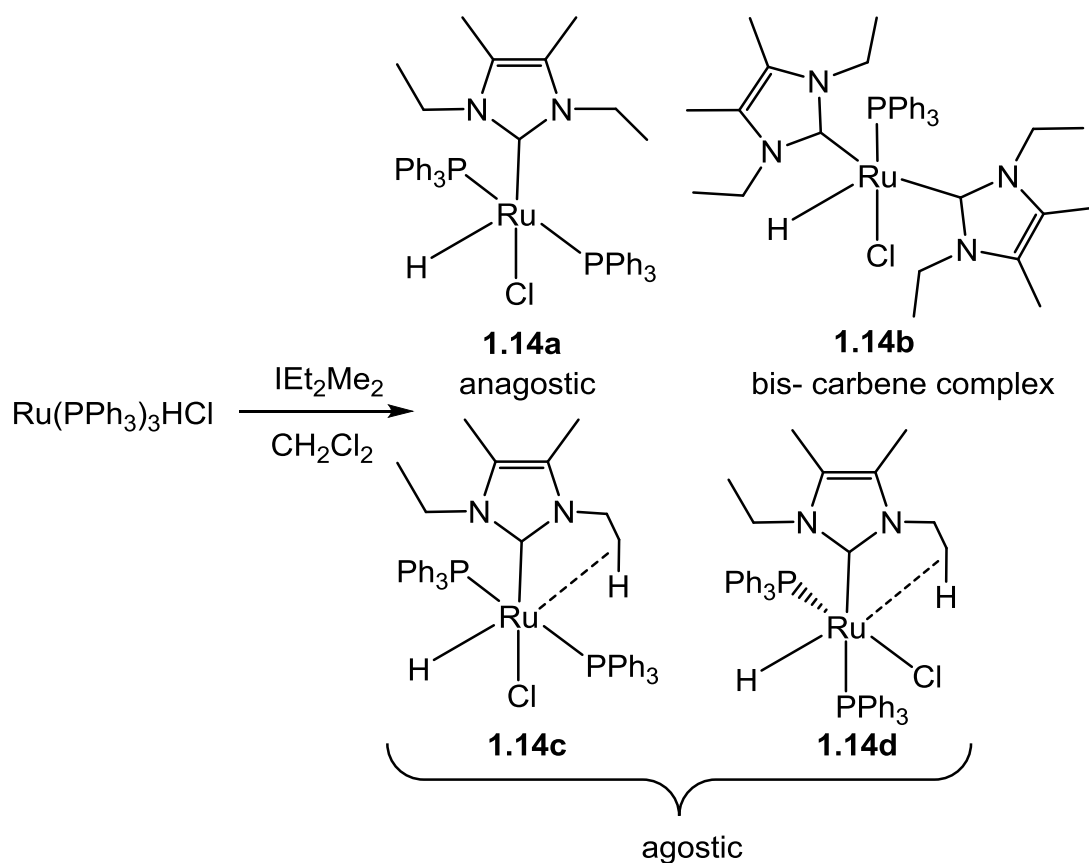
1.5 C-H activation of NHCs in Ru, Rh and Ir complexes

Whittlesey and co-workers have reported C-H activation of N-alkyl substituted NHCs at ruthenium. Thus, $\text{Ru}(\text{PPh}_3)_3(\text{CO})\text{H}_2$ reacted with IEt_2Me_2 to form $\text{Ru}(\text{IEt}_2\text{Me}_2)(\text{PPh}_3)_2(\text{CO})\text{H}_2$ **1.11**, which upon addition of the hydrogen acceptor $\text{CH}_2=\text{CHSiMe}_3$ generated the corresponding C-H activated complex, $\text{Ru}(\text{IEt}_2\text{Me}_2)(\text{PPh}_3)_2(\text{CO})\text{H}$, **1.12**. In contrast, when $\text{Ru}(\text{PPh}_3)_3(\text{CO})\text{H}_2$ was reacted with $\text{I}^i\text{Pr}_2\text{Me}_2$, direct activation to form $\text{Ru}(\text{I}^i\text{Pr}_2\text{Me}_2)(\text{PPh}_3)_2(\text{CO})\text{H}$ **1.13** took place without the need for the alkene (Scheme 1.7).⁴⁷



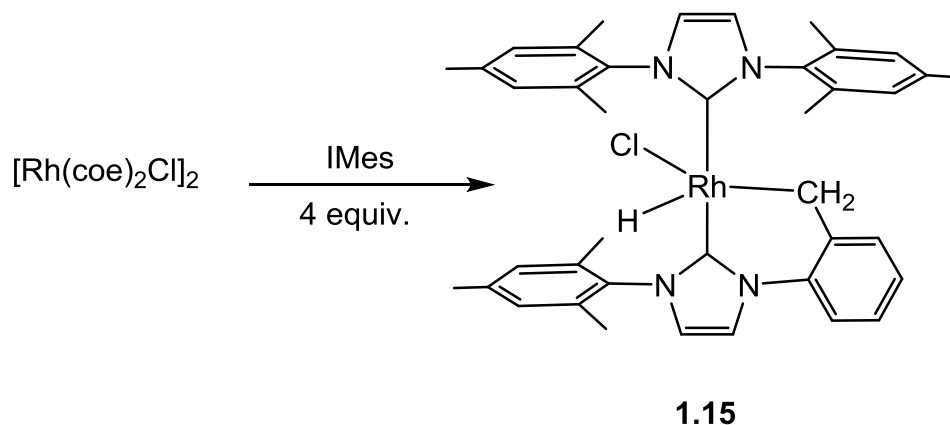
Scheme 1.7: Alkene induced C-H bond activation of IEt_2Me_2 (top) and direct C-H activation of iPr_2Me_2 (bottom)

Reaction with $\text{Ru}(\text{PPh}_3)_3\text{HCl}$ and IEt_2Me_2 did not lead to any clean C-H activation, but formed agostic **1.14a**, bis-carbene **1.14b** and agostic **1.14c-d** products (Scheme 1.8). Exposing the mixture of products to ethene failed to induce complete C-H activation and instead resulted in decomposition and mainly formed imidazolium salt.⁴⁸



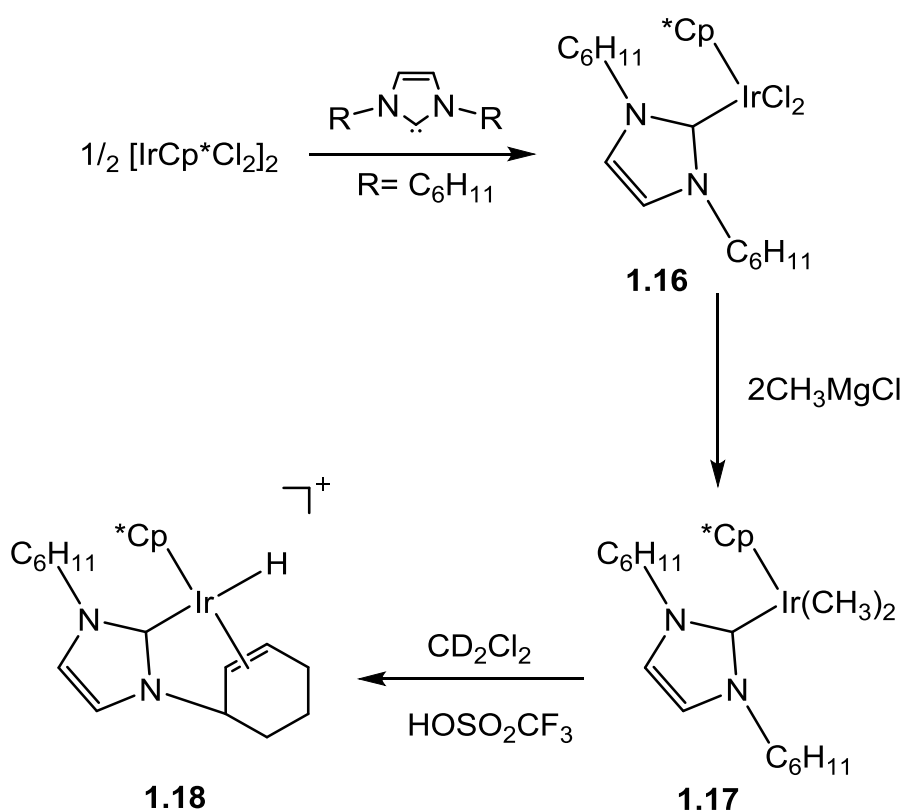
Scheme 1.8: Formation of four products upon reaction of $\text{Ru(PPh}_3\text{)}_3\text{HCl}$ with IEt_2Me_2

Nolan and co-workers reacted IMes with $[\text{Rh}(\text{coe})_2\text{Cl}]_2$ at room temperature to form the cyclometallated complex $\text{Rh}(\text{IMes})(\text{IMes}')\text{HCl}$ **1.15** resulting from the C-H bond activation of an aryl methyl C-H bond of one of the IMes ligands (Scheme 1.9).⁴⁹



Scheme 1.9: C-H activation in a Rh-NHC complex

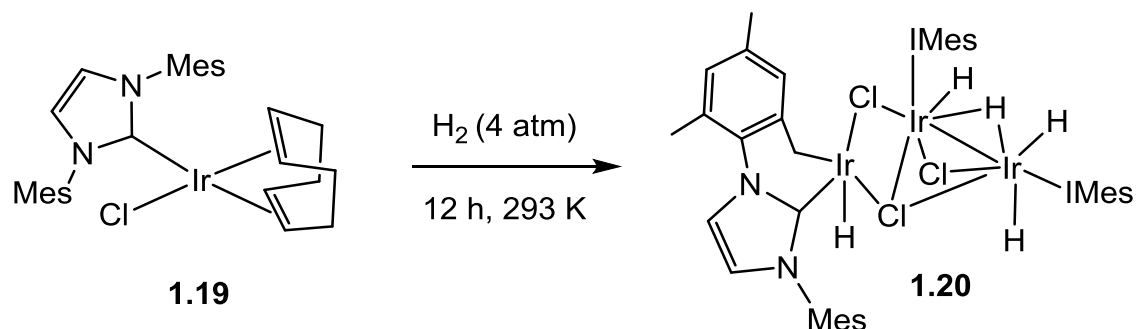
Herrmann et al prepared a new iridium (III) NHC complex where the cyclohexyl substituent underwent C-H activation (Scheme 1.10). They reacted $[\text{IrCp}^*\text{Cl}_2]_2$ with one equivalent of ICy to afford complex **1.16** containing an intact ICy ligand. Addition of two equiv. of CH_3MgCl afforded the corresponding dimethyl complex **1.17** which still retained the unactivated ICy ligand. One equivalent of HOTf was added to **1.17** resulting in the elimination of two equiv. of CH_4 to form **1.18** as a result of C-H activation of the cyclohexyl substituent followed by dehydrogenation.⁵⁰



Scheme 1.10: Functionalization of ICy by a C-H activation process at an iridium (III) centre

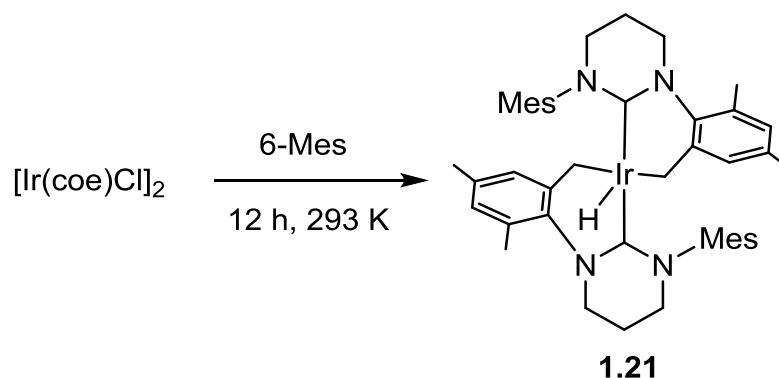
Aldridge and co-workers reported Ir complexes bearing NHCs which undergo C-H activation.⁵¹⁻⁵⁴ The hydrogenation of two highly unsaturated mono-NHC Ir(I) systems (IPr and IMes) were described in 2011.⁵¹ Although the loss of the cod ligand was observed in both reactions, they afforded different products. $\text{Ir}(\text{IPr})(\text{cod})\text{Cl}$ generated a highly reactive trimer $[\text{Ir}(\text{IPr})(\text{H}_2)\text{Cl}]_3$, whereas the IMes complex **1.19** underwent C-H bond

activation to afford $\text{Ir}_3(\text{IMes})_2(\text{IMes}')\text{Cl}_3\text{H}_5$ **1.20** where one IMes ligand was activated at one methyl substituent (Scheme 1.11).



Scheme 1.11: Hydrogenation of **1.19** to afford the C-H activated complex **1.20**

In contrast the reaction of the six membered NHC 6-Mes with $[\text{Ir}(\text{coe})_2\text{Cl}]_2$ afforded $\text{Ir}(\text{6-Mes}')_2\text{H}$ **1.21** which contained two activated NHC ligands (Scheme 1.12).⁵⁵ This double activation chemistry is in contrast with the behaviour of the less strongly donating and less bulky IMes ligand, which generates $\text{Rh}(\text{IMes})(\text{IMes}')\text{HCl}$ **1.15** as shown in Scheme 1.9 and $\text{Ir}(\text{IMes})(\text{IMes}')\text{HCl}$ **1.22** (Figure 1.7).^{49,56} More discussion on ring expanded NHC complexes will be presented in detail in Chapter 4.



Scheme 1.12: Ir bis-NHC complex displaying double C-H activation

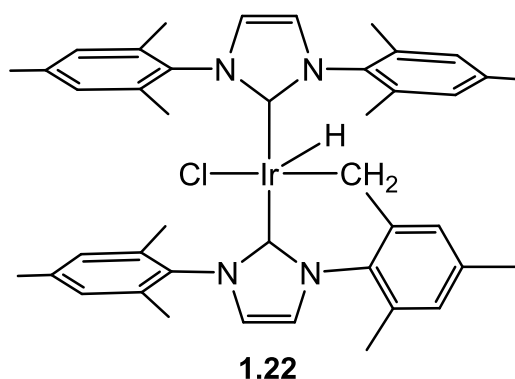
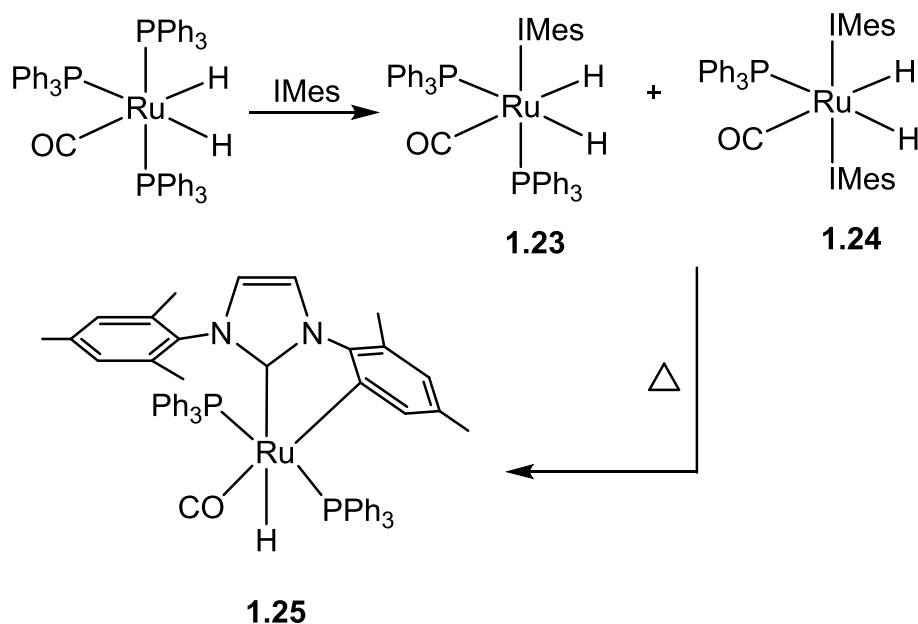


Figure 1.7: An Ir bis-IMes complex showing cyclometallation of one IMes ligand

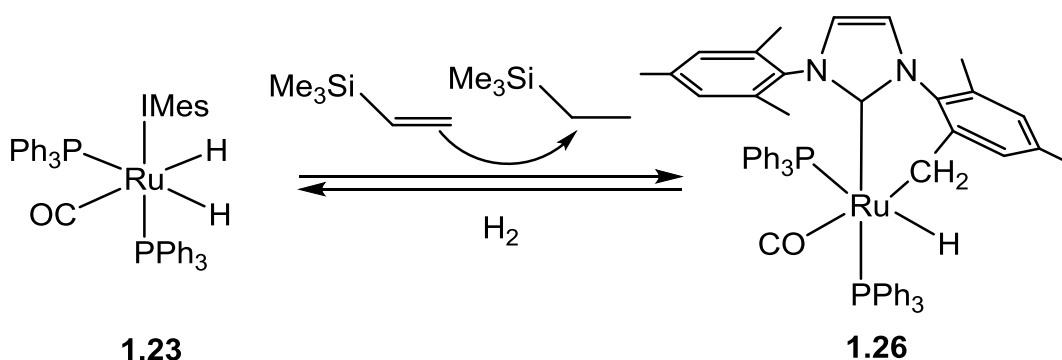
1.6 C-C and C-H bond activations reactions of NHCs

Thermolysis of a benzene solution of $\text{Ru}(\text{PPh}_3)_3(\text{CO})\text{H}_2$ with IMes at 353 K for 14 days led to the formation of $\text{Ru}(\text{IMes})(\text{PPh}_3)_2(\text{CO})\text{H}_2$ **1.23** and $\text{Ru}(\text{IMes})_2(\text{PPh}_3)(\text{CO})\text{H}_2$ **1.24**. Heating the reaction mixture further at 383 K for 2 days afforded the C-C insertion product **1.25** resulting from the cleavage of an Ar-CH₃ bond. At no stage in the formation of the C-C activated complex was a ArCH₂-H cleavage product detected (Scheme 1.13).³⁸



Scheme 1.13: Example of C-C bond activation

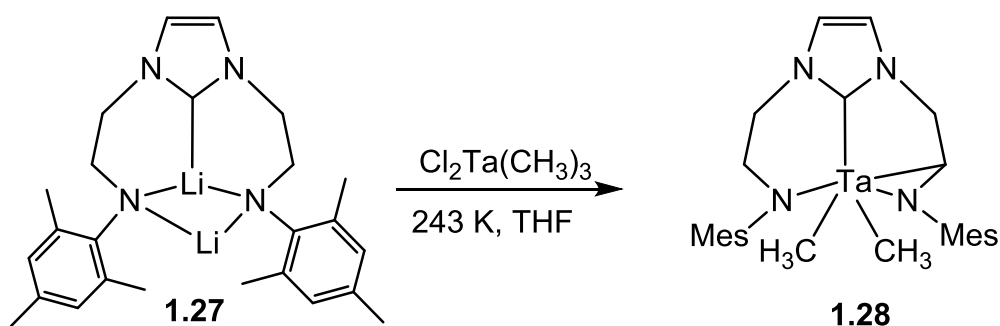
However, facile C-H activation of **1.23** took place at room temperature upon the addition of a hydrogen acceptor to give Ru(IMes')(PPh₃)₂(CO)H **1.26** (Scheme 1.14).³⁸



Scheme 1.14: Formation of Ru(IMes')(PPh₃)₂(CO)H

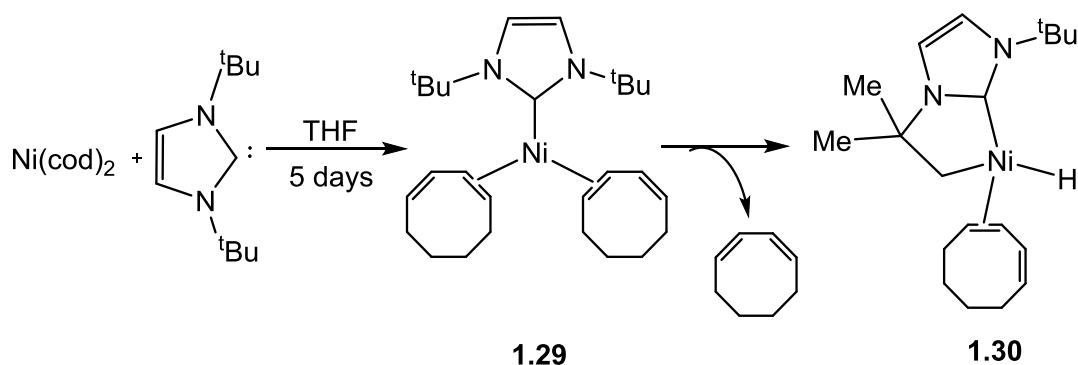
1.7 C-H activation of NHCs in early and late transition metals

Ru, Ir and Rh have the most established track record for C-H activation in NHCs, but it is also possible to cleave carbene C-H bonds using both earlier (Ta, Hf, Ti, V)^{57,58} and later (Ni) transition metals. In the case of Ta, C-H activation does not take place at the N-group, but on one of the amido backbone arms.⁵⁹ Thus, Fryzuk and co-workers described the reaction of TaCl₂Me₃ with **1.27** to form **1.28** upon C-H bond activation (Scheme 1.15).⁵⁹



Scheme 1.15: Synthesis of a metallated [NCNC] Ta alkyl derivative

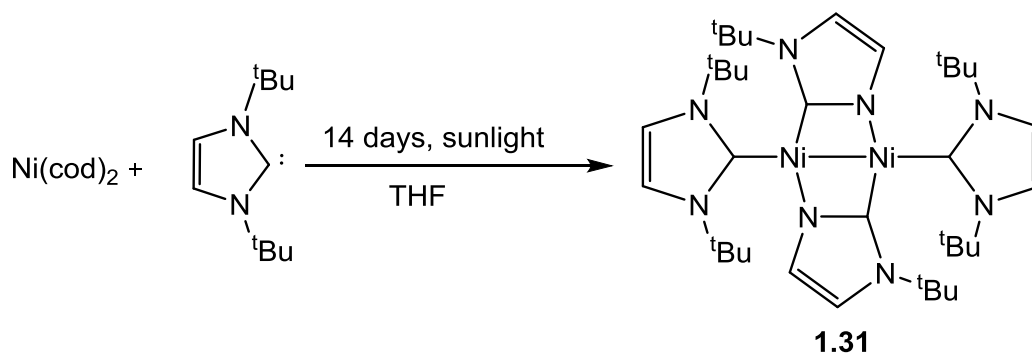
Caddick and co-workers illustrated intramolecular alkyl C-H activation of ^tBu by Ni(cod)₂ to form **1.30**. Addition of ^tBu to Ni(cod)₂ initially gave the 3-coordinate Ni-^tBu bis diene complex **1.29**, which upon elimination of a single cyclooctadiene allowed C-H cleavage of the ^tBu group (Scheme 1.16).⁶⁰



Scheme 1.16: Intramolecular alkyl C-H activation of $t\text{Bu}$ on Ni.

1.8 Metal induced C-N bond activation reaction of NHCs

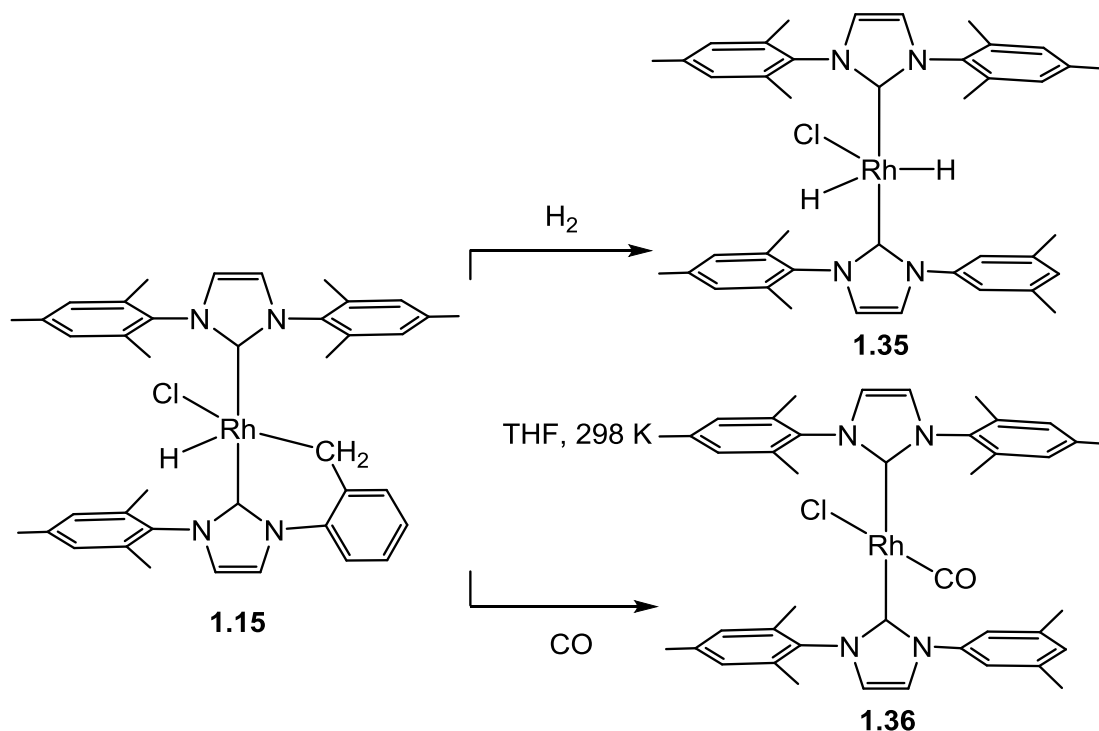
The first example of C-N activation of NHCs was described in 2004 by Cloke, Caddick and co-workers (Scheme 1.17).⁶⁰ Exposure of a THF solution of Ni(cod)_2 and $t\text{Bu}$ to sunlight for 2 weeks yielded the dinuclear Ni(II) species **1.31** containing two C-N activated $t\text{Bu}$ ligands. Shorter irradiation times led to the isolation of an intermediate species containing a C-H activated N^tBu group **1.30**, as shown above which upon heating with additional $t\text{Bu}$ at 353 K afforded the same final C-N activated product, along with isobutene.⁶⁰



Scheme 1.17: Nickel induced C-N bond activation of an NHC

A number of other examples of metal induced C-N activation have now been reported.⁶¹⁻⁶⁷ Treatment of $\text{Ru(PPh}_3)_3(\text{CO})\text{HCl}$ with $i\text{Pr}_2\text{Me}_2$ in THF at 343 K afforded a mixture of products consisting not only of the C-H activated carbene complex $\text{cis-Ru}(i\text{Pr}_2\text{Me}_2)'(\text{PPh}_3)_2(\text{CO})\text{H}$ **1.13**, but also more unexpectedly, of **1.32** formed through C-N activation of one of the N^iPr linkages in the carbene (Scheme 1.18). Repeating the same reaction but at 323 K and leaving it for 6 days gave complete conversion to complex **1.32**

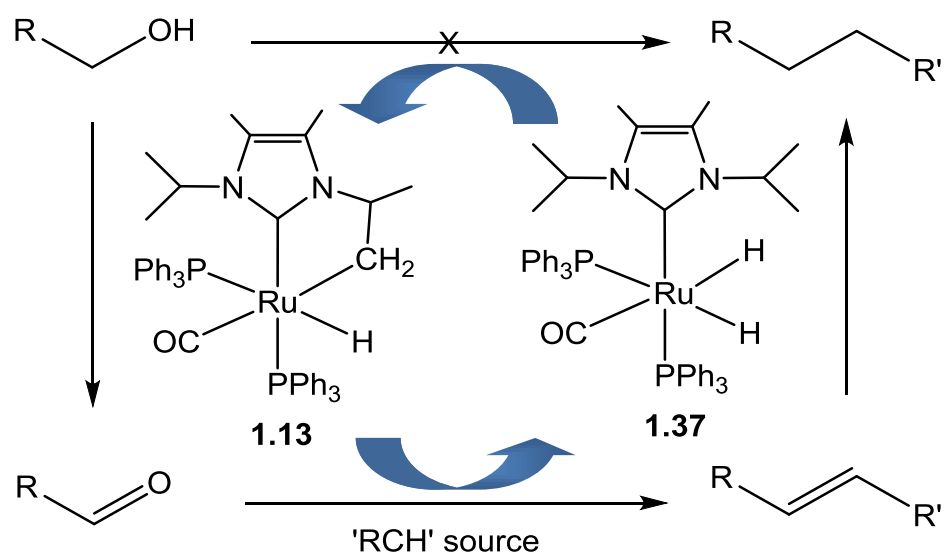
The synthesis of $\text{Rh}(\text{IMes})(\text{IMes}')\text{HCl}$ **1.15** which contained an activated methyl group on the IMes was reported by Nolan and co-workers. However, C-H activation can also be reversed by the addition of H_2 to form $\text{Rh}(\text{IMes})_2\text{H}_2\text{Cl}$ **1.35**. Adding CO to **1.15** generates the mono carbonyl complex $\text{Rh}(\text{IMes})_2(\text{CO})\text{Cl}$ **1.36** (Scheme 1.20).⁴⁹



Scheme 1.20: Reactivity of **1.15** with H_2 and CO

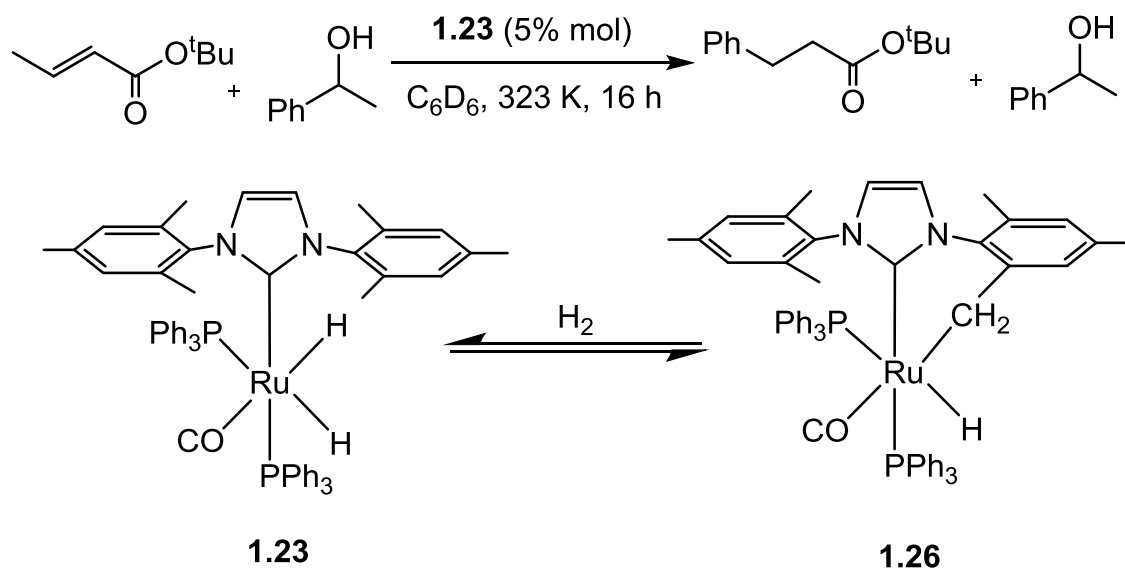
1.10 Catalysis with C-H activated NHC metal complexes

Cyclometallation is a well-established reaction for transition metal NHC complexes, particularly involving late metals such as Ru, Rh and Ir. In some cases where metallation can be reversed by reaction with H_2 or a hydrogen donor, the reaction can become part of a catalytic cycle. An example is shown in Scheme 1.21 for the catalytic 'borrowing hydrogen' process. The metallated N-ⁱPr carbene complex **1.13** picks up the H_2 released during the oxidation of alcohol to an aldehyde to form the corresponding dihydride complex **1.37**. This can then bring about the hydrogenation of an alkene (formed for example by reaction of aldehyde with $\text{Ph}_3\text{P}=\text{CHR}'$), reforming the metallated complex and completing the catalytic cycle.^{47,70}



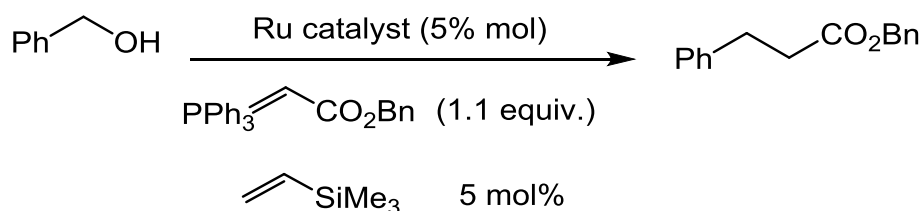
Scheme 1.21

The addition of NHCs to metal complexes makes them suitable for a broad spectrum of catalytic applications, which include transfer hydrogenation.⁸ Ruthenium NHC complexes have been shown to perform efficient transfer hydrogenation reactions with alcohols and alkenes based on the reversible C-H activation of **1.23** (Scheme 1.22).



Scheme 1.22: Transfer hydrogenation reaction between alcohol and alkene (top) and reversible dehydrogenation/hydrogenation pathway of **1.23** (bottom).

Whittlesey and co-workers have also shown the ability of **1.23** to take part in indirect Wittig reactions, which involves the conversion of an alcohol to alkane (Scheme 1.23). The activity of **1.23** is somewhat greater than that of the all-phosphine analogue, Ru(PPh₃)₃(CO)H₂ (Table 1.1).⁷¹

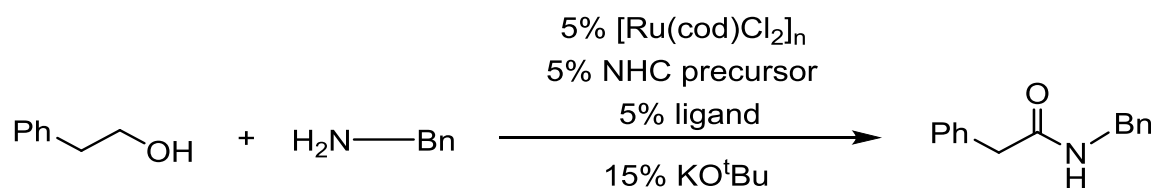


Scheme 1.23: Ruthenium catalysed indirect Wittig reaction of benzyl alcohol

Precursor (5 mol %)	Conversion (%)
Ru(IMes)(PPh ₃) ₂ COH ₂	90
Ru(PPh ₃) ₃ (CO)H ₂	80

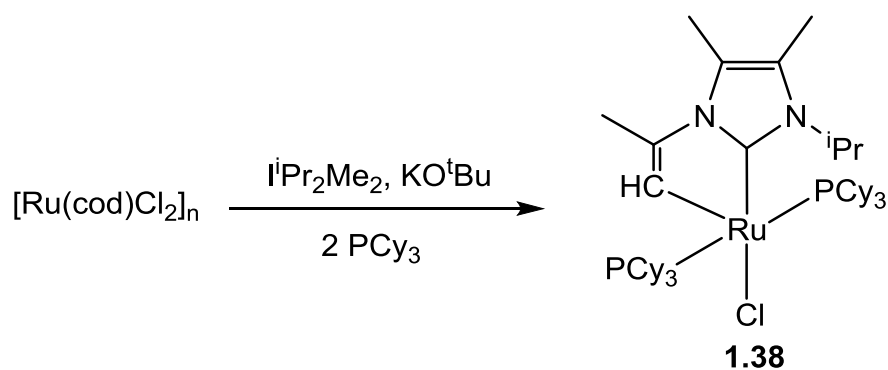
Table 1.1: Effect of ruthenium complexes upon the indirect Wittig reaction of benzyl alcohol to alkane

The synthesis of amides is one of the most important reactions in organic chemistry. Madsen has shown that an in-situ generated ruthenium catalyst prepared by combining Ru(PPh₃)₃Cl₂, an imidazolium salt and a base is capable of generating amides from a combination of alcohols and amine.^{72,73} Only low yields of products were formed, but these could be improved significantly by replacing the ruthenium phosphine precursor by [Ru(cod)Cl₂]_n (Scheme 1.24). However the nature of the active catalyst in these reactions was unknown.



Scheme 1.24: Conversion to an amide using Ru complexes

Wolf and co-workers showed that combining $[\text{Ru}(\text{cod})\text{Cl}_2]_n$, iPr_2Me_2 , PCy_3 and KO^tBu gave the alkenyl carbene complex $\text{Ru}(\text{iPr}_2\text{Me}_2)(\text{PCy}_3)_2\text{Cl}$ **1.33** (Scheme 1.25).⁷⁴ However no catalytic turnover could be observed when compound **1.38** was tested as a catalyst for the dehydrogenative coupling of 2-phenyl ethanol and benzylamine, indicating that this species is not the active fragment formed in Madsen's in-situ reaction.



Scheme 1.25: Triple alkyl C-H activated isopropenyl carbene complex

1.11 Thesis synopsis

This thesis describes the use of five and six-membered NHCs as supporting ligands for the formation of new ruthenium and rhodium complexes. The results are separated into 3 Chapters, each describing a different aspect of NHC chemistry.

Chapter 2 illustrates the use of $[\text{Ru}(\text{cod})\text{Cl}_2]_n$, $\text{Ru}(\text{PPh}_3)_3\text{Cl}_2$ and $\text{Ru}(\text{DMSO})_4\text{Cl}_2$ as precursors and their reactivity with 5-NHCs (IPr_2Me_2 , IEt_2Me_2 and I^tBu) to afford an array of C-H activated Ru complexes.

Chapter 3 describes the reactivity of the previously reported $[\text{Ru}(\text{NHC})_4\text{H}]^+$ species towards amine boranes and the catalytic transfer hydrogenation of a series of organic substrates.

Chapter 4 describes the synthesis and reactivity of new ruthenium and rhodium complexes bearing the small 6-Me and 6-Et ligands.

References

- (1) Hahn, F. E.; Jahnke, M. C. *Angew. Chem. Int. Ed.* **2008**, *47*, 3122.
- (2) Arduengo, A. J.; Harlow, R. L.; Kline, M. J. *Am. Chem. Soc.* **1991**, *113*, 361.
- (3) Crabtree, R. H. *J. Organomet. Chem.* **2005**, *690*, 5451.
- (4) Herrmann, W. A.; Elison, M.; Fischer, J.; Köcher, C.; Artus, G. R. J. *Angew. Chem. Int. Ed.* **1995**, *34*, 2371.
- (5) Herrmann, W. A.; Köcher, C. *Angew. Chem. Int. Ed.* **1997**, *36*, 2162.
- (6) Herrmann, W. A. *Angew. Chem. Int. Ed.* **2002**, *41*, 1290.
- (7) Díez-González, S.; Marion, N.; Nolan, S. P. *Chem. Rev.* **2009**, *109*, 3612.
- (8) Demir, S.; Özdemir, I.; Çetinkaya, B. *J. Organomet. Chem.* **2009**, *694*, 4025.
- (9) Tolman, C. A. *Chem. Rev.* **1977**, *77*, 313.
- (10) Huang, J. K.; Schanz, H. J.; Stevens, E. D.; Nolan, S. P. *Organometallics* **1999**, *18*, 5375.
- (11) Hillier, A. C.; Sommer, W. J.; Yong, B. S.; Petersen, J. L.; Cavallo, L.; Nolan, S. P. *Organometallics* **2003**, *22*, 4322.
- (12) Clavier, H.; Nolan, S. P. *Chem. Commun.* **2010**, *46*, 841.
- (13) Scott, N. M.; Dorta, R.; Stevens, E. D.; Correa, A.; Cavallo, L.; Nolan, S. P. *J. Am. Chem. Soc.* **2005**, *127*, 3516.
- (14) Hu, X. L.; Tang, Y. J.; Gantzel, P.; Meyer, K. *Organometallics* **2003**, *22*, 612.
- (15) Scholl, M.; Ding, S.; Lee, C. W.; Grubbs, R. H. *Org. Lett.* **1999**, *1*, 953.
- (16) Chung, C. K.; Grubbs, R. H. *Org. Lett.* **2008**, *10*, 2693.
- (17) Crabtree, R. *Acc. Chem. Res.* **1979**, *12*, 331.
- (18) Lee, H. M.; Jiang, T.; Stevens, E. D.; Nolan, S. P. *Organometallics* **2001**, *20*, 1255.
- (19) McGuinness, D. S.; Saendig, N.; Yates, B. F.; Cavell, K. J. *J. Am. Chem. Soc.* **2001**, *123*, 4029.
- (20) McGuinness, D. S.; Cavell, K. J.; Yates, B. F.; Skelton, B. W.; White, A. H. *J. Am. Chem. Soc.* **2001**, *123*, 8317.

- (21) Gründemann, S.; Kovacevic, A.; Albrecht, M.; Faller, J. W.; Crabtree, R. H. *J. Am. Chem. Soc.* **2002**, *124*, 10473.
- (22) Kovacevic, A.; Gründemann, S.; Miecznikowski, J. R.; Clot, E.; Eisenstein, O.; Crabtree, R. H. *Chem. Commun.* **2002**, 2580.
- (23) Danopoulos, A. A.; Winston, S.; Hursthouse, M. B. *J. Chem. Soc., Dalton Trans.* **2002**, 3090.
- (24) Clement, N. D.; Cavell, K. J.; Jones, C.; Elsevier, C. J. *Angew. Chem. Int. Ed.* **2004**, *43*, 1277.
- (25) Giunta, D.; Hölscher, M.; Lehmann, C. W.; Mynott, R.; Wirtz, C.; Leitner, W. *Adv. Synth. Catal.* **2003**, *345*, 1139.
- (26) Chilvers, M. J.; Jazzar, R. F. R.; Mahon, M. F.; Whittlesey, M. K. *Adv. Synth. Catal.* **2003**, *345*, 1111.
- (27) Chatwin, S. L.; Diggle, R. A.; Jazzar, R. F. R.; Macgregor, S. A.; Mahon, M. F.; Whittlesey, M. K. *Inorg. Chem.* **2003**, *42*, 7695.
- (28) Chianese, A. R.; Kovacevic, A.; Zeglis, B. M.; Faller, J. W.; Crabtree, R. H. *Organometallics* **2004**, *23*, 2461.
- (29) Burling, S.; Mahon, M. F.; Paine, B. M.; Whittlesey, M. K.; Williams, J. M. J. *Organometallics* **2004**, *23*, 4537.
- (30) Davies, C. J. E.; Lowe, J. P.; Mahon, M. F.; Poulten, R. C.; Whittlesey, M. K. *Organometallics* **2013**, *32*, 4927.
- (31) Pan, B. F.; Pierre, S.; Bezpalko, M. W.; Napoline, J. W.; Foxman, B. M.; Thomas, C. M. *Organometallics* **2013**, *32*, 704.
- (32) Jazzar, R. F. R.; Bhatia, P. H.; Mahon, M. F.; Whittlesey, M. K. *Organometallics* **2003**, *22*, 670.
- (33) Burling, S.; Kociok-Köhn, G.; Mahon, M. F.; Whittlesey, M. K.; Williams, J. M. J. *Organometallics* **2005**, *24*, 5868.
- (34) Dorta, R.; Stevens, E. D.; Nolan, S. P. *J. Am. Chem. Soc.* **2004**, *126*, 5054.
- (35) Segarra, C.; Mas-Marzá, E.; Mata, J. A.; Peris, E. *Organometallics* **2012**, *31*, 5169.
- (36) Crabtree, R. H. *Coord. Chem. Rev.* **2013**, *257*, 755.
- (37) Poulain, A.; Iglesias, M.; Albrecht, M. *Curr. Org. Chem.* **2011**, *15*, 3325.

- (38) Jazzar, R. F. R.; Macgregor, S. A.; Mahon, M. F.; Richards, S. P.; Whittlesey, M. K. *J. Am. Chem. Soc.* **2002**, *124*, 4944.
- (39) Burling, S.; Mahon, M. F.; Powell, R. E.; Whittlesey, M. K.; Williams, J. M. J. *J. Am. Chem. Soc.* **2006**, *128*, 13702.
- (40) Crudden, C. M.; Allen, D. P. *Coord. Chem. Rev.* **2004**, *248*, 2247.
- (41) Hitchcock, P. B.; Lappert, M. F.; Pye, P. L. *J. Chem. Soc., Chem. Commun.* **1977**, 196.
- (42) Hong, S. H.; Chlenov, A.; Day, M. W.; Grubbs, R. H. *Angew. Chem. Int. Ed.* **2007**, *46*, 5148.
- (43) Crabtree, R. H. *J. Chem. Soc., Dalton Trans* **2001**, 2437.
- (44) Abdur-Rashid, K.; Fedorkiw, T.; Lough, A. J.; Morris, R. H. *Organometallics* **2004**, *23*, 86.
- (45) Corberán, R.; Sanaú, M.; Peris, E. *Organometallics* **2006**, *25*, 4002.
- (46) Mathew, J.; Koga, N.; Suresh, C. H. *Organometallics* **2008**, *27*, 4666.
- (47) Burling, S.; Paine, B. M.; Nama, D.; Brown, V. S.; Mahon, M. F.; Prior, T. J.; Pregosin, P. S.; Whittlesey, M. K.; Williams, J. M. J. *J. Am. Chem. Soc.* **2007**, *129*, 1987.
- (48) Burling, S.; Mas-Marzá, E.; Valpuesta, J. E. V.; Mahon, M. F.; Whittlesey, M. K. *Organometallics* **2009**, *28*, 6676.
- (49) Huang, J. K.; Stevens, E. D.; Nolan, S. P. *Organometallics* **2000**, *19*, 1194.
- (50) Prinz, M.; Grosche, M.; Herdtweck, E.; Herrmann, W. A. *Organometallics* **2000**, *19*, 1692.
- (51) Tang, C. Y.; Lednik, J.; Vidovic, D.; Thompson, A. L.; Aldridge, S. *Chem. Commun.* **2011**, *47*, 2523.
- (52) Tang, C. Y.; Phillips, N.; Kelly, M. J.; Aldridge, S. *Chem. Commun.* **2012**, *48*, 11999.
- (53) Tang, C. Y.; Smith, W.; Vidovic, D.; Thompson, A. L.; Chaplin, A. B.; Aldridge, S. *Organometallics* **2009**, *28*, 3059.
- (54) Tang, C. Y.; Thompson, A. L.; Aldridge, S. *J. Am. Chem. Soc.* **2010**, *132*, 10578.
- (55) Phillips, N.; Rowles, J.; Kelly, M. J.; Riddlestone, I.; Rees, N. H.; Dervisi, A.; Fallis, I. A.; Aldridge, S. *Organometallics* **2012**, *31*, 8075.

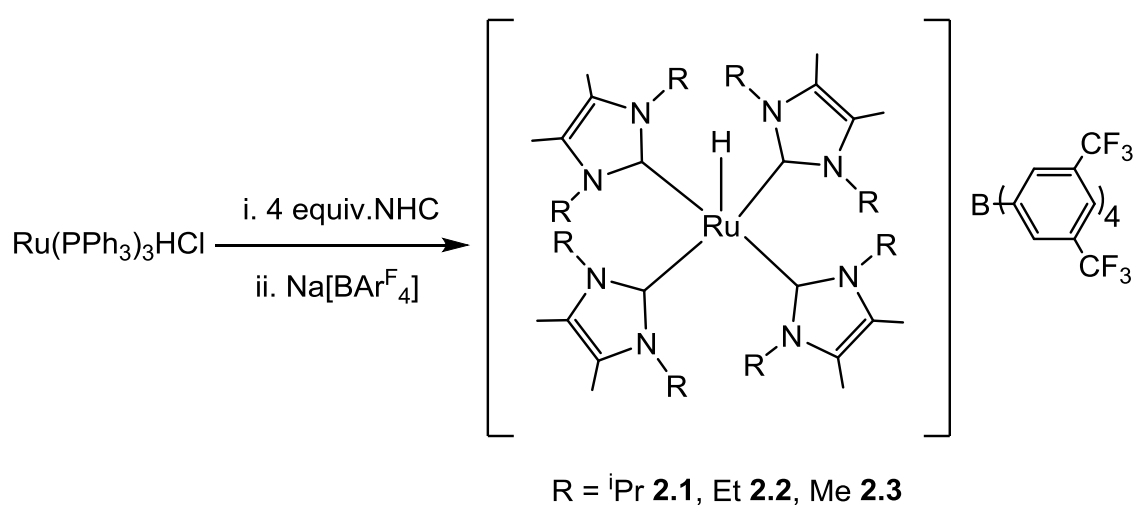
- (56) Tang, C. Y.; Smith, W.; Thompson, A. L.; Vidovic, D.; Aldridge, S. *Angew. Chem. Int. Ed.* **2011**, *50*, 1359.
- (57) Spencer, L. P.; Fryzuk, M. D. *J. Organomet. Chem.* **2005**, *690*, 5788.
- (58) Downing, S. P.; Danopoulos, A. A. *Organometallics* **2006**, *25*, 1337.
- (59) Spencer, L. P.; Beddie, C.; Hall, M. B.; Fryzuk, M. D. *J. Am. Chem. Soc.* **2006**, *128*, 12531.
- (60) Caddick, S.; Cloke, F. G. N.; Hitchcock, P. B.; Lewis, A. K. D. *Angew. Chem. Int. Ed.* **2004**, *43*, 5824.
- (61) Hu, Y.-C.; Tsai, C.-C.; Shih, W.-C.; Yap, G. P. A.; Ong, T.-G. *Organometallics* **2010**, *29*, 516.
- (62) Mas-Marzá, E.; Poyatos, M.; Sanaú, M.; Peris, E. *Organometallics* **2004**, *23*, 323.
- (63) Mas-Marzá, E.; Poyatos, M.; Sanaú, M.; Peris, E. *Inorg. Chem.* **2004**, *43*, 2213.
- (64) Cabeza, J. A.; del Río, I.; Miguel, D.; Sánchez-Vega, M. G. *Angew. Chem. Int. Ed.* **2008**, *47*, 1920.
- (65) Cooke, C. E.; Jennings, M. C.; Katz, M. J.; Pomeroy, R. K.; Clyburne, J. A. C. *Organometallics* **2008**, *27*, 5777.
- (66) Ye, J.; Zhang, X.; Chen, W.; Shimada, S. *Organometallics* **2008**, *27*, 4166.
- (67) Han, Y.; Hong, Y.-T.; Huynh, H. V. *J. Organomet. Chem.* **2008**, *693*, 3159.
- (68) Häller, L. J. L.; Page, M. J.; Erhardt, S.; Macgregor, S. A.; Mahon, M. F.; Abu Naser, M.; Vélez, A.; Whittlesey, M. K. *J. Am. Chem. Soc.* **2010**, *132*, 18408.
- (69) Fortman, G. C.; Jacobsen, H.; Cavallo, L.; Nolan, S. P. *Chem. Commun.* **2011**, *47*, 9723.
- (70) Page, M. J.; Mahon, M. F.; Whittlesey, M. K. *Dalton Trans.* **2011**, *40*, 7858.
- (71) Edwards, M. G.; Jazzar, R. F. R.; Paine, B. M.; Shermer, D. J.; Whittlesey, M. K.; Williams, J. M. J.; Edney, D. D. *Chem. Commun.* **2004**, 90.
- (72) Dam, J. H.; Osztrovszky, G.; Nordstrøm, L. U.; Madsen, R. *Chem. Eur. J.* **2010**, *16*, 6820.

- (73) Nordstrøm, L. U.; Vogt, H.; Madsen, R. *J. Am. Chem. Soc.* **2008**, *130*, 17672.
- (74) Wolf, R.; Plois, M. *Eur. J. Inorg. Chem.* **2010**, 4419.

2. INTRODUCTION

2.1 Ruthenium hydride NHC complexes

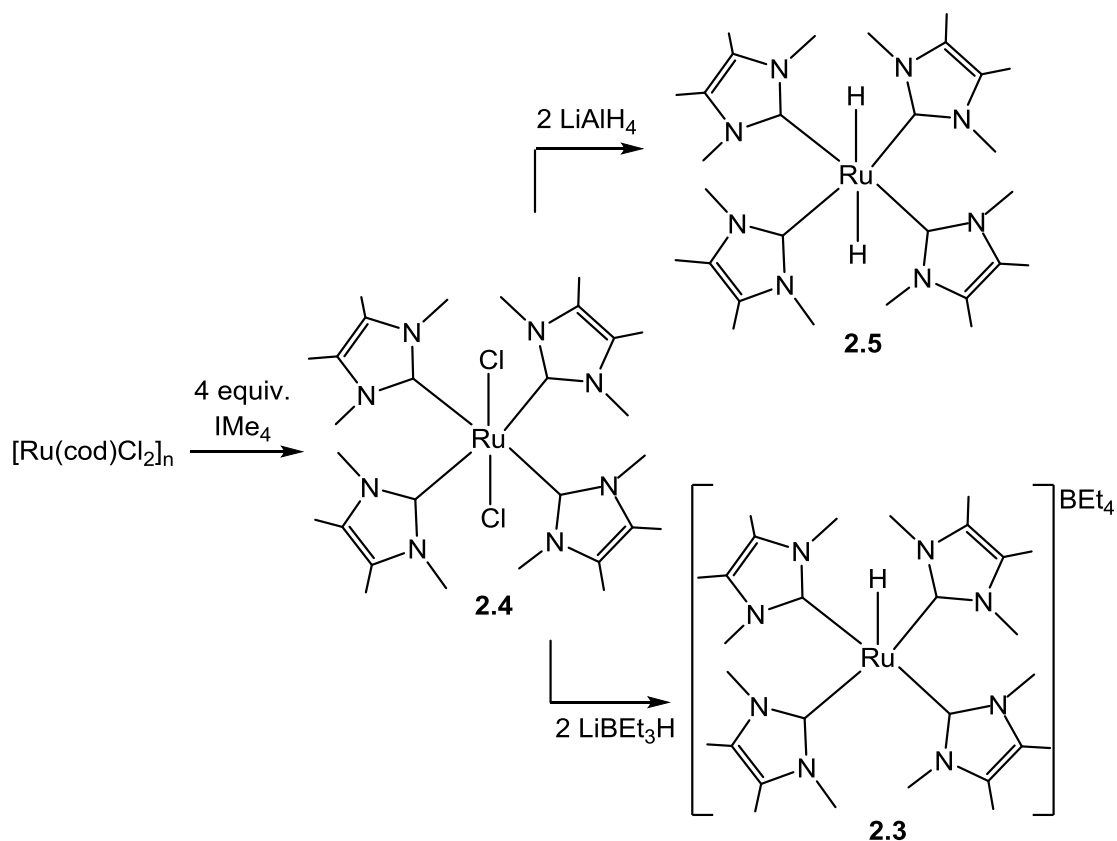
In 2009 our group reported the synthesis of a series of $[\text{Ru}(\text{NHC})_4\text{H}]^+$ salts containing the ligands $^i\text{Pr}_2\text{Me}_2$, IEt_2Me_2 and IMe_4 .¹ Treatment of $\text{Ru}(\text{PPh}_3)_3\text{HCl}$ with four equiv. of these NHCs afforded the five-coordinate cations $[\text{Ru}(\text{NHC})_4\text{H}]^+$ as purple powders. Metathesis with $\text{Na}[\text{BAr}^{\text{F}}_4]$ in either MeCN or toluene allowed isolation of the structurally characterised $[\text{BAr}^{\text{F}}_4]$ salts **2.1-2.3** (Scheme 2.1).



Scheme 2.1: Synthesis of $[\text{Ru}(\text{NHC})_4\text{H}][\text{BAr}^{\text{F}}_4]$ salts

The ability of the 16-electron Ru-NHC species to bind small molecules was reported to vary with the N-substituents on the carbene ligands. Thus, $[\text{Ru}(^i\text{Pr}_2\text{Me}_2)_4\text{H}]^+$ reversibly coordinates O_2 , but is unreactive towards either H_2 or N_2 . The N-ethyl and N-Me complexes are oxidised by O_2 but reversibly coordinate H_2 and N_2 .^{1,2}

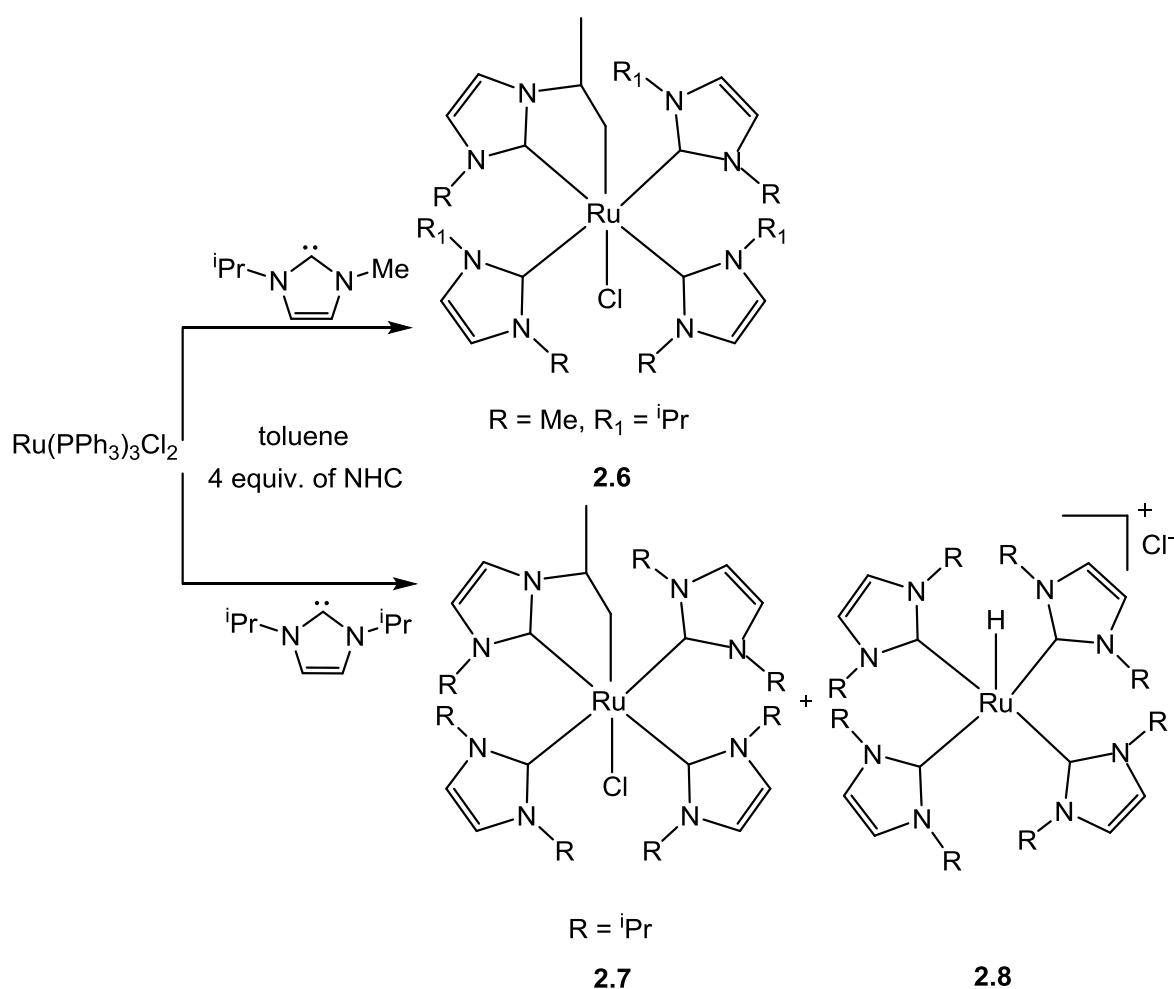
Shortly afterwards, Wolf and co-workers reported the synthesis of tetrakiscarbene hydride complexes $\text{Ru}(\text{IMe}_4)_4\text{H}_2$ and $[\text{Ru}(\text{IMe}_4)_4\text{H}][\text{BEt}_4]$ from the dichloride complex $\text{Ru}(\text{IMe}_4)_4\text{Cl}_2$ **2.4** (Scheme 2.2).³



Scheme 2.2: Synthesis of ruthenium hydride complexes via $\text{Ru}(\text{IME}_4)_4\text{Cl}_2$

Complex **2.4** was formed initially from the reaction of $\text{Ru}(\text{PPh}_3)_3\text{Cl}_2$ with IME_4 , although the PPh_3 by-product was difficult to separate. Changing the precursor to $[\text{Ru}(\text{cod})\text{Cl}_2]_n$ and reacting it with four equiv. of IME_4 cleanly afforded **2.4**. Treatment with LiAlH_4 afforded the neutral dihydride complex **2.5**, whereas treatment of **2.4** with LiBHET_3 took a completely different course and generated the cation $[\text{Ru}(\text{IME}_4)_4\text{H}]^+$ **2.3**, with $[\text{BEt}_4]^-$ as the anion.³

Radius et al carried out experiments in order to synthesise new tetrakis carbene dichloride complexes of ruthenium with a range of N-alkyl substituted NHCs. Reaction with the unsymmetrical NHC $iPrMe$, gave four isomers of $Ru(iPrMe)_4Cl_2$. At higher temperature, HCl elimination took place leading to formation of **2.6** (along with isomers which were not structurally characterised) via C-H activation of one of the methyl groups on an iPr arm. When the reaction was attempted with iPr , a mixture of products was also formed including the C-H activated product, $Ru(iPr)_3(iPr')$ Cl **2.7**, as well as the cationic hydride complex $[Ru(iPr)_4H]^+$ **2.8**, and imidazolium salt, which formed by reaction of the eliminated HCl (Scheme 2.3).⁴

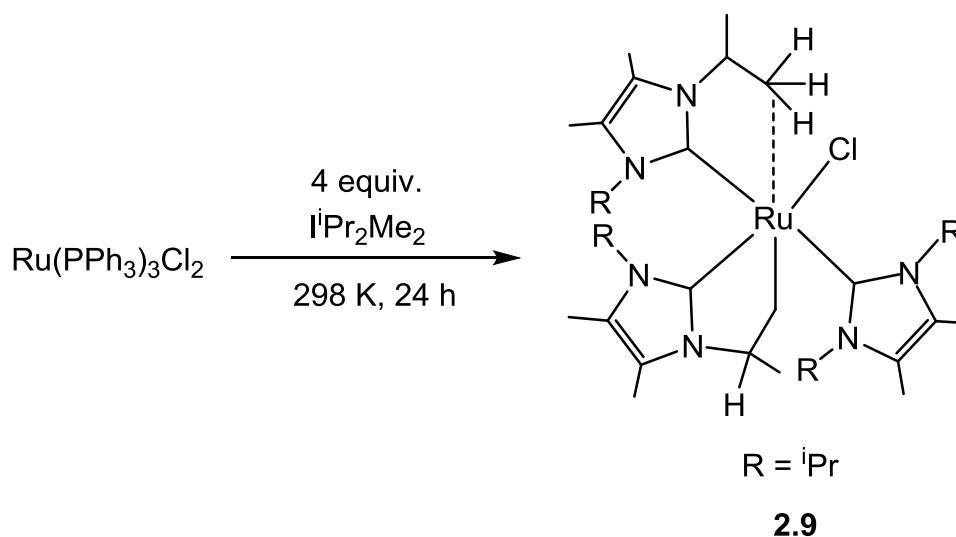


Scheme 2.3: Synthesis of tetrakis carbene ruthenium complexes

In light of these findings by Wolf and Radius, we attempted to use a range of ruthenium dichloride starting materials including $[\text{Ru}(\text{cod})\text{Cl}_2]_n$, $\text{Ru}(\text{PPh}_3)_3\text{Cl}_2$ and $\text{Ru}(\text{DMSO})_4\text{Cl}_2$, in efforts to prepare a range of new cyclometallated NHC complexes.

2.2 Synthesis of $\text{Ru}(\text{iPr}_2\text{Me}_2')(\text{iPr}_2\text{Me}_2)_2\text{Cl}$ (**2.9**)

A toluene solution of $\text{Ru}(\text{PPh}_3)_3\text{Cl}_2$ containing four equiv. of iPr_2Me_2 was stirred for 24 h at 298 K to afford the C-H activated triscarbene chloride complex $\text{Ru}(\text{iPr}_2\text{Me}_2')(\text{iPr}_2\text{Me}_2)_2\text{Cl}$ **2.9**. This was isolated as an orange solid in 43% yield (Scheme 2.4) and characterised through a combination of X-ray crystallography and 1D and 2D NMR spectroscopy.



Scheme 2.4: Synthesis of $\text{Ru}(\text{iPr}_2\text{Me}_2')(\text{iPr}_2\text{Me}_2)_2\text{Cl}$

Crystals suitable for X-ray diffraction were obtained from slow diffusion from hexane into a concentrated benzene solution of the complex. The X-ray structure is shown in Figure 2.3 along with selected bond lengths and angles.

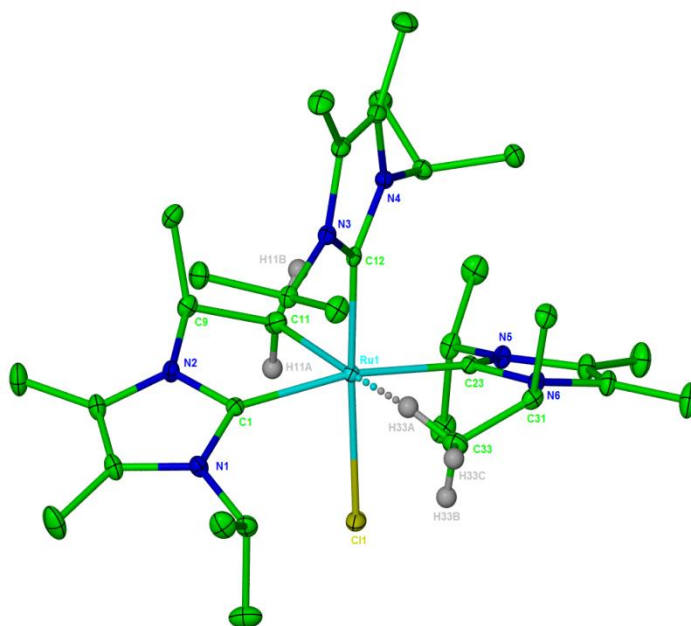


Figure 2.3: Molecular structure of $\text{Ru}(\text{iPr}_2\text{Me}_2')(\text{iPr}_2\text{Me}_2)_2\text{Cl}$ (**2.9**) (thermal ellipsoids at 30% probability; hydrogen atoms except those on the cyclometallated and agostic arm are removed for clarity). Selected bond lengths [Å] and angles [°]: Ru(1)-C(1) 2.0669(16), Ru(1)-C(11) 2.1446(18), Ru(1)-C(12) 2.0268(15), Ru(1)-C(23) 2.10829(16), Ru(1)-Cl(1) 2.5240(4), C(1)-Ru(1)-C(11) 76.32(6), C(1)-Ru(1)-C(23) 168.32(6), C(11)-Ru(1)-C(23) 104.27(6).

The molecular structure comprises of a distorted octahedral geometry with a chloride and three carbene ligands, a metallated iPr arm and, in the sixth coordination site trans to the metallated arm, an agostic interaction to an iPr methyl group. The agostic distances [Ru \cdots H(33a) 1.97 Å, Ru \cdots C(33) 2.703(2) Å] are shorter than those found in analogous Ru-NHC complexes^{5,6} and are in the range associated with strong interactions.⁷⁻¹⁰ The three Ru-C_{NHC} distances are all different with the distance to the agostic NHC significantly longer [Ru(1)-C(23) 2.1082(16) Å] than to either of the remaining two NHC ligands [Ru(1)-C(1) 2.0669(16) Å; Ru(1)-C(12) 2.0268(15) Å].

The ^1H NMR spectrum of **2.9** showed four septets (marked as * in Figure 2.4) between 5.8 and 6.8 ppm, arising from the methine protons of the unactivated iPr groups. Two septets at 3.7 and 4.0 ppm (*) arise from the methine protons on the agostically bound and C-H activated iPr arms

respectively; assignment of these was made by ^1H COSY. There are eleven ^iPr methyl groups, with five of these doublet resonances overlapping between 1.5 -2.1 ppm. The remaining six signals (marked as #) are clearer and are located between 0.0 – 1.5 ppm.

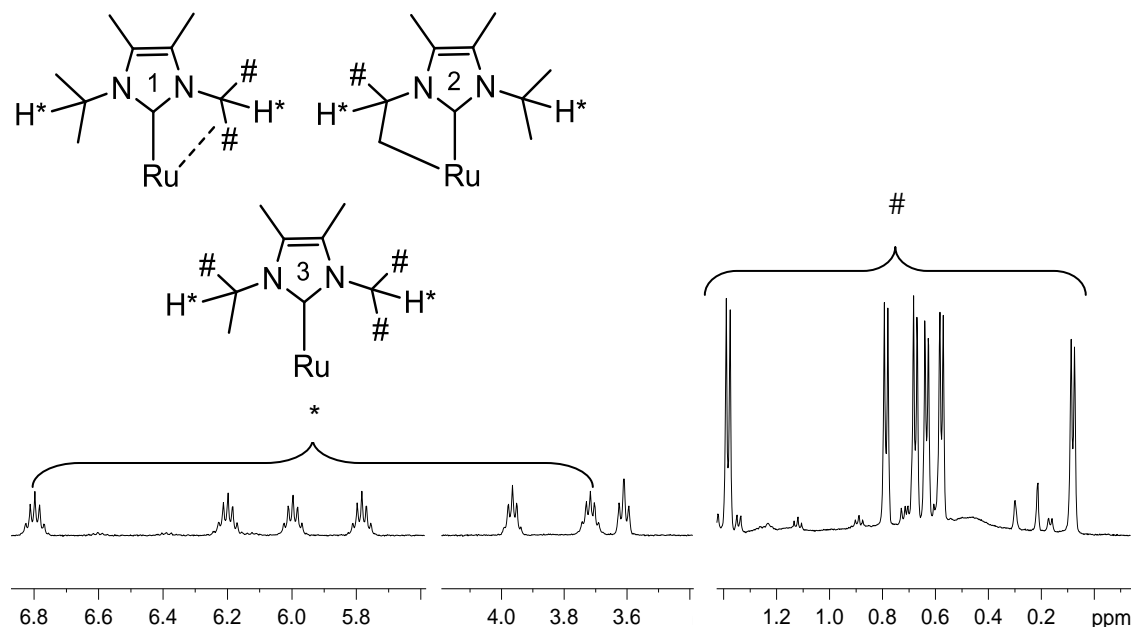


Figure 2.4: Partial ^1H NMR spectrum of **2.9** (C_6D_6 , 500 MHz, 298 K)

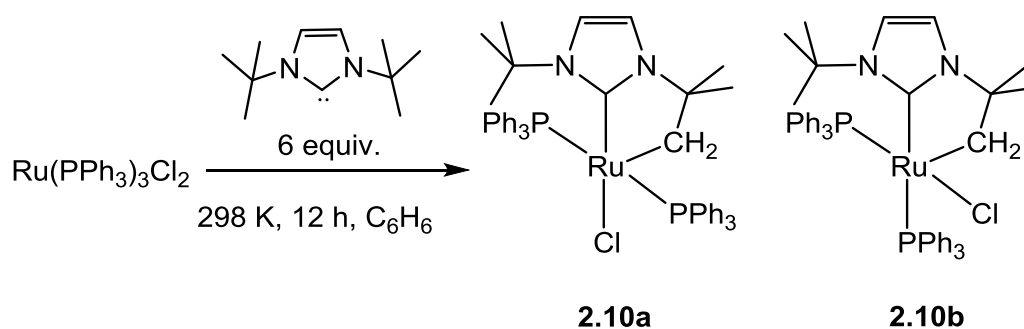
The $^{13}\text{C}\{^1\text{H}\}$ NMR spectrum showed three characteristically high frequency singlets at 203, 202 and 200 ppm, assigned to the carbenic carbons of the agostic, C-H activated and unactivated ligands respectively on the basis of ^1H - ^{13}C HSQC experiments.

Employing the same approach used by Wolf and co-workers³ (Scheme 2.2), reactions of $[\text{Ru}(\text{cod})\text{Cl}_2]_n$ with an excess (4 equiv.) of ^iBu , IEt_2Me_2 and $^i\text{Pr}_2\text{Me}_2$ were attempted in toluene solution at 373 K for 4 h. No Ru-NHC products could be isolated from the reaction involving ^iBu , most likely because of its very bulky nature. The reaction with the N-ethyl-substituted carbene gave one major product, which was identified as the cationic tetrakis(carbene)hydride complex $[\text{Ru}(\text{IEt}_2\text{Me}_2)_4\text{H}]^+$ on the basis of the very low frequency hydride resonance (-41.0 ppm).¹ In the case of $^i\text{Pr}_2\text{Me}_2$, a homogeneous red-orange solution was formed from which a mixture of purple and orange microcrystalline solids were isolated. The former was characterised as $[\text{Ru}(^i\text{Pr}_2\text{Me}_2)_4\text{H}]^+$ while the latter was identified as **2.9**.

Studies on the reactivity of **2.9** focused on the potential reversibility of C-H activation. Thus, addition of 1 atm H₂ to a benzene solution of **2.9** resulted in the rapid formation of a mixture of products at room temperature, implying that the complex adds H₂ in an uncontrolled way. It may be possible to overcome this by carrying out the reaction with H₂ at low temperature and following progress by low temperature NMR spectroscopy.

2.3 Synthesis of Ru(^tBu')(PPh₃)₂Cl (**2.10a/b**)

A solution of Ru(PPh₃)₃Cl₂ and six equiv. of ^tBu was stirred for 12 h in benzene at 298 K to afford the C-H activated complex Ru(^tBu')(PPh₃)₂Cl **2.10a/b** as a mixture of trans and cis phosphine isomers (Scheme 2.5).



Scheme 2.5: Synthesis of Ru(^tBu')(PPh₃)₂Cl

By ³¹P{¹H} NMR spectroscopy (Figure 2.5), the major product was the trans phosphine isomer **2.10a**, which displayed a singlet resonance at 40.3 ppm, while the cis-phosphine isomer **2.10b** exhibited two doublet resonances ($J_{PP} = 23.8\text{Hz}$) at 36.1 and 62.0 ppm.

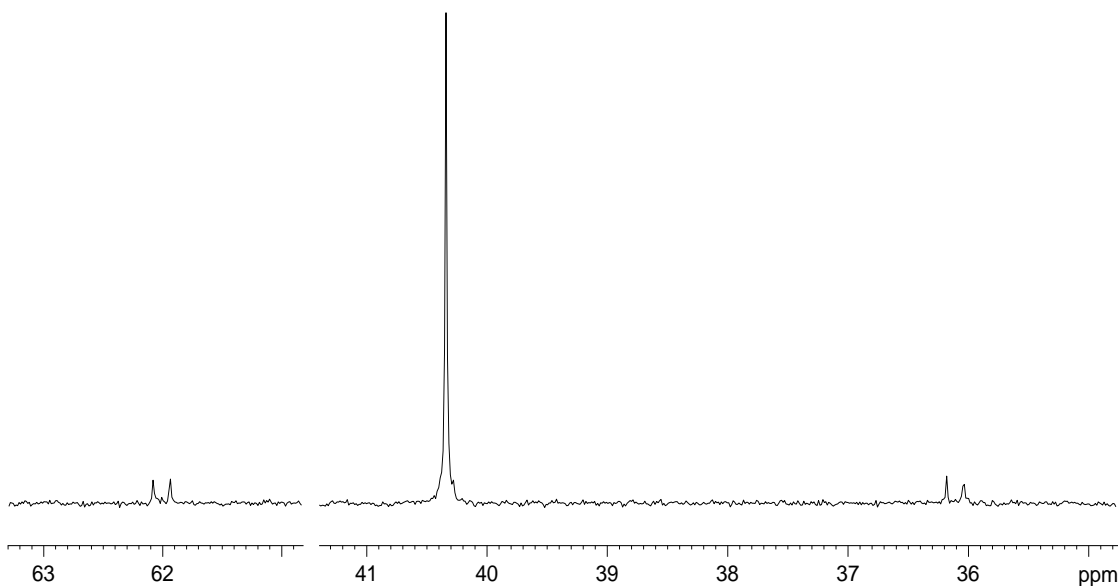


Figure 2.5: $^{31}\text{P}\{^1\text{H}\}$ NMR spectrum of the two isomers of **2.10** (CD_2Cl_2 , 162 MHz, 298 K)

The ^1H NMR spectrum of **2.10a** displayed two singlets at 6.9 and 6.7 ppm for the inequivalent backbone protons. A triplet at 2.2 ppm ($J_{\text{HP}} = 8.5$ Hz) was assigned to the CH_2 of the activated arm of the carbene; it exhibited a correlation to a ^{13}C methylene resonance (based on the PENDANT spectrum) at 12.3 ppm. Two singlets at 0.8 and 0.5 ppm with relative integrals of 9 and 6 respectively arose from the remaining N-Me groups of the ^iBu ligand, and were correlated by ^1H COSY and HSQC NMR spectroscopy. The very low concentration of the cis-isomer **2.10b** limited any detailed spectroscopic characterisation.

Dark red crystals of **2.10a** were isolated from a benzene/hexane solution and proved suitable for X-ray diffraction (Figure 2.6).

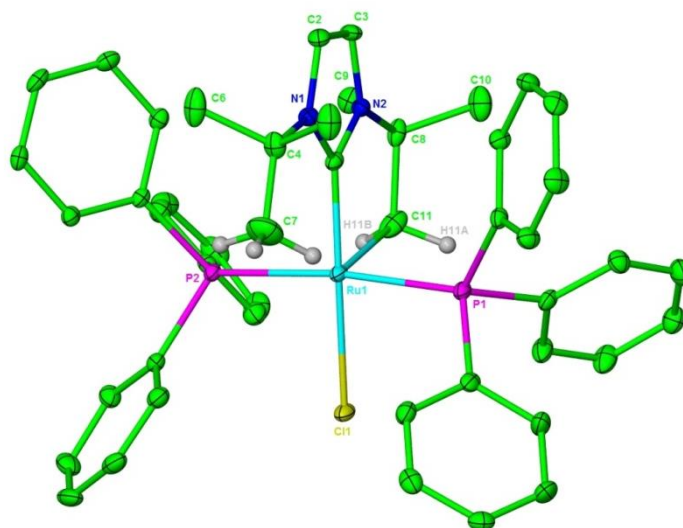
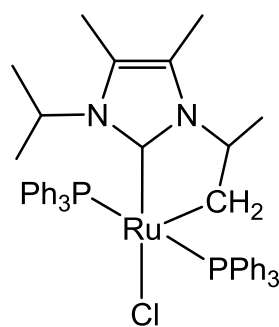


Figure 2.6: Molecular structure of the major trans phosphine isomer of $\text{Ru}(\text{iBu}')(\text{PPh}_3)_2\text{Cl}$ (**2.10a**) (thermal ellipsoids at 30% probability; hydrogen atoms except those on the cyclometallated arm are removed for clarity). Selected bond lengths [Å] and angles [°]: Ru(1)-C(1) 1.964(3), Ru(1)-C(11) 2.187(5), Ru(1)-P(1) 2.3626(9), Ru(1)-P(2) 2.3621(9), Ru(1)-Cl(1) 2.4712(9), C(1)-Ru(1)-C(11) 77.99(15), C(1)-Ru(1)-Cl(1) 176.27(11), P(1)-Ru(1)-P(2) 172.97(3).

The two phosphorus atoms, along with the chloride and carbenic carbon, formed the base of a square pyramid with the Ru 0.002 Å out of the plane and the methylene group of the activated arm in the fifth, apical position.

The X-ray crystal structure of **2.10a** can be compared with that of the previously reported iPr_2Me_2 analogue¹¹ **2.11** (Figure 2.7) since the two complexes adopt essentially identical geometries. The Ru-C_{NHC} bond lengths are the same, although the Ru-P bond lengths in **2.10a** are slightly longer than those in **2.11**, (Table 2.1), probably due to the bulky tertiary butyl groups forcing the phosphorus atoms away from the ruthenium centre. Steric bulk may also account for the bond length between the Ru and the activated arm being significantly longer in **2.10a**.



2.11

Figure 2.7: Ru($1^i\text{Pr}_2\text{Me}_2'$)(PPh₃)₂Cl

	2.10a	Ru($1^i\text{Pr}_2\text{Me}_2'$)(PPh₃)₂Cl 2.11
Ru(1)-C(1)	1.964 (3)	1.9695(17)
Ru(1)-C(11)	2.187 (5)	2.116(2)
Ru(1)-P(1)	2.3626(9)	2.3326(4)
Ru(1)-P(2)	2.3621(9)	2.3290(4)
C(1)-Ru(1)-C(4)	77.99(15)	76.61(8)
P(1)-Ru(1)-P(2)	177.226(15)	177.264(15)

Table 2.1: Comparison of bond lengths [Å] and angles [°] in **2.10a** and **2.11**

Again, studies on the reactivity of **2.10a** focused on the possible reversibility of the C-H activation. The addition of H₂ (1 atm) to a CD₂Cl₂ solution of **2.10a** failed to result in simple reversal of C-H activation, but instead gave a complex mixture of products. The ¹H NMR spectrum did display two triplets at -20.0 and -20.2 ppm indicating that hydride containing products were formed, but we were unable to isolate a single major product out of the reaction.

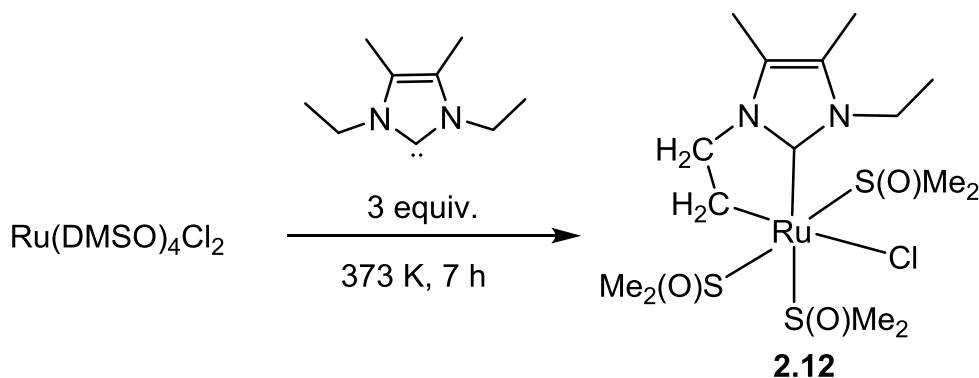
2.4 Reactivity of Ru(DMSO)₄Cl₂ towards NHCs

After the first few reports on transition metal complexes with sulfoxides in the early sixties^{12,13}, the chemistry of this class of compounds has increased both quickly and widely. The interest in these compounds expanded, as they were shown to be useful starting materials to the synthesis

of new organometallic and coordination compounds.¹² Furthermore, they have been studied widely in basic coordination chemistry, for the ambidentate nature of sulfoxides, and their cis and trans effects.¹³ All these studies are related to the strength and nature of the metal-sulfoxide bond. Therefore, an understanding of the parameters affecting the bonding mode of sulfoxides in metal complexes is a fundamental aspect of their coordination chemistry. Previous work and our interest in ruthenium(II) halide complexes guided us to investigate the reactivity of Ru(DMSO)₄Cl₂ towards NHCs.

2.5 Synthesis of Ru(I-Et₂Me₂')(DMSO)₃Cl (**2.12**)

Treatment of Ru(DMSO)₄Cl₂ with three equiv. of I-Et₂Me₂' in toluene gave no reaction at 298 K but, upon heating at 373 K, afforded the C-H activated carbene tris-DMSO complex Ru(I-Et₂Me₂')(DMSO)₃Cl **2.12** (Scheme 2.6) as a light brown powder in 56% yield. Crystals suitable for X-ray crystallography were obtained by slow diffusion of hexane into a concentrated solution of the complex in benzene.



Scheme 2.6: Synthesis of Ru(I-Et₂Me₂')(DMSO)₃Cl

The structure of **2.12** (Figure 2.8) revealed a distorted octahedral geometry with a mer-arrangement of three S-bonded DMSO ligands, two of which are trans to each other, and the third trans to the activated arm of the NHC. The observed S-bound coordination of the DMSO ligands is as expected due to the soft nature of the Ru(II) centre. The Ru–S distances vary between 2.2803(5)–2.3268(5) Å and are in accordance with other Ru(II) S-bound DMSO complexes.¹²⁻¹⁴

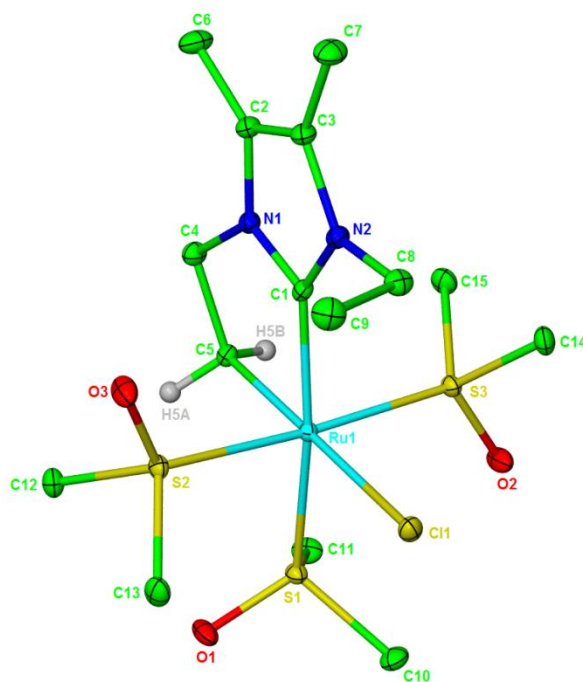


Figure 2.8. Molecular structure of $\text{Ru}(\text{IEt}_2\text{Me}_2')(\text{DMSO})_3\text{Cl}$ (**2.12**) (thermal ellipsoids at 30% probability; hydrogen atoms, except those on the cyclometallated arm, are removed for clarity) Selected bond lengths [\AA] and angles [$^\circ$]: Ru(1)-C(1) 2.062(2), Ru(1)-C(5) 2.130(2), Ru(1)-S(1) 2.3178(5), Ru(1)-S(2) 2.3268(5), Ru(1)-S(3) 2.2803(5), Ru(1)-Cl(1) 2.5398(5), C(1)-Ru(1)-C(2) 92.83(7), C(1)-Ru(1)-C(3) 93.87(8), C(1)-Ru(1)-C(4) 167.06(7), C(3)-Ru(1)-Cl(1) 174.79(6), S(1)-Ru(1)-S(2) 92.304(18), S(2)-Ru(1)-S(3) 174.127(19), S(1)-Ru(1)-C(1) 170.55(6).

The ^1H NMR spectrum of **2.12** (Figure 2.9) showed three methyl singlets in a 1:1:1 ratio between 2.5-3.2 ppm for the DMSO ligands. The protons of the activated arm gave rise to two doublets of doublets, one at 3.6, the other at 1.9 ppm. The ^1H COSY spectrum (Figure 2.10) showed that each proton was coupled to the other and then also to a different proton of the diastereotopic NCH_2 group which showed multiplet resonances at 1.9 and 3.6 ppm.

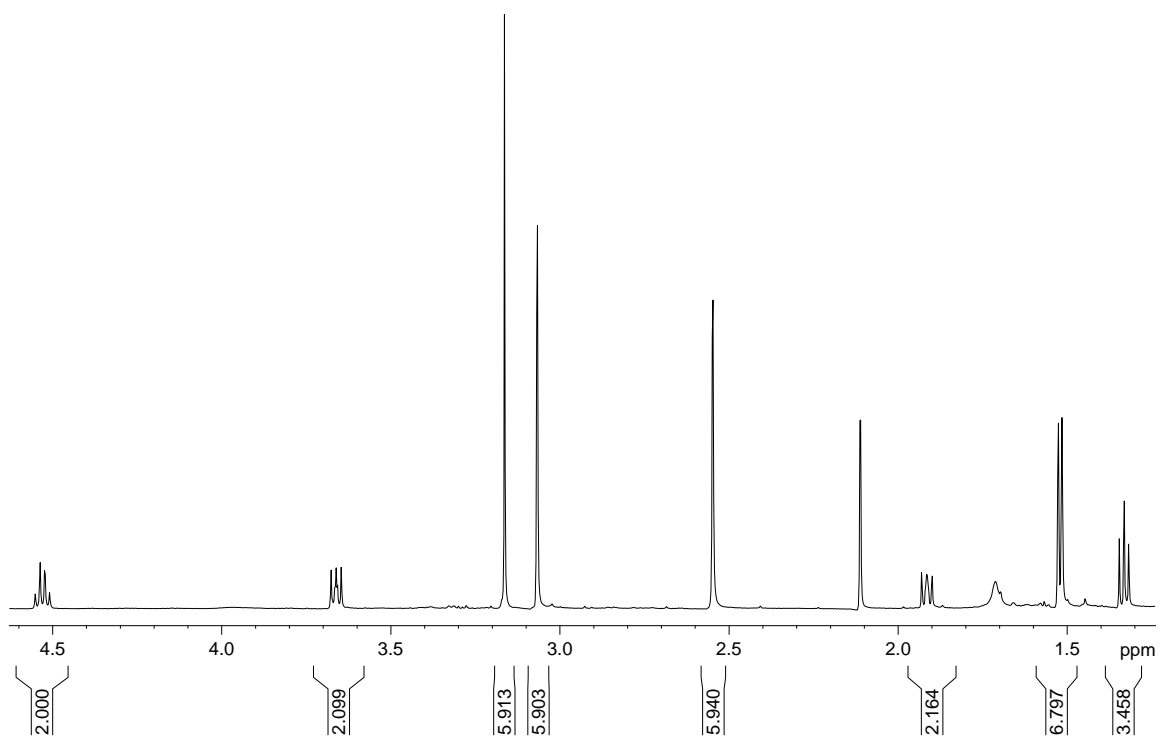


Figure 2.9: ^1H NMR spectrum of **2.12** (C_6D_6 , 500 MHz, 298 K)

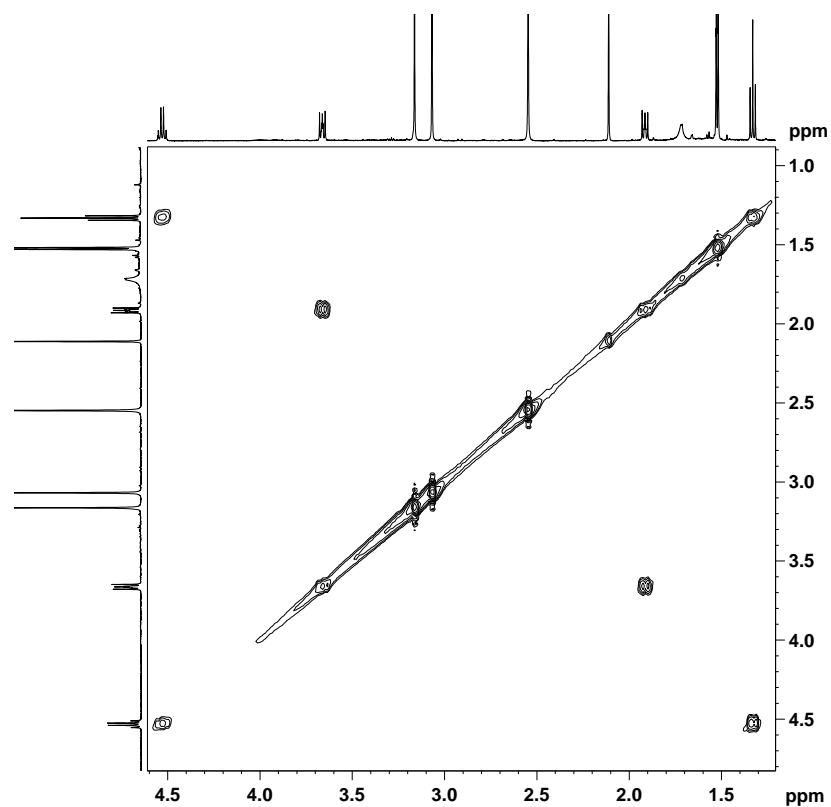
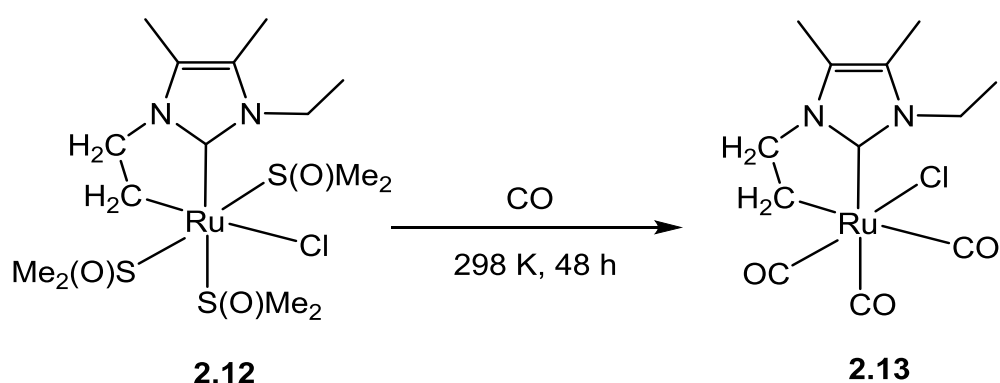


Figure 2.10: ^1H COSY spectrum of **2.12** highlighting the coupling of the N- CH_2 + Ru- CH_2 resonances (C_6D_6 , 500 MHz, 298 K)

2.6. Reactivity of Ru(IEt₂Me₂')(DMSO)₃Cl

Upon heating **2.12** under vacuum at 348 K for 5 h, there was no evidence for any dissociation of the DMSO ligands. Dissolution of the complex in chlorinated solvents (CD₂Cl₂ or CDCl₃) led to immediate colour changes from yellow to green. The resulting ¹H NMR spectra showed loss of all starting material resonances and formation of a characteristically high frequency resonance at 10.8 ppm, assigned to [IEt₂Me₂H]Cl. It is possible that traces of acid contamination in such solvents may result in the complex undergoing protonation and dissociation of the NHC ligand in the form of the imidazolium salt.



Scheme 2.7: Synthesis of Ru(IEt₂Me₂')(CO)₃Cl

A slow substitution reaction was observed upon treatment of **2.12** with CO (1 atm) to form the tricarbonyl complex Ru(IEt₂Me₂')(CO)₃Cl **2.13** (Scheme 2.7). The ¹H NMR spectrum recorded after 72 h at room temperature showed the presence of a signal for free DMSO at 1.7 ppm, along with residual signals of the starting material at 2.6, 3.0 and 3.1 ppm. After replenishing the CO and leaving for an additional 2 days all of the starting material had reacted and the ¹H NMR spectrum now showed the peak at 1.7 ppm, along with a triplet and five multiplets at 1.0, 2.2, 2.5, 3.4, 3.6 and 4.0 ppm respectively. ¹H COSY was used to assign the resonances at 2.2, 2.5, 3.4 and 4.0 ppm to the inequivalent protons of the activated arm (marked as # in Figure 2.11). The methylene protons from the remaining N-Et group were also inequivalent and appeared at 3.6 and 3.4 ppm (marked as *). In a separate experiment, complete substitution of the three DMSO ligands by CO was observed after 48 h at 353 K in benzene to afford **2.13** rather than five

days at 298 K.

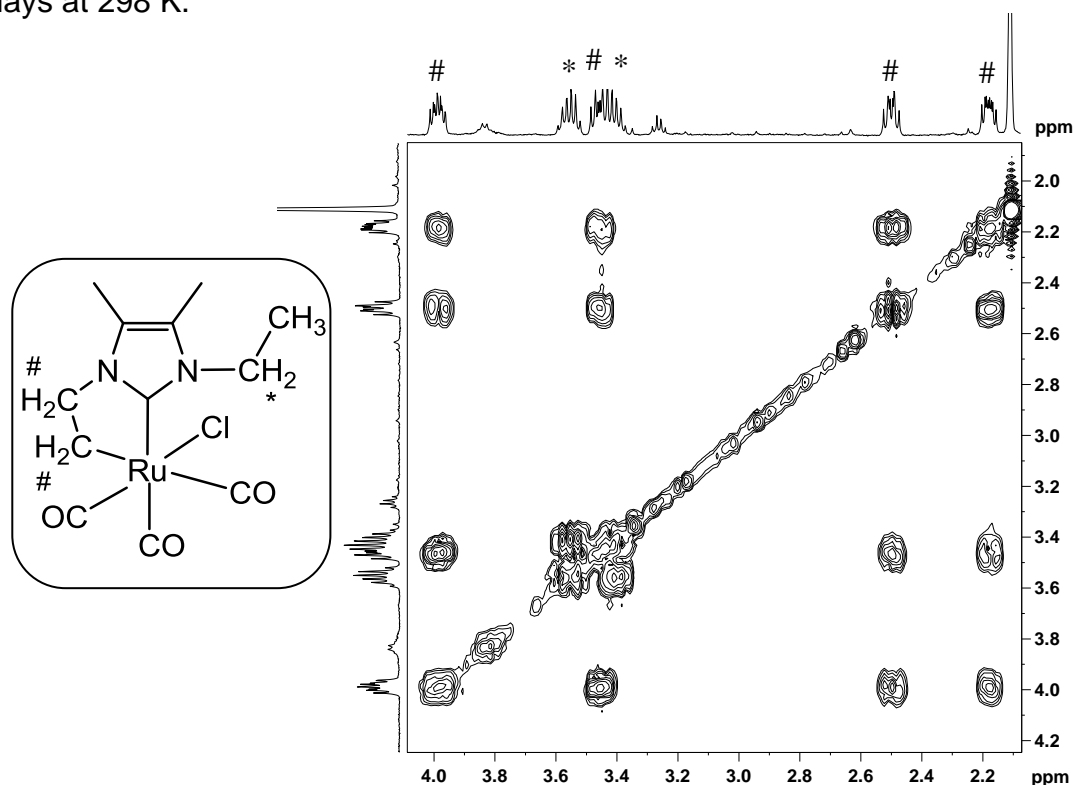


Figure 2.11: ^1H COSY spectrum of **2.13** showing the N-Et regions of the spectrum (C_6D_6 , 500 MHz, 298 K)

The X-ray crystal structure of **2.13** (Figure 2.12) showed a considerably distorted octahedral structure in which the three CO ligands were now arranged in a fac-orientation. The carbonyl ligand *trans* to the π -donor Cl displayed a significantly shorter Ru–CO distance (1.8651(19) Å) than those *trans* to the NHC and metallated arms (1.9486(19) and 1.9898(19) Å, respectively).

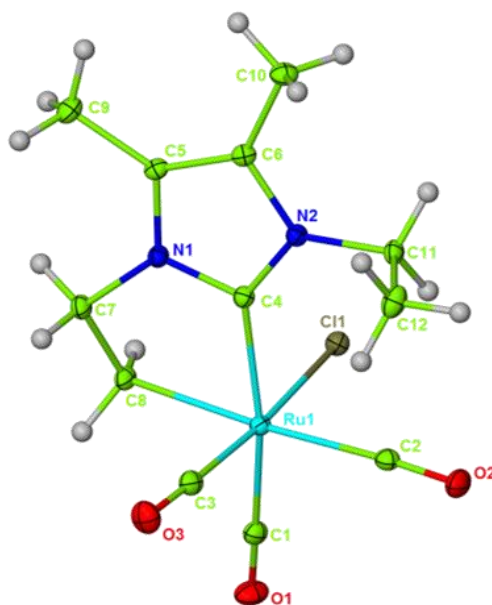


Figure 2.12: Molecular structure of $\text{Ru}(\text{IEt}_2\text{Me}_2')(\text{CO})_3\text{Cl}$ (**2.13**) (thermal ellipsoids at 30% probability; hydrogen atoms except those on the cyclometallated arm, removed for clarity) Selected bond lengths [\AA] and angles [$^\circ$]: Ru(1)-C(1) 1.9486(19), Ru(1)-C(2) 1.9898(19), Ru(1)-C(3) 1.8651(19), Ru(1)-C(4) 2.0924(17), Ru(1)-C(8) 2.1656(17), Ru(1)-Cl(1) 2.4573(4) C(1)-Ru(1)-C(2) 92.83(7), C(1)-Ru(1)-C(3) 93.87(8), C(1)-Ru(1)-C(4) 167.06(7), C(3)-Ru(1)-Cl(1) 174.79(6).

In the $^{13}\text{C}\{^1\text{H}\}$ NMR spectrum, there were four high frequency singlets at 195, 193, 189 and 184 ppm which were subsequently assigned by repeating the reaction with ^{13}CO . The reaction with 1 atm ^{13}CO was set up and after one month,¹⁵ the $^{13}\text{C}\{^1\text{H}\}$ NMR spectrum of **2.13** displayed two doublet of doublets and one triplet, all with coupling constants of ca. 3 Hz consistent with the fac-arrangement in the X-ray structure (Figure 2.13).

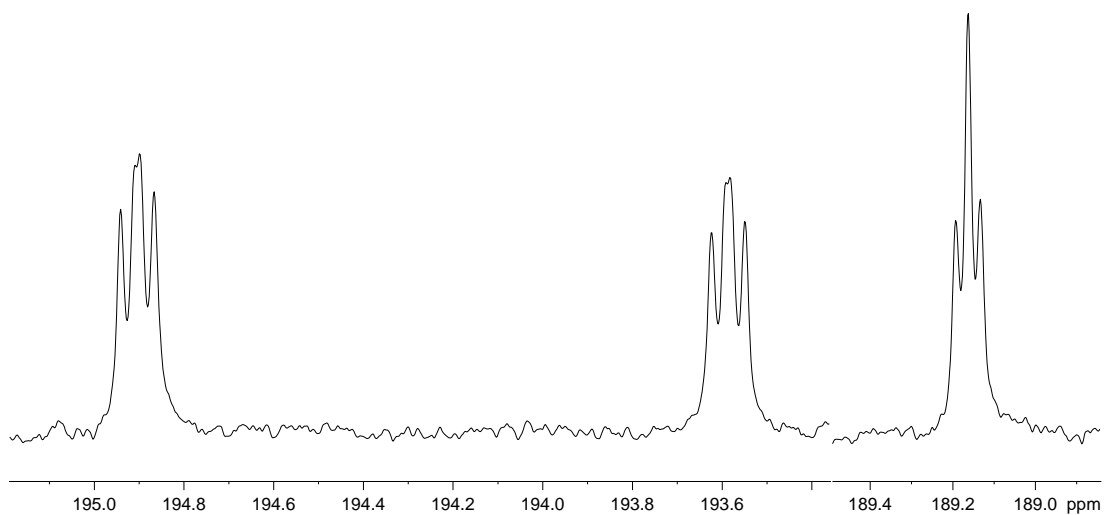


Figure 2.13: High frequency region of the $^{13}\text{C}\{^1\text{H}\}$ NMR spectrum of ^{13}CO labelled **2.13** (C_6D_6 , 125 MHz, 298 K)

The ^{13}C labelling experiment allowed an usual ^{13}C - ^{13}C COSY spectrum to be recorded which showed the anticipated coupling of all three CO ligands to one another (Figure 2.14).

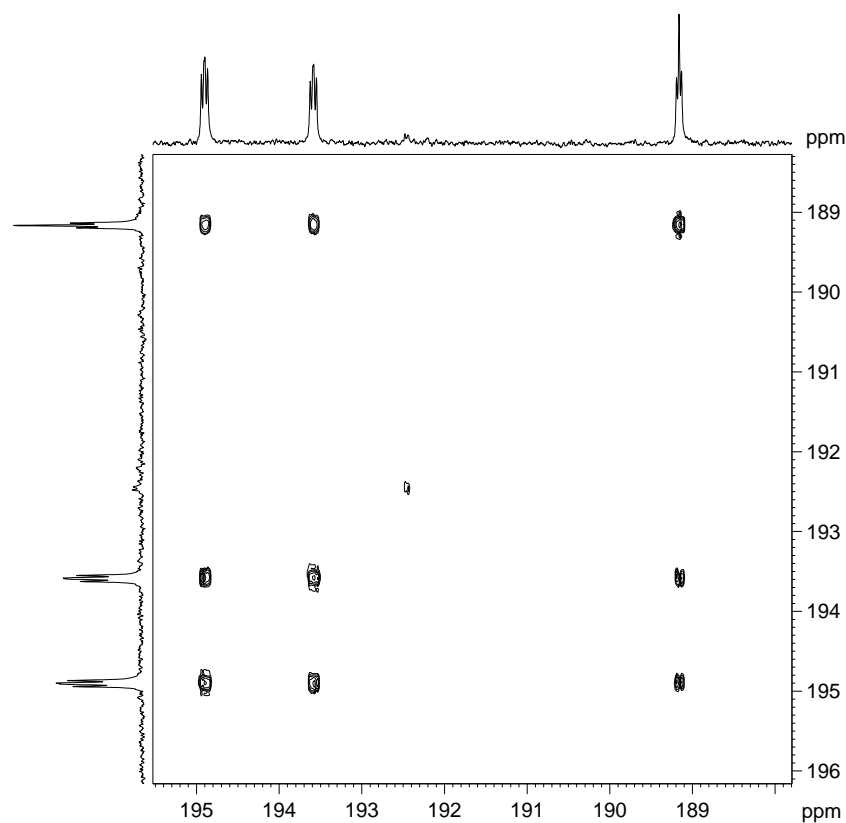


Figure 2.14: ^{13}C - ^{13}C COSY spectrum of ^{13}CO labelled **2.13** (C_6D_6 , 100 MHz, 298 K)

Another useful spectroscopic technique, infrared, was used to assign the carbonyl bands. Table 2.2 shows the carbonyl bands for both the ^{12}CO and ^{13}CO isotopomers.

Complex	ν_{CO} (cm^{-1} , KBr disk)
$\text{Ru}(\text{IEt}_2\text{Me}_2')(^{12}\text{CO})_3\text{Cl}$	2000, 2027, 2085
$\text{Ru}(\text{IEt}_2\text{Me}_2')(^{13}\text{CO})_3\text{Cl}$	1955, 1982, 2038

Table 2.2: IR carbonyl stretching bands of $\text{Ru}(\text{IEt}_2\text{Me}_2')(\text{CO})_3\text{Cl}$ containing either ^{12}CO or ^{13}CO .

As expected the carbonyl bands for the complex containing ^{13}CO are at lower frequency than the bands found in the ^{12}CO labelled sample. The difference in ν_{CO} for the ^{12}CO and ^{13}CO isotopomers can be determined by the reduced masses and is calculated as 46 cm^{-1} . The predicted ^{13}CO peaks of 1954, 1981 and 2039 cm^{-1} are virtually identical to the experimentally measured frequencies.

The reaction with ^{13}CO was repeated again, and the $^{13}\text{C}\{^1\text{H}\}$ NMR spectrum recorded after one week. Interestingly, five peaks were now observed (Figure 2.15), three from **2.13** and two doublet resonances at 197 and 192 ppm with $^2J_{\text{CC}}$ ca. 4 Hz (# in Figure 2.15) assigned to the intermediate dicarbonyl complex **2.14** (Scheme 2.8). This slowly converted to **2.13** over one month at room temperature.

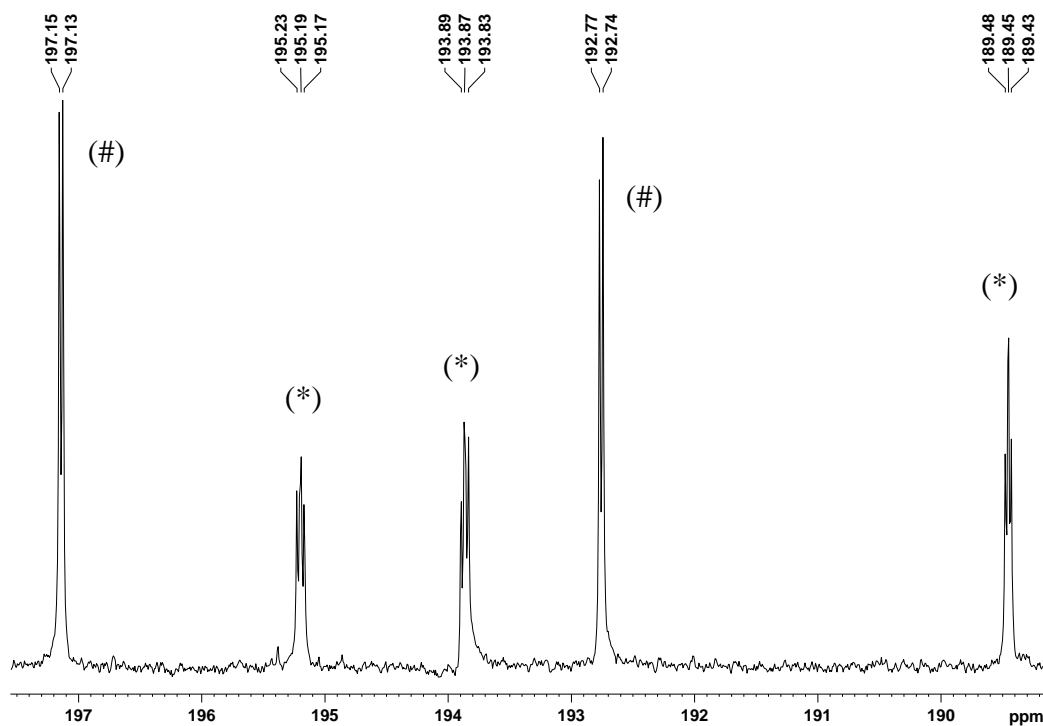
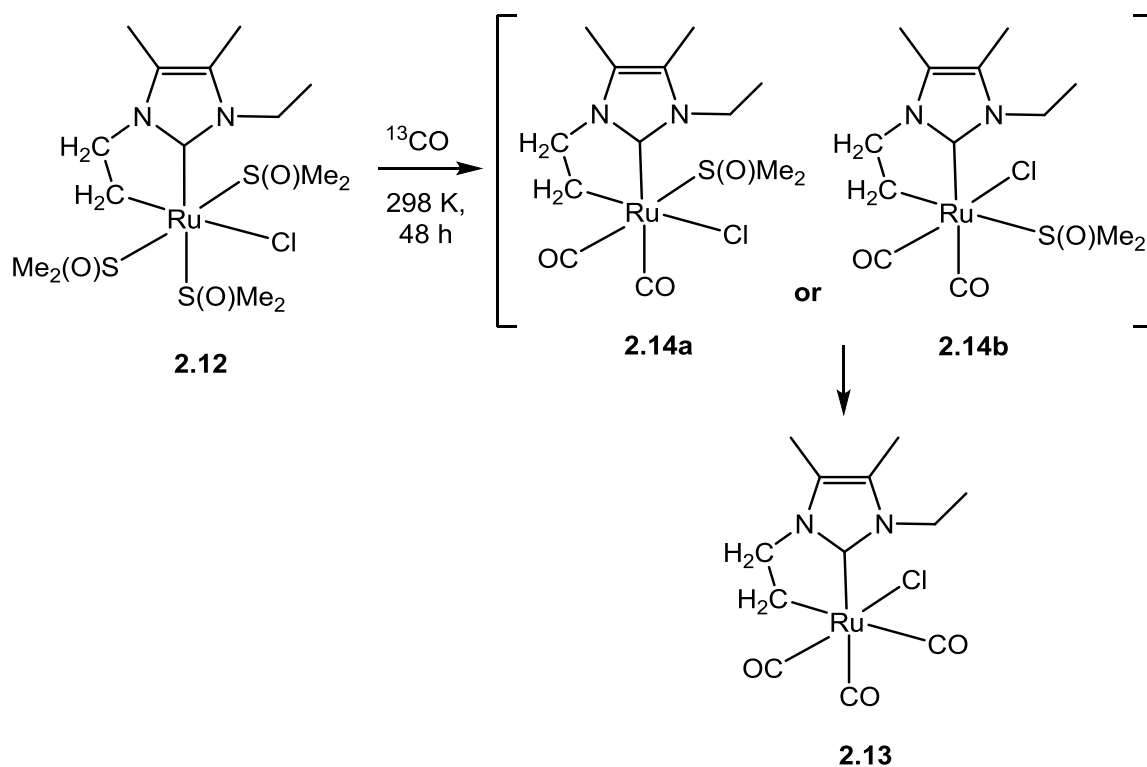


Figure 2.15: High frequency region of the $^{13}\text{C}\{^1\text{H}\}$ NMR spectrum of **2.13** and **2.14** (C_6D_6 , 125 MHz, 298 K)

Due to the fact that the intermediate dicarbonyl complex was only present as part of a mixture with **2.12** and **2.13**, it could not be isolated. Therefore the exact geometry of **2.14** in terms of the relative positions of the DMSO and Cl ligands is not known (possible isomers a and b are shown in Scheme 2.8). The magnitude of $^2J_{\text{CC}}$ implies that the CO ligands are cis, but the arrangement of the DMSO and chloride ligand then remains ambiguous. It is clear that CO substitutes two DMSO ligands to give either **2.14a** or **2.14b**, however the formation of **2.14b** requires isomerisation of **2.12**, but then has the same ligand geometry as the final product. The alternative isomer **2.14a** would need to isomerise en route to **2.13** (Scheme 2.8).

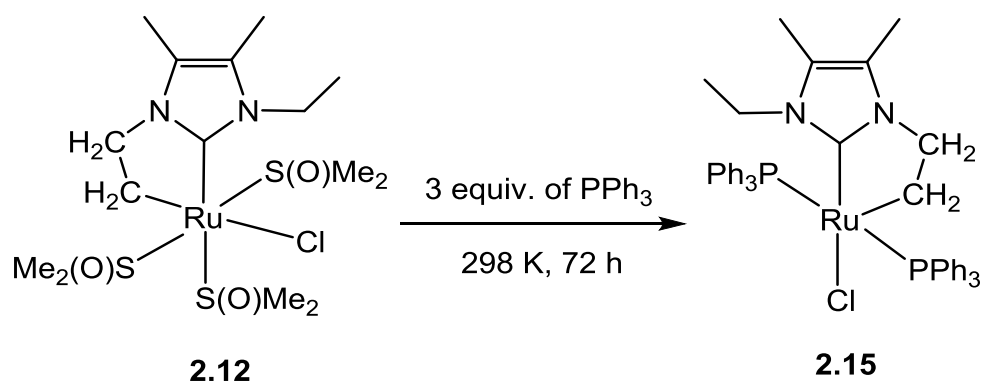


Scheme 2.8: Pathway for reaction of **2.12** with CO

The reaction of **2.12** with CO indicates that the DMSO ligands are substitutionally labile with strongly coordinating ligands. Unsurprisingly, 2 equiv. of IEt_2Me_2 also reacted with **2.12** at 298 K over 7 days to afford the cationic hydride product $[\text{Ru}(\text{IEt}_2\text{Me}_2)_4\text{H}]^+$, along with traces of imidazolium salt. Even though only two equiv. of IEt_2Me_2 were used, there is obviously a strong driving force to make the four carbene containing product. Attempts to react **2.12** with either IMe_4 or $\text{I}^i\text{Pr}_2\text{Me}_2$ gave only mixtures of products.

2.7 Reactivity of **2.12** towards PPh_3 : Synthesis of $\text{Ru}(\text{IEt}_2\text{Me}_2')(\text{PPh}_3)_2\text{Cl}$ (**2.15**)

$\text{Ru}(\text{IEt}_2\text{Me}_2')(\text{DMSO})_3\text{Cl}$ and three equiv. of PPh_3 were dissolved in C_6D_6 affording a dark brown solution. After 72 h, a brown precipitate was observed, which was isolated and dried *in vacuo*. ^1H , $^{31}\text{P}\{^1\text{H}\}$ and $^{13}\text{C}\{^1\text{H}\}$ NMR spectroscopy were used to characterise this product as the C-H activated bis-phosphine complex $\text{Ru}(\text{IEt}_2\text{Me}_2')(\text{PPh}_3)_2\text{Cl}$ **2.15** (Scheme 2.9).



Scheme 2.9: Synthesis of Ru(I(Et₂Me₂')(PPh₃)₂)Cl

The ¹H NMR spectrum in THF-*d*₈ revealed a doublet of doublets and a quintet at 1.4 ppm (*J* = 7.6 Hz) and 2.1 ppm (*J* = 7.6 Hz) respectively, which were assigned to the protons of the N-CH₂ and Ru-CH₂ groups respectively in the activated arm (Figure 2.16).

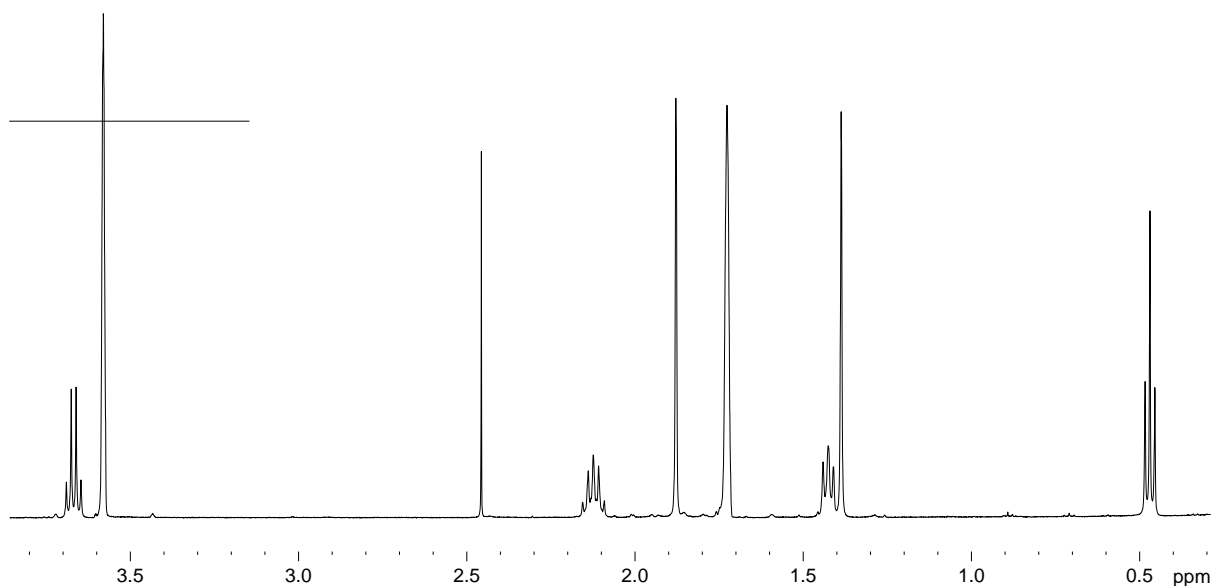


Figure 2.16: Alkyl region of the ¹H NMR spectrum of **2.15** (THF-*d*₈, 500 MHz, 298 K)

The ³¹P{¹H} NMR spectrum revealed a singlet at 40.2 ppm consistent with the trans-PPh₃ geometry. No other peaks were present showing there were no isomers, unlike the case of **2.10a/b** (Scheme 2.5). The ¹³C{¹H} NMR spectrum showed two distinctive triplet resonances at δ 184.7 (²*J*_{CP} = 14.0 Hz) assigned to Ru-C_{NHC} and δ -3.6 (*J*_{CP} = 7.3 Hz) for the Ru-CH₂ group. All the product peaks were correlated by ¹H COSY and HSQC.

The structure was further verified using X-ray crystallography, using crystals obtained by slow diffusion of hexane into a concentrated solution of the complex in THF (Figure 2.17).

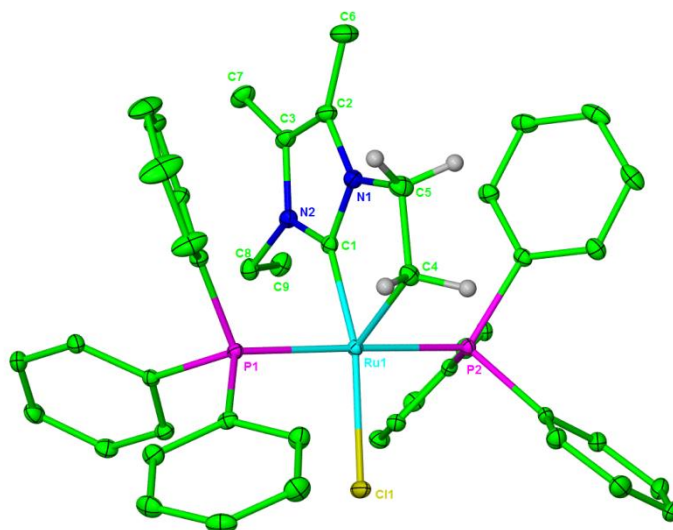


Figure 2.17. Molecular structure of $\text{Ru}(\text{I}(\text{Et}_2\text{Me}_2')(\text{PPh}_3)_2\text{Cl})$ (**2.15**) (thermal ellipsoids at 30% probability; hydrogen atoms except those on the cyclometallated arm, removed for clarity) Selected bond lengths [\AA] and angles [$^\circ$]: Ru(1)-C(1) 1.9639(16), Ru(1)-C(4) 1.21157(17), Ru(1)-C(3) 1.8651(19), Ru(1)-P(1) 2.3365(4), Ru(1)-P(2) 2.3267(4), Ru(1)-Cl(1) 2.4456(4) P(1)-Ru(1)-P(2) 177.226(15), C(1)-Ru(1)-Cl(1) 160.70(5).

A comparison of the bond lengths and angles in **2.15** and the $\text{I}^*\text{Pr}_2\text{Me}_2$ analogue **2.11** reveals essentially no differences (Table 2.3).

	2.15	2.11
Ru(1)-C(1)	1.9639(16)	1.9695(17)
Ru(1)-C(4)	2.1157(17)	2.116(2)
Ru(1)-P(1)	2.3365(4)	2.3326(4)
Ru(1)-P(2)	2.3267(4)	2.3290(4)
C(1)-Ru(1)-C(4)	77.90(7)	76.61(8)
P(1)-Ru(1)-P(2)	177.226(15)	177.264(15)

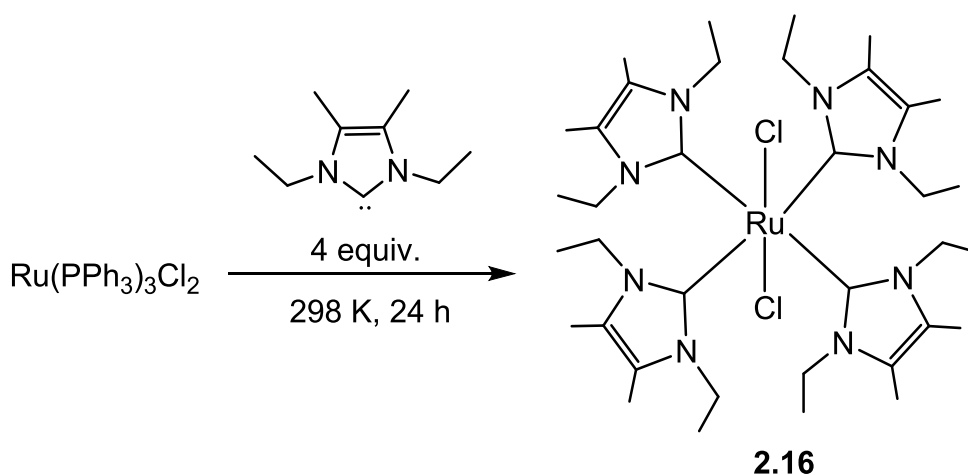
Table 2.3: Selected bond lengths [\AA] and angles [$^\circ$] for **2.15** and **2.11**

As previously reported, **2.11** had been prepared directly from $\text{Ru}(\text{PPh}_3)_3\text{HCl}$ and $\text{I}^t\text{Pr}_2\text{Me}_2$.¹¹ It was also reported that when this route was attempted using IEt_2Me_2 , no clean C-H activation was observed, and instead, a mixture of products was formed.

2.8 Attempts to prepare $\text{Ru}(\text{IEt}_2\text{Me}_2)(\text{PPh}_3)_2\text{Cl}$ using an alternative route

After successfully preparing **2.15** from **2.12** by the addition of excess PPh_3 , we were interested in looking for a 'one-step' route to **2.15**, since the I^tBu analogue **2.10a** could be prepared via reaction of $\text{Ru}(\text{PPh}_3)_3\text{Cl}_2$ and two equiv. of NHC. $\text{Ru}(\text{PPh}_3)_3\text{Cl}_2$ and two equiv. of IEt_2Me_2 were charged to an NMR tube and dissolved in C_6D_6 . After 7 days at room temperature a brown precipitate was observed. The ^1H NMR spectrum of this precipitate (in CD_2Cl_2) displayed peaks due to **2.15**, but also revealed a signal at 10.8 ppm for $[\text{IEt}_2\text{Me}_2\text{H}]^+$. It is reasonable to propose that as only one IEt_2Me_2 goes to the product, the second equivalent of IEt_2Me_2 must remove HCl to afford the activated Ru complex and imidazolium salt. This showed the reaction of **2.12** with PPh_3 is a much cleaner route to form $\text{Ru}(\text{IEt}_2\text{Me}_2)(\text{PPh}_3)_2\text{Cl}$.

Upon reacting $\text{Ru}(\text{PPh}_3)_3\text{Cl}_2$ with four equiv. of IEt_2Me_2 in toluene at 298 K for 24 h, a brown/ red powder was isolated in 52% yield and shown by X-ray crystallography (Figure 2.18) to be the dichloride complex $\text{Ru}(\text{IEt}_2\text{Me}_2)_4\text{Cl}_2$ (**2.16**) shown in Scheme 2.10.



Scheme 2.10: Synthesis of $\text{Ru}(\text{IEt}_2\text{Me}_2)_4\text{Cl}_2$

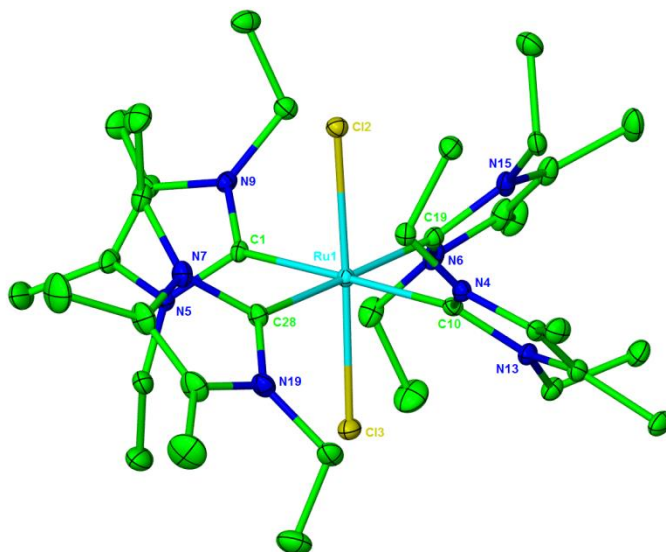


Figure 2.18: Molecular structure of $\text{Ru}(\text{I}(\text{Et}_2\text{Me}_2)_4\text{Cl}_2$ (**2.16**) (thermal ellipsoids at 30% probability; hydrogen atoms arm removed for clarity) Selected bond lengths [\AA] and angles [$^\circ$]: $\text{Ru}(1)\text{-C}(1)$ 2.1234(17), $\text{Ru}(1)\text{-C}(10)$ 2.1164(18), $\text{Ru}(1)\text{-C}(19)$ 2.094(2), $\text{Ru}(1)\text{-C}(28)$ 2.131(2), $\text{Ru}(1)\text{-Cl}(2)$ 2.4514(6) $\text{Ru}(1)\text{-Cl}(3)$ 2.4700(6), $\text{C}(1)\text{-Ru}(1)\text{-C}(10)$ 178.57(15), $\text{C}(1)\text{-Ru}(1)\text{-C}(28)$ 90.66(9).

The X-ray crystal structure (Figure 2.18) revealed a trans arrangement of chloride ligands. The bond lengths and angles are comparable, for the most part to those of the $\text{I}(\text{Me}_4)$ analogue prepared by Wolf and co-workers (Table 2.4).³ The Ru-C distances in both complexes are the same, although the Ru-Cl bond lengths are somewhat shorter in **2.16**. This may reflect the ability of the substituents on the $\text{I}(\text{Et}_2\text{Me}_2)$ ligands to bend away from the metal centre more than in the case of $\text{I}(\text{Me}_4)$ allowing a slightly closer approach of the chlorides.

The ^1H NMR spectrum of the complex displayed two doublet of quartets from the diastereotopic methylene protons of the ethyl arms and triplet from the Me groups. The carbenic carbons appeared at 198.8 ppm in the $^{13}\text{C}\{^1\text{H}\}$ NMR spectrum, almost identical to the chemical shift reported for $\text{Ru}(\text{I}(\text{Me}_4)_4\text{Cl}_2$.³

	2.16	Ru(IME₄)₄Cl₂
Ru(1)-C(10)	2.1164(18)	2.113(3)
Ru(1)-C(1)	2.1234(17)	2.113(3)
Ru(1)-C(28)	2.131(2)	2.113(3)
Ru(1)-C(19)	2.094(2)	2.113(3)
Ru(1) – Cl(2)	2.4514(6)	2.465(2)
Ru(1) – Cl(3)	2.4700(6)	2.516(2)
Cl(2)-Ru(1)-Cl(3)	178.16(2)	180(1)

Table 2.4: Selected bond lengths [Å] and angles [°] in **2.16** and Ru(IME₄)₄Cl₂

2.9 CHAPTER SUMMARY

In an effort to make new $\text{Ru}(\text{NHC})_x$ ($x = 1-4$) complexes, we have combined different Ru dichloride precursors including $[\text{Ru}(\text{cod})\text{Cl}_2]_n$, $\text{Ru}(\text{PPh}_3)_3\text{Cl}_2$ and $\text{Ru}(\text{DMSO})_4\text{Cl}_2$ with a series of N-alkyl substituted carbenes. The addition of $\text{I}^i\text{Pr}_2\text{Me}_2$ to $[\text{Ru}(\text{cod})\text{Cl}_2]_n$ or $\text{Ru}(\text{PPh}_3)_3\text{Cl}_2$ afforded $\text{Ru}(\text{I}^i\text{Pr}_2\text{Me}_2)(\text{I}^i\text{Pr}_2\text{Me}_2)_2\text{Cl}$, which contained a C-H activated carbene as well as one showing an agostic interaction. The reaction of $\text{Ru}(\text{PPh}_3)_3\text{Cl}_2$ with I^tBu generated only the mono C-H activated carbene product $\text{Ru}(\text{I}^t\text{Bu})(\text{PPh}_3)_2\text{Cl}$. Changing the Ru precursor to $\text{Ru}(\text{DMSO})_4\text{Cl}_2$ and reacting with IEt_2Me_2 resulted in C-H activation to give $\text{Ru}(\text{IEt}_2\text{Me}_2)(\text{DMSO})_3\text{Cl}$.

The latter proved to be the most susceptible to reactivity studies. Thus, treatment with CO at room temperature brought about substitution of all three DMSO ligands to afford the tricarbonyl complex $\text{Ru}(\text{IEt}_2\text{Me}_2)(\text{CO})_3\text{Cl}$. The latter was also reacted with PPh_3 to give the bis-phosphine species $\text{Ru}(\text{IEt}_2\text{Me}_2)(\text{PPh}_3)_2\text{Cl}$. Attempts to generate $\text{Ru}(\text{IEt}_2\text{Me}_2)(\text{PPh}_3)_2\text{Cl}$ by an alternative reaction of IEt_2Me_2 with $\text{Ru}(\text{PPh}_3)_3\text{Cl}_2$ proved unsuccessful when two equiv. of carbene were used, although with four equiv. of NHC, the dichloride complex $\text{Ru}(\text{IEt}_2\text{Me}_2)_4\text{Cl}_2$ was produced.

2.10 EXPERIMENTAL

2.10.1 General methods

All manipulations were carried out by using standard Schlenk, high vacuum and glovebox techniques with dried and degassed solvents. Deuterated solvents (Sigma–Aldrich) were vacuum transferred from K (C_6D_6 , THF- d_8) or CaH_2 (CD_2Cl_2). Hydrogen (BOC, 99.9 %), ^{12}CO (BOC, 99.9%) and ^{13}CO (Cambridge Isotope Laboratories) were used as received. NMR spectra were recorded at 298 K (unless otherwise stated) on Bruker Avance 500 and 400 MHz NMR spectrometers and referenced as follows for 1H and $^{13}C\{^1H\}$ spectra: C_6D_6 (1H , $\delta = 7.16$ ppm; ^{13}C , $\delta = 128.0$ ppm), C_4D_8O (1H , $\delta = 3.58$ ppm; ^{13}C , $\delta = 25.4$ ppm), CD_2Cl_2 (1H , $\delta = 5.32$ ppm; ^{13}C , $\delta = 54.0$ ppm). $^{31}P\{^1H\}$ NMR chemical shifts were referenced to 85% H_3PO_4 ($\delta = 0.0$ ppm). IR spectra were recorded on a Nicolet Nexus FTIR spectrometer as KBr disks. Elemental analysis was performed by London Metropolitan University, UK.

Preparation of Carbenes

2.10.2 Synthesis of $I^iPr_2Me_2=S$. 1,2-diisopropyl-2-thiourea (11.33 g, 70.7 mmol), 3-hydroxy-2-butanone (6.23 g, 70.7 mmol) and 1-hexanol (180 mL) were refluxed at 433 K for 12 h. The solvent was removed in *vacuo*. The residue was washed with Et_2O (2 x 20 mL) and H_2O (2 x 30 mL). The precipitate was recrystallised from Et_2O/H_2O (1:1) and filtered to afford a white powder (10.86g, 72% yield). NMR data were in agreement with the literature.¹⁶

2.10.3 Synthesis of $I^iPr_2Me_2$. $I^iPr_2Me_2=S$ (2.10 g, 9.91 mmol), THF (60 mL) and chopped pieces of potassium (1.00 g, 25.6 mmol) were refluxed at 253 K for 4 h under argon. After cooling, the suspension was filtered through celite and the filtrate reduced to dryness, to afford a cream powder (1.58 g, 89% yield). NMR data were in agreement with the literature.¹⁶

2.10.4 Synthesis of $I^Et_2Me_2$. 1,3-diethyl-4,5-dimethylimidazole-2-(3H)-thione (1.80 g, 10.0 mmol), THF (60 mL) and chopped pieces of potassium (1.00 g, 25.6 mmol) were refluxed for 4 h. After cooling, the suspension was filtered through celite and the filtrate reduced to dryness to afford an orange solid (1.08 g, 73% yield). NMR data were in agreement with the literature.¹⁶

2.10.5 Synthesis I^tBu.¹⁷ A suspension of 1,3-di-tert-butylimidazolium chloride (0.85 g, 3.93 mmol) and KN(SiMe₃)₂ (0.85 g, 4.25 mmol) in THF (30 mL) was stirred for 1 h at 298 K. It was then filtered through a celite pad, and the solvent removed under vacuum to afford a white powder (0.50 g, 71% yield). ¹H NMR (C₆D₆, 500 MHz): δ 6.79 (s, 2H, CH), 1.51 (s, 18 H, C(CH₃)₃).

Preparation of Ruthenium precursors

2.10.6 Synthesis of Ru(PPh₃)₃Cl₂.¹⁸ RuCl₃·3H₂O (1.09 g, 4.17 mmol) in dry MeOH (250 mL) was refluxed for 5 min under Ar and then cooled. Triphenylphosphine (6.01 g, 22.9 mmol) was added and the solution refluxed for 3 h. After cooling to room temperature, the mixture was cannula filtered and the filtrate reduced to dryness. After washing the residue with Et₂O (3 x 20 mL), a brown powder was isolated (3.50 g, 88% yield).

2.10.7 Synthesis of Ru(DMSO)₄Cl₂.¹⁹ RuCl₃·3H₂O (1.00 g, 3.83 mmol) in DMSO (5 mL) was refluxed at 433 K for 5 min and then cooled. The solution was reduced to half volume and acetone (20 mL) was added to precipitate a yellow solid. This was filtered and washed with non-dried, non-degassed acetone (2 x 20 mL) and Et₂O (2 x 20 mL) to afford 935 mg (51% yield) of product.

Preparation of Ruthenium complexes

2.10.8 Synthesis of Ru(IⁱPr₂Me₂')(IⁱPr₂Me₂)₂'Cl (2.9). Ru(PPh₃)Cl₂ (50 mg, 0.05 mmol) and IⁱPr₂Me₂ (35 mg, 0.19 mmol) were dissolved in toluene (5 mL) in an ampoule fitted with a J. Youngs PTFE tap and stirred at 298 K for 24 h. The solution was filtered, and the orange product isolated upon addition of hexane (5 mL) (15 mg, 43% yield). Recrystallization from benzene/hexane afforded X-ray quality crystals. Analysis for C₃₃H₅₉N₆ClRu·0.5C₆H₆ (715.38) %: calcd. C 60.44, H 8.73, N 11.75; found C 60.42, H 8.58, N 11.73. ¹H NMR (C₆D₆, 500 MHz): δ = 6.79 [sept, ³J_{HH} = 7.2 Hz, 1 H, NCH(CH₃)₂], 6.19 [sept, ³J_{HH} = 7.2 Hz, 1 H, NCH(CH₃)₂], 5.99 [sept, ³J_{HH} = 7.2 Hz, 1 H, NCH(CH₃)₂], 5.78 [sept, ³J_{HH} = 6.8 Hz, 1 H, NCH(CH₃)₂], 3.96 [sept, ³J_{HH} = 7.2 Hz, 1 H, NCH(CH₃)₂], 3.72 [sept, ³J_{HH} = 7.0 Hz, 1 H, NCH(CH₃)₂], 3.60 (t, J_{HH} = 7.7 Hz, 1 H, RuCH₂), 2.04 (s, 3 H, NCCH₃), 2.02 [m, 3 H, NCH(CH₃)₂], 2.01 [m, 3 H, NCH(CH₃)₂], 2.00 (s, 3 H, NCCH₃), 1.85 (s, 6 H, NCCH₃), 1.72 (m, 1 H,

RuCH₂), 1.66 (s, 3 H, NCCH₃), 1.58 [m, 3 H, NCH(CH₃)₂], 1.57 (s, 3 H, NCCH₃), 1.55 [m, 3 H, NCH(CH₃)₂], 1.52 [d, ³J_{HH} = 7.2 Hz, 3 H, NCH(CH₃)₂], 1.38 [d, ³J_{HH} = 7.2 Hz, 3 H, NCH(CH₃)₂], 0.78 [d, ³J_{HH} = 7.2 Hz, 3 H, NCH(CH₃)₂], 0.67 [d, ³J_{HH} = 7.2 Hz, 3 H, NCH(CH₃)₂], 0.63 [d, ³J_{HH} = 7.2 Hz, 3 H, NCH(CH₃)₂], 0.57 [d, ³J_{HH} = 7.2 Hz, 3 H, NCH(CH₃)₂], 0.08 [d, ³J_{HH} = 7.2 Hz, 3 H, NCH(CH₃)₂] ppm. ¹³C{¹H} NMR (C₆D₆, 125 MHz): δ = 202.6 (s, NCN), 202.2 (s, NCN), 199.6 (s, NCN), 124.3, 121.9, 121.5 (s, NCCH₃), 60.0, 52.1, 51.7, 51.0, 50.4, 49.3, [s, NCH(CH₃)₂], 25.2, 24.4, 23.6, 22.7, 22.3, 22.1, 22.0, 21.0, 21.0, 20.8, 19.6 [s, NCH(CH₃)₂], 15.2 (s, RuCH₂), 11.0, 10.9, 10.8, 10.7, 9.3, 9.2 (s, NCCH₃) ppm.

2.10.9 Synthesis of Ru(^tBu')(PPh₃)₂Cl (2.10a/b). Ru(PPh₃)₃Cl₂ (50 mg, 0.05 mmol) and ^tBu (56 mg, 0.31 mmol) were dissolved in benzene (5 mL) in an ampoule fitted with a J. Youngs PTFE tap and stirred at 298 K for 24 h. The solution was filtered, and the filtrate layered with hexane to form dark red crystals (10 mg, 23% yield). Analysis for C₄₇H₄₉N₂P₂ClRu (840.34) %: calcd. C 67.17, H 5.88, N 3.33; found C 67.03, H 5.70, N 3.46. ¹H NMR (CD₂Cl₂, 500 MHz, 298 K): NMR data for **2.10a**: δ = 7.65–6.85 (br., 30 H, C₆H₅), 6.93 (s, 1H, NCH), 6.71 (s, 1 H, NCH), 2.22 (t, ³J_{HP} = 8.7 Hz, 2 H, CH₂), 0.78 (s, 9 H, CH₃), 0.45 (s, 6 H, CH₃) ppm. Selected* ¹³C{¹H} NMR (CD₂Cl₂, 100 MHz): δ = 186.5 (t, ²J_{CP} = 12 Hz, NCN), 118.1 (s, NCH) 117.7 (s, NCH), 30.6 (s, CH₃), 30.4 (s, CH₃), 12.3 (s, RuCH₂) ppm. *Resonances from the PPh₃ ligands were not assigned. ³¹P{¹H} (CD₂Cl₂, 162 MHz): δ = 40.3 (s) ppm. NMR data for **2.28b**: δ = 62.0 (d, ²J_{PP} = 23.8 Hz), 36.1 (d, ²J_{PP} = 23.8 Hz) ppm.

2.10.10 Synthesis of Ru(IEt₂Me₂')(DMSO)₃Cl (2.12). Ru(DMSO)₄Cl₂ (100 mg, 0.21 mmol) and IEt₂Me₂ (94 mg, 0.67 mmol) were charged to an ampoule fitted with a J. Youngs PTFE tap, dissolved in toluene (5 mL), and then heated at 373 K for 7 h. The reaction mixture was filtered, and the precipitate washed with hexane (3 x 10 mL) and dried under vacuum to obtain a light brown powder (60 mg, 56% yield). Recrystallization from benzene/hexane afforded X-ray quality crystals. Analysis for C₁₅H₃₃N₂O₃ClS₃Ru·0.8C₆H₆ (583.82) %: calcd C 40.73, H 6.52, N 4.79; found C 40.72 H 6.36, N 4.56. ¹H NMR (C₆D₆, 500 MHz): δ = 4.53 (q, ³J_{HH} = 7.1 Hz, 2 H, CH₂), 3.65 (dd, J_{HH} = 9.2, J_{HH} = 5.9 Hz, 2 H, CH₂), 3.19 [s, 6 H,

SO(CH₃)₂], 3.15 [s, 6 H, SO(CH₃)₂], 2.55 [s, 6 H, SO(CH₃)₂], 1.91 (dd, $J_{\text{HH}} = 9.2$, $J_{\text{HH}} = 5.9$ Hz, 2 H, CH₂), 1.53 (s, 3 H, NCCH₃), 1.52 (s, 3 H, NCCH₃), 1.31 (t, $^3J_{\text{HH}} = 7.1$ Hz, 3 H, CH₃) ppm. $^{13}\text{C}\{^1\text{H}\}$ NMR (C₆D₆, 125 MHz): $\delta = 180.7$ (s, NCN), 124.0 (s, CH), 123.5 (s, CH), 50.0 (s, CH₂), 45.2 (s, SOCH₃), 44.9 (s, SOCH₃), 43.6 (s, SOCH₃), 41.7 (s, CH₃), 16.4 (s, CH₃), 9.4 (s, CH₃), 8.4 (s, CH₃), 4.7 (s, CH₂) ppm.

2.10.11 Synthesis of Ru(IEt₂Me₂')₃(CO)₃Cl (2.13).

Ru(IEt₂Me₂')₃(DMSO)₃Cl (10 mg, 0.15 mmol) was charged into an ampoule with a J Youngs resealable tap and dissolved in C₆H₆ (5 mL) and 1 atm of CO added. The mixture was heated at 353 K for 2 h, cooled, freeze-pump-thaw degassed and the CO atmosphere replenished. The sample was heated again at 353 K for 48 h and then reduced to dryness. The residue was redissolved in a minimum amount of benzene (2 mL), whereupon crystals were formed within 2 h (Yield 30 mg, 53%). Analysis for C₁₂H₁₅N₂O₃ClRu (371.79) %: calcd. C 38.77, H 4.07, N 7.53; found C 38.86, H 4.12, N 7.44. ^1H NMR (C₆D₆, 500 MHz): $\delta = 3.99$ (ddd, $J_{\text{HH}} = 11.8$, $J_{\text{HH}} = 8.0$, $J_{\text{HH}} = 5.0$ Hz, 1 H, NCH₂CH₂Ru), 3.55 (dq, $^2J_{\text{HH}} = 14.6$, $^3J_{\text{HH}} = 7.4$ Hz, 1 H, NCH₂CH₃), 3.46 (dt, $J_{\text{HH}} = 11.5$, $J_{\text{HH}} = 7.5$ Hz, 1 H, NCH₂CH₂Ru), 3.43 (m, 2 H, NCH₂CH₂Ru), 2.50 (dt, $J_{\text{HH}} = 10.5$, $J_{\text{HH}} = 7.5$ Hz, 1 H, NCH₂CH₂Ru), 2.18 (ddd, $J_{\text{HH}} = 10.5$, $J_{\text{HH}} = 8.0$, $J_{\text{HH}} = 5.0$ Hz, 1 H, NCH₂CH₂Ru), 1.27 (s, 3 H, NCCH₃), 1.26 (s, 3 H, NCCH₃), 0.99 (t, $^3J_{\text{HH}} = 7.4$ Hz, 3 H, CH₂CH₃) ppm. $^{13}\text{C}\{^1\text{H}\}$ NMR (C₆D₆, 125 MHz): $\delta = 195.5$ (s, CO: ^{13}C labelled sample, dd, $^2J_{\text{CC}} = 4.5$, $^2J_{\text{CC}} = 3.0$ Hz), 194.2 (s, CO: ^{13}C labelled sample, dd, $^2J_{\text{CC}} = 4.5$ Hz, $^2J_{\text{CC}} = 3.0$ Hz), 189.7 (s, CO: ^{13}C labelled sample, t, $^2J_{\text{CC}} = 3.0$ Hz), 174.0 (s, NCN), 124.3 (s, NCCH₃), 124.2 (s, NCCH₃), 51.2 (s, NCH₂), 43.2 (s, NCH₂), 16.5 (s, CH₃), 15.5 (s, RuCH₂), 9.2 (s, CH₃), 8.4 (s, CH₃) ppm. IR: $\nu = 2085$ (s), 2027 (s), 2000 (s) cm⁻¹. [^{13}C labelled sample: $\nu = 2038$ (s), 1982 (s), 1954 (s) cm⁻¹].

2.10.12 Synthesis of Ru(IEt₂Me₂')₃(PPh₃)₂Cl (2.15).

Ru(IEt₂Me₂')₃(DMSO)₃Cl (10 mg, 0.02 mmol) and PPh₃ (15 mg, 0.06 mmol) were charged into an NMR tube with a J Youngs resealable tap and dissolved in C₆D₆. After 24 h a brown solid was observed. The solid was filtered, washed with hexane (1 x 2 mL) and vacuum dried. Yield: 8 mg (51%). Recrystallization from THF/hexane afforded X-ray quality crystals. Analysis for C₄₅H₄₅N₂P₂ClRu: (812.32) %: calcd. C 66.54, H 5.58, N 3.45; found: C

66.41 H 5.46 N 3.40. ^1H NMR (THF- d_8 , 500 MHz): δ = 7.62-7.14 (br., 30 H, PC_6H_5), 3.66 (q, $^3J_{\text{HH}} = 7.3$ Hz, 2 H, CH_2), 2.12 (quint, $^3J_{\text{P,H}} = ^3J_{\text{HH}} = 8.0$ Hz, 2 H, RuCH_2), 1.39 (s, 3 H, CH_3), 0.47 (t, $^3J_{\text{HH}} = 7.0$ Hz, 3 H, CH_3) ppm. $^{13}\text{C}\{^1\text{H}\}$ NMR (THF- d_8 , 125 MHz): δ = 184.8 (t, $^2J_{\text{CP}} = 14$ Hz, NCN), 137.5 (vt, $|^2J_{\text{CP}} + ^4J_{\text{CP}}| = 16$ Hz, PC_6H_5), 135.8 (s, PC_6H_5), 129.4 (s, PC_6H_5), 128.3 (vt, $|^2J_{\text{CP}} + ^4J_{\text{CP}}| = 5$ Hz, PC_6H_5), 124.3 (s, NCCH_3), 123.2 (s, NCCH_3), 48.7 (s, NCH_2), 42.8 (s, NCH_2), 15.2 (s, CH_3), 10.1 (s, CH_3), 9.1 (s, CH_3), -3.4 (t, $J_{\text{CP}} = 7.3$ Hz, RuCH_2) ppm. $^{31}\text{P}\{^1\text{H}\}$ (THF- d_8 , 162 MHz): δ = 39.1 (s) ppm.

2.10.13 Synthesis of $\text{Ru}(\text{IEt}_2\text{Me}_2)_4\text{Cl}_2$ (2.16). $\text{Ru}(\text{PPh}_3)_3\text{Cl}_2$ (200 mg, 0.21 mmol) and IEt_2Me_2 (126 mg, 0.83 mmol) were charged to an ampoule fitted with a J. Youngs PTFE tap, dissolved in toluene (5 mL) and stirred at 298 K for 24 h. Undissolved solids were filtered off and hexane (5 mL) was added to the filtrate which was stirred for 30 min until a precipitate was observed. Small traces of light brown precipitate were filtered off. Filtrate was taken to dryness, red oily precipitate was observed. The precipitate was washed with hexane (10 mL), to afford a brown/ red powder (85 mg, 52% yield). Analysis for $\text{C}_{36}\text{H}_{64}\text{N}_8\text{Cl}_2\text{Ru}$ (780.87) %: calcd. C 55.37, H 8.26, N 14.34; found C 55.29, H 8.14, N 14.25. ^1H NMR (C_6D_6 , 500 MHz): δ = 4.77 (m, $^2J_{\text{HH}} = 13.6$, $^3J_{\text{HH}} = 7.1$ Hz, 8 H, CH_2CH_3), 3.58 (m, $^2J_{\text{HH}} = 13.6$, $^3J_{\text{HH}} = 7.1$ Hz, 8 H, CH_2CH_3), 1.96 (s, 24 H, CCH_3), 1.35 (t, $^3J_{\text{HH}} = 7.1$ Hz, 24 H, CH_2CH_3) ppm. $^{13}\text{C}\{^1\text{H}\}$ NMR (C_6D_6 , 125 MHz): δ = 198.8 (s, NCN), 124.8 (s, CCH_3), 43.5 (s, CH_2CH_3), 18.6 (s, CH_2CH_3), 10.3 (s, CCH_3) ppm.

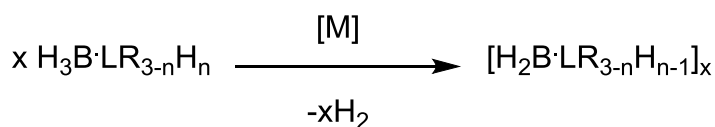
References

- (1) Burling, S.; Häller, L. J. L.; Mas-Marzá, E.; Moreno, A.; Macgregor, S. A.; Mahon, M. F.; Pregosin, P. S.; Whittlesey, M. K., *Chem. Eur. J.* **2009**, *15*, 10912.
- (2) Häller, L. J. L.; Mas-Marzá, E.; Moreno, A.; Lowe, J. P.; Macgregor, S. A.; Mahon, M. F.; Pregosin, P. S.; Whittlesey, M. K. *J. Am. Chem. Soc.*, **2009**, *131*, 9618.
- (3) Wolf, R.; Plois, M.; Hepp, A., *Eur. J. Inorg. Chem.* **2010**, 918.
- (4) Würtemberger, M.; Ott, T.; Doering, C.; Schaub, T.; Radius, U., *Eur. J. Inorg. Chem.* **2011**, 405.
- (5) Burling, S.; Kociok-Köhn, G.; Mahon, M. F.; Whittlesey, M. K.; Williams, J. M. J., *Organometallics* **2005**, *24*, 5868.
- (6) Häller, L. J. L.; Page, M. J.; Macgregor, S. A.; Mahon, M. F.; Whittlesey, M. K., *J. Am. Chem. Soc.* **2009**, *131*, 4604.
- (7) Baratta, W.; Herdtweck, E.; Rigo, P. *Angew. Chem. Int. Ed.* **1999**, *38*, 1629.
- (8) Baratta, W.; Mealli, C.; Herdtweck, E.; Ienco, A.; Mason, S. A.; Rigo, P., *J. Am. Chem. Soc.* **2004**, *126*, 5549.
- (9) Abdur-Rashid, K.; Fedorkiw, T.; Lough, A. J.; Morris, R. H., *Organometallics* **2004**, *23*, 86.
- (10) Scott, N. M.; Dorta, R.; Stevens, E. D.; Correa, A.; Cavallo, L.; Nolan, S. P., *J. Am. Chem. Soc.* **2005**, *127*, 3516.
- (11) Burling, S.; Mas-Marzá, E.; Valpuesta, J. E. V.; Mahon, M. F.; Whittlesey, M. K., *Organometallics* **2009**, *28*, 6676.
- (12) Mercer, A.; Trotter, J., *J. Chem. Soc., Dalton Trans.* **1975**, 2480.
- (13) Calligaris, M.; Carugo, O. *Coord. Chem. Rev.* **1996**, *153*, 83.
- (14) Iengo, E.; Mestroni, G.; Geremia, S.; Calligaris, M.; Alessio, E., *J. Chem. Soc., Dalton Trans.* **1999**, 3361.
- (15) The slow reaction time arises due to the low pressure of ^{13}CO used.
- (16) Kühn, N.; Kratz, T. *Synthesis*, **1993**, 561.
- (17) Arduengo, A. J.; Krafczyk, R.; Schmutzler, R.; Craig, H. A.; Goerlich, J. R.; Marshall, W. J.; Unverzagt, M. *Tetrahedron* **1999**, *55*, 14523.

- (18) Hallman, P. S.; Stephenson, T. A.; Wilkinson, G. *Inorg. Synth.* **1982**, 12, 237.
- (19) Evans, I. P.; Spencer, A.; Wilkinson, G. *J. Chem. Soc., Dalton Trans.* **1973**, 204.

3. INTRODUCTION

The coordination and subsequent activation of B-H bonds has attracted considerable research interest since this process is involved in a number of environmentally important catalytic processes.¹⁻⁴ Ammonia borane in particular has attracted significant interest as a hydrogen source in hydrogenation reactions since it possesses a high H₂ content (19.6 wt %) and can be readily accessed.⁵⁻⁷ As thermal dehydrocoupling requires high kinetic barriers⁸, much research has focused on the release of H₂, via the catalytic dehydrocoupling of amine- and phosphine- boranes as this reaction could be utilized in transfer hydrogen reactions (Scheme 3.1).⁹⁻¹² The products resulting from the dehydrocoupling of amine- and phosphine- boranes are highly attractive for the synthesis of polymeric materials.^{4,13-17}



Scheme 3.1: General scheme for the catalytic dehydrocoupling of amine- and phosphine-boranes, where L = N or P and n = 1-3

3.1 Coordination of Amine- and phosphine- boranes to metal centres

The mechanisms for the catalytic dehydrocoupling of amine- and phosphine-boranes are in most cases not fully understood. To overcome this, research into the coordination and subsequent activation of the substrates has been investigated. The dehydrocoupling of amine- and phosphine-boranes must proceed through a mechanism involving the activation of B-H and N-H bonds. However before this chemistry can take place, the substrate must approach and coordinate to the metal centre to form a σ -complex.¹⁸⁻²¹ Much work has therefore concentrated on isolating examples of such species and then establishing their role in subsequent stoichiometric and catalytic steps.

Complexes formed from the η^1 -coordination of tertiary amine- and phosphine- borane adducts are well known, but they are unable to undergo dehydrogenation. Known as Shimoi complexes²²⁻²⁴, they have been isolated

across a range of metal centres from chromium and tungsten in group 6 to manganese and ruthenium in groups 7-8 (Figure 3.1).²²⁻²⁴

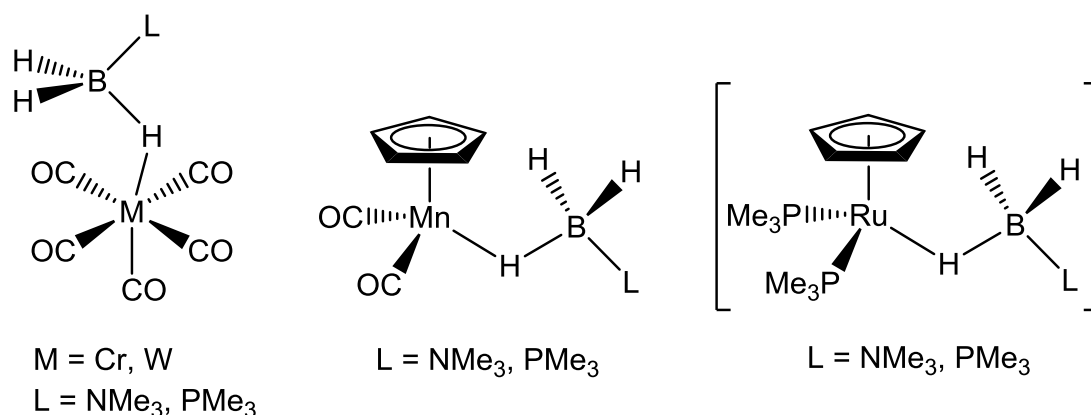
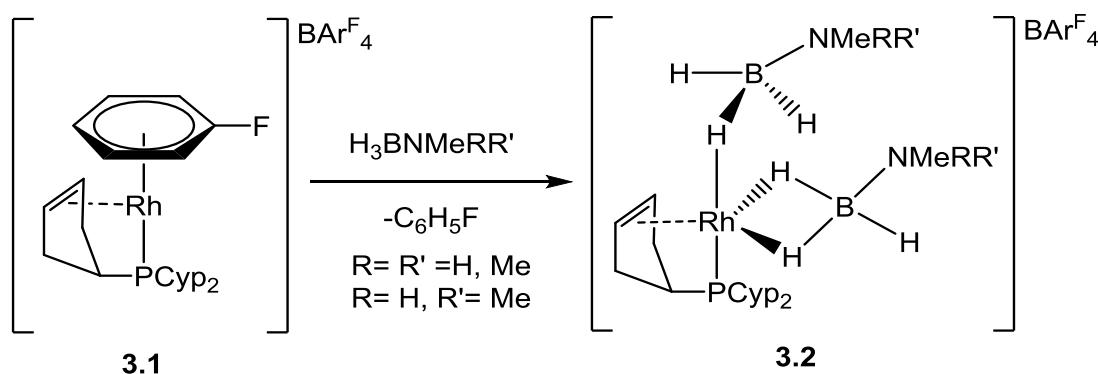


Figure 3.1: A series of isolated Shimoi complexes

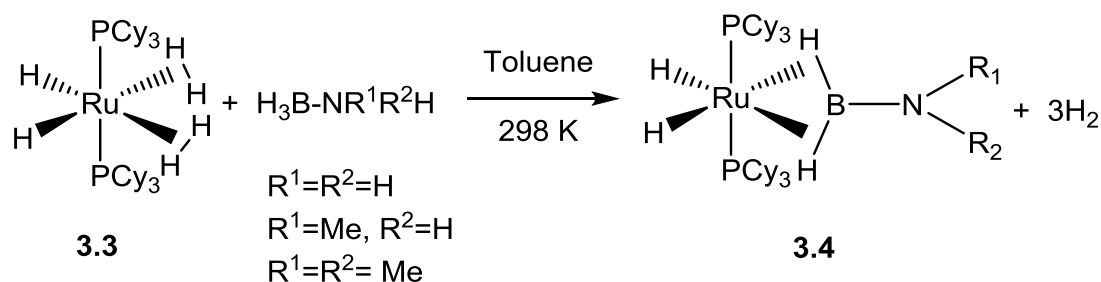
η^2 -coordination of amine- and phosphine- boranes is more unusual, and in contrast to η^1 -coordination, an η^2 -bonding mode can arise if the metal centre is able to donate electron density into a vacant p orbital of boron. This back donation occurs via the 'side-on' orientation of the B-H bond.³

The reaction of the rhodium precursor **3.1** with H₃B.NMeH₂, H₃B.NMe₂H (dimethylamine borane, or DMAB) and H₃B.NMe₃ allowed Weller and co-workers to isolate a series of complexes (**3.2**) exhibiting both η^1 - and η^2 -coordination of the B-H bonds (Scheme 3.2). These complexes represented the first examples of bis(σ -amine-borane) coordination.^{25,26}



Scheme 3.2: η^1 - and η^2 - B-H coordination at a cationic rhodium centre

Following this chemistry, Sabo-Etienne reported the synthesis of the first 'true' bis (σ -B-H) aminoborane ruthenium complexes (Scheme 3.3). The reaction of $\text{Ru}(\text{PCy}_3)_2(\text{H})_2(\eta^2\text{-H}_2)_2$ **3.3** with amine boranes in toluene took place at room temperature. After working up the reactions $[\text{Ru}(\eta^2;\eta^2\text{-H}_2\text{B-NR}'\text{R}_2)(\text{PCy}_3)_2\text{H}_2]$ **3.4** were isolated and structurally characterised.³



Scheme 3.3: Synthesis of ruthenium bis (σ -B-H) amine boranes complexes

The coordination modes of amino boranes have been investigated by a number of groups. Weller and co-workers observed a $[\text{Rh-AB}][\text{BAR}^{\text{F}}_4]$ species which appeared to be the end product of the reaction between DMAB and $[\text{Rh}(\text{P}^i\text{Bu}_3)_2][\text{BAR}^{\text{F}}_4]$, but was only analysed spectroscopically.²⁶ More recently Weller and Sabo-Etienne described isoelectronic ruthenium, rhodium, and iridium bis(σ -B-H) aminoborane complexes (Figure 3.2).²⁷ NHC analogues of the Rh and Ir species were reported by Aldridge and co-workers coordinating $\text{H}_2\text{B-N}^i\text{Pr}_2$ (Figure 3.2).¹⁸

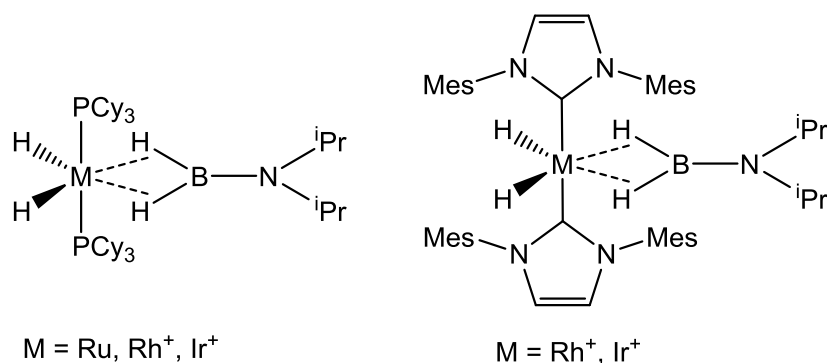
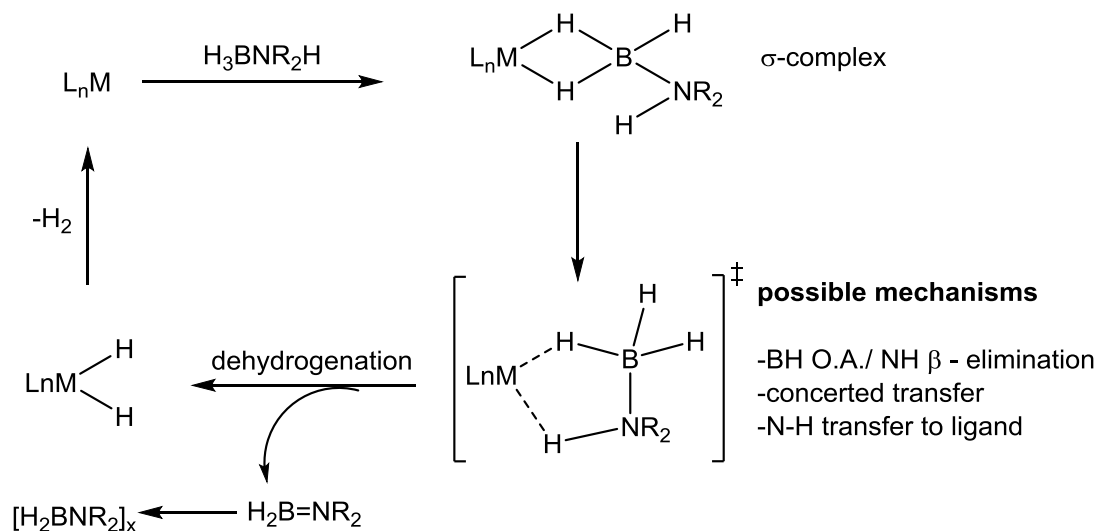


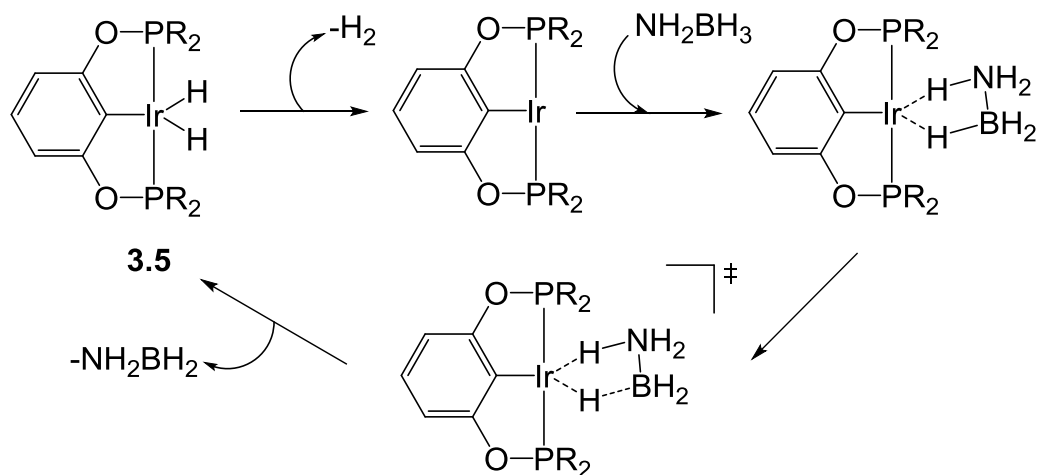
Figure 3.2: A series of Ru, Rh and Ir bis(σ -B-H) aminoborane complexes

Although the formation of amine borane σ -complexes can be accepted as the initial step in a homogeneous reaction pathway, the mechanism by which these coordinated substrates undergo dehydrocoupling is uncertain. A possible mechanism was reported by Weller and co-workers in 2008 (Scheme 3.4).²⁶



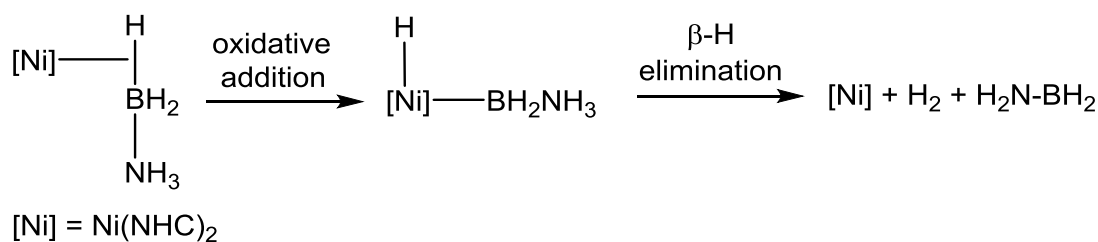
Scheme 3.4: Reaction pathway for the dehydrocoupling of amine borane

Computational studies have shown a number of possibilities regarding the coordination of the amine boranes, which revealed that it is dependent on the metal centre.^{28,29} Previous work on Cp_2Ti derivatives support the stepwise intermolecular transfer of the NH and then the BH proton to the titanium centre.²⁸ However an Ir-pincer complex **3.5** reported by Paul and co-workers, displayed a different route, which is thought to involve a concerted removal pathway as shown in Scheme 3.5.²⁹



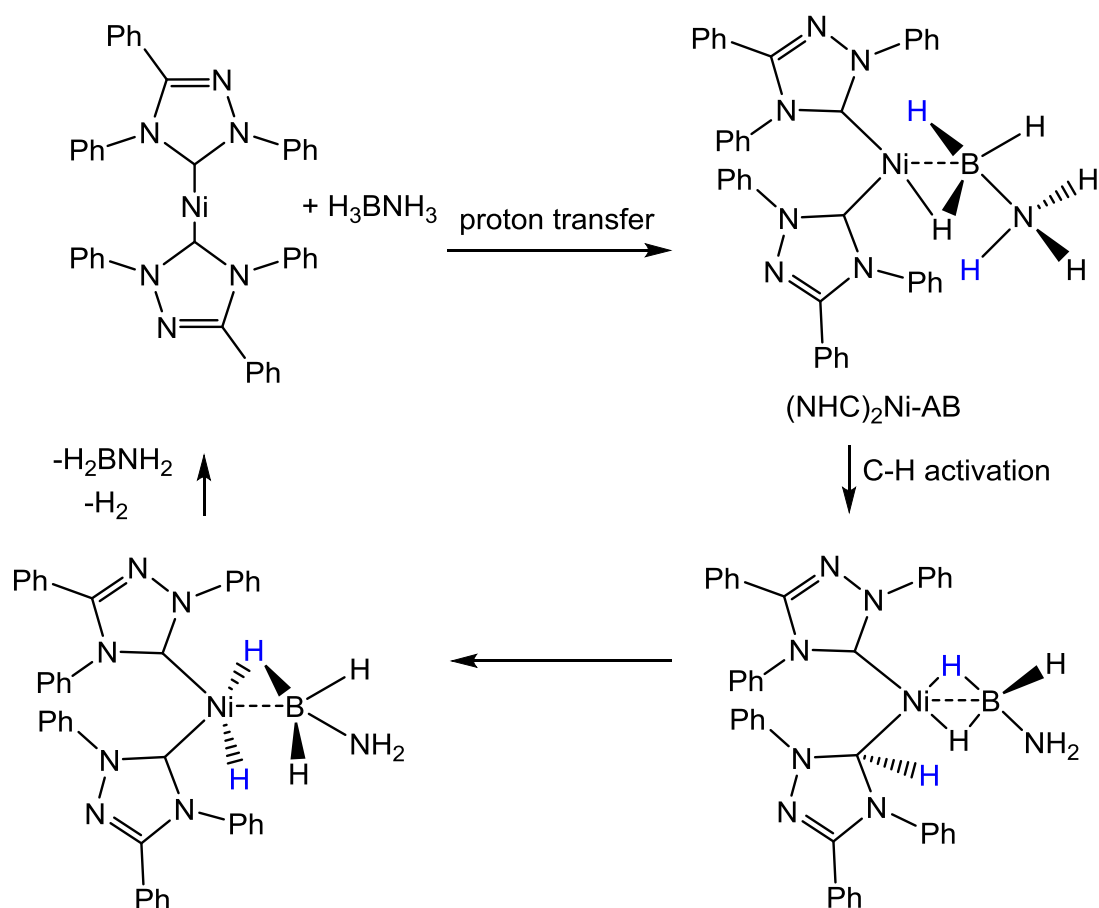
Scheme 3.5: Pathway for AB dehydrogenation employing **3.5**

Baker et al in 2007 reported a highly effective Ni-NHC catalyst for the dehydrocoupling of amine boranes and suggested that this could take place via oxidative addition of the B-H bond with subsequent NH β -elimination (Scheme 3.6).³⁰



Scheme 3.6: Proposed initial steps of nickel-catalysed AB dehydrocoupling

A year later Hall et al carried out DFT calculations on this Ni-NHC system^{30,31} which revealed possible auxiliary ligand involvement with transfer of an NH proton to the carbenic carbon followed by C-H activation and then B-H activation to dehydrocouple the amine borane (Scheme 3.7).³¹

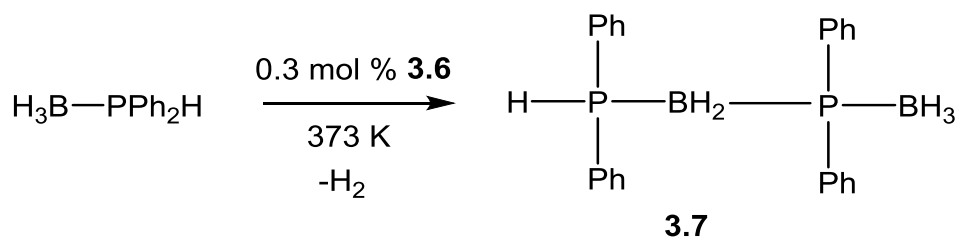


Scheme 3.7: Dehydrocoupling of amine borane with $\text{Ni}(\text{NHC})_2$ via auxiliary ligand involvement

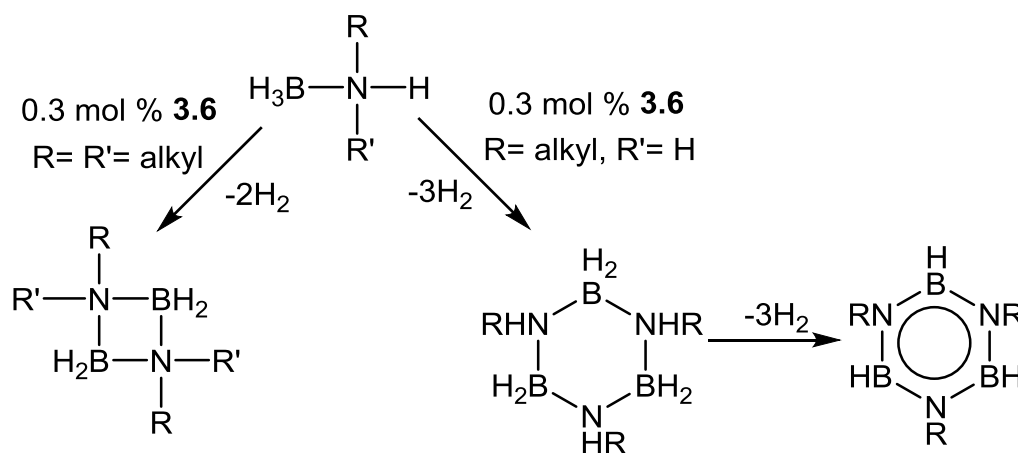
3.2 Dehydrocoupling of amine and phosphine boranes

The thermal dehydrocoupling of amine- and phosphine-boranes has been known since the 1950s.³² A range of products, such as cyclic amino boranes $[\text{R}_2\text{B-NR}'_2]_x$ ($x = 2$ or 3) and borazine $[\text{RB-NR}']_3$ derivatives, as well as phosphinoboranes $[\text{R}_2\text{B-PR}'_2]_3$ were isolated and characterised. However, high temperatures were required in the absence of a catalyst.^{8,32,33} Hence, considerable efforts have been made to develop protocols for the catalytic dehydrocoupling of amine- and phosphine boranes which could allow access to these species under milder conditions. In 1999, Manners³⁴ et al reported the first example of metal-catalysed dehydrocoupling, when $[\text{Rh}(\text{cod})(\mu\text{-Cl})]_2$ **3.6** was used at 0.3 mol % loading to dehydrocouple $\text{H}_3\text{B.PPh}_2\text{H}$, which generated the dimer **3.7** (Scheme 3.8). Soon after, the scope of this catalyst was extended to amine borane systems to give a range of cyclic dimers from

secondary amine-boranes and borazines from primary amine-boranes (Scheme 3.9).^{35,36}



Scheme 3.8: Rh catalysed dehydrocoupling of the phosphine-borane, $\text{H}_3\text{B.PPh}_2\text{H}$



Scheme 3.9: Rh catalysed dehydrocoupling of $\text{H}_3\text{B.NRR}'\text{H}$

Since these first examples of catalytic dehydrocoupling of amine- and phosphine boranes, the research in this field has expanded rapidly. Fagnou and co-workers explained that catalysts effective for the transfer hydrogenation of alcohols could function for the dehydrocoupling of amine boranes. A range of ruthenium catalysts were therefore investigated in the dehydrocoupling of ammonia boranes.³⁷ A series of ruthenium $[\text{Ru}(\text{R}_2\text{PCH}_2\text{CH}_2\text{NH}_2)_2\text{Cl}_2]$ complexes **3.8** ($\text{R} = \text{}^t\text{Bu}, \text{}^i\text{Pr}, \text{Ph}$) (Figure 3.3) based on previous work by Morris and co-workers³⁸ proved to be effective catalysts. These complexes, although requiring activation by KO^tBu , were able to release 1 equiv. H_2 from $\text{H}_3\text{B.NH}_3$ within 5 min at room temperature at ruthenium loadings as low as 0.03 mol %.³⁸

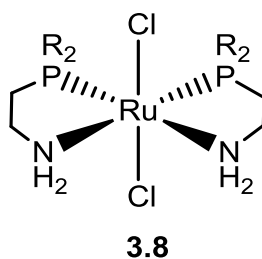
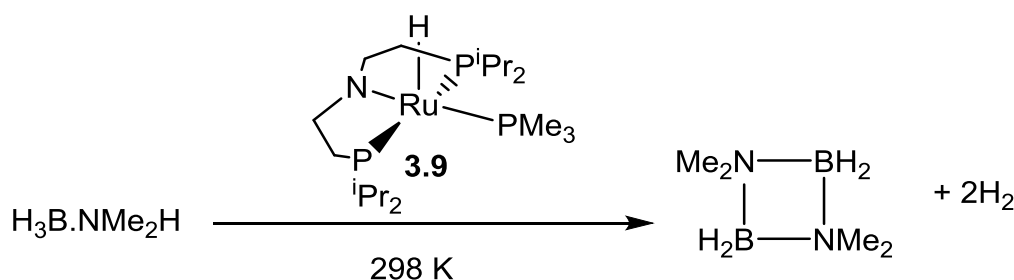


Figure 3.3: $[\text{Ru}(\text{R}_2\text{PCH}_2\text{CH}_2\text{NH}_2)_2\text{Cl}_2]$ ($\text{R} = \text{}^t\text{Bu}, \text{}^i\text{Pr}, \text{Ph}$) catalysts prepared by Fagnou

Schneider and co-workers employed the Ru-PNP complex **3.9** (0.1%) for dehydrocoupling of $\text{H}_3\text{B}\cdot\text{NMe}_2\text{H}$. The complex was able to generate more than one equivalent of H_2 at room temperature (Scheme 3.10), and because of the presence of the Ru-H ligand, no prior activation by base was required.³⁹⁻⁴¹

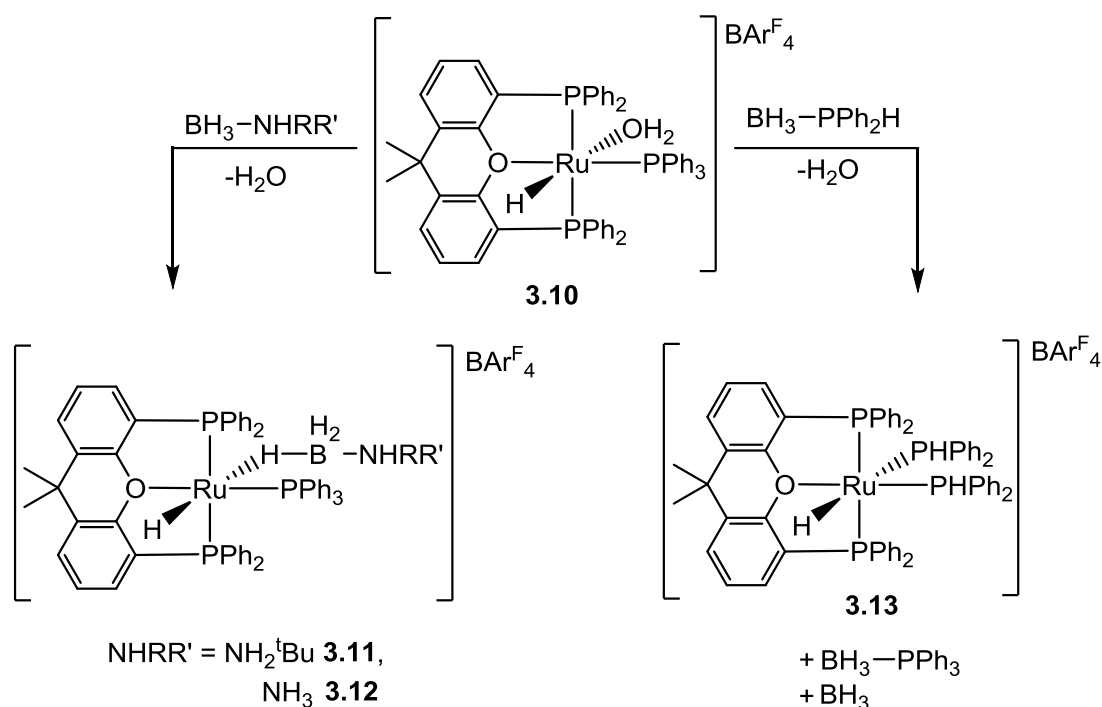


Scheme 3.10: Ru catalysed dehydrocoupling of DMAB

3.3 Coordination and dehydrocoupling of amine and phosphine boranes by Ru(P-P)L derivatives

In 2011, our group reported the reactivity of a series of ruthenium complexes containing the chelating phosphine ligands xantphos and dppf towards amine- and phosphine-boranes.⁴² The coordination of amine-boranes to $[\text{Ru}(\text{xantphos})(\text{PPh}_3)(\text{OH}_2)\text{H}][\text{BAR}^{\text{F}}_4]$ **3.10**, allowed the isolation and structural characterisation of the $\eta^1\text{-B-H}$ Shimoi-type complexes $[\text{Ru}(\text{xantphos})(\text{PPh}_3)(\text{H}_3\text{B}\cdot\text{NH}_2\text{}^t\text{Bu})\text{H}][\text{BAR}^{\text{F}}_4]$ **3.11** and $[\text{Ru}(\text{xantphos})(\text{PPh}_3)(\text{H}_3\text{B}\cdot\text{NH}_3)\text{H}][\text{BAR}^{\text{F}}_4]$ **3.12**. In contrast, the phosphine-borane $\text{H}_3\text{B}\cdot\text{PPh}_2$ underwent P-B bond cleavage to yield the bis-secondary phosphine complex $[\text{Ru}(\text{xantphos})(\text{PPh}_2)_2\text{H}][\text{BPh}_4]$ **3.13** (Scheme 3.11). The cationic and neutral ruthenium dppf complexes $[\text{Ru}(\text{dppf})(\eta^6\text{-C}_6\text{H}_5\text{PPh}_2)\text{H}][\text{BAR}^{\text{F}}_4]$, $[\text{Ru}(\text{dppf})(\text{PPh}_3)\text{HCl}]$ and $[\text{Ru}(\text{ICy})(\text{dppf})\text{HCl}]$ showed no

coordination of amine boranes, but catalysed the room temperature dehydrocoupling of DMAB to $(\text{H}_2\text{B-NMe}_2)_2$, with the highest level of activity shown by the ICy complex.



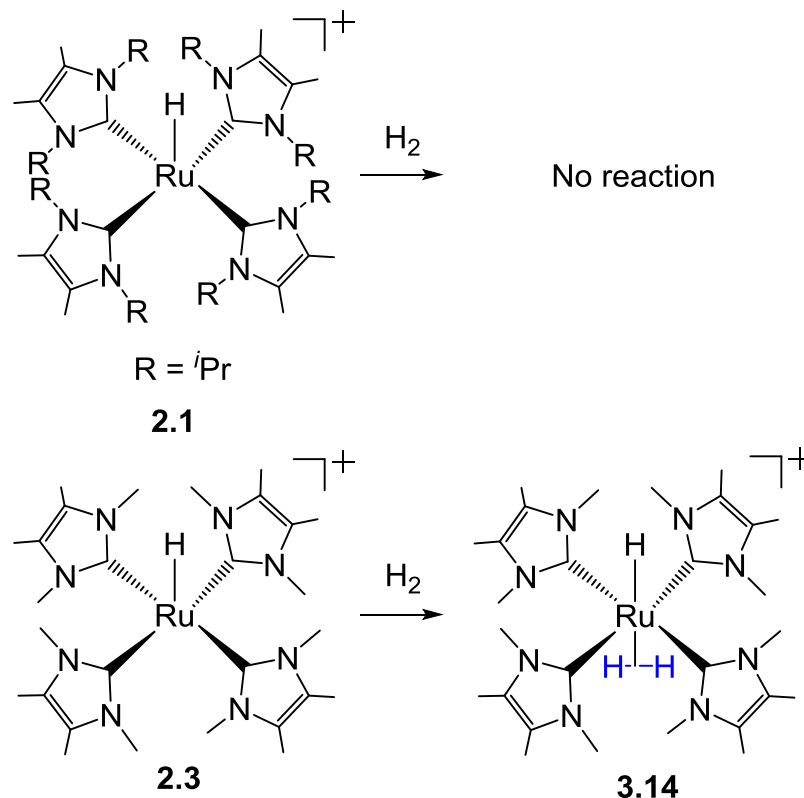
Scheme 3.11: Synthesis of ruthenium amine-borane complexes and a bis-PPh₂ complex

These ruthenium systems are all essentially based on RuL_3 or $[\text{RuL}_4]^+$ skeletons ($\text{L}=\text{P}, \text{O}, \text{C}_{\text{NHC}}$ donor). Hence, as a natural extension of these species, we were interested in establishing whether $[\text{Ru}(\text{NHC})_4\text{H}]^+$ would show simple coordination of amine boranes, or alternatively, catalytic dehydrocoupling reactivity.

3.4 Reactivity of $[\text{Ru}(\text{NHC})_4\text{H}]^+$ with H_2

As mentioned in Chapter 2 (Scheme 2.6) our group reported the synthesis of a series of $[\text{Ru}(\text{NHC})_4\text{H}]^+$ species which reacted readily with small molecules (O_2 , N_2 and H_2) as a function of the size of the NHC substituents.⁴³ Thus, H_2 did not react with $[\text{Ru}(\text{i}^i\text{Pr}_2\text{Me}_2)_4\text{H}]^+$ (NB: anion typically BAr_4^{F}) **2.1** due to the steric inhibition provided by the four bulky $\text{i}^i\text{Pr}_2\text{Me}_2$ ligands, whereas addition of 1 atm of H_2 to THF- d_8 solutions of $[\text{Ru}(\text{IME}_4)_4\text{H}]^+$ **2.3** resulted in a colour change from purple to red and complete

conversion to the dihydrogen hydride complex $[\text{Ru}(\text{IMe}_4)_4(\eta^2\text{-H}_2)\text{H}]^+$ **3.14** at 298 K (Scheme 3.12). In the case of the IEt_2Me_2 analogue $[\text{Ru}(\text{IEt}_2\text{Me}_2)_4\text{H}]^+$ **2.2**, $[\text{Ru}(\text{IEt}_2\text{Me}_2)_4(\eta^2\text{-H}_2)\text{H}]^+$ could only be characterised at low temperature by ^1H NMR spectroscopy due to the lability of the dihydrogen ligand.



Scheme 3.12: Reactivity of $[\text{Ru}(\text{NHC})_4\text{H}]^+$ (anion is BAR_4^{F}) towards H_2

3.5 Reactivity of $[\text{Ru}(\text{NHC})_4\text{H}]^+$ with amine boranes

In light of the inability of **2.1** to bind H_2 , it was unsurprising to find that addition of one equivalent of DMAB to a CD_2Cl_2 solution of the complex resulted in neither coordination nor dehydrocoupling of DMAB. In contrast to the reaction with **2.1**, immediate evolution of H_2 from a 1:1 mixture of **2.3** and DMAB was observed upon dissolution in $\text{THF-}d_8$ with a resultant colour change of the solution from purple to colourless. The NMR tube containing the reaction mixture was left to stand at 298 K for 2 h to let the bubbling subside and ^1H and ^{11}B NMR spectra then recorded. The chemical shifts and relative integrals of product signals in the ^1H NMR spectrum agree with those of **3.14**, although whereas the Ru-H signal is sharp and the $\eta^2\text{-H}_2$ resonance is broad in the spectrum of **3.14**, formation via reaction with DMAB swaps the appearance of the signals around (Figure 3.4).

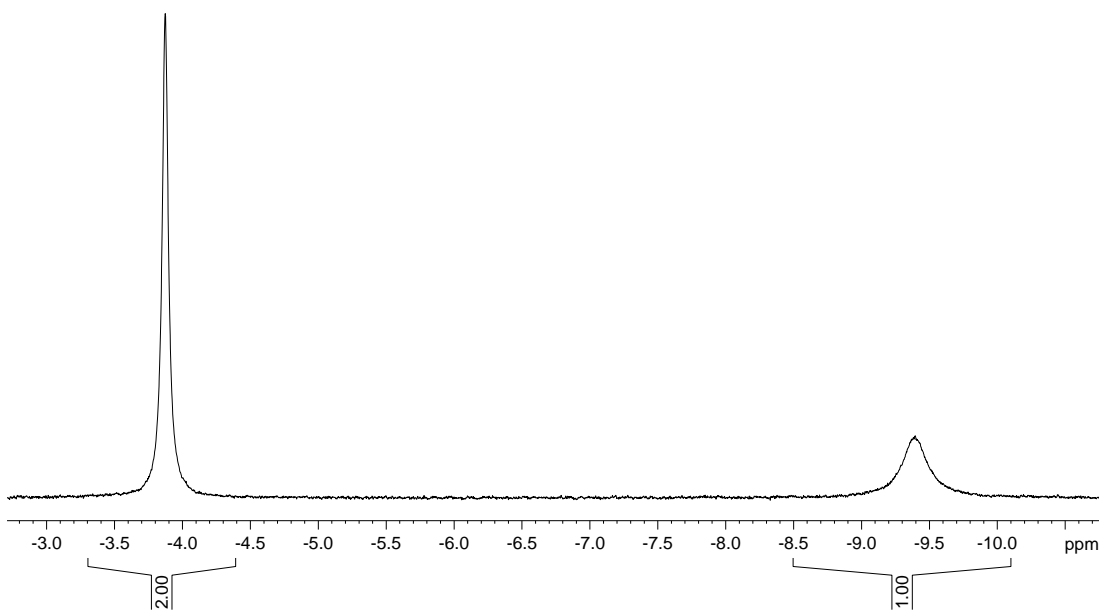


Figure 3.4: Hydride region of the ^1H NMR spectrum of a solution of **2.3** and DMAB ($\text{THF-}d_8$, 298 K, 500 MHz)

^{11}B NMR spectroscopy (Figure 3.5) confirmed full conversion of DMAB to the dehydrocoupled products $(\text{Me}_2\text{NBH}_2)_2$ at 5.3 ppm (A) and what is believed to be $(\text{Me}_2\text{N})_2\text{BH}$ at 28.8 ppm (B) (Scheme 3.13).³⁹

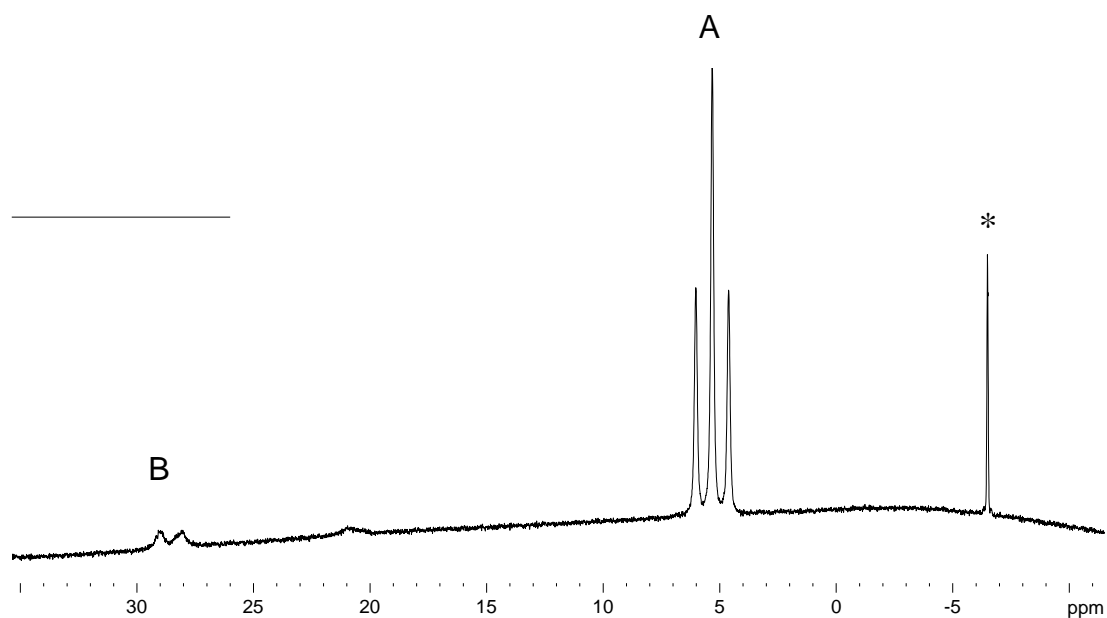
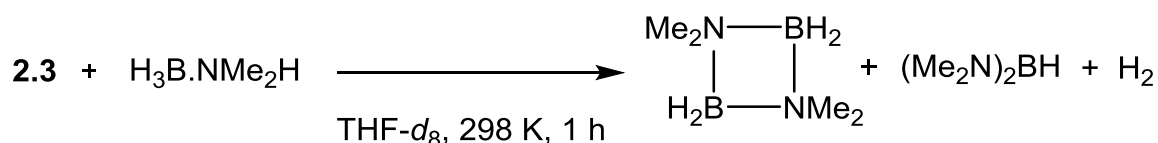


Figure 3.5: ^{11}B NMR spectrum showing the products from the stoichiometric reaction of **2.3** and DMAB ($\text{THF-}d_8$, 298 K, 160 MHz) *denotes BAr^{F}_4



Scheme 3.13: Dehydrocoupling of DMAB using **2.3**

It is not clear as to why the appearance of the hydride and dihydrogen signals of **3.14** change depending upon generation from H₂ or DMAB. To provide further evidence for [Ru(NHC)₄H]⁺ species reacting with amine boranes via dehydrogenation and H₂ coordination, the IEt₂Me₂ analogue **2.2** was treated with DMAB. Although the room temperature ¹H NMR spectrum showed no signals for H₂ coordination, cooling to 232 K revealed a broad signal at -3.9 ppm and a sharper signal at -8.6 ppm in a 2:1 ratio. These chemical shifts, appearance and temperature at which the signals are seen match the repeated observations for H₂ addition to **2.2**.

There is clearly a difference in reactivity between **2.3** and the Ru-xantphos and dppf complexes (**3.11-3.13**), as the former now dehydrogenate and bind the resulting H₂ rather than either coordinate DMAB or catalyse dehydrogenative loss of H₂. The ability of the [Ru(NHC)₄H]⁺ species to remove H₂ and retain it suggested that transfer of the H₂ to an organic substrate might be possible.⁴⁴⁻⁴⁶

3.6 Catalytic dehydrogenation and transfer hydrogenation with amine boranes

Initial experiments revealed that [Ru(IMe₄)₄H]⁺ (**2.3**) was unable to bring about the direct hydrogenation of organic substrates with H₂. Thus, addition of acetophenone to a THF-*d*₈ solution of **2.3** (10 mol %) under 1 atm H₂ resulted in no conversion to the corresponding alcohol even upon heating to 353 K for 2 h.

However, when DMAB was used as the hydrogen source rather than H₂, 77% conversion to 1-phenylethanol was measured by ¹H NMR spectroscopy after 1 h. The ¹¹B NMR spectrum (Figure 3.6) showed total disappearance of the DMAB resonance at -15.5 ppm and appearance of [Me₂N-BH₂]₂ at 5.3 ppm. The identity of a second product signal at 28.8 ppm

was initially believed to be due to $(\text{Me}_2\text{N})_2\text{BH}$ as noted on p.11, however, closer analysis of the ^1H NMR spectrum showed doublet and quartet resonances for the alcohol product but no OH proton. At present, we believe that this could indicate formation of a species such as that shown in Scheme 3.14 in which the alcohol is coordinated to B.

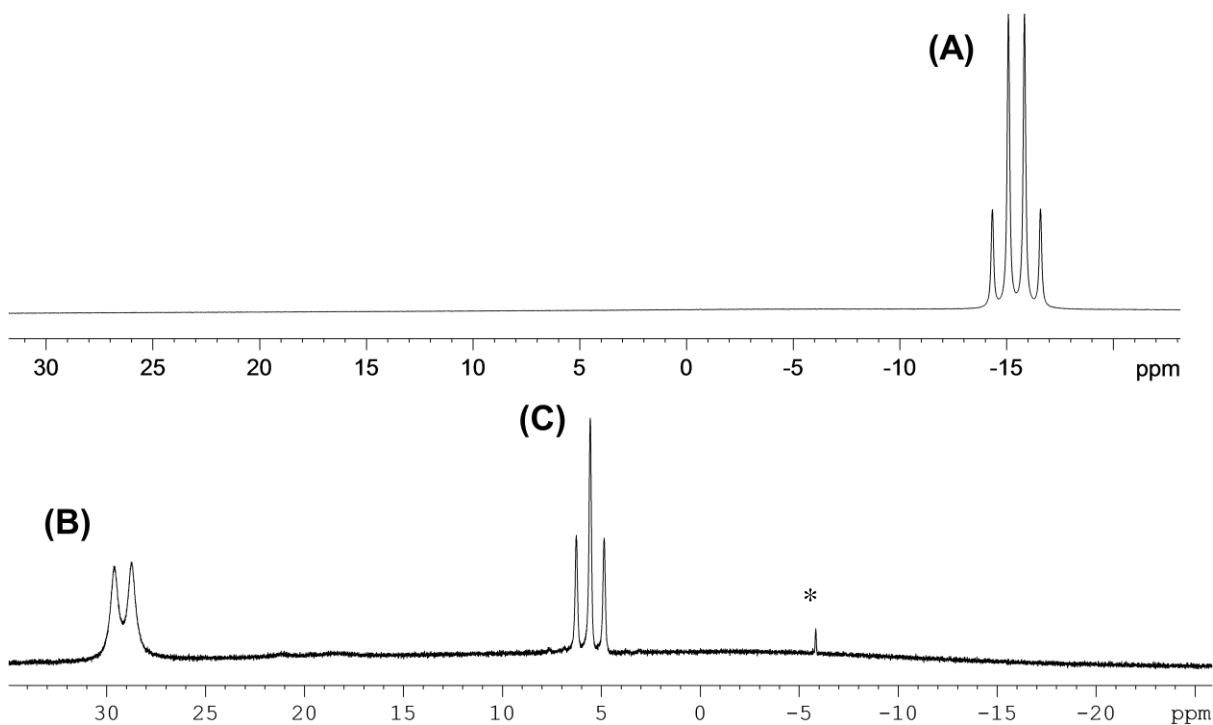
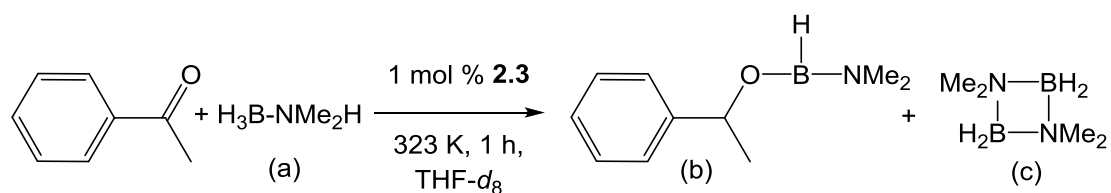
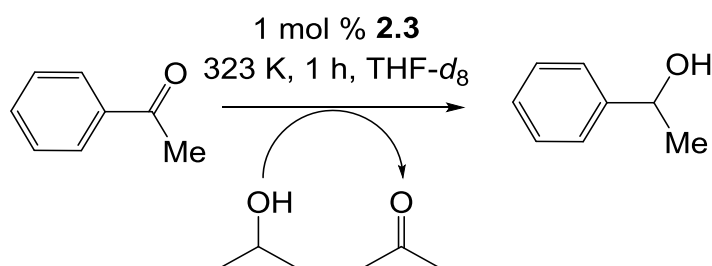


Figure 3.6: ^{11}B NMR spectrum illustrating dehydrocoupling of DMAB by **2.3** (THF- d_8 at 298 K, 160 MHz) * denotes BAr^{F}_4



Scheme 3.14: Transfer hydrogenation of acetophenone utilizing DMAB as H_2 source

Interestingly, when ⁱPrOH was used as the hydrogen source instead of DMAB for the [Ru(IMe₄)₄H]⁺ catalysed reduction of acetophenone, only 35% conversion to alcohol was achieved in 2 h at 343 K. Further heating for an additional 48 h resulted in only a slight increase to 41% most likely due to degradation of the Ru catalyst, as evidenced by change of colour of the solution from purple to green (Scheme 3.15).



Scheme 3.15: Transfer hydrogenation of acetophenone utilizing ⁱPrOH as H₂ source

3.7 Optimisation of Ru catalysed transfer hydrogenation of ketones by amine boranes

There are many examples of commonly used amine boranes, five of which were investigated to identify the most suitable one to carry out the catalysis (Table 3.1).

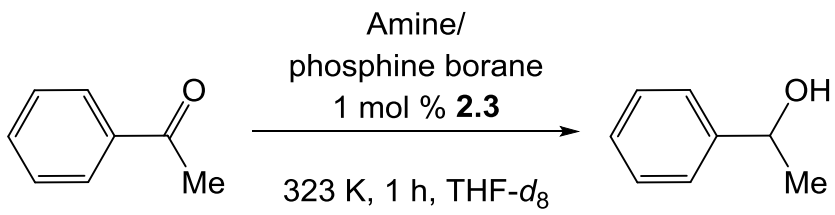
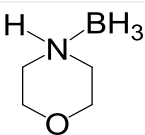
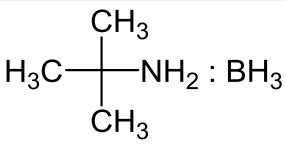
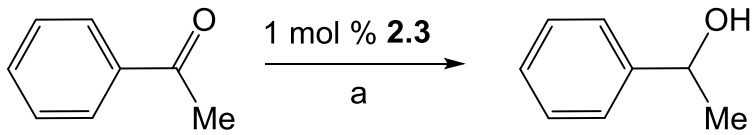
		
Amine/Phosphine borane	Time (h)	Conversion (%) of acetophenone
$\text{H}_3\text{B.NH}_3$	1	80
	1	70
	1	<1
$\text{H}_3\text{B.NMe}_2\text{H}$	1	77
$\text{Ph}_2\text{PH:BH}_3$	1	<1
Reaction conditions: acetophenone (136 mmol), catalyst (1.36 mmol), amine/phosphine borane (136 mmol), THF- d_8 (1 mL).		

Table 3.1: Amine- and phosphine borane screening for their use in catalytic transfer hydrogenation

Table 3.1 summarises the results on the use of alternative amine boranes to DMAB. Both $\text{H}_3\text{B.NH}_3$ and morpholine borane brought about comparable conversions whereas the bulkier $^t\text{BuNH}_2\text{BH}_3$ was essentially unreactive. The same applied to the secondary phosphine borane Ph_2PHBH_3 . Although $\text{H}_3\text{B.NH}_3$ displayed better conversion of acetophenone by ^1H NMR spectroscopy, DMAB was selected for the catalytic transfer hydrogenation because it displayed more informative ^1H and ^{11}B NMR spectra.

3.8 Optimised temperature for catalytic transfer hydrogenation of acetophenone to 1-phenyl ethanol

At 298 K, the transfer hydrogenation reaction was quite slow and only 15% conversion of acetophenone was observed after 1 h with 1 mol % **2.3** and DMAB. Increasing the temperature to 343 K gave 85% conversion along with complete consumption of DMAB. When the reaction was repeated at 343 K but in the absence of any **2.3**, 60% conversion of ketone was observed. This revealed that a background reaction occurred at 343 K and in order to overcome this, the reaction temperature was lowered to 323 K. At this temperature, there was no reaction observed over 1 h in the absence of the Ru complex and therefore all subsequent catalytic runs were carried out at the optimised temperature of 323 K (Table 3.2).

		
Temperature (K)	Time (h)	Conversion (%) of acetophenone
298	1	15
343	1	85
343 ^b	1	60
323	1	77
323 ^b	1	0
	12	52

^aacetophenone (136 mmol), **2.3** (1.36 mmol), DMAB (136 mmol), THF-*d*₈ (1 mL), 323 K, 1 h. ^breaction performed in the absence of **2.3**

Table 3.2: Influence of temperature on Ru catalysed transfer hydrogenation of acetophenone

3.9 Influence of NHC and solvent on transfer hydrogenation

As shown in Table 3.3, **2.3** proved to be the most active catalyst for conversion of acetophenone. The IEt₂Me₂ analogue showed comparable reactivity whereas the I^tPr₂Me₂, was totally inactive. A preliminary study showed a solvent effect for **2.3** with THF leading to higher conversion than benzene.

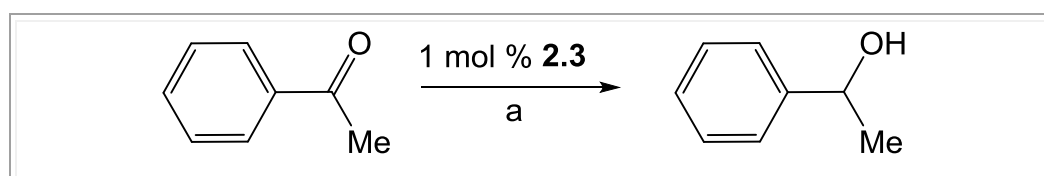
		
Catalyst	Solvent	Conversion (%) of acetophenone
2.3	THF- <i>d</i> ₈	77
2.2	THF- <i>d</i> ₈	70
2.1	THF- <i>d</i> ₈	<1
2.3	C ₆ D ₆	49
^a acetophenone (136 mmol), catalyst (1.36 mmol), DMAB (136 mmol), solvent (1 mL), 323 K, 1 h		

Table 3.3: Solvent and catalyst screening

3.10 Transfer hydrogenation of nitriles

Due to their importance in pharmaceuticals and material science, amines constitute a widely used class of chemicals in industry.⁴⁷⁻⁴⁹ The reduction of nitriles is usually a straightforward route to produce amines, however, conventional stoichiometric reduction methods involve the use of strong reducing agents such as LiAlH₄. Nowadays, the hydrogenation of nitriles is typically performed using metal catalysts which include a series of ruthenium complexes containing phosphine ligands, but these require drastic conditions such as high temperatures⁵⁰⁻⁵⁴ Milder conditions for the hydrogenation of aromatic nitriles were found by applying ruthenium/carbene catalysts.⁴⁸ These findings led us to investigate the hydrogenation of a

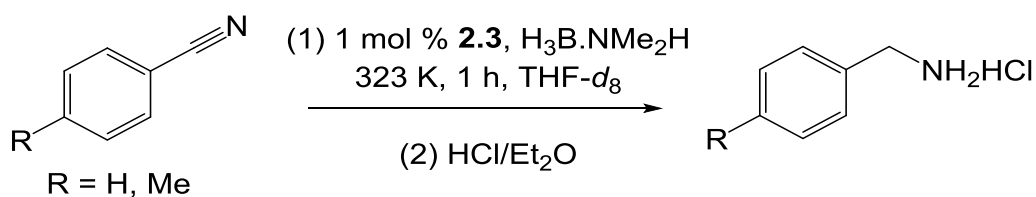
selection of nitriles using **2.3** and see whether analogous reductions could be performed.

An NMR tube was charged with a THF-*d*₈ solution of **2.3** (1 mol %), nitrile and 2-6 equiv. DMAB. In the case of benzonitrile and *p*-tolynitrile, heating for 1 h at 323 K with only 2 equiv. of DMAB resulted in complete conversion to [Me₂N.BH₂]₂ and yet again a higher frequency ¹¹B signal at 28.8 ppm. Butyronitrile proved harder to reduce and a total of 6 equiv. DMAB for 5 days at 323 K was needed for reasonable conversion of the starting material (Table 3.4).

R	Time	Conversion (%) to amine	Isolated yield (%) of amine
<i>p</i> -MeC ₆ H ₄	1 h	100	75
C ₆ H ₅	1 h	100	68
ⁿ Pr	5 days	87	
^a nitrile (136 mmol), 2.3 (1.36 mmol), DMAB (272 mmol), THF- <i>d</i> ₈ (1 mL), 323 K, 1 h			

Table 3.4: [Ru(IMe₄)₄H]⁺ catalysed transfer hydrogenation reaction of nitriles

Table 3.4 shows conversions to amine based on the aromatic signals of the products. However, the NH and CH₂ signals were harder to assign, raising the possibility again that there is some interaction of the amine with a boron containing species. To overcome this uncertainty, the amines were isolated as the hydrochloride salts⁵⁵ as shown in Scheme 3.16. As expected, isolated yields were lower than spectroscopic conversions (Table 3.4).



Scheme 3.16: $[\text{Ru}(\text{IMe}_4)_4\text{H}]^+$ catalysed transfer hydrogenation reaction of nitriles and conversion to the hydrochloride salts

Further studies on the catalysis with $[\text{Ru}(\text{IMe}_4)_4\text{H}]^+$ of polar substrates (ketones, nitriles) with DMAB are needed to definitely confirm product identifications. Moreover, in the case of nitrile reduction, establishing the role of imines as intermediates will be necessary.

3.11 Transfer hydrogenation of alkynes and alkenes

Catalytic C–H bond making and breaking is one of the most useful synthetic applications of organometallic chemistry.^{56,57} Hydrogenation of alkenes is classically performed by direct hydrogenation using molecular H_2 .⁵⁸⁻⁶⁰ In contrast transfer hydrogenation of alkenes requires H_2 from a hydrogen source. However both methods involve, in most cases, a metal-dihydride species, or a monohydride complex when a ligand is assisting the H_2 or hydrogen donor activation.

A NMR tube containing $\text{THF-}d_8$ was charged with 1 mol % **2.3**, alkene and 1 equiv. DMAB and heated at 323 K for 1 h. For both styrene and trimethylvinylsilane, ^1H NMR spectroscopy revealed formation of the corresponding reduction products. Conversions to the alkane products are given in Table 3.5.

$\text{RHC}=\text{CH}_2 \xrightarrow{1 \text{ mol } \% \mathbf{2.3}^a} \text{RH}_2\text{C}-\text{CH}_3$		
R	Time (h)	Conversion (%) of alkane
Ph	1	94
Me ₃ Si	1	100
^a 1.36 mmol of catalyst, 136 mmol of DMAB and 136 mmol of selected alkene in THF- <i>d</i> ₈ and heated at 323 K.		

Table 3.5: [Ru(IME₄)₄H]⁺ catalysed transfer hydrogenation of alkenes

These conversions are significantly greater than those reported by Albrecht and co-workers, they used the Ru catalyst **3.15** (Figure 3.6), ⁱPrOH as the H₂ source and only obtained a moderate 30% yield conversion to ethylbenzene over 12 h at 353 K.⁵⁸

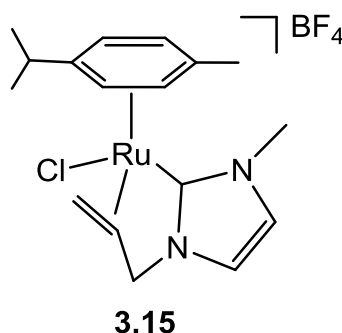


Figure 3.6: Ru-NHC complex employed in transfer hydrogenation reactions reported by Albrecht et al

A series of alkynes were also tested to see if they hydrogenated to the corresponding alkenes in the presence of **2.3** and DMAB. Trimethylsilylacetylene and phenylacetylene were both investigated; a similar procedure was followed as for the alkenes described above, but at 343 K and 12 h reaction time. At 323 K, very little conversion was observed after 1 h. Raising the temperature to 343 K proved to bring about reasonable conversions, perhaps due to tighter bonding of alkynes as opposed to alkenes. Interestingly in both cases, styrene and trimethylvinylsilane were

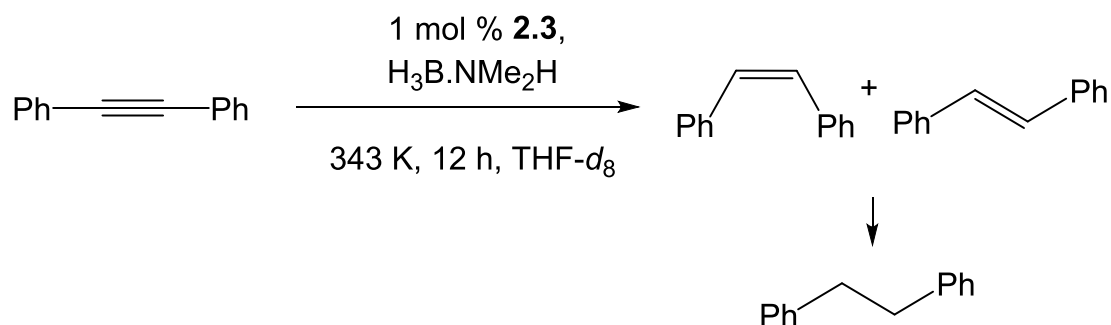
observed in the ^1H NMR spectrum after 1 h, however with time, these alkenes were further hydrogenated to generate the corresponding alkanes (Table 3.6).

$\text{RC}\equiv\text{CH} \xrightarrow{1 \text{ mol } \% \text{ 2.3}^a} \text{RHC}=\text{CH}_2 \longrightarrow \text{RH}_2\text{C}-\text{CH}_3$		
Substrate	Time (h)	Conversion (%) to alkane
Ph	12	75
Me_3Si	12	100

^a1.36 mmol of **2.3**, 136 mmol of DMAB and 136 mmol alkene, $\text{THF-}d_8$, 343 K.

Table 3.6: $[\text{Ru}(\text{IME}_4)_4\text{H}]^+$ catalysed transfer hydrogenation of alkynes

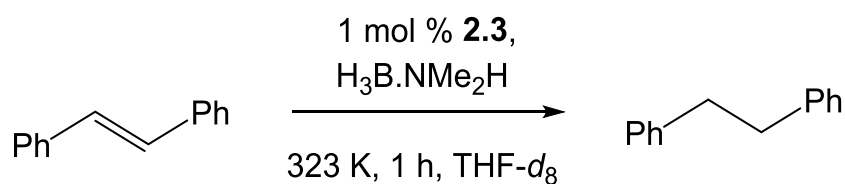
Hydrogenation reactions of internal alkynes took a different pathway. An NMR tube containing $\text{THF-}d_8$, **2.3**, diphenylacetylene and DMAB was heated and the ^1H NMR spectrum monitored after 1 h at 343 K. Interestingly, signals for both *cis*- and *trans*-stilbene were present in a 1:1.5 ratio, along with signals for dibenzyl (Scheme 3.17). Heating the reaction for an additional 12 h and monitoring the ^1H NMR spectrum again revealed the presence of only dibenzyl and trace amounts of *trans*-stilbene.



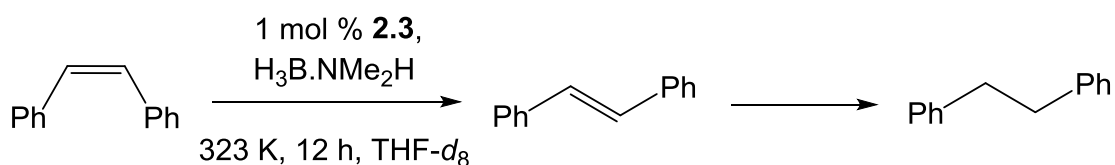
Scheme 3.17: Catalytic transfer hydrogenation of $\text{PhC}\equiv\text{CPh}$

To probe the isomerisation/hydrogenation steps in more detail, both *cis*- and *trans*-stilbene were separately hydrogenated with **2.3** and DMAB at 323 K, and the reactions monitored by ^1H NMR spectroscopy. After 1 h, *trans*-stilbene was hydrogenated to dibenzyl in 45% yield (Scheme 3.18), whereas

cis-stilbene first isomerised to the trans-isomer, which then underwent hydrogenation (Scheme 3.19).



Scheme 3.18: Hydrogenation of trans-stilbene



Scheme 3.19: Isomerisation of cis-stilbene followed by hydrogenation of trans-stilbene

The hydrogenation of cis-stilbene was followed spectroscopically over 12 h as shown in Figure 3.7. The ¹H NMR spectrum displays the reactivity of cis-stilbene towards DMAB and **2.3**, which isomerises to the more stable trans isomer rapidly within 1 h. With time, the amount of cis stilbene decreases and after 12 h the substrate is fully consumed.

The same catalytic procedure was followed for MeO₂CC≡CCO₂Me and the ¹H NMR spectrum recorded after 1 h. During this time, the alkyne had been hydrogenated and both dimethyl fumarate and dimethyl maleate were formed along with MeO₂CCH₂CH₂CO₂Me (Scheme 3.20). Heating the reaction mixture at 343 K for a total of 12 h afforded 50% conversion to the alkane.

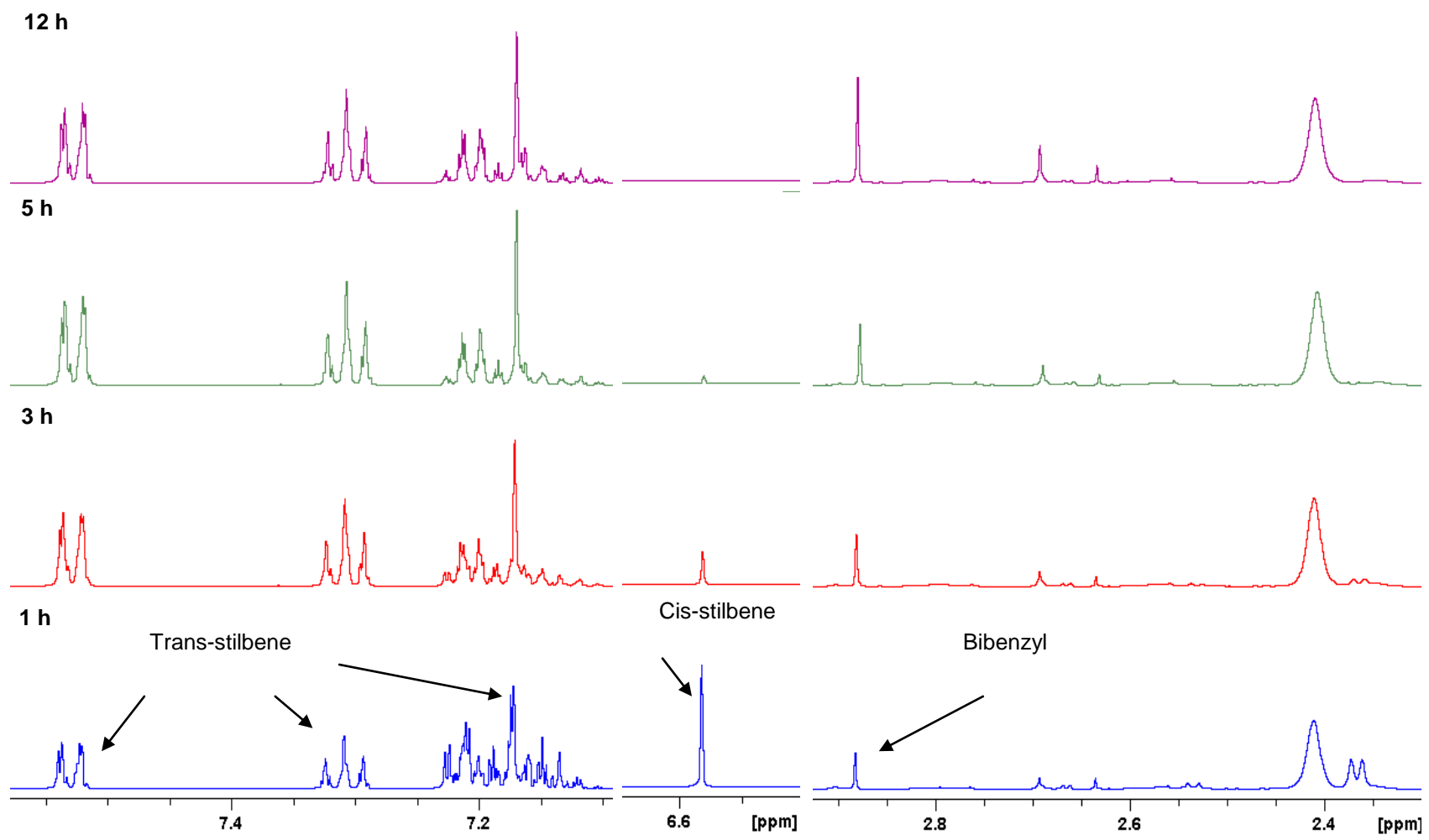
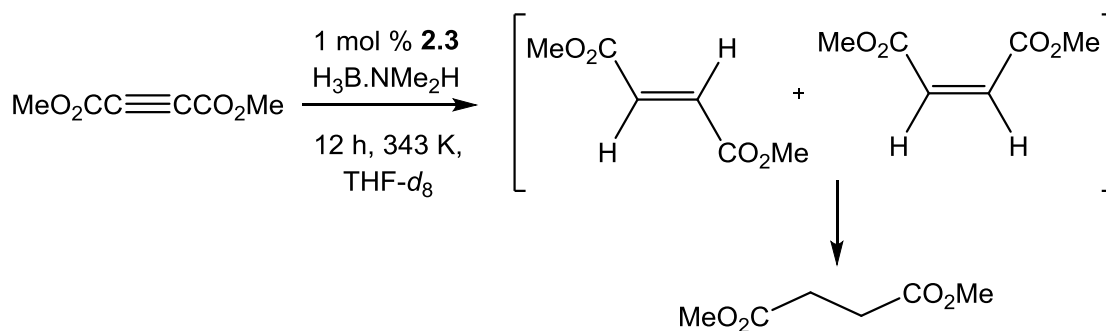


Figure 3.7: ¹H NMR spectra displaying the isomerisation of cis-stilbene followed by hydrogenation (THF-*d*₈, 298 K, 500MHz)



Scheme 3.20: $[\text{Ru}(\text{IMe}_4)_4\text{H}]^+$ catalysed transfer hydrogenation of $\text{MeO}_2\text{CC}\equiv\text{CCO}_2\text{Me}$

To understand the process in detail, each alkene was reacted separately with DMAB in the presence of 1 mol % **2.3** at 323 K for 1 h. The ^1H NMR spectrum of the dimethyl fumarate reaction showed complete conversion to the alkane. In the case of dimethyl maleate, isomerisation to the trans isomer was seen along with formation of alkane (Figure 3.8).

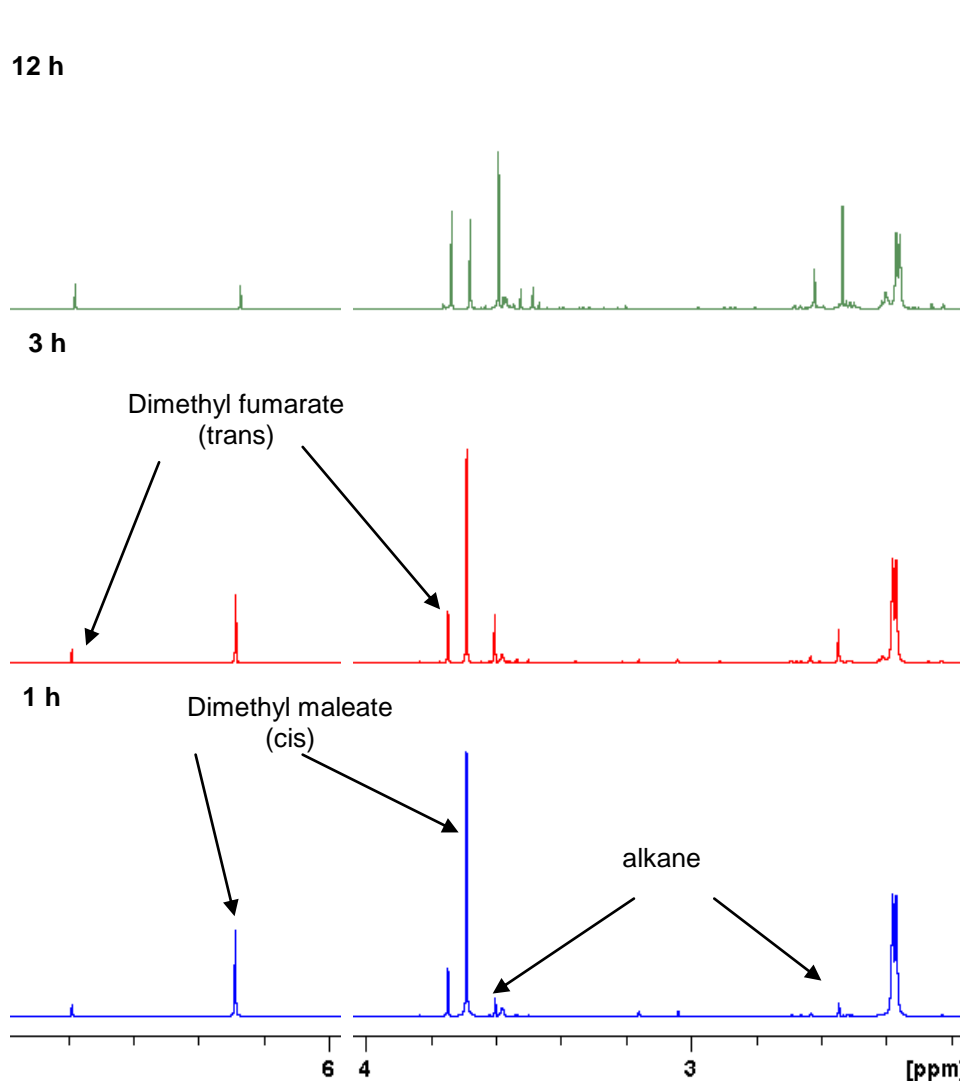
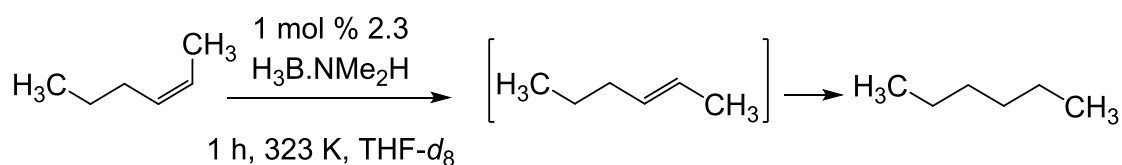


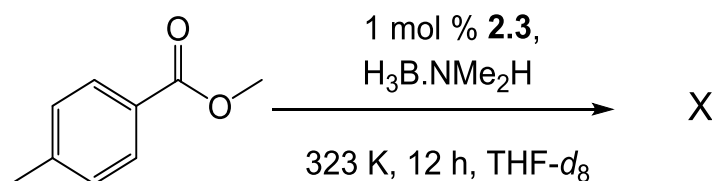
Figure 3.8: ^1H NMR spectra showing the ruthenium induced isomerisation of dimethyl maleate to dimethyl fumarate along with hydrogenation to alkane (THF- d_8 , 298 K, 500MHz)

The catalytic transfer hydrogenation of cis-2-hexene showed an identical isomerisation to the trans isomer before hydrogenation to hexane took place. No reaction took place in the absence of the Ru complex (Scheme 3.21).



Scheme 3.21: $[\text{Ru}(\text{IME}_4)_4\text{H}]^+$ catalysed isomerisation and reduction of cis-2-hexene

The catalytic transfer hydrogenation of an aromatic ester was briefly investigated. No reaction was observed for 4-methyl-4-methylbenzoate in the presence of DMAB and 1 mol % **2.3** over 1 h at 323 K (Scheme 3.22). Heating the reaction mixture for a total 12 h showed no change and only displayed the starting materials.



Scheme 3.22: Attempted catalytic transfer hydrogenation of methyl-4-methylbenzoate

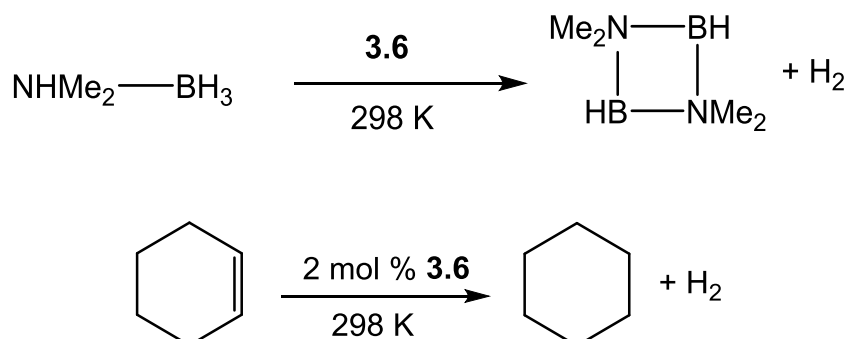
3.12 Comment on catalytic activity of other reported examples employing amine boranes

Although many groups have reported catalytic transfer hydrogenation reactions of organic substrates, many of them were only described for selected substrates. Our system appears to be able to hydrogenate a range of substrates which suggest it maybe more versatile. Selected examples are described below which can be compared with our catalytic system.

An early example by Manners and co-workers reported the use of rhodium colloids for the catalytic reduction of alkenes with DMAB.⁴⁴ During the course of the catalytic dehydrocoupling of Me₂NHBH₃ with **3.6**, (Scheme 3.23) the formation of small quantities of cyclooctane was consistently observed in the reaction mixtures. This presumably resulted from the catalytic hydrogenation of 1,5 cyclooctadiene, which was present in solution upon reduction of the precatalyst to Rh colloids. It was apparent that the active catalyst for the dehydrocoupling reaction also acted as a catalyst for alkene hydrogenation, without the necessity for an external H₂ source. To test for quantitative hydrogenation of alkenes via this route, stoichiometric reactions were performed using commercially available DMAB and cyclohexene in the presence of colloidal Rh as a catalyst.⁴⁴

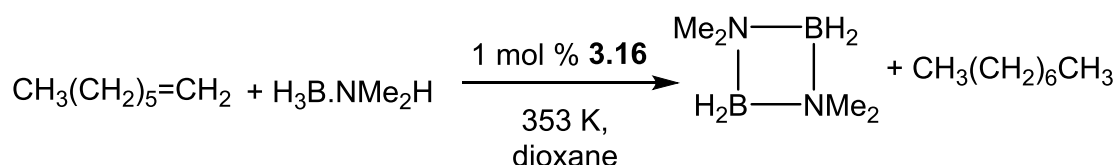
A typical experiment consisted of 1 equiv. DMAB, 1 equiv. cyclohexene and 2 mol % **3.6** dissolved in C₆D₆ and after 8 h the hydrogenation reaction

had reached 38% conversion. A blank reaction between DMAB and cyclohexene in the absence of precatalyst displayed no evidence of dehydrocoupling-hydrogenation reactivity.⁴⁴



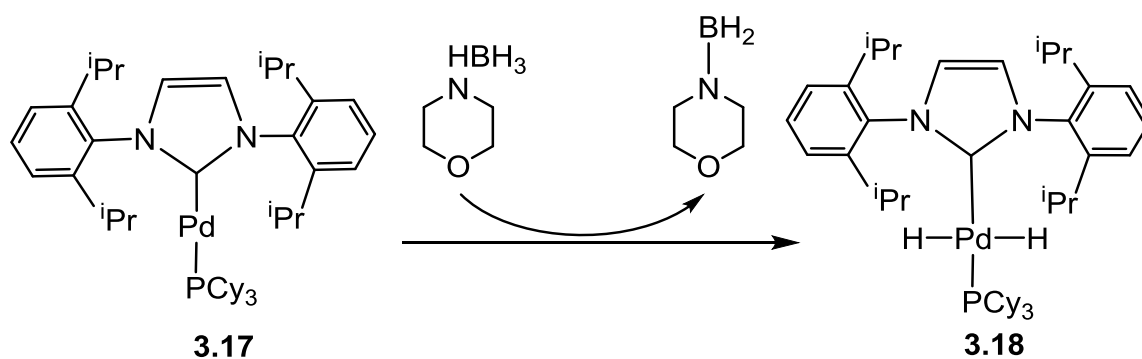
Scheme 3.23: Rhodium colloids for the catalytic reduction of alkenes with DMAB

In 2007 Berke and co-workers reported a series of Re complexes which could dehydrogenate amine boranes and then perform transfer hydrogenation reactions.^{45,46} Equal amounts of DMAB and 1-octene were mixed with 1 mol % of $\text{Re}(\text{P}^i\text{Pr}_3)_2(\text{NO})\text{H}_2\text{Br}_2$ (**3.16**) in dioxane. After 1 h at 353 K, 93% conversion of 1-octene to octane was reported (Scheme 3.24).^{45,46}



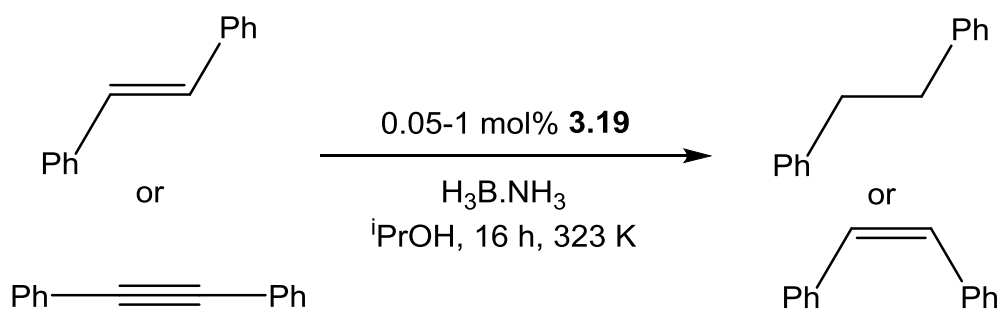
Scheme 3.24: Rhenium catalysed transfer hydrogenation reaction of alkenes with DMAB as source of H_2 ⁴⁵

More recently, Cazin and co-workers described the use of the Pd-NHC complex $\text{Pd}(\text{IPr})(\text{PCy}_3)$ **3.17** as an active catalyst in the dehydrocoupling of amine boranes and the subsequent hydrogenation of unsaturated compounds.⁶² The Pd(0) complex **3.17** was shown to dehydrogenate morpholine borane to afford the Pd(II) dihydride complex **3.18** (Scheme 3.25).



Scheme 3.25: Formation of the dihydride complex **3.18** by dehydrogenation of morpholine borane

This chemistry encouraged the group to see whether these complexes could react with $\text{H}_3\text{B.NH}_3$, generate H_2 and subsequently use this H_2 to hydrogenate C-C multiple bonds. The best catalytic activity for reducing alkynes/alkenes was observed with $\text{Pd}(\text{SiPr})(\text{PCy}_3)$ **3.19** in $i\text{PrOH}$ with low catalyst loading of 0.05 mol % (Scheme 3.26).



Scheme 3.26: Pd catalysed hydrogenation using $\text{H}_3\text{B.NH}_3$

Many groups have reported the hydrogenation of a series of organic substrates, with⁶³ and without^{47-49,56,58,64} amine boranes as the hydrogen source but some of the effective conversions have emerged with the use of amine boranes.^{58,62,65} Our results showed DMAB to be an excellent hydrogen source in the catalytic transfer hydrogenation reactions of ketones, nitriles, alkynes and alkenes, which took place under mild conditions. Interestingly **2.3** also showed evidence for alkene isomerisation during the hydrogenation reactions of internal alkynes and selected alkenes.

Since the exact catalytic fragment in our system is unknown, the mechanism in which the transfer hydrogenations reactions proceed can only be postulated at this time. Experiments should be carried out in the future to help elucidate the mechanism, one of which includes the addition of deuterated reagents such as Me_2DNBH_3 and Me_2HNBD_3 to determine for polar reagents which way round H-D addition occurs.

3.13 CHAPTER SUMMARY

The catalytic transfer hydrogenation of ketones, nitriles, alkenes and alkynes using **2.3** and DMAB has been described at low catalyst loadings, moderate temperatures and in short reaction times of 1 h to bring about good conversions. The results obtained are at least comparable with those reported in the literature which typically require more drastic conditions to achieve reasonable yields.

The true catalytic intermediate remains to be established. The stoichiometric reduction of DMAB by both $[\text{Ru}(\text{IMe}_4)_4\text{H}]^+$ and $[\text{Ru}(\text{IEt}_2\text{Me}_2)_4\text{H}]^+$ leads to formation of what appears to be the corresponding dihydrogen hydride complexes $[\text{Ru}(\text{NHC})_4(\eta^2\text{-H}_2)\text{H}]^+$, although whether those lie off the catalytic cycle or mediate H_2 transfer from amine boranes will be the subject of future studies.

3.14 Experimental

3.14.1 General methods

All manipulations were carried out by using standard Schlenk, high vacuum and glovebox techniques with dried and degassed solvents. Deuterated solvents (Sigma–Aldrich) were vacuum transferred from potassium (C_6D_6 and $\text{THF-}d_8$). Hydrogen (BOC, 99.9 %) was used as received. NMR spectra were recorded at 298 K on Bruker Avance 500 and 400 MHz NMR spectrometers and referenced as follows for ^1H spectra: benzene (^1H , $\delta = 7.16$ ppm), tetrahydrofuran (^1H , $\delta = 3.58$ ppm). $^{11}\text{B}\{^1\text{H}\}$ NMR chemical shifts were referenced to $\text{BF}_3\cdot\text{OEt}_2$ ($\delta = 0.0$ ppm). Ammonia borane, morpholine borane, dimethylamine borane, tert-butyl borane and phosphine borane (Sigma Aldrich) were all used as received. All organic substrates; acetophenone, fluoroacetophenone, 4-methyl acetophenone, 2-methyl acetophenone, 4

methoxyacetophenone, pinacolone, phenylacetylene, styrene, diphenylacetylene, trans-stilbene, cis-stilbene, *p*-tolunitrile, benzonitrile, trimethylsilylacetylene, trimethylvinylsilane, dimethyl acetylenecarboxylate, dimethyl fumarate, dimethyl maleate, butyronitrile, N-benzylideneaniline, methyl-4 methylbenzoate and cis-2-hexene (Sigma Aldrich) were used as received.

3.14.2 Synthesis of 1,3,4,5-tetramethylimidazole-2-ylidene (IME₄)⁶⁶

1,3,4,5-tetramethylimidazole-2-(3H)-thione (1.80 g, 10.0 mmol), THF (60 mL) and chopped pieces of potassium (1.00 g, 25.6 mmol) were refluxed for 4 h. After cooling, the suspension was filtered through celite and the filtrate reduced to dryness which afforded an orange solid (1.08 g, 73% yield). NMR data were in agreement with the literature.

3.14.3 Synthesis of [Ru(IME₄)₄H][BAR^F₄]⁴³ [Ru(PPh₃)₃HCl] (300 mg, 0.32 mmol) and IME₄ (322 mg, 2.60 mmol) were heated at 343 K in THF (5 mL) for 12 h in an ampoule fitted with a J. Youngs PTFE valve. The reaction mixture was cooled to room temperature and the yellow solid formed isolated by cannula filtration, washed with hexane (2 x 5 mL) and dried under vacuum. The resulting solid (140 mg) and Na[BAR^F₄] (196 mg) were stirred at room temperature in toluene (10 mL) for 3 h. The suspension was cannula filtered and then the filtrate was reduced to dryness to afford a purple solid and dried under vacuum. (299 mg, 63% yield). NMR data were in agreement with the literature.⁴³

3.14.4 General procedure for catalytic transfer hydrogenation of ketones and alkenes [Ru(IME₄)₄H][BAR^F₄] (2 mg, 1.36 mmol), ketone (136 mmol) and DMAB (8 mg, 136 mmol) were heated at 323 K in THF-*d*₈ in an NMR tube fitted with a J. Youngs PTFE valve.

3.14.5 General procedure for catalytic transfer hydrogenation of nitriles [Ru(IME₄)₄H][BAR^F₄] (2 mg, 1.36 mmol), nitrile (136 mmol) and DMAB (16 mg, 272 mmol) were heated at 323 K in THF-*d*₈ in an NMR tube fitted with a J. Youngs PTFE valve.

3.14.6 General procedure for catalytic transfer hydrogenation of alkynes [Ru(IME₄)₄H][BAR^F₄] (2 mg, 1.36 mmol), alkyne (136 mmol) and DMAB (8 mg, 136 mmol) were heated at 343 K in THF-*d*₈ in an NMR tube fitted with a J. Youngs PTFE valve.

3.14.7 Isolation of hydrochloride amine salts⁵⁵ [Ru(IMe₄)₄H][BAr^F₄] (30 mg, 20.0 mmol), benzonitrile (211 μ L, 2.05 mol) and DMAB (242 mg, 4.10 mol) were heated at 323 K in THF-*d*₈ in an ampoule fitted with a J. Youngs PTFE valve and then cooled to room temperature. The reaction mixture was diluted with hexane (250 mL) and washed with NaOH solution (1M, 2 x 50 mL). The organic layer was dried (MgSO₄) and then HCl in diethyl ether (1M, 1 equiv.) was added. A precipitate was formed which was collected by reduced pressure filtration. The precipitate was dissolved in minimum amount of ethanol followed by ethyl acetate and left to crystallise. Yield 68%. NMR data were in agreement with the literature.⁵⁵ The same procedure was used for p-tolunitrile which afforded 75 % yield.

References

- (1) Mkhaliid, I. A. I.; Barnard, J. H.; Marder, T. B.; Murphy, J. M.; Hartwig, J. F. *Chem. Rev.* **2010**, *110*, 890.
- (2) Kumar, R.; Jagirdar, B. R. *Inorg. Chem.* **2013**, *52*, 28.
- (3) Alcaraz, G.; Sabo-Etienne, S. *Angew. Chem., Int. Ed.* **2010**, *49*, 7170.
- (4) Staubitz, A.; Robertson, A. P. M.; Manners, I. *Chem. Rev.* **2010**, *110*, 4079.
- (5) Stephens, F. H.; Pons, V.; Baker, R. T. *Dalton Trans.* **2007**, 2613.
- (6) Marder, T. B. *Angew. Chem., Int. Ed.* **2007**, *46*, 8116.
- (7) Smythe, N. C.; Gordon, J. C. *Eur. J. Inorg. Chem.* **2010**, 509.
- (8) Wagner, R. I.; Caserio, F. F. *J. Inorg. Nucl. Chem.* **1959**, *11*, 259.
- (9) Hamilton, C. W.; Baker, R. T.; Staubitz, A.; Manners, I. *Chem. Soc. Rev.* **2009**, *38*, 279.
- (10) Denney, M. C.; Pons, V.; Hebden, T. J.; Heinekey, D. M.; Goldberg, K. I. *J. Am. Chem. Soc.* **2006**, *128*, 12048.
- (11) Jaska, C. A.; Manners, I. *J. Am. Chem. Soc.* **2004**, *126*, 9776.
- (12) Jana, A.; Schulzke, C.; Roesky, H. W. *J. Am. Chem. Soc.* **2009**, *131*, 4600.
- (13) Staubitz, A.; Robertson, A. P. M.; Sloan, M. E.; Manners, I. *Chem. Rev.* **2010**, *110*, 4023.
- (14) Staubitz, A.; Sloan, M. E.; Robertson, A. P. M.; Friedrich, A.; Schneider, S.; Gates, P. J.; Günne, J. S. A. D.; Manners, I. *J. Am. Chem. Soc.* **2010**, *132*, 13332.
- (15) Staubitz, A.; Soto, A. P.; Manners, I. *Angew. Chem., Int. Ed.* **2008**, *47*, 6212.
- (16) Pons, V.; Baker, R. T. *Angew. Chem., Int. Ed.* **2008**, *47*, 9600.
- (17) Dorn, H.; Rodezno, J. M.; Brunnhöfer, B.; Rivard, E.; Massey, J. A.; Manners, I. *Macromolecules* **2003**, *36*, 291.
- (18) Tang, C. Y.; Thompson, A. L.; Aldridge, S. *Angew. Chem., Int. Ed.* **2010**, *49*, 921.
- (19) Dallanegra, R.; Chaplin, A. B.; Tsim, J.; Weller, A. S. *Chem. Commun.* **2010**, *46*, 3092.
- (20) Chaplin, A. B.; Weller, A. S. *Angew. Chem., Int. Ed.* **2010**, *49*, 581.

- (21) Douglas, T. M.; Chaplin, A. B.; Weller, A. S.; Yang, X. Z.; Hall, M. B. *J. Am. Chem. Soc.* **2009**, *131*, 15440.
- (22) Kakizawa, T.; Kawano, Y.; Shimoi, M. *Organometallics* **2001**, *20*, 3211.
- (23) Kawano, Y.; Hashiva, M.; Shimoi, M. *Organometallics* **2006**, *25*, 4420.
- (24) Shimoi, M.; Nagai, S.; Ichikawa, M.; Kawano, Y.; Katoh, K.; Uruichi, M.; Ogino, H. *J. Am. Chem. Soc.* **1999**, *121*, 11704.
- (25) Dallanegra, R.; Chaplin, A. B.; Weller, A. S. *Angew. Chem., Int. Ed.* **2009**, *48*, 6875.
- (26) Douglas, T. M.; Chaplin, A. B.; Weller, A. S. *J. Am. Chem. Soc.* **2008**, *130*, 14432.
- (27) Alcaraz, G.; Chaplin, A. B.; Stevens, C. J.; Clot, E.; Vendier, L.; Weller, A. S.; Sabo-Etienne, S. *Organometallics* **2010**, *29*, 5591.
- (28) Luo, Y.; Ohno, K. *Organometallics* **2007**, *26*, 3597.
- (29) Paul, A.; Musgrave, C. B. *Angew. Chem., Int. Ed.* **2007**, *46*, 8153.
- (30) Keaton, R. J.; Blacquiere, J. M.; Baker, R. T. *J. Am. Chem. Soc.* **2007**, *129*, 1844.
- (31) Yang, X.; Hall, M. B. *J. Am. Chem. Soc.* **2008**, *130*, 1798.
- (32) Burg, A. B.; Wagner, R. I. *J. Am. Chem. Soc.* **1953**, *75*, 3872.
- (33) Gee, W.; Holden, J. B.; Shaw, R. A.; Smith, B. C. *J. Chem. Soc.* **1965**, 3171.
- (34) Dorn, H.; Singh, R. A.; Massey, J. A.; Lough, A. J.; Manners, I. *Angew. Chem., Int. Ed.* **1999**, *38*, 3321.
- (35) Jaska, C. A.; Temple, K.; Lough, A. J.; Manners, I. *Chem. Commun.* **2001**, 962.
- (36) Jaska, C. A.; Temple, K.; Lough, A. J.; Manners, I. *J. Am. Chem. Soc.* **2003**, *125*, 9424.
- (37) Blaquiere, N.; Diallo-Garcia, S.; Gorelsky, S. I.; Black, D. A.; Fagnou, K. *J. Am. Chem. Soc.* **2008**, *130*, 14034.
- (38) Morris, R.; Habtemariam, A.; Guo, Z. J.; Parsons, S.; Sadler, P. J. *Inorg. Chim. Acta* **2002**, *339*, 551.
- (39) Friedrich, A.; Drees, M.; Schneider, S. *Chem. Eur. J.* **2009**, *15*, 10339.
- (40) Kass, M.; Friedrich, A.; Drees, M.; Schneider, S. *Angew. Chem., Int. Ed.* **2009**, *48*, 905.

- (41) Marziale, A. N.; Friedrich, A.; Klopsch, I.; Drees, M.; Celinski, V. R.; Günne, J. S. A. D.; Schneider, S. *J. Am. Chem. Soc.* **2013**, *135*, 13342.
- (42) Ledger, A. E. W.; Ellul, C. E.; Mahon, M. F.; Williams, J. M. J.; Whittlesey, M. K. *Chem. Eur. J.* **2011**, *17*, 8704.
- (43) Burling, S.; Häller, L. J. L.; Mas-Marzá, E.; Moreno, A.; Macgregor, S. A.; Mahon, M. F.; Pregosin, P. S.; Whittlesey, M. K. *Chem. Eur. J.* **2009**, *15*, 10912.
- (44) Jaska, C. A.; Manners, I. *J. Am. Chem. Soc.* **2004**, *126*, 2698.
- (45) Jiang, Y.; Berke, H. *Chem. Commun.* **2007**, 3571.
- (46) Jiang, Y.; Blacque, O.; Fox, T.; Frech, C. M.; Berke, H. *Organometallics* **2009**, *28*, 5493.
- (47) Miao, X.; Bidange, J.; Dixneuf, P. H.; Fischmeister, C.; Bruneau, C.; Dubois, J.-L.; Couturier, J.-L. *Chemcatchem* **2012**, *4*, 1911.
- (48) Addis, D.; Enthaler, S.; Junge, K.; Wendt, B.; Beller, M. *Tetrahedron Lett.* **2009**, *50*, 3654.
- (49) Werkmeister, S.; Bornschein, C.; Junge, K.; Beller, M. *Chem. Eur. J.* **2013**, *19*, 4437.
- (50) Suarez, T.; Fontal, B. *J. Mol. Catal. A: Chem.* **1988**, *45*, 335.
- (51) Yoshida, T.; Okano, T.; Otsuka, S. *J. Chem. Soc.-Chem. Commun.* **1979**, 870.
- (52) Chong, S. C.; Lee, B. N. *Catal. Lett.* **1992**, *14*, 135.
- (53) Enthaler, S.; Addis, D.; Junge, K.; Erre, G.; Beller, M. *Chem. Eur. J.* **2008**, *14*, 9491.
- (54) Enthaler, S.; Junge, K.; Addis, D.; Erre, G.; Beller, M. *ChemSuschem* **2008**, *1*, 1006.
- (55) Nixon, T. D.; Whittlesey, M. K.; Williams, J. M. J. *Tetrahedron Lett.* **2011**, *52*, 6652.
- (56) Horn, S.; Gandolfi, C.; Albrecht, M. *Eur. J. Inorg. Chem.* **2011**, 2863.
- (57) Wienhöfer, G.; Westerhaus, F. A.; Jagadeesh, R. V.; Junge, K.; Junge, H.; Beller, M. *Chem. Commun.* **2012**, *48*, 4827.
- (58) Horn, S.; Albrecht, M. *Chem. Commun.* **2011**, *47*, 8802.
- (59) Young, J. F.; Osborn, J. A.; Jardine, F. H.; Wilkinson, G. *Chem. Commun.* **1965**, 131.

- (60) Hallman, P. S.; Evans, D.; Osborn, J. A.; Wilkinson, G. *Chem. Commun.* **1967**, 305.
- (61) Gandolfi, C.; Heckenroth, M.; Neels, A.; Laurency, G.; Albrecht, M. *Organometallics* **2009**, *28*, 5112.
- (62) Hartmann, C. E.; Jurčák, V.; Songis, O.; Cazin, C. S. J. *Chem. Commun.* **2013**, *49*, 1005.
- (63) Yang, X.; Zhao, L.; Fox, T.; Wang, Z.-X.; Berke, H. *Angew. Chem., Int. Ed.* **2010**, *49*, 2058.
- (64) Werkmeister, S.; Bornschein, C.; Junge, K.; Beller, M. *Eur. J. Org. Chem.* **2013**, 3671.
- (65) Dharmasena, U. L.; Foucault, H. M.; dos Santos, E. N.; Fogg, D. E.; Nolan, S. P. *Organometallics* **2005**, *24*, 1056.
- (66) Kuhn, N.; Kratz, T. *Synthesis* **1993**, 561.

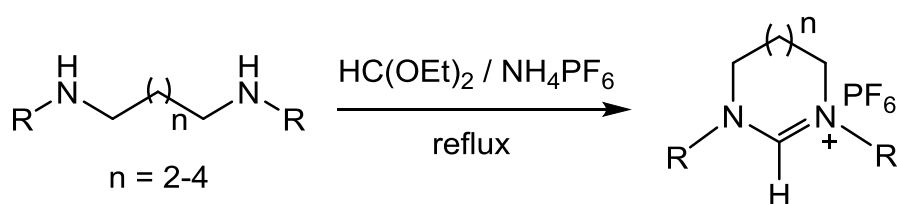
4. INTRODUCTION

4.1 Ring expanded N-heterocyclic carbenes (RE-NHCs)

Since the isolation of the first free N-heterocyclic carbenes (NHCs), there have been plenty of new developments with respect to the types and sizes of carbenes that may be synthesised. While the coordination of NHCs towards various metals have been reported, most cases have involved five-membered ring NHCs.^{1,2} Only very recently have studies on six- and seven-membered-ring NHCs been reported.³⁻¹³ These so-called ring expanded N-heterocyclic carbenes (RE-NHCs) are very basic and show unique structural features.¹⁴ They have been shown to exhibit much wider N-C-N angles than their five-membered counterparts which results in an increase in the steric hindrance around the metal core. Placing the N-substituents in close proximity to a metal centre not only blocks specific coordination sites, but may also facilitate intramolecular C-H activation of the carbene ligand.

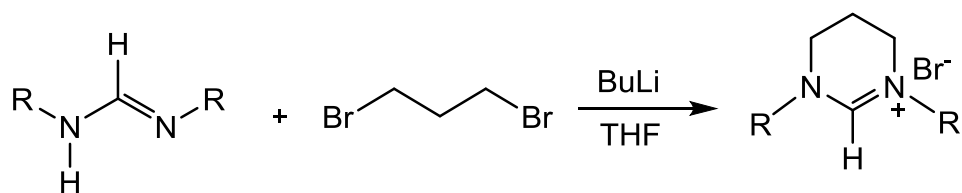
4.2 Synthesis of RE-NHCs

The synthesis of cyclic amidinium salts bearing N-alkyl or aryl substituents has been achieved by cyclization of substituted diamines. The reaction of N,N'-disubstituted diamines with triethylorthoformate in the presence of ammonium hexafluorophosphate yields the cyclic amidinium salts (Scheme 4.1).¹⁵



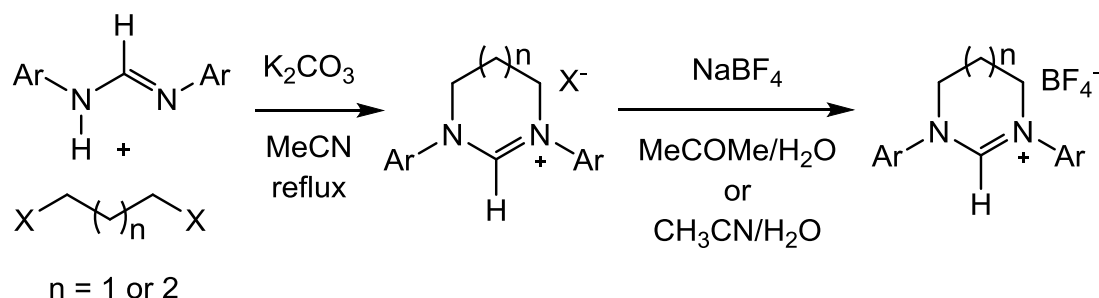
Scheme 4.1: Synthesis of cyclic amidinium salts via diamines

In 2006 Bertrand published a different process for the preparation of these carbene salts. 1,3-dibromopropane was added to a THF solution of the lithium salt of the formamidine and, after stirring overnight at room temperature, the corresponding salt was isolated (Scheme 4.2).¹⁶



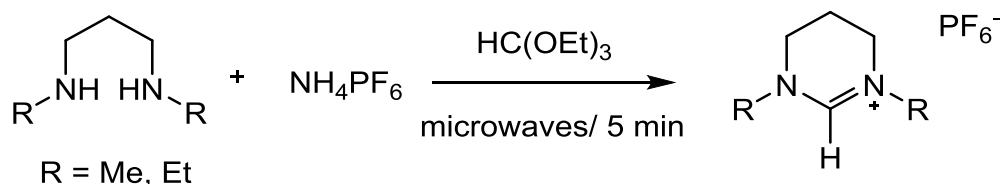
Scheme 4.2: Synthesis of carbene salts via formamidines

Soon after Cavell and co-workers modified Bertrand's procedure and reported a more efficient route to synthesising several six- and seven membered ring carbenes. The modified synthetic route allowed the reaction to be carried out on large scales, under aerobic conditions and to afford high yields for a series of ring sizes and N-substituents (Scheme 4.3).¹⁷



Scheme 4.3: Modified route to carbene salts via formamidines

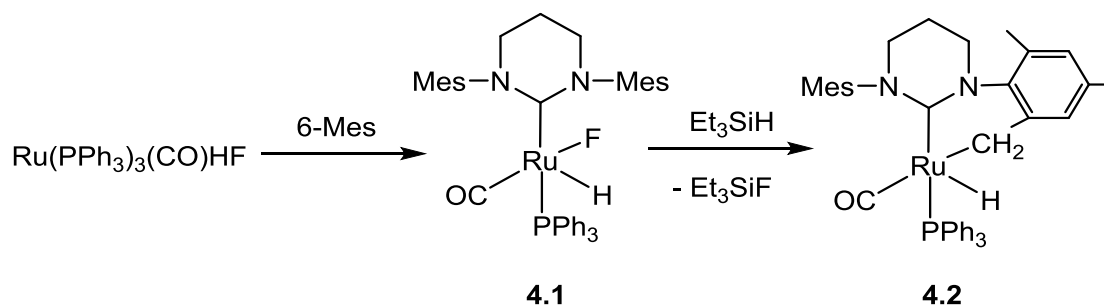
As already mentioned, the preparation of cyclic amidinium salts with a saturated backbone is usually achieved via condensation of a N,N'-disubstituted α,ω -alkanediamine and an inorganic ammonium salt with triethyl orthoester in the presence of formic acid.¹⁵ Although numerous variations have been made on this experimental procedure¹⁸, they all still require heating under reflux for prolonged times ranging between a few hours and few days to reach desirable yields. In 2008 Delaude and co-workers reported the facile microwave-assisted synthesis of cyclic amidinium salts (Scheme 4.4).¹⁹ Interestingly, this method was not that efficient for salts bearing N-Ar substituents but worked well for N-alkyl substituents.



Scheme 4.4: Synthesis of RE-NHC precursors using microwaves

4.3 Group 8 and 9 transition metal complexes bearing RE-NHCs

In 2009 our group reported the reactivity of the six-membered NHCs 6-Mes and 6-ⁱPr towards the ruthenium hydride halide complexes $\text{Ru}(\text{PPh}_3)_3(\text{CO})\text{HF}$ and $\text{Ru}(\text{PPh}_3)_3(\text{CO})\text{HCl}$.⁴ $\text{Ru}(\text{PPh}_3)_3(\text{CO})\text{HF}$ reacted with two equiv. of 6-Mes to afford the mono-carbene product $\text{Ru}(6\text{-Mes})(\text{PPh}_3)(\text{CO})\text{HF}$ **4.1**. However, with the addition of Et_3SiH , the C-H activated complex $\text{Ru}(6\text{-Mes}')(\text{PPh}_3)(\text{CO})\text{H}$ **4.2** was generated (Scheme 4.5).⁴



Scheme 4.5: Synthesis of Ru 6-Mes complexes

The reaction of 6-Mes with the hydride chloride complex $\text{Ru}(\text{PPh}_3)_3(\text{CO})\text{HCl}$ was quite different from that of the hydride fluoride precursor as it yielded the C-H activated complex directly in the absence of Et_3SiH , along with small amounts of two other products, $\text{Ru}(6\text{-Mes})(\text{PPh}_3)(\text{CO})\text{HCl}$ and $\text{Ru}(\text{PPh}_3)_3(\text{CO})\text{H}_2$. To prevent the formation of a mixture of products, the ratio of 6-Mes was lowered; $\text{Ru}(6\text{-Mes})(\text{PPh}_3)(\text{CO})\text{HCl}$ was now formed as the major product with the C-H activated complex as the minor product. Treatment of $\text{Ru}(\text{PPh}_3)_3(\text{CO})\text{HCl}$ with 6 equiv. of 6-ⁱPr gave fewer products and directly afforded complete conversion to the C-H activated complex $\text{Ru}(6\text{-}^i\text{Pr}')(\text{PPh}_3)_2(\text{CO})\text{H}$ **4.3** (Scheme 4.6).⁴

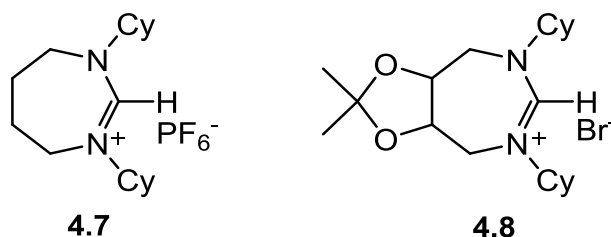
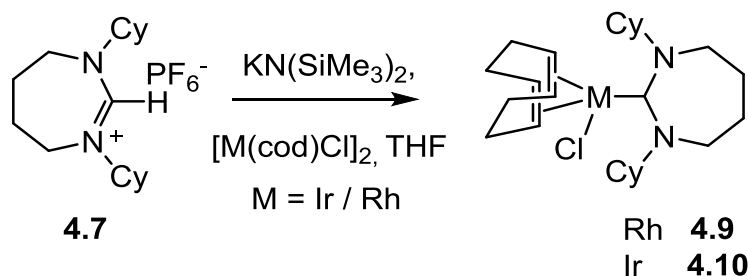


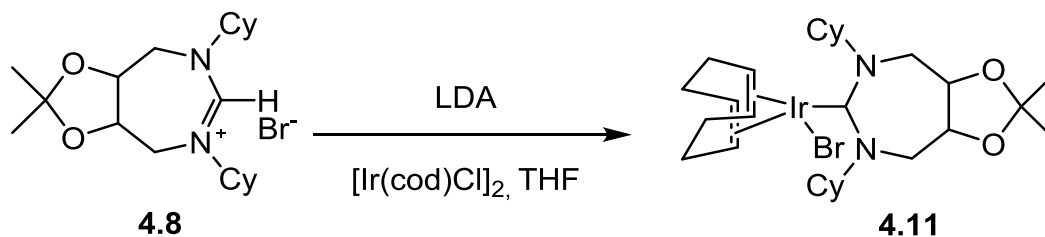
Figure 4.1: Examples of new saturated 7-NHC salts

Rh(I) and Ir(I) complexes of **4.7** were successfully isolated in the form of **4.9** and **4.10** (Scheme 4.8), however only the Ir complex **4.11** of the backbone substituted carbene could be synthesised (Scheme 4.9).²¹



Scheme 4.8: Rh and Ir complexes bearing 1,3-dicyclohexyl-1,3-diazepan-2-ylidene

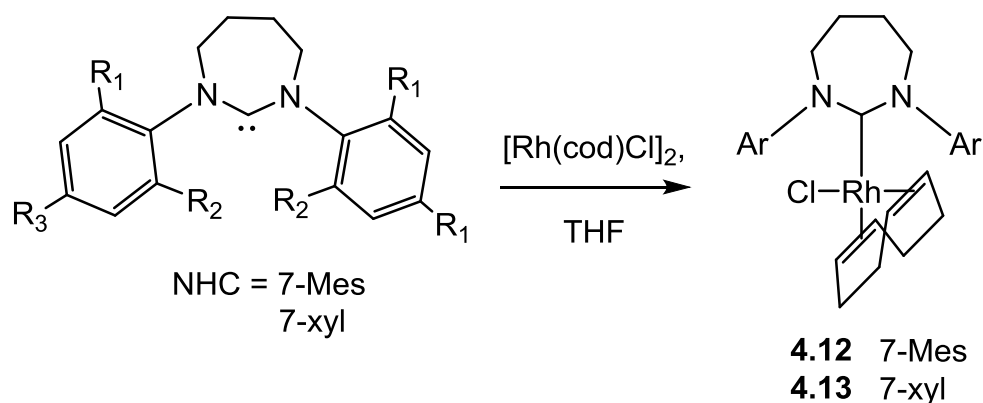
The in situ deprotonation of **4.8** with $\text{LiN}[(\text{CH}_3)_2\text{CH}]_2$ followed by addition of $[\text{Ir}(\text{cod})\text{Cl}]_2$ afforded complex **4.11**, in which halogen exchange had taken place between the metal chloride and the LiBr present in solution. Due to low yields of **4.8**, and the unstable nature of the corresponding carbene, further studies with other metals were not pursued (Scheme 4.9).²¹



Scheme 4.9: Synthesis of an Ir-NHC complex

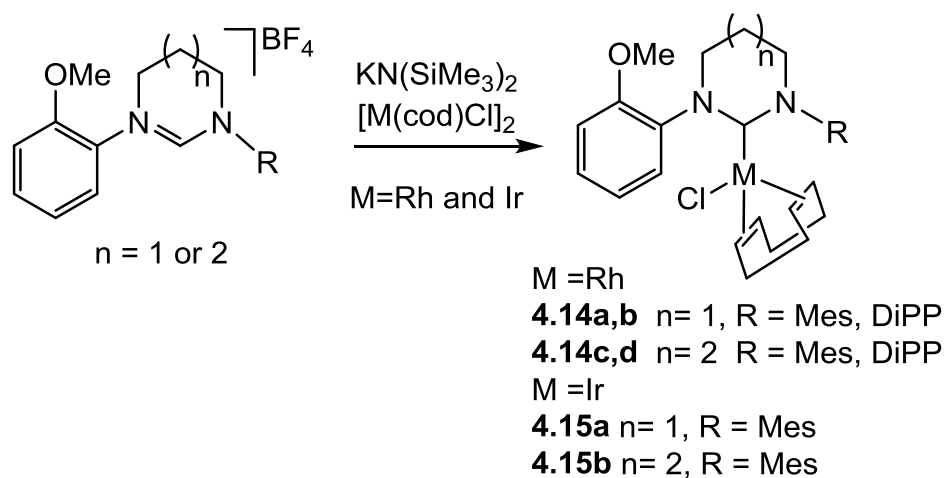
The first examples with Rh and seven membered NHCs bearing aromatic substituents were reported by Cavell in 2009.³ Treatment of

[Rh(cod)Cl]₂ with 2 equiv. of 7-Mes or 7-xyl afforded the complexes Rh(7-Mes)(cod)Cl **4.12** and Rh(7-xyl)(cod)Cl **4.13** as yellow, air-stable solids (Scheme 4.10). The corresponding 7-oTol complex was generated by in situ deprotonation of 7-oTol.HBF₄ with KN(SiMe₃)₂ followed by subsequent reaction with [Rh(cod)Cl]₂. Attempts to synthesise a stable Rh 7-dipp complex failed, due to the steric demands imposed by the bulky isopropyl substituents.³



Scheme 4.10: Synthesis of Rh complexes bearing 7-Mes and 7-xyl

In 2009 Cavell and co-workers reported Rh and Ir complexes of RE-NHCs with methoxy-functionalised substituents (Scheme 4.11). The catalytic activity of these complexes was tested in the direct hydrogenation of a range of substrates, including 1-cyclooctene and 2-methyl styrene which revealed enhanced activity under mild conditions of temperature and hydrogen pressure. Some of these results are shown in Table 4.1.²²



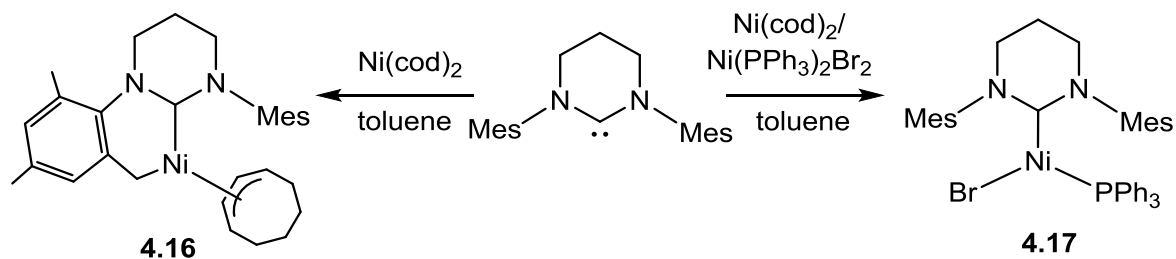
Scheme 4.11: Rh and Ir complexes bearing methoxy functionalised NHCs

Substrate	Complex	Conversion (%)
1-cyclooctene	4.14a/c	>99
	4.15a/b	>99
2-methyl styrene	4.14a	99
	4.14b	97
1-methyl cyclohexene	4.14a/b	81-89
	4.14c/d	31-46
Reaction conditions: 24 h, 298 K, 1 mol % catalyst, 3.5 atm (H ₂), solvent (EtOH), (5 mL), 1 mmol of alkene		

Table 4.1

4.4 Group 10 and 11 transition metal complexes bearing RE-NHCs

The reactivity of 6-Mes with Ni(cod)₂ afforded the C-H activated 6-Mes nickel(II) complex **4.16**, whereas the novel three co-ordinate Ni(I) species Ni(6-Mes)(PPh₃)Br **4.17** was generated if the reaction was carried out in the presence of Ni(PPh₃)₂Br₂ (Scheme 4.12).²³



Scheme 4.12: Synthesis of 6-Mes nickel complexes

NHC Nickel complexes have been used in a wide range of catalytic transformations including cross-coupling reactions and cycloadditions.^{8,24-28} Complexes bearing five membered ring carbenes with bulky N-substituents are usually used for catalysis but, in most cases, the nature of the active nickel–NHC species is unclear as generation typically takes place in-situ. The Ni(II) species **4.16** proved to be susceptible to facile decomposition upon mild heating therefore limiting any catalytic potential. In contrast, the three co-ordinate Ni(I) species **4.17** proved to be a useful precursor for catalytic

hydrodehalogenation and cross-coupling reactions,²⁹ showing activity even towards aryl fluorides.²³

After reporting examples of three-co-ordinate Ni(I) complexes in 2010, our group investigated the preparation of a series of well-defined Ni(I) complexes bearing a set of easily modified NHC ligands. The preparation of a series of Ni(NHC)(PPh₃)Br complexes **4.18-4.21** incorporating six-, seven- and eight- membered RE-NHC ligands were reported using the comproportionation reaction of Ni(0) and Ni(II) precursors (Ni(cod)₂ and Ni(PPh₃)₂Br₂) in the presence of two equiv. of the appropriate carbene (Figure 4.2).²⁹

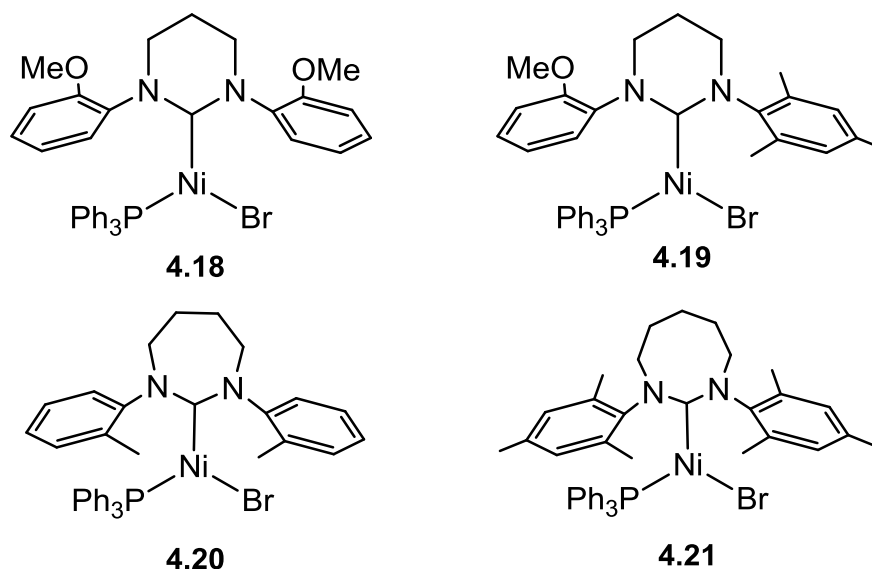
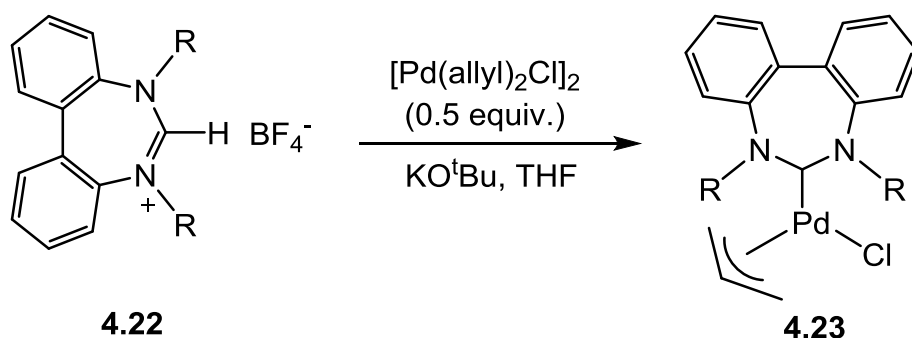


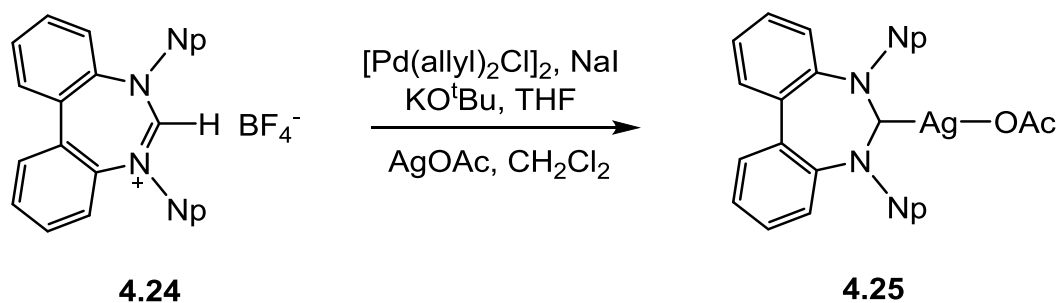
Figure 4.2: Examples of Ni(NHC)(PPh₃)Br complexes

The amidinium salt **4.22** was a novel NHC precursor which led Stahl and co-workers to focus on the preparation of NHC-coordinated Pd(II) complexes. This was easily carried out by deprotonating **4.22** with KO^tBu to give **4.4**. In the presence of a THF solution of [Pd(allyl)₂Cl]₂, this generated the air stable complex **4.23** (Scheme 4.13).³⁰



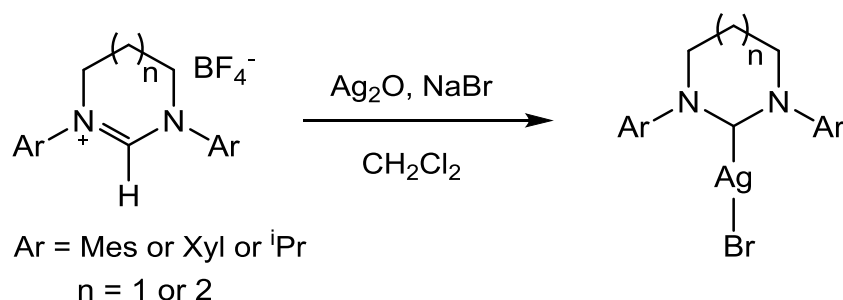
Scheme 4.13: Synthesis of a Pd-NHC complex bearing 7-NHC

After reporting the first example of a seven membered NHC ligand for transition metals, Stahl went on to develop this class of ligands by varying the N-substituents and attempted to synthesise new Ag(I) and Pd(II) complexes. In the case of the neopentyl derivative **4.24** it was found that addition of AgOAc as a route to Pd(NHC)(OAc)₂ gave instead the Ag-NHC complex **4.25** (Scheme 4.14).³¹



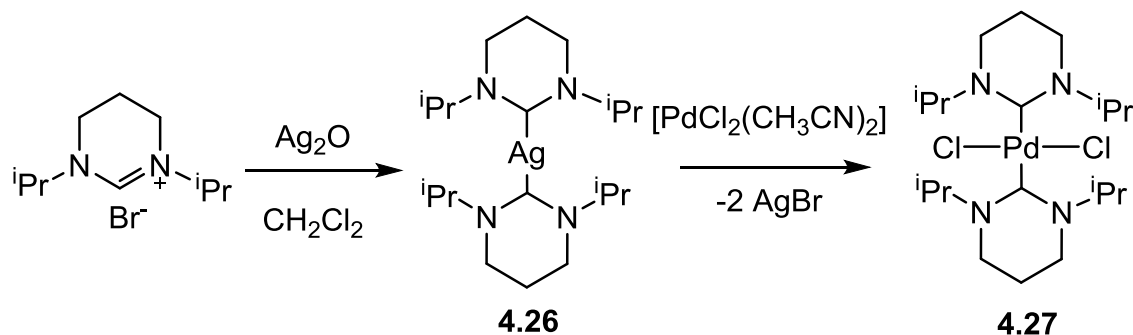
Scheme 4.14: Synthesis of Ag-NHC complex

As already mentioned, Cavell reported in 2008 a more efficient route to the synthesis of several six- and seven membered carbenes, which led to the synthesis of a number of silver complexes. As shown in Scheme 4.15, reaction of the amidinium salts with a slight excess of Ag₂O afforded the corresponding silver complexes in good yields.¹⁷



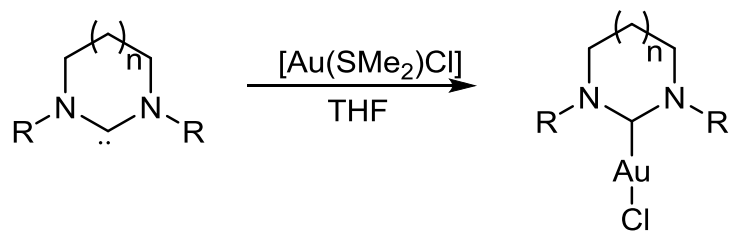
Scheme 4.15: Silver complexes bearing six and seven membered ring NHCs

All the examples described so far with RE-NHCs have produced mono-carbene metal complexes. In 2004, Buchmeiser and co-workers reported examples of bis-NHC complexes of Ag **4.26** and Pd **4.27** (Scheme 4.16). The latter was shown to be a highly active catalyst for Heck reactions of aryl bromides and chlorides.³²



Scheme 4.16: Synthesis of bis-NHC Ag and Pd complexes

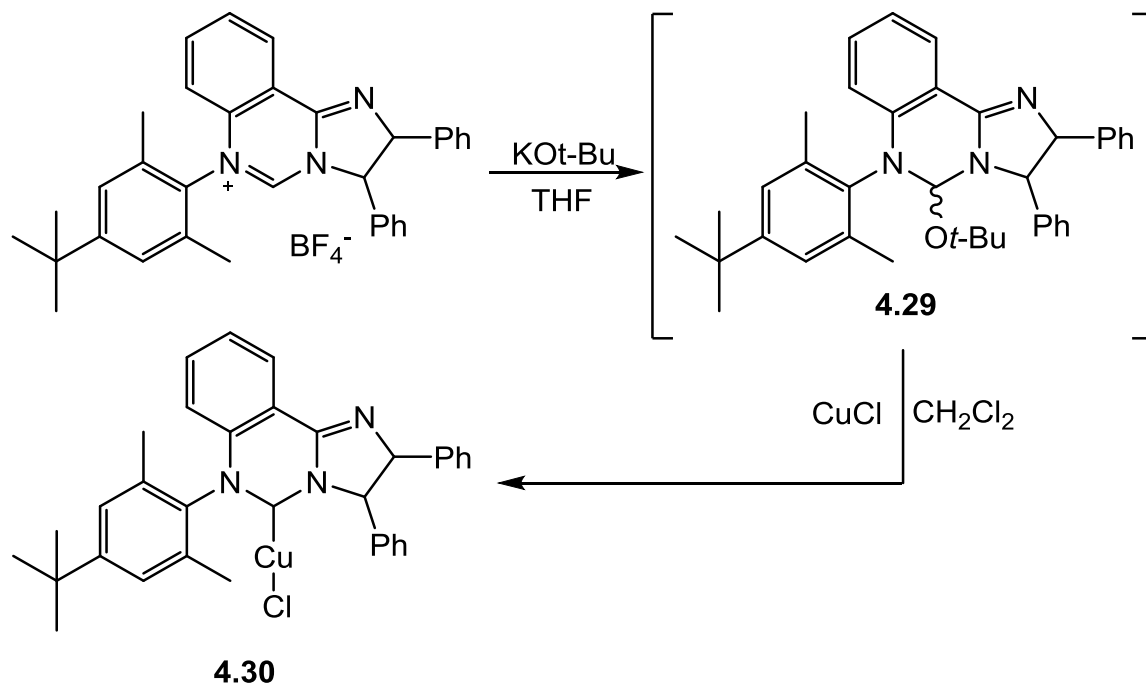
More recently Cavell reported the synthesis and characterization of novel six- and seven membered expanded ring NHC complexes of the general formula Au(NHC)Cl **4.28a-d**. The six- and seven-membered NHC complexes were synthesised in a facile method via the addition of the desired free carbene (generated in situ) to a stirred THF suspension of the commercially available Au(SMe₂)Cl under inert conditions (Scheme 4.17).³³



- 4.28a** (R=Mes) (n=1)
4.28b (R=DIPP) (n=1)
4.28c (R=Mes) (n=2)
4.28d (R=DIPP) (n=2)

Scheme 4.17: Synthesis of Au-NHC complexes

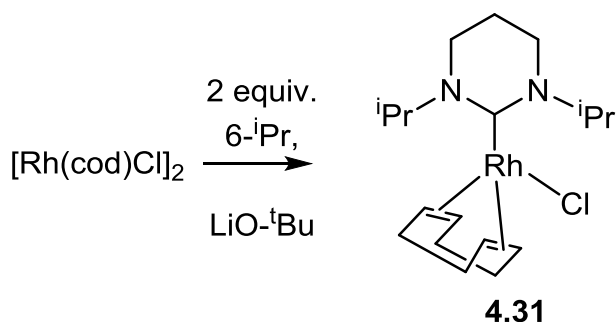
In 2012, McQuade reported the synthesis of the Cu-6-NHC species **4.30** in good yields. The alkoxy adduct **4.29** was considered to be a good precursor based on the observation that the epimeric mixture equilibrates to a single isomer in dichloromethane, suggesting that the $C_{NHC}-O$ bond is labile (Scheme 4.18).³⁴



Scheme 4.18: Synthesis of a Cu complex bearing a RE-NHC

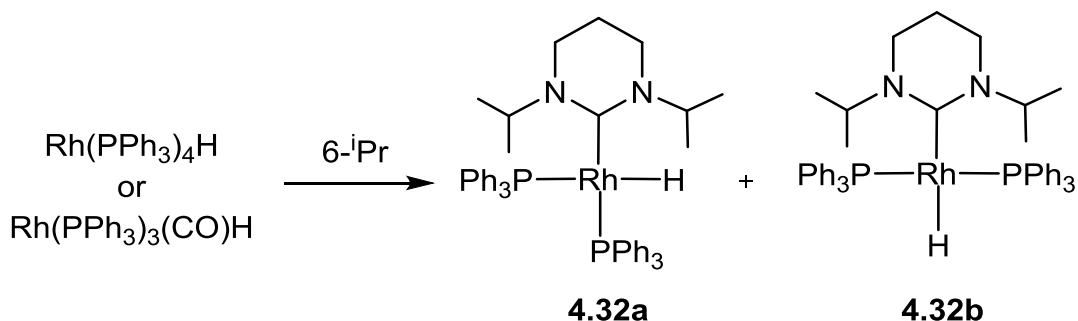
4.5 RE-NHCs with small N-substituents

In 1996 Hermann and co-workers generated the first examples of mono- and bis-NHC Rh complexes with NHCs of low steric demand such as 1,3-dimethylimidazolin-2-ylidene.³⁵ Buchmeiser and co-workers reported the reactivity of $[\text{Rh}(\text{cod})\text{Cl}]_2$ with 6-ⁱPr which generated the mono-carbene complex $\text{Rh}(6\text{-}^i\text{Pr})(\text{cod})\text{Br}$ **4.31** (Scheme 4.19).³²



Scheme 4.19: Synthesis of an Rh complex bearing 6-ⁱPr

In 2012, our group investigated the reactivity of the 6-membered NHC 6-ⁱPr towards $\text{Rh}(\text{PPh}_3)_4\text{H}$ and $\text{Rh}(\text{PPh}_3)_3(\text{CO})\text{H}$. Addition of three equiv. of 6-ⁱPr to a toluene solution of $\text{Rh}(\text{PPh}_3)_4\text{H}$ at 343 K for 2-3 h afforded the monocarbene complex $\text{Rh}(6\text{-}^i\text{Pr})(\text{PPh}_3)_2\text{H}$ **4.32** as a 1:2 mixture of the cis- and trans-phosphine isomers **4.32a/b** (Scheme 4.20).³⁶



Scheme 4.20: Synthesis of $\text{Rh}(6\text{-}^i\text{Pr})(\text{PPh}_3)_2\text{H}$

The same products were also ultimately formed from the carbonyl precursor $\text{Rh}(\text{PPh}_3)_3(\text{CO})\text{H}$, which reacted with 6-ⁱPr at room temperature. However, with the carbonyl precursor, the formation of two additional species at early times was observed which were identified as the cis- and trans-isomers of the monocarbonyl complex $\text{Rh}(6\text{-}^i\text{Pr})(\text{PPh}_3)(\text{CO})\text{H}$. Upon leaving the reaction mixture at room temperature overnight, both isomers of $\text{Rh}(6\text{-}^i\text{Pr})$

ⁱPr)(PPh₃)(CO)H disappeared, leaving **4.32a/b** as the only products. This transformation was achievable in 2 h if the reaction mixture was warmed to 343 K.³⁶

The studies described in Chapter 2 and 3 portrayed the synthesis and reactivity of 5-NHCs towards a variety of ruthenium precursors. In light of our group's work (Scheme 4.5, 4.6 and 4.20), we attempted the synthesis of new ruthenium and rhodium complexes bearing the small 6-NHCs, 6-Me and 6-Et (Figure 4.3), as these have had little consideration in the literature.^{10,37-39}

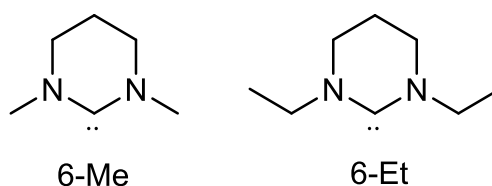


Figure 4.3: 6-NHCs used in our studies

4.6 Preparation of the salts [6-MeH]PF₆ and [6-EtH]PF₆

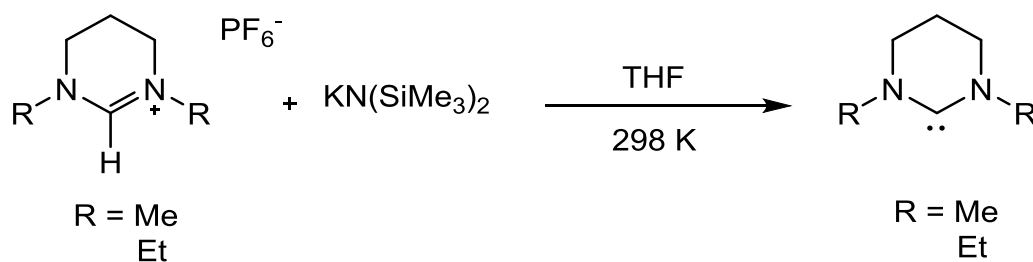
The hexafluorophosphate salts [6-MeH]PF₆ and [6-EtH]PF₆ were prepared following the procedure reported by Delaude and co-workers (Scheme 4.4).¹⁹ A microwave vial was charged with N,N'-dimethyl-1,3-propanediamine (1 mmol) and NH₄PF₆ (1 mmol) in triethyl orthoformate (5 mL) and irradiated for 5 min at 418 K with 25 W microwave power to afford [6-MeH]PF₆ in 66% yield. The same method was applied to synthesise [6-EtH]PF₆ (also isolated in 66% yield) starting from N,N'-diethyl-1,3-propanediamine.

It should be pointed out that the 6-Me and 6-Et BF₄ salts were extremely hygroscopic and quickly became deliquescent upon exposure to air, therefore preventing further reactivity studies. However the corresponding hexafluorophosphate salts were not hygroscopic and were more suitable to carry out reactivity studies towards Ru and Rh precursors.

4.7 Generating the free carbenes 6-Me and 6-Et

In initial tests on an NMR scale, both [6-MeH]PF₆ and [6-EtH]PF₆ were rapidly deprotonated by KN(SiMe₃)₂ in THF-*d*₈ to give the respective carbenes

within 30 min at 298 K, as evidenced by the loss of the high frequency C2-proton resonances at 7.93 and 7.94 ppm respectively (Scheme 4.21).



Scheme 4.21: Synthesis of the free carbenes

Interestingly, the NMR spectra of the salts in C_6D_6 were extremely broad and unresolved. The C2-proton signals could not be observed definitively, making it impossible to analyse the success of deprotonation (Figure 4.4). For this reason, the free carbenes were generated in THF rather than benzene, the solvent then removed under vacuum and the residue redissolved in C_6H_6 before addition to benzene solutions of Ru and Rh precursors.

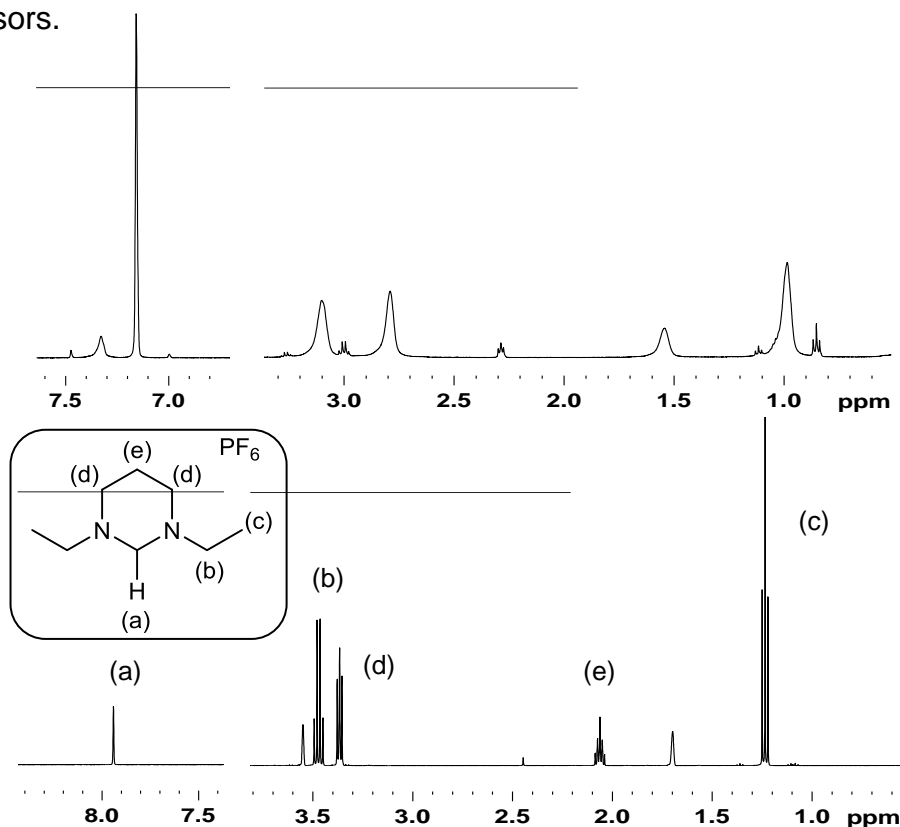
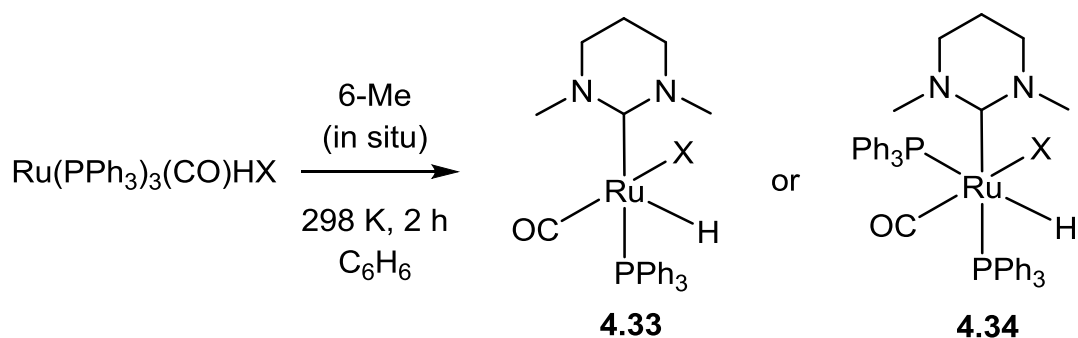


Figure 4.4: ^1H NMR spectrum of $[\text{6 EtH}]^+$ in C_6D_6 (top) and $\text{THF-}d_8$ (bottom)

4.8 Reactions of ruthenium precursors with 6-Me/6-Et

In light of the reactions of $\text{Ru}(\text{PPh}_3)_3(\text{CO})\text{HX}$ ($\text{X}=\text{F},\text{Cl}$) complexes with 6-ⁱPr shown in Schemes 4.5 and 4.6, we anticipated that C-H activation of the RE-NHC could occur for 6-Et, whereas in the case of 6-Me, formation of a 5- or 6-coordinate non-activated species (**4.33** or **4.34**) was most likely (Scheme 4.22).



Scheme 4.22: Reaction of $\text{Ru}(\text{PPh}_3)_3(\text{CO})\text{HX}$ with 6-Me

Addition of three equiv. in-situ generated 6-Me to $\text{Ru}(\text{PPh}_3)_3(\text{CO})\text{HCl}$ in C_6D_6 at 298 K led to colour change from red to brown over a period of ca. 2 h. Addition of hexane gave a yellow precipitate, which showed a triplet hydride resonance at -7.75 ppm ($^2J_{\text{HP}} = 22.5$ Hz) consistent with a bis-phosphine containing product with the Ru-H cis to the two phosphine ligands. This ruled out the possibility of the product being the 5-coordinate mono-phosphine complex **4.33**.

The remaining signals of the ^1H NMR spectrum of the 6-coordinate complex $\text{Ru}(6\text{-Me})(\text{PPh}_3)\text{COHCl}$ **4.34** should be straightforward to assign and would possibly contain a singlet, triplet and a quintet with integrals of 6:4:2 respectively for the 6-Me. As this was not observed (Figure 4.5) it was apparent that **4.34** could not have been generated either. The ^1H NMR spectrum displayed a multiplet, two triplets and a singlet with relative integrals of 2:2:2:3 (Figure 4.5). These signals were assigned to the $\text{N-CH}_2\text{CH}_2$, NCH_2 , NCH_2 and N-CH_3 protons of the carbene using HSQC spectroscopy (Figure 4.6). However there was another singlet at 2.7 ppm which integrated to 2H, suggestive of a $\text{Ru-CH}_2\text{-N}$ group, which pointed to the possibility of a C-H activated 6-Me carbene, although this would produce a highly strained 4

membered ruthenacycle. The product was thus tentatively identified as **4.35** (Scheme 4.23). The crude product was also analysed by $^{31}\text{P}\{^1\text{H}\}$ NMR spectroscopy. A singlet was apparent at 60.8 ppm consistent with a single trans-phosphine product, along with trace amounts of free PPh_3 and $\text{PPh}_3=\text{O}$.

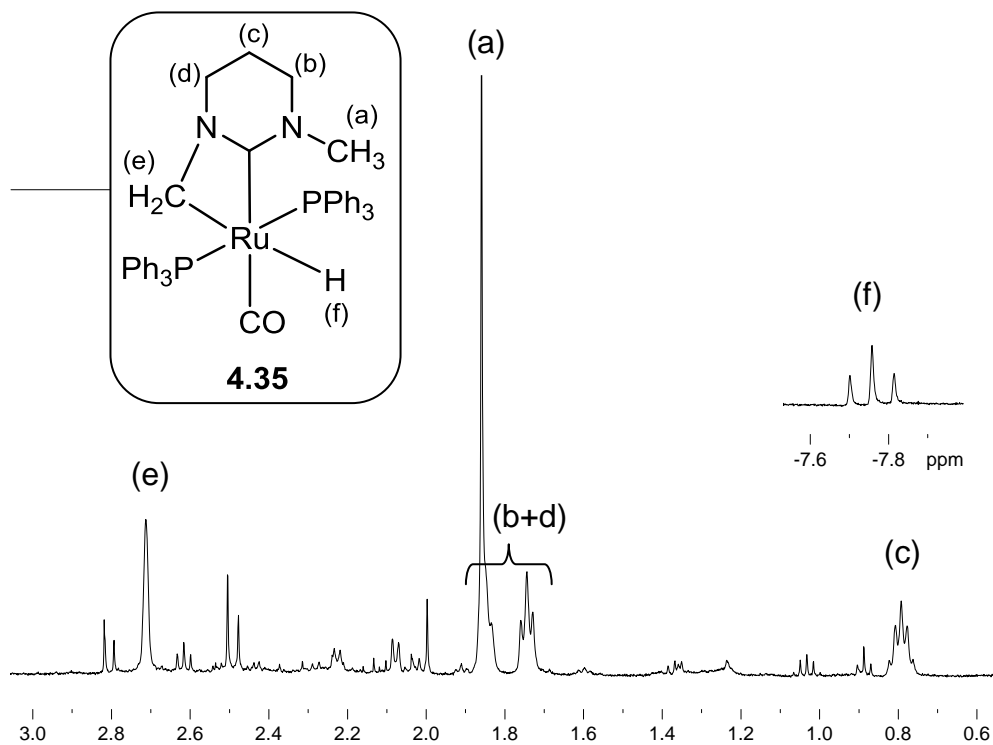
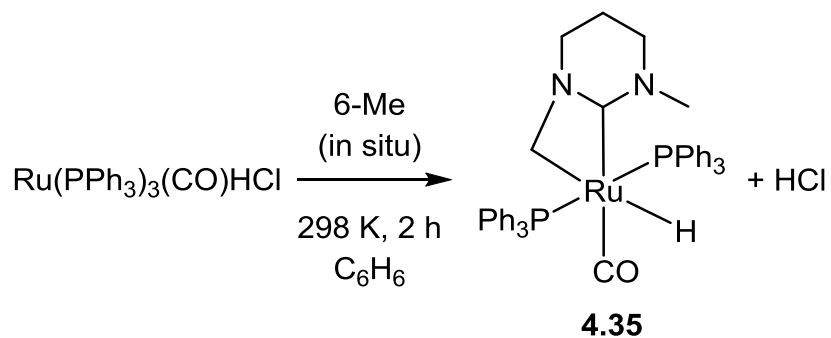


Figure 4.5: Partial ^1H NMR spectrum of **4.35** (C_6D_6 , 500 MHz)



Scheme 4.23: Reaction of $\text{Ru}(\text{PPh}_3)_3(\text{CO})\text{HCl}$ with 6-Me

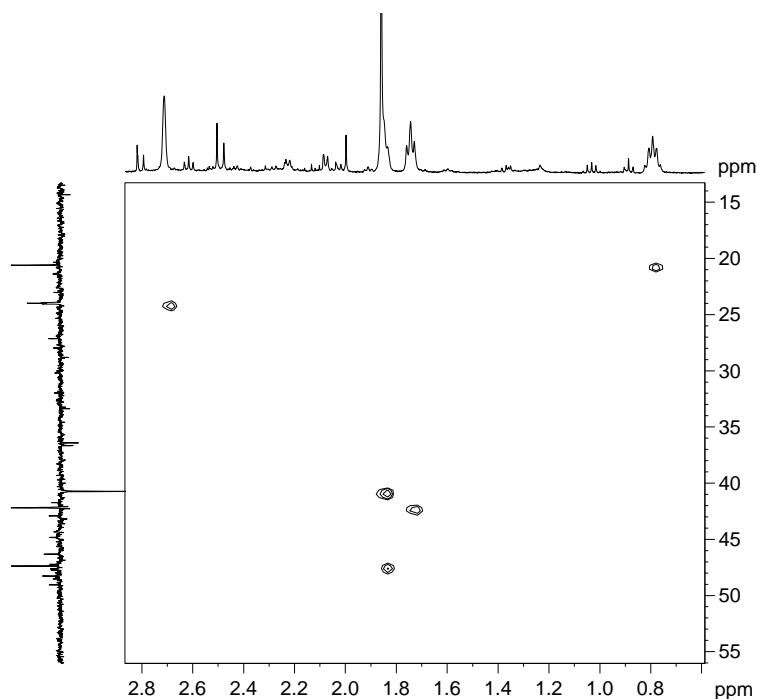


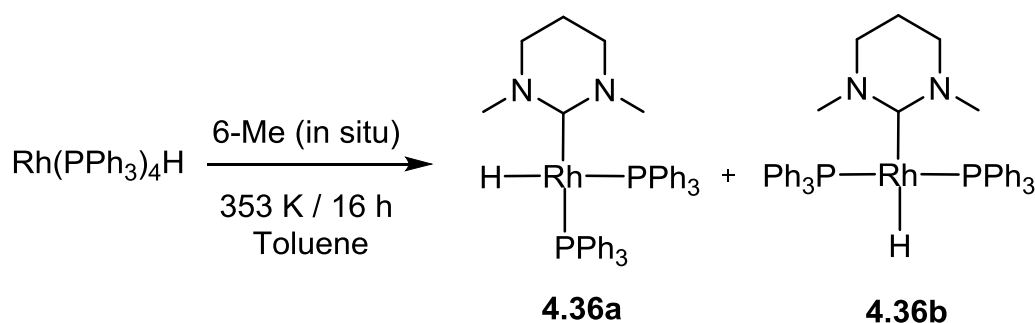
Figure 4.6: ^1H - ^{13}C HSQC NMR spectrum of **4.35**

More definitive evidence for **4.35** being a non-halide containing product came from the fact that the same ^1H and $^{31}\text{P}\{^1\text{H}\}$ NMR spectra were generated when the starting material was changed from $\text{Ru}(\text{PPh}_3)_3(\text{CO})\text{HCl}$ to $\text{Ru}(\text{PPh}_3)_3(\text{CO})\text{HF}$. Multiple attempts were made to isolate and crystallise **4.35**, but these were unsuccessful.

Preliminary reactions of the hydride halide ruthenium precursors and 6-Et were carried out and the product formed also appeared to be C-H activated like **4.35** on the basis of observations in the ^1H and ^{31}P NMR spectra. Failure to crystallise any compound prevented any additional reactions from being carried out.

4.9 Synthesis of Rh(6-Me)(PPh₃)₂H (4.36)

Addition of three equiv. 6-Me to a benzene solution of Rh(PPh₃)₄H resulted in very little reaction over 2 days at room temperature. Upon heating to 353 K for 16 h, the hydride complex Rh(6-Me)(PPh₃)₂H (**4.36**) was formed and isolated as an orange powder in 54% yield. This complex was present in solution as a mixture of cis- and trans-phosphine isomers in a ratio of ca. 1:20 (Scheme 4.24). The major trans-phosphine isomer **4.36b** was characterised through a combination of X-ray crystallography and 1D and 2D NMR spectroscopy.



Scheme 4.24: Preparation of cis-/trans- isomers of Rh(6-Me)(PPh₃)₂H

The ¹H NMR spectrum of the major trans-P,P isomer **4.36b** is shown in Figure 4.7. The hydride region showed the expected triplet of doublets signal at -9.2 ppm with ²J_{HP} and ¹J_{HRh} splittings of 23 and 11 Hz respectively. Higher frequency signals at 1.0 ppm (quintet), 2.0 ppm (triplet) and 3.2 ppm (singlet) were assigned to the protons at the C5, C4/C6 and N-Me positions, respectively. The hydride resonance for the cis-isomer **4.36a** was visible at -5.2 ppm, but the low concentration of the compound made assignment of other signals uncertain. Only **4.36b** could be seen in the ³¹P{¹H} NMR spectrum and showed the expected doublet resonance, with a ¹J_{PRh} coupling constant of 180 Hz.

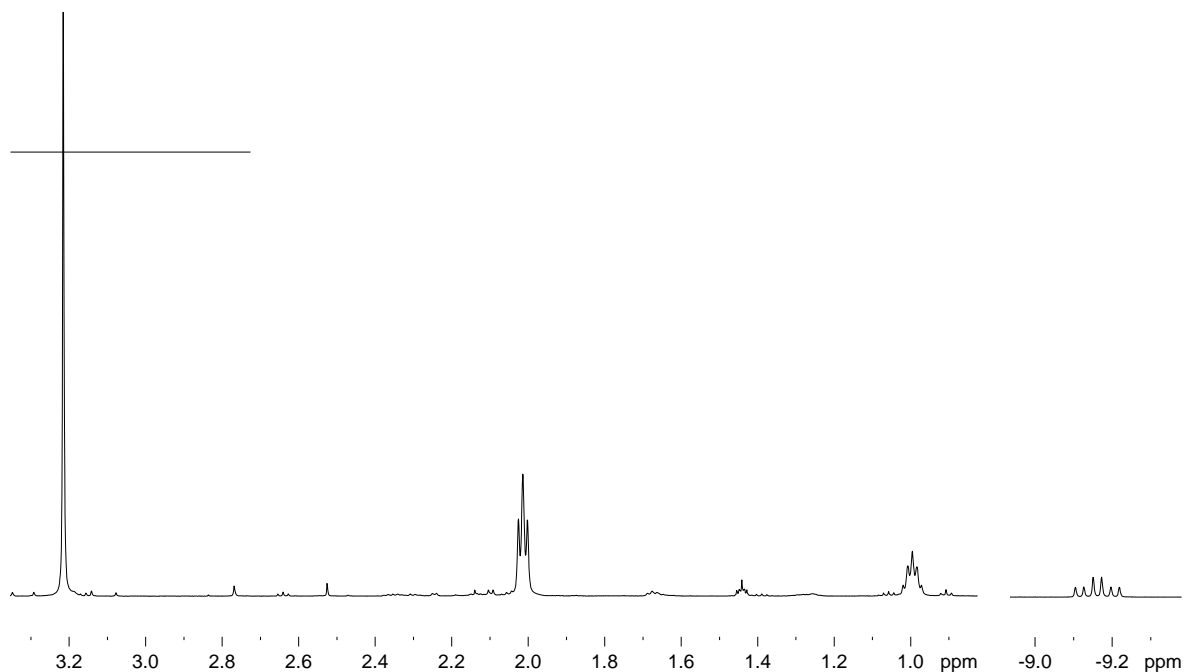


Figure 4.7: Partial ^1H NMR spectrum of the trans-phosphine isomer **4.36b**
(C_6D_6 , 500 MHz)

The X-ray crystal structure of **4.36b** showed the single hydride, two PPh_3 ligands and 6-Me ligand in a distorted square planar geometry ($\text{P-Rh-P} = 155.03(2)^\circ$) (Figure 4.8). The Rh-C_{NHC} distance in **4.36b** ($2.081(1) \text{ \AA}$) was shortened significantly compared to that in the 6- ^iPr analogue **4.32b** ($2.0928(13) \text{ \AA}$)³⁶ presumably as a result of lower repulsion between the metal and N-Me vs N- ^iPr substituents.

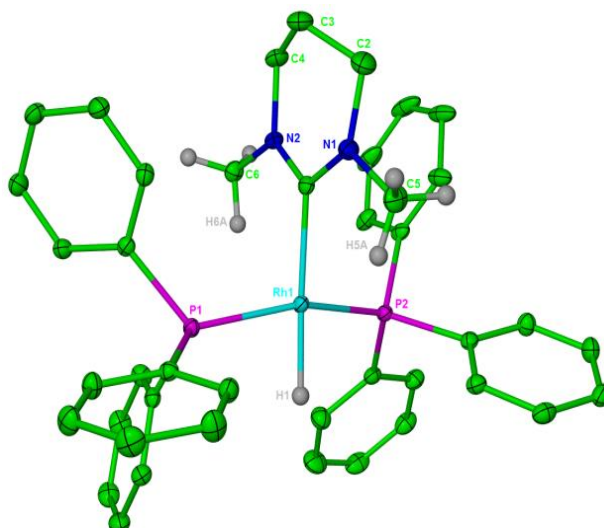
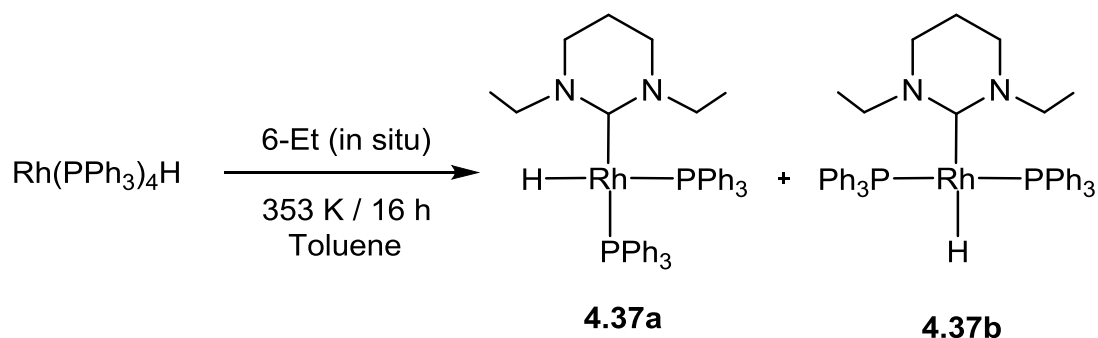


Figure 4.8: Molecular structure of trans-phosphine isomer of Rh(6-Me)(PPh₃)₂H (**4.36b**). Ellipsoids are shown at the 30% level. Hydrogen atoms except for Rh-H and N-Me are removed for clarity. Selected bond lengths (Å) and angles (°): Rh(1)-P(1) 2.2294(5), Rh(1)-P(2) 2.2388(5), Rh(1)-C(1) 2.081(1), P(1)-Rh(1)-C(1) 101.54(6), P(1)-Rh(1)-P(2) 155.03(2).

4.10 Synthesis of Rh(6-Et)(PPh₃)₂H (**4.37**)

Reaction of Rh(PPh₃)₄H with 6-Et under identical conditions to those used to prepare **4.36** gave Rh(6-Et)(PPh₃)₂H (**4.37**) as an orange powder in 64% yield. Like **4.36**, this complex was also present in solution as a mixture of cis- and trans-phosphine isomers, but now in a ratio of ca. 1:9 (Scheme 4.25).



Scheme 4.25: Preparation of cis-/trans- isomers of Rh(6-Et)(PPh₃)₂H

The greater concentration of the cis isomer **4.37a** allowed identification of both forms by NMR spectroscopy. The major trans-isomer **4.37b** was identified by the appearance of a triplet of doublets hydride resonance at -9.8

ppm with couplings of 25.0 Hz ($^2J_{HP}$) and 11.0 Hz ($^1J_{HRh}$). The cis-isomer exhibited a doublet of doublet of doublets hydride signal at -5.4 ppm with couplings of 106.9 Hz ($^2J_{HP}$), 30.5 Hz ($^2J_{HP}$ or $^1J_{HRh}$) and 25.9 Hz ($^2J_{HP}$ or $^1J_{HRh}$). The $^{31}\text{P}\{^1\text{H}\}$ NMR spectrum showed a doublet at 45.8 ppm with coupling of 180 Hz ($^1J_{PRh}$) for the trans-isomer and two doublets of doublets for the cis-isomer (Figure 4.9).

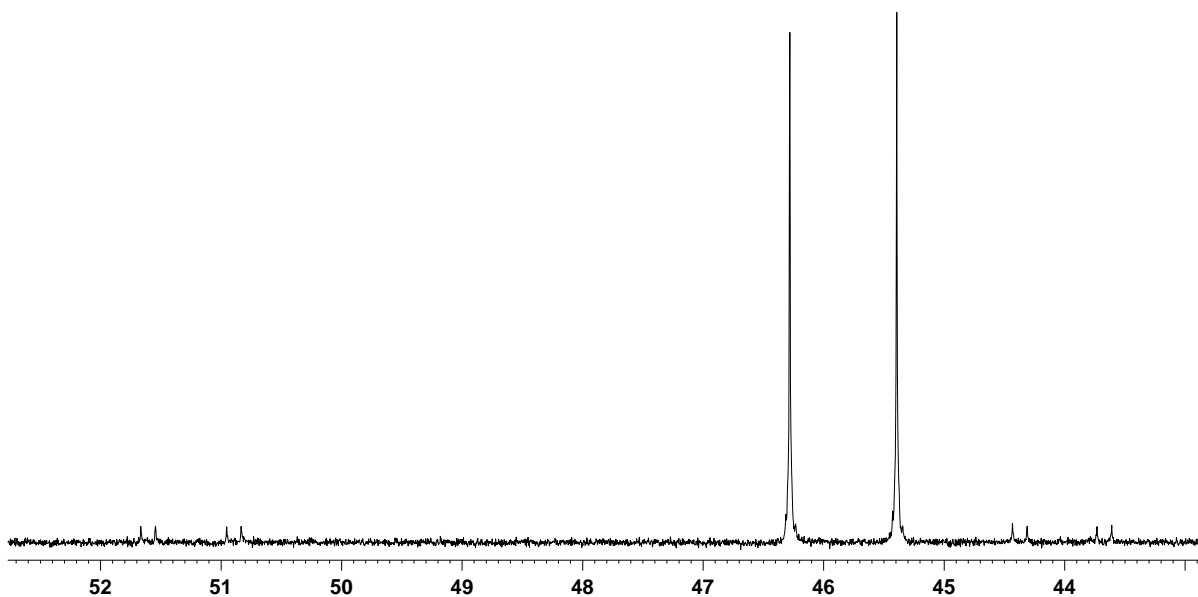


Figure 4.9: $^{31}\text{P}\{^1\text{H}\}$ NMR spectrum of **4.37a/b** (C_6D_6 , 298K, 202 MHz)

As in the 6-Me case, the X-ray crystal structure of the trans-phosphine isomer **4.37b** revealed a distorted square planar geometry at the rhodium centre with a P-Rh-P angle of $150.11(2)^\circ$ (Figure 4.10). The Rh- C_{NHC} distance in **4.37b** ($2.086(2)$ Å) was the same within error as that in **4.32b** ($2.0928(13)$ Å), but at the low end, making it more similar to that of **4.36b** ($2.081(2)$ Å). This further supports the close approach of NHCs with small N-groups to the Rh in these types of complexes. The relatively short Rh \cdots C(9) and Rh \cdots H(7B) distances of 3.086 Å and 2.341 Å (shown by a dotted line) indicated that there could be an agostic interaction. Previous work by Aldridge et al reported that it is unlikely that there could be any agostic interaction stabilizing the metal centre with Rh \cdots C contacts being >3.8 Å.⁴⁰ However, Nolan and co-workers reported Rh(^tBu)($^i\text{Bu}'$)HCl where the empty coordination site in the 16-electron complex was taken up by a strong agostic interaction with Rh \cdots C and

Rh \cdots H distances of 2.704 Å and 2.073 Å respectively.⁴¹ Based on these findings, the Rh \cdots H(7B) distance in **4.37b** perhaps suggests a very weak agostic interaction.

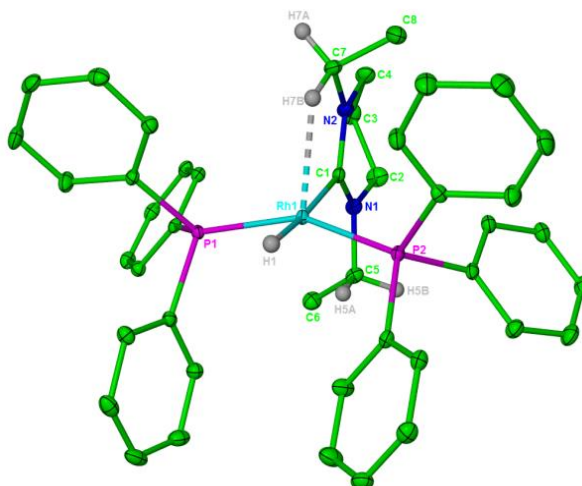
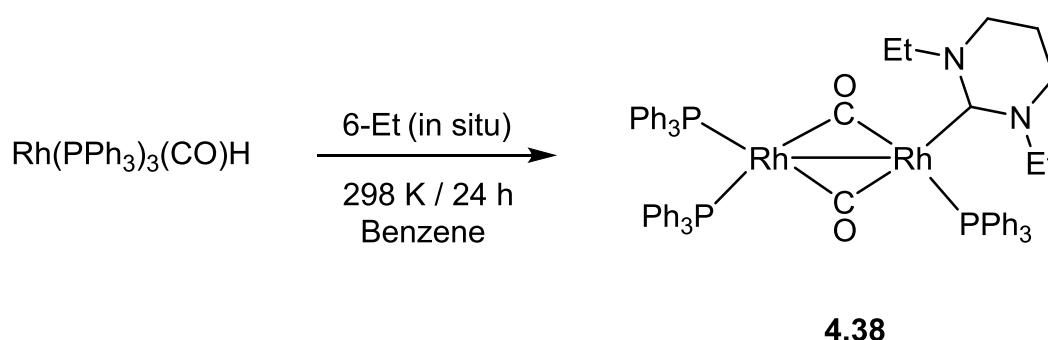


Figure 4.10: Molecular structure of Rh(6-Et)(PPh₃)₂H **4.37b**. Ellipsoids are shown at the 30% level. Hydrogen atoms except for Rh-H and N-CH₂ are removed for clarity. Selected bond lengths (Å) and angles (°): Rh(1)-P(1) 2.2266(5), Rh(1)-P(2) 2.2492(5), Ru(1)-C(1) 2.086(1), P(1)-Rh(1)-C(1) 102.23(6), P(1)-Rh(1)-P(2) 150.11(2).

There is substantial asymmetry of the metal-carbene bonding in both **4.36b** and **4.37b**, which is exemplified by the difference in the N-C-Rh angles of 118.22(12)/125.47(13)° (**4.36b**) and 117.17(14)/126.45(15)° (**4.37b**).

4.11 Reaction of Rh(PPh₃)₃(CO)H with NHCs

Given that both Rh(PPh₃)₄H and Rh(PPh₃)₃(CO)H gave the same final product upon reaction with 6-*i*-Pr (Scheme 4.5), both 6-Me and 6-Et were reacted with the carbonyl precursor. An NMR tube was charged with three equiv. of 6-Et and Rh(PPh₃)₃(CO)H in benzene and left to stand at 298 K. During the reaction, gas evolution was observed. After 24 h, the solvent was concentrated and hexane added to afford a few dark red crystals that proved to be the dinuclear compound [(PPh₃)₂Rh(μ-CO)₂Rh(6-Et)(PPh₃)] (**4.38**) (Scheme 4.26). The product was characterised through a combination of X-ray crystallography and ³¹P{¹H} NMR spectroscopy.



Scheme 4.26: Synthesis of [(PPh₃)₂Rh(μ-CO)₂Rh(6-Et)(PPh₃)] **4.38**

The X-ray crystal structure of **4.38** (Figure 4.11) consists of a square-planar Rh(1)-carbene-PPh₃ fragment (C(1)-Rh(1)-P(1) 96.81(9)°; C(27)-Rh(1)-C(28) 93.07(12)°) connected to a distorted tetrahedral Rh(2)-(PPh₃)₂ unit (P(2)-Rh(2)-P(3) 121.25(3)°) via two bridging CO ligands and a Rh-Rh bond. These distortions are probably due to a large steric interaction between the P(2) and P(3) phosphine ligands. The Rh(2)-P(2) and Rh(2)-P(3) bond distances are the same (2.3291(8)° and 2.3407(8)° respectively), whereas the Rh(1)-P(1) distance (2.2739(8)°) is significantly shorter presumably as a result of the different geometries of the two metal centres.

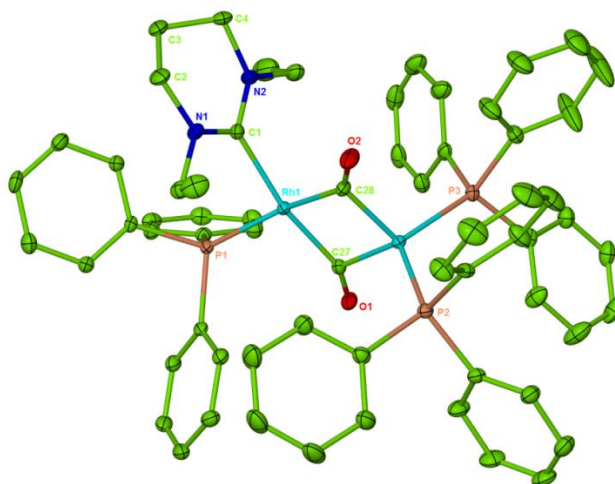
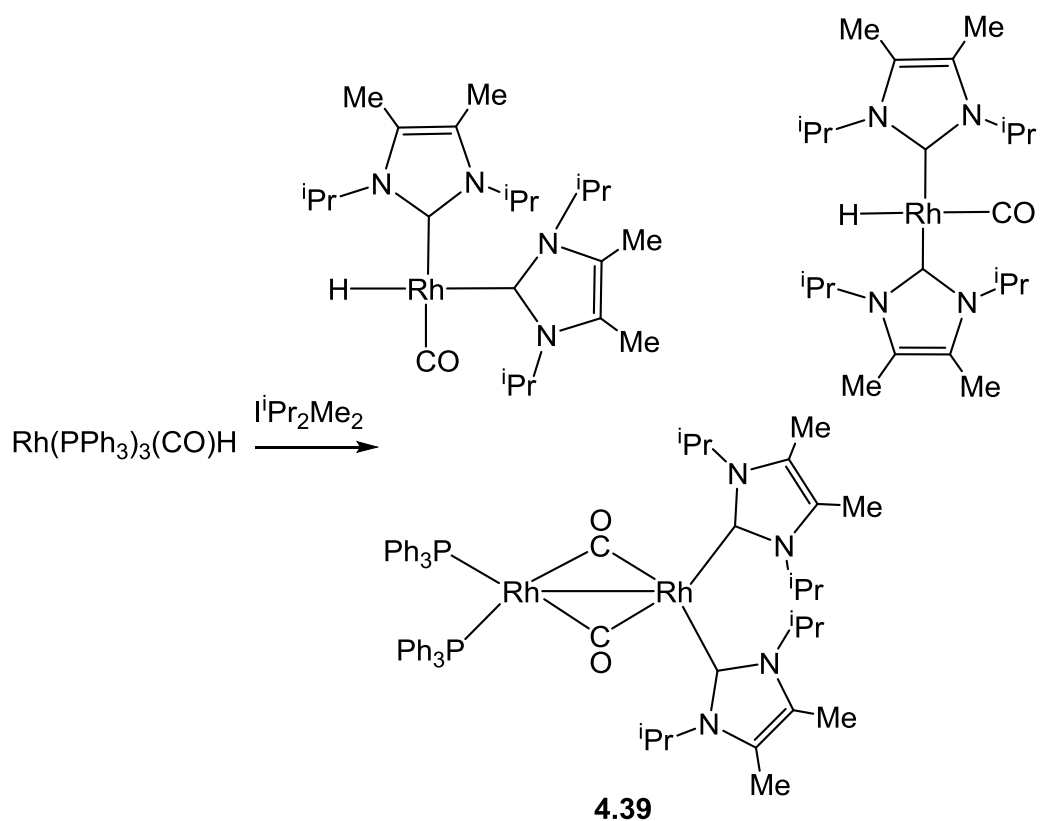


Figure 4.11: Molecular structure of $[(PPh_3)_2Rh(\mu-CO)_2Rh(6-Et)(PPh_3)]$ **4.38**. Ellipsoids are shown at the 30% level. Hydrogen atoms are removed for clarity. Selected bond lengths (Å) and angles (°): Rh(1)-C(1) 2.090(3), Rh(1)-C(27) 1.984(3), Rh(1)-C(28) 2.023(3), Rh(2)-C(28) 1.938(3), Rh(2)-C(27) 1.990(3), Rh(1)-P(1) 2.2739(8), Rh(2)-P(2) 2.3291(8), Rh(2)-P(3) 2.3407(8), C(27)-Rh(1)-C(28) 93.07(12).

The product generated can be contrasted with the symmetrical μ -CO bridging dimer **4.39** (Scheme 4.39) which is formed in the reaction of $Rh(PPh_3)_3(CO)H$ and six equiv. of $I^iPr_2Me_2$. An isomeric mixture of the mononuclear bis-carbene complex $Rh(I^iPr_2Me_2)_2(CO)H$ was formed along with the carbonyl bridged dimer (Scheme 4.27).⁴² The Rh-Rh bond distance of 2.694 Å is identical to that found in **4.39** (2.6939 Å).



Scheme 4.27: Synthesis of Rh bis- $i\text{Pr}_2\text{Me}_2$ complexes and a bridged dimer

4.38 can also be compared to the dimer **4.40** reported by Freeman⁴³, which also consisted of two rhodium atoms and bridging carbonyls (Figure 4.12). Like **4.38**, **4.40** comprised of square-planar and distorted-tetrahedral fragments. The Rh(1)-Rh(2) bond distance in **4.40** (2.718 (1) Å) is slightly longer than that in **4.38**.

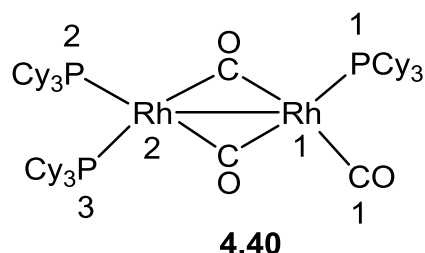


Figure 4.12: Dimer $(\text{PCy}_3)_2\text{Rh}(\mu\text{-CO})_2\text{Rh}(\text{CO})\text{PCy}_3$ reported by Freeman

The $^{31}\text{P}\{^1\text{H}\}$ NMR spectrum of redissolved single crystals of **4.38** in $\text{THF-}d_8$ displayed a doublet at 40.2 ppm ($J_{\text{PRh}} = 183$ Hz) and a doublet of doublets at 35.3 ppm ($J_{\text{PRh}} = 235$ Hz, $^2J_{\text{PRh}} = 8$ Hz) (Figure 4.13).

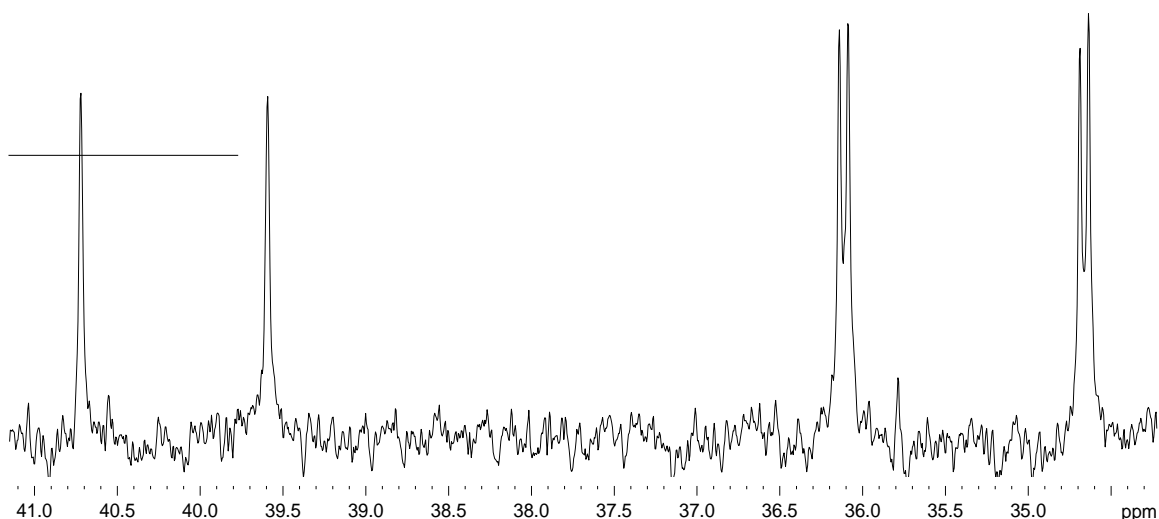


Figure 4.13: $^{31}\text{P}\{^1\text{H}\}$ NMR spectrum of **4.38** (THF- d_8 , 298 K, 161 MHz)

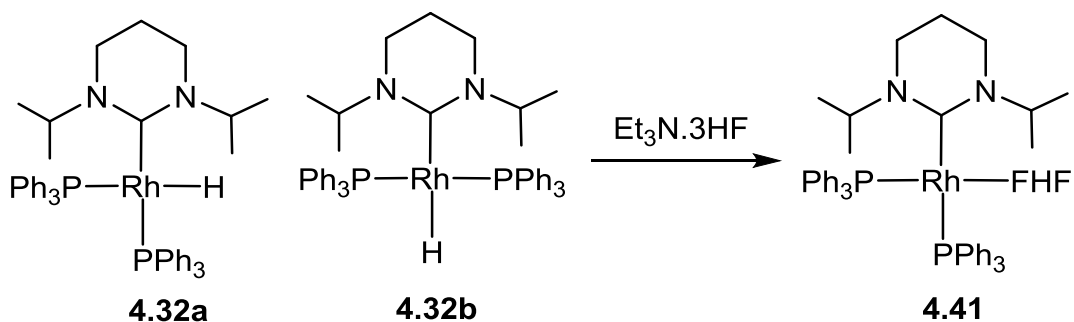
The room temperature $^{31}\text{P}\{^1\text{H}\}$ NMR spectrum of **4.40** consisted of a doublet of doublets at δ 50.5 ($^1J_{\text{PRh}} = 223$ Hz, $^2J_{\text{PRh}} = 9$ Hz) and a doublet at δ 42.8 ($J_{\text{PRh}} = 156$ Hz). Upon lowering the temperature to 183 K, the signal at 50.5 ppm resolved into two broad doublets at 49.0 ppm ($^1J_{\text{PRh}} = 240$ Hz) and 52.0 ppm ($^1J_{\text{PRh}} = 240$ Hz) assigned to the phosphines P(2) and P(3) on Rh(2). From the crystal structure it was evident that the P(2)Rh(2)P(3) plane was rotated 80.3° with respect to the Rh(2)(CO)(CO)Rh(2) plane and therefore P(2) and P(3) occupied non equivalent sites with respect to P(1) and C(1). Rapid oscillation of P(2) and P(3) through the 90° tetrahedral position to the opposite and equivalent 80.3° position would make P(2) and P(3) magnetically equivalent and as a result explained the presence of the two broad doublets.

A CH_2Cl_2 solution of **4.38** was analysed by IR spectroscopy and displayed a broad peak at 1717 cm^{-1} for the bridging CO. This value is comparable with that in **4.39** at 1708 cm^{-1} .

The reaction with $\text{Rh}(\text{PPh}_3)_3(\text{CO})\text{H}$ and 6-Me was carried out under the same conditions described with 6-Et to see if the reaction also generated a dimer. Following the reaction by ^{31}P NMR spectroscopy, the starting material at 41.2 ppm was observed along with a doublet and a doublet of doublets at 42.9 and 38.1 ppm respectively from the product. Heating the sample for 2 h at 343 K led to complete conversion to product although, the 6-Me derivative only formed an oily precipitate.

4.12 Preparation of the bifluoride complexes Rh(6-NHC)(PPh₃)₂(FHF)

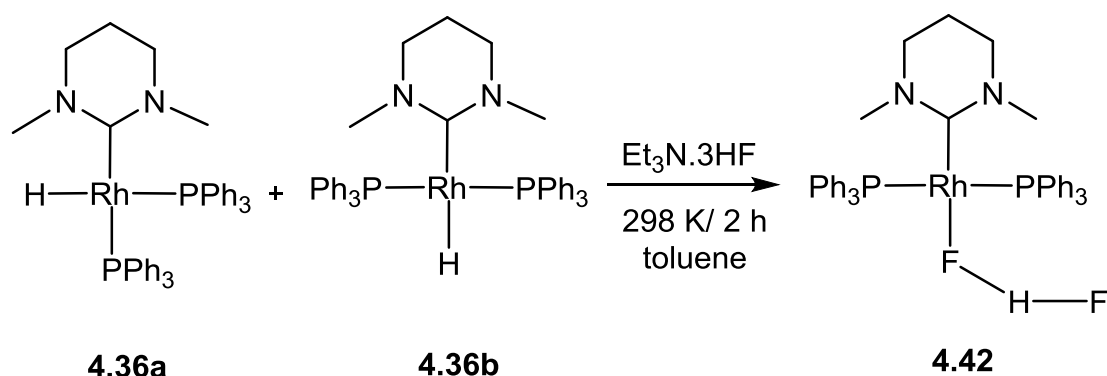
The reported reactivity of Rh(6-ⁱPr)(PPh₃)₂H **4.32** towards Et₃N·3HF to afford the bifluoride complex **4.41** (Scheme 4.28)³⁶ led us to probe the reactivity of both **4.35a/b** and **4.36a/b** towards this reagent.



Scheme 4.28: Preparation of Rh(6-ⁱPr)(PPh₃)₂(FHF)

4.13 Synthesis of Rh(6-Me)(PPh₃)₂(FHF) (**4.42**)

A toluene solution of **4.36a/b** and one equivalent of Et₃N·3HF stirred for 2 h at 298 K afforded the bifluoride complex Rh(6-Me)(PPh₃)₂(FHF) **4.42**, which was isolated as a yellow powder in 44% yield (Scheme 4.29).



Scheme 4.29: Synthesis of Rh(6-Me)(PPh₃)₂(FHF)

The ³¹P{¹H} NMR spectrum of **4.42** displayed a single broad doublet of doublet resonance at 26.1 ppm (¹J_{PRh} = 173 Hz, ²J_{PF} = 13 Hz) consistent with (i) formation of a single isomer of the product and (ii) this isomer having a trans arrangement of phosphines rather than the cis-P,P geometry found in the 6-ⁱPr analogue **4.41**.

The appearance of the signals for the FHF ligand were, unsurprisingly, temperature dependent. In the room temperature ^1H NMR spectrum recorded in $\text{THF-}d_8$, the bifluoride proton appeared as a single, very broad resonance, (Figure 4.14) which partially resolved into the expected doublet of doublets ($J_{\text{HF}} = 379, 42$ Hz) and shifted ca. 0.9-1.0 ppm with cooling to 190 K. The broadening of the FHF signal in $\text{THF-}d_8$ most likely reflects some interaction with the solvent.⁴⁴

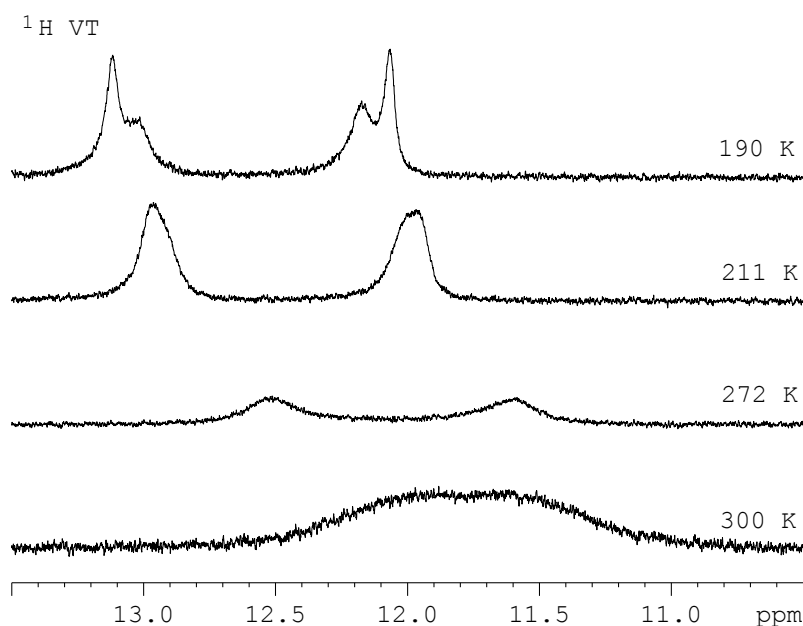


Figure 4.14: Variable temperature ^1H NMR spectra of **4.42** in $\text{THF-}d_8$ (400 MHz)

The room temperature ^{19}F NMR spectrum in $\text{THF-}d_8$ exhibited two broad singlets at -316.4 (proximal Rh-F-H-F) ppm and -181.3 (distal Rh-F-H-F) ppm. Upon cooling to 190 K, the ^{19}F NMR spectrum resolved to a doublet of doublets signal at -176.9 ppm with $^1J_{\text{FH}}$ and $^2J_{\text{FF}}$ of 381 Hz and 127 Hz respectively and a broad doublet at -312.0 ppm with $^2J_{\text{FF}}$ ca. 125 Hz (Figure 4.15).

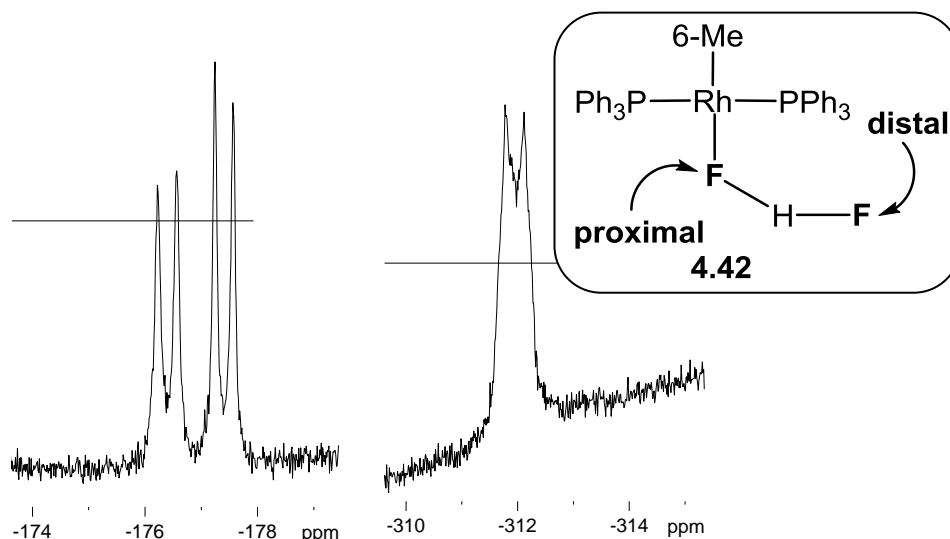


Figure 4.15: 190 K ^{19}F NMR spectrum of **4.42** (THF- d_8 , 470 MHz)

Complex **4.42** was less soluble in C_6D_6 and $\text{tol-}d_8$, but at the same time exhibited very different spectra to those measured in THF- d_8 . In the ^1H NMR spectrum in $\text{tol-}d_8$ at 298 K, a broad doublet at 12.8 ppm ($J \approx 390$ Hz) was observed for the bifluoride proton (Figure 4.16). Upon cooling to 224 K, there was only partial resolution of the bifluoride signal, which now exhibited an additional $^1J_{\text{HF}(\text{proximal})}$ splitting of ≈ 38 Hz.

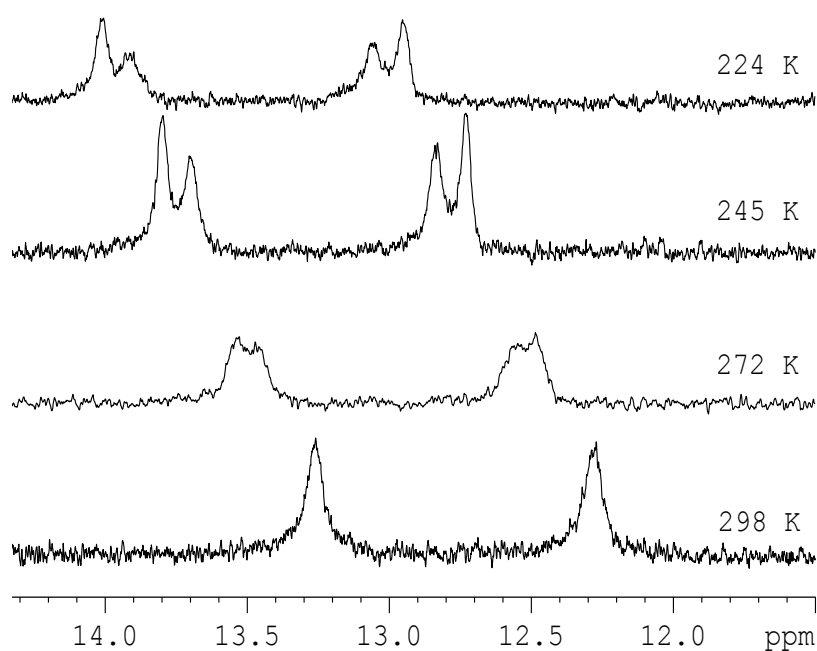


Figure 4.16: Variable temperature ^1H NMR spectra of **4.42** in $\text{tol-}d_8$ (400 MHz)

The structure of **4.42** was confirmed by X-ray crystallography as shown in Figure 4.17. The four coordinate rhodium centre was distorted from a regular square plane with trans C-Rh-P and trans-P-Rh-P angles of $172.75(7)^\circ$ and $162.28(2)^\circ$ respectively. The positioning of the FHF ligand trans to the NHC resulted in a minor lengthening of the Rh-F distance ($2.1460(12)$ Å) relative to that in the **4.41** where the F is opposite to phosphine ($2.1217(13)$ Å).

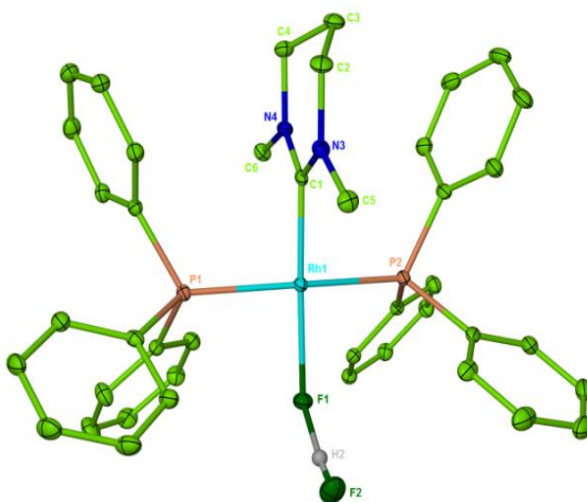
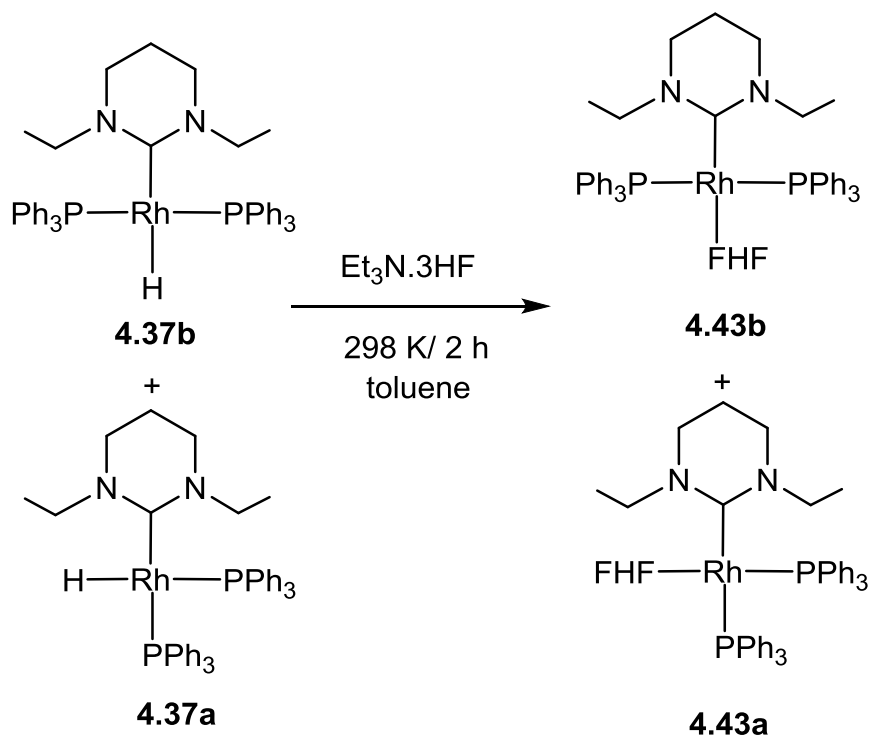


Figure 4.17: Molecular structure of Rh(6-Me)(PPh₃)₂(FHF) **4.42**. Ellipsoids are shown at the 30% level. Hydrogen atoms except for Rh-FHF and those on the N-substituents of the NHCs are removed for clarity. Selected bond lengths (Å) and angles (°): Rh(1)–P(1) 2.3016(6), Rh(1)–P(2) 2.2785(6), Rh(1)–C(1) 1.968(2), Rh(1)–F(1) 2.1460(12), P(1)–Rh(1)–C(1) 93.11(6), P(1)–Rh(1)–P(2) 162.28.

4.14 Synthesis of Rh(6-Et)(PPh₃)₂(FHF) (4.43)

The 6-Et FHF analogue was prepared by the same methodology as for 4.42 (Scheme 4.30) and isolated as a yellow solid in 43% yield.



Scheme 4.30: Synthesis of cis-/trans-isomers of Rh(6-Et)(PPh₃)₂(FHF) 4.43

A ³¹P {¹H} NMR spectrum of the material run immediately after dissolution in THF-*d*₈ displayed a doublet of doublets at 27.7 ppm indicating that the trans-phosphine isomer 4.43b had been formed, with only trace amounts of the cis isomer observed. However upon leaving the sample in solution for 24 h, signals for the cis-isomer were now much clearer. The isomers eventually equilibrated over 24 h at 298 K to a 1:1 mixture. The two isomers were straightforward to differentiate by ³¹P {¹H} NMR spectroscopy; the cis-isomer displayed two doublet of doublet of doublet resonances with quite different P-Rh (219 Hz and 123 Hz) and P-F (181 Hz and 22 Hz) couplings, while the trans-isomer appeared as just a doublet of doublets with ¹J_{PRh} and ²J_{PF} values of 173 Hz and 17 Hz respectively (Figure 4.18).

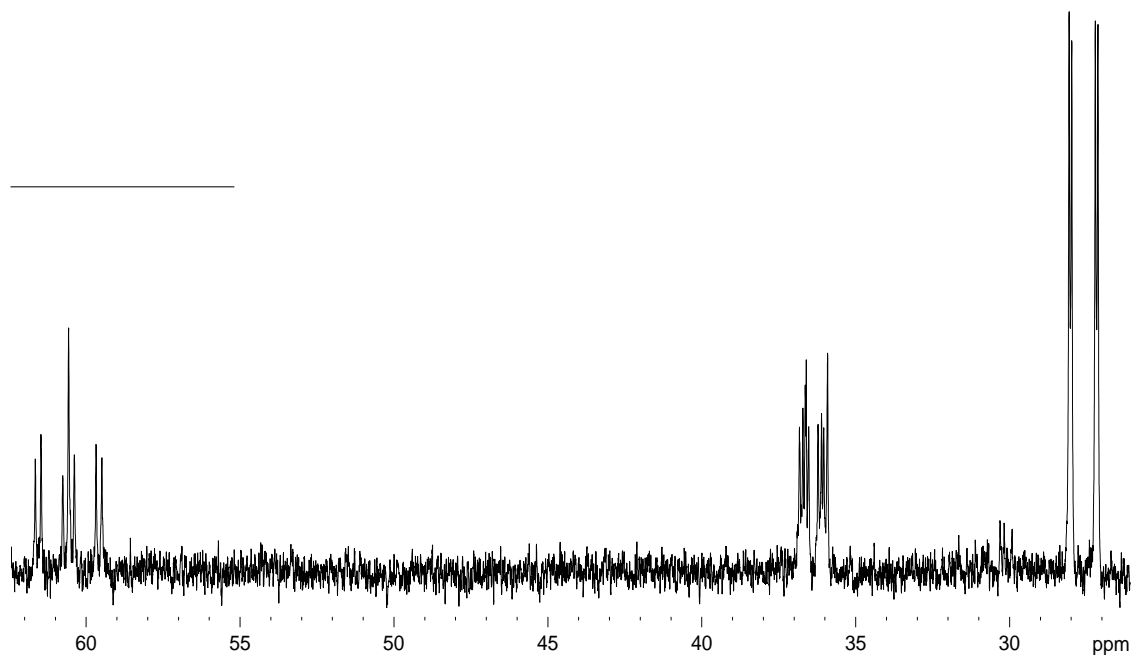


Figure 4.18: $^{31}\text{P}\{^1\text{H}\}$ NMR spectrum of **4.43a/b** ($\text{THF-}d_8$, 298 K, 202 MHz)

Interestingly, the corresponding ^1H NMR spectrum displayed only a single albeit very broad, high frequency singlet at 11.8 ppm for the bifluoride ligand, despite the FHF ligand being in two different environments in the two isomers. Another feature was the appearance of a highly deshielded methylene signal at ca. 6.1 ppm for the cis-isomer which possibly reflects its very close proximity to the FHF (Figure 4.19).

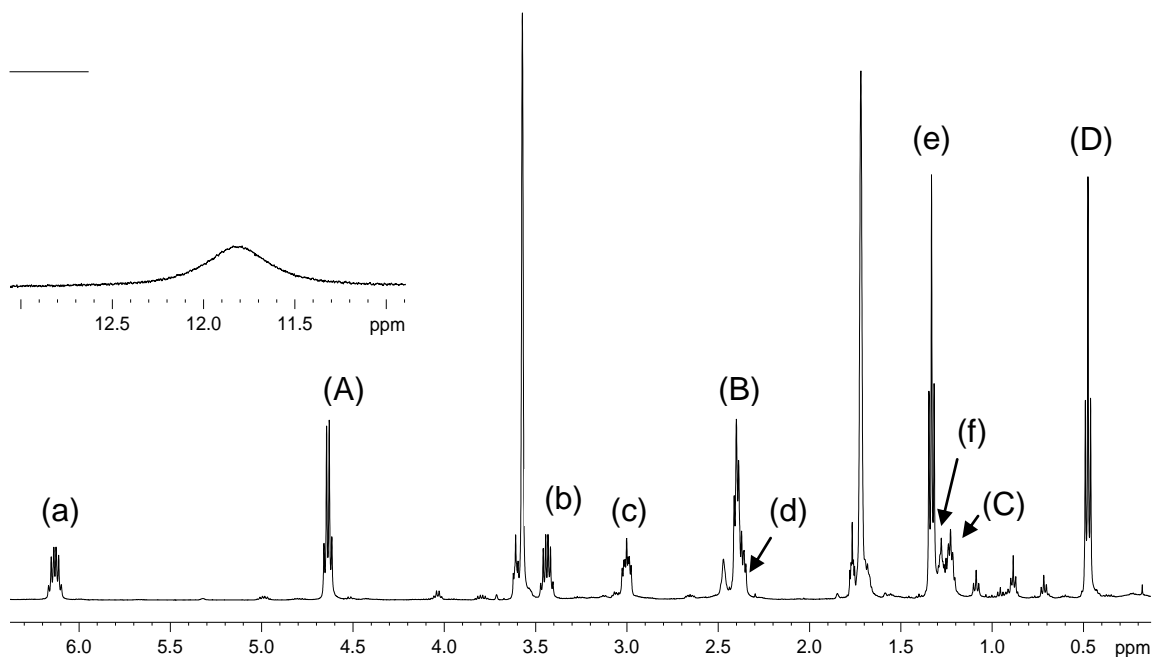
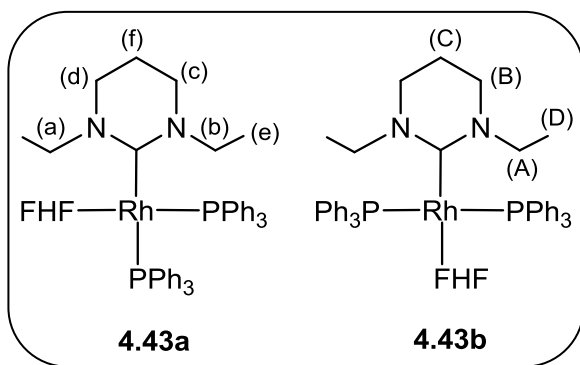


Figure 4.19: ^1H NMR spectrum of the two isomers of **4.43** (THF- d_8 , 298 K, 500 MHz)

The ^{19}F NMR spectrum of the isomeric mixture **4.43a/b** was only partially resolved at 298 K. The signals for the two distal fluorine nuclei at -273.3 and -310.6 ppm were assigned to the trans and cis isomers respectively. The proximal fluorine for both isomers appeared as a single, very broad resonance at -181.0 ppm, but upon cooling to 218 K, this resolved into two still relatively broad doublets at -177.3 and -179.1 ppm, with $^1J_{\text{FH}}$ coupling constants of ca. 372 and 380 Hz respectively (Figure 4.20).

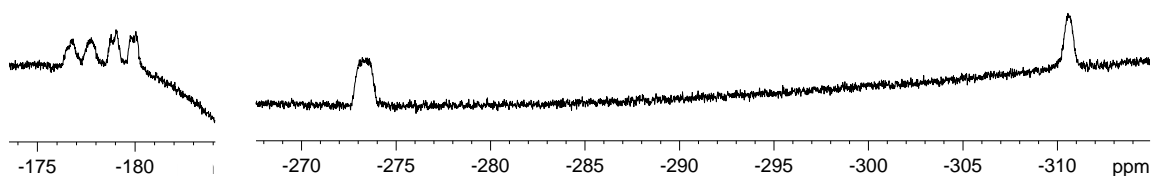


Figure 4.20: Low temperature (218 K) ^{19}F NMR spectrum of a mixture of **4.43a/b** (THF- d_8 , 376 MHz)

4.43b was further characterised using X-ray crystallography (Figure 4.21). The trans-NHC-Rh-FHF geometry resulted in a minor lengthening of the Rh-F distances (**4.42**: 2.1460(12) Å; **4.43b**: 2.1354(17) Å) relative to the trans-P-Rh-FHF arrangement in **4.41** (2.1217(13) Å). The Rh-F...F angles of **4.42** (122.96(6)°) and **4.43b** (121.41(9)°) were significantly more acute than that in **4.41** (127.44°), this value being at the bottom end of the range reported for other M-FHF species.⁴⁵⁻⁴⁸

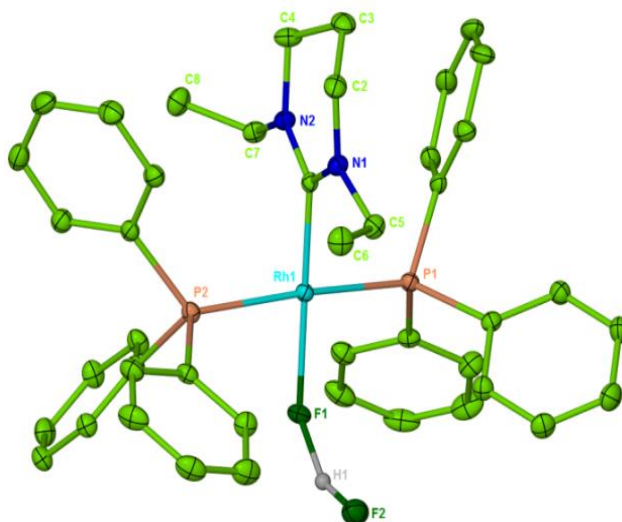


Figure 4.21: Molecular structure of Rh(6-Et)(PPh₃)₂(FHF) **4.43b**. Ellipsoids are shown at the 30% level. Hydrogen atoms except for Rh-FHF and those on the N-substituents of the NHCs are removed for clarity. Selected bond lengths (Å) and angles (°): Rh(1)–P(1) 2.2899(8), Rh(1)–P(2) 2.3172(8), Rh(1)–C(1) 1.969(3), Rh(1)–F(1) 2.1354(17), P(1)–Rh(1)–C(1) 92.77(8), P(1)–Rh(1)–P(2) 171.33(3).

Like the Rh hydride complexes **4.36b** and **4.37b**, some tilting of the NHC ligands was observed, with N-C-Rh angles of 117.88(14)/125.51(14)° in **4.42** and 120.41(19)/123.49(20)° in **4.43**.

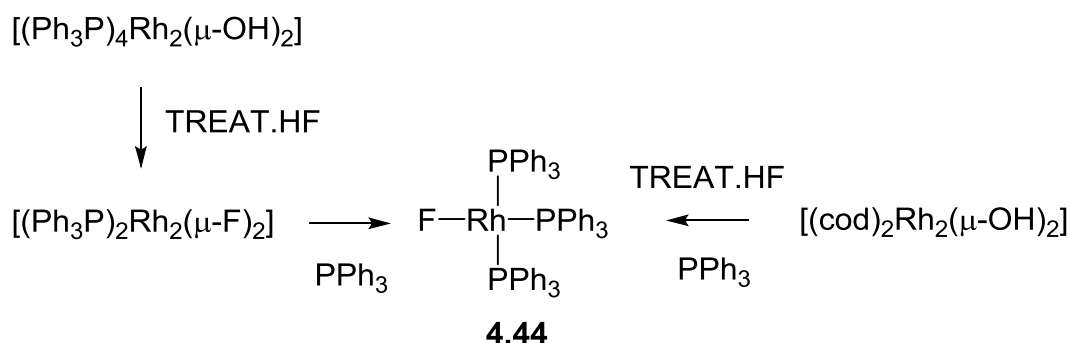
As mentioned previously, the initial formation of cis-Rh(6-Et)(PPh₃)₂(FHF) **4.43a** was followed by isomerisation to a ca. 1:1 mixture with the trans-isomer over hours in solution at 298 K. Multiple experiments at different temperature and solvents and were carried out to see whether the mixture of isomers went through to one isomer. An NMR tube containing **4.43a/b** in THF-*d*₈ was heated at 323 K and monitored by ³¹P NMR

spectroscopy at 1 h intervals, but the ratio remained as 1:1 over 12 hrs. Similarly, changing the solvent to C₆D₆ also had no effect on the mixture of isomers.

The bifluoride compounds Rh(6-Me)(PPh₃)₂(FHF) **4.42** and Rh(6-Et)(PPh₃)₂(FHF) **4.43a/b** were further characterised by IR spectroscopy. **4.42** displayed two broad ν_{FHF} bands at 2506 and 1897 cm⁻¹ whereas **4.43a/b** displayed three signals at 1883, 2422 and 2334 cm⁻¹. The 6-ⁱPr analogue **4.41** showed a comparable lower frequency feature at 1921 cm⁻¹ and two distinct, higher frequency bands at 2465 and 2328 cm⁻¹.

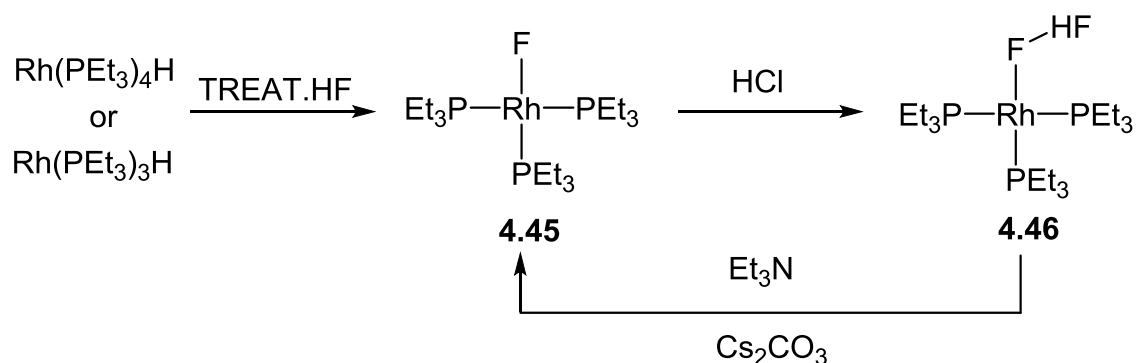
4.15 Comment on the formation of Rh FHF complexes

The formation of the bifluoride complexes from TREAT.HF contrasts with work reported by Grushin and Braun on the use of this reagent to form Rh-F complexes. In 2004, Grushin described two efficient routes to synthesise Rh(PPh₃)₃F **4.44**, both of which involved the use of TREAT.HF as a mild HF source. Treatment of [(Ph₃P)₄Rh₂(μ-OH)₂] with 2-3 equiv. of TREAT.HF afforded the dinuclear fluoride product [(Ph₃P)₄Rh₂(μ-F)₂], which upon addition of PPh₃, gave Rh(PPh₃)₃F **4.44**. The second route is similar in many respects; addition of TREAT.HF in the presence of excess PPh₃ to [(cod)₂Rh₂(μ-OH)₂] (Scheme 4.31).⁴⁹



Scheme 4.31: Synthesis of Rh(PPh₃)₃F

Braun reported that reaction of $\text{Rh}(\text{PEt}_3)_4\text{H}$ or $\text{Rh}(\text{PEt}_3)_3\text{H}$ with TREAT.HF gave $\text{Rh}(\text{PEt}_3)_3\text{F}$ **4.45** (Scheme 4.32).^{50,51}



Scheme 4.32: Synthesis of $\text{Rh}(\text{PEt}_3)_3\text{F}$

The formation of the bifluoride compound $\text{Rh}(\text{PEt}_3)_3(\text{FHF})$ **4.46** took place upon addition of HCl to $\text{Rh}(\text{PEt}_3)_3\text{F}$. The HF was shown to be loosely bound as it was easily removed by addition of Et_3N and Cs_2CO_3 to give full conversion to **4.45**.^{50,51}

4.16 Intermolecular and intramolecular exchange of the bifluoride complexes

Since the first example of a transition metal bifluoride complex, $\text{trans-Pt}(\text{PCy}_3)_2(\text{FHF})\text{H}$ reported by Coulson in 1976⁵², investigations of the fluxional properties of bifluoride ligands have only been carried out on this complex⁴⁶ and $\text{trans-Pd}(\text{PPh}_3)_2(\text{FHF})\text{Ph}$.⁴⁸ The solution behaviour of the M-FHF species can be studied using NMR methods including magnetization transfer. Our isolation of Rh bifluoride complexes provided an opportunity to extend studies of FHF dynamics to a different metal centre and would also show if the influence of the trans-ligand (-phosphine in **4.41**, NHC in **4.42**) had an effect (we excluded **4.43** because of the mixture of isomers).

An NMR tube was charged with **4.42** (5 mg) in $\text{THF-}d_8$ (0.5 mL) and a series of ^{19}F magnetization transfer experiments were carried out. During these experiments one of the fluorine resonances is selectively excited by irradiating it with a 180° pulse; after this, by waiting a series of time delays, a spectrum can be acquired. The same procedure was carried out for **4.41** (Figure 4.22). The results revealed there was exchange between the distal

and proximal fluorine resonances for **4.42** taking place at 298 K, whereas for **4.41**, exchange was not observed until 313 K. Monitoring the exchange rate as a function of temperature gave similar ΔH^\ddagger values for the two compounds (**4.41**: $51 \pm 5 \text{ kJ mol}^{-1}$; **4.42**: $60 \pm 6 \text{ kJ mol}^{-1}$). At first sight, a difference was apparent between the two calculated ΔS^\ddagger values (**4.41**: $-70 \pm 17 \text{ J mol}^{-1} \text{ K}^{-1}$; **4.42**: $-27 \pm 18 \text{ J mol}^{-1} \text{ K}^{-1}$), although taking into account the error bars, this difference could be as little as $7 \text{ J mol}^{-1} \text{ K}^{-1}$.

Further experiments were carried out with different concentrations of the samples. Diluting the samples by up to three-fold had no effect on the rate of exchange, suggesting that the activation parameters reflect an intramolecular process. This observation is similar to what Grushin had reported for the isoelectronic square-planar system $\text{Pd}(\text{PPh}_3)_2(\text{FHF})\text{Ph}$ where the bifluoride ligand is proposed to undergo exchange via temporary κ^2 -coordination.³⁷ An Eyring plot is shown below in Figure 4.23 which displays the ^{19}F magnetisation data collected for **4.41** and **4.42**.

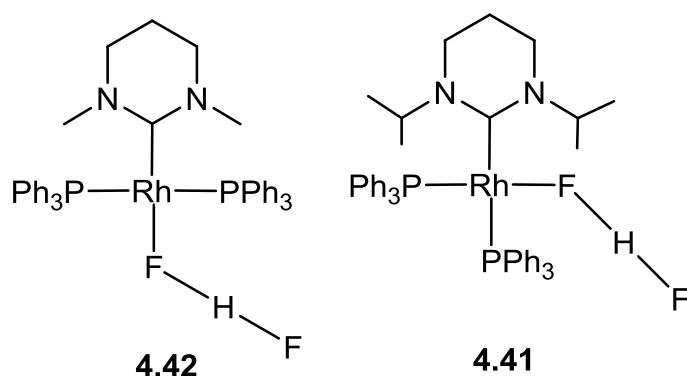


Figure 4.22: $\text{Rh}(6\text{-Me})(\text{PPh}_3)_2(\text{FHF})$ and $\text{Rh}(6\text{-}^i\text{Pr})(\text{PPh}_3)_2(\text{FHF})$

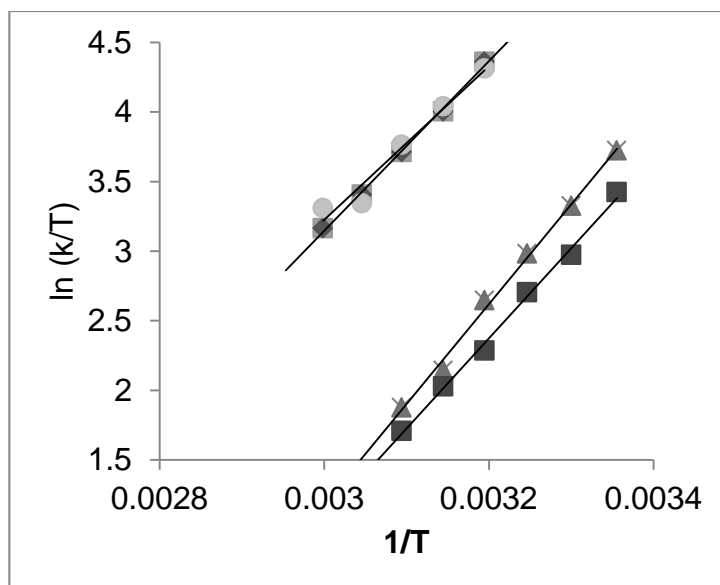
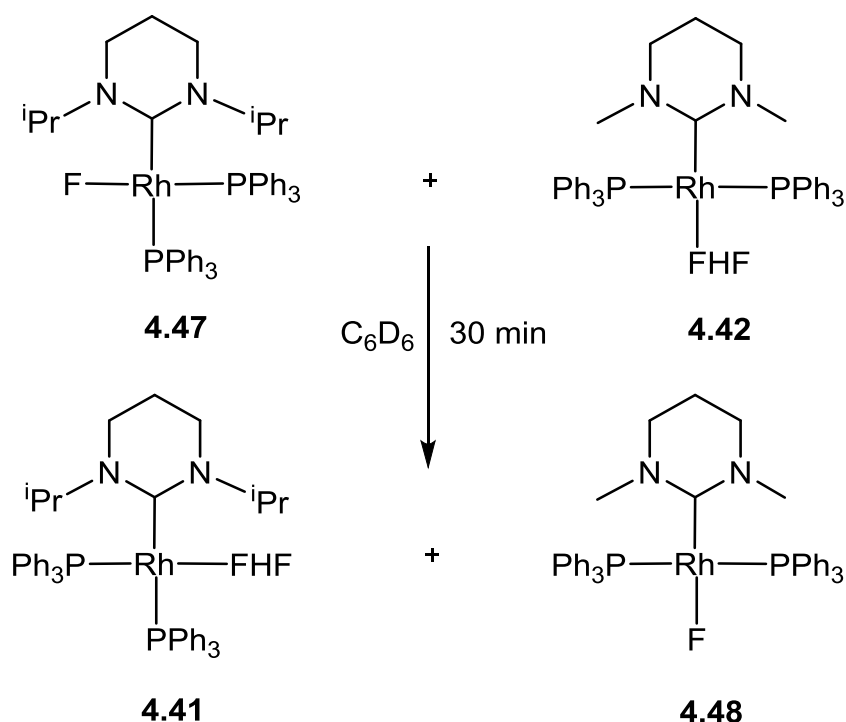


Figure 4.23: Eyring plot for ^{19}F magnetization data. Upper line: 3.51×10^{-2} M of **4.41** (squares/diamonds), 1.76×10^{-2} M of **4.41** (circles). Lower line: 2.79×10^{-2} M of **4.42** (squares), 1.35×10^{-2} M of **4.42** (triangles/spikes).

Complexes **4.41** and **4.42** successfully displayed intramolecular exchange as described above, but it was also of interest to see whether the bifluoride complexes were able to undergo intermolecular exchange. Approximately 5 mg of **4.42** and the Rh(6-*i*Pr)F complex Rh(6-*i*Pr)(PPh₃)₂F **4.47** were added to an NMR tube in C₆D₆ and the ^{19}F NMR spectrum recorded after 30 min. It was evident that intermolecular exchange had taken place, as the signals for **4.41** (-175.9 and -272.6 ppm) and Rh(6-Me)(PPh₃)₂F **4.48** (-332.7 ppm) were now visible along with those of the starting materials (Scheme 4.33).

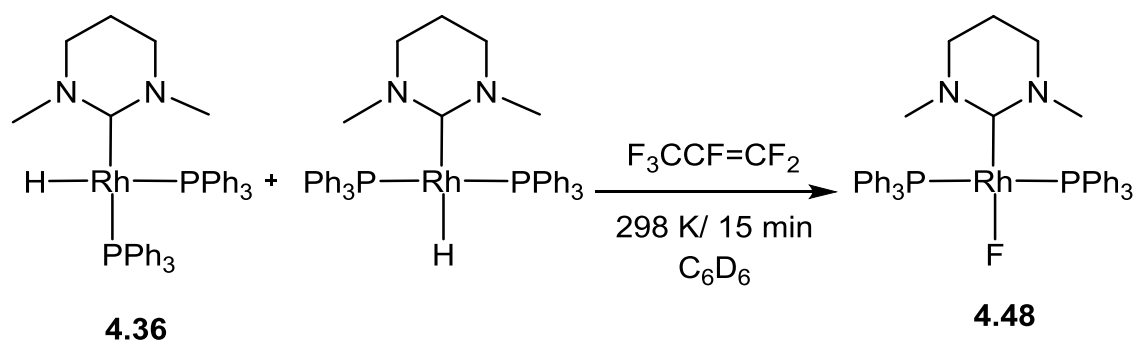


Scheme 4.33: Intermolecular exchange with **4.47** and **4.42**

Similarly, addition of a single equivalent of **4.41** to a C_6D_6 solution of **4.48** showed the presence of **4.42** and cis/trans **4.47**.

4.17 Synthesis of $Rh(6-Me)(PPh_3)_2F$ (**4.48**)

The yields of **4.42** and **4.43** were relatively low due to their partial solubility in alkane solvents, and so it proved difficult to use them as precursors to the corresponding fluoride complexes via reaction with $[Me_4N]F$, the route used to prepare $Rh(6-iPr)(PPh_3)_2F$ **4.47**. However C-F activation of $F_3CCF=CF_2$ by **4.36** and **4.37** provided a direct route to $Rh(NHC)(PPh_3)_2F$, the fluoride compounds being the only rhodium containing products of the reactions. A benzene solution containing **4.36** and 1 atm perfluoropropene was stirred at 298 K for 15 min. The reaction mixture was reduced to dryness, extracted with minimum amount of benzene and precipitated under vigorous stirring of hexane to afford $Rh(6-Me)(PPh_3)_2F$ **4.48** as a yellow powder in 25% yield (Scheme 4.34). Low yields were observed due to partial solubility in alkane solvents, which also thwarted efforts to crystallise **4.48**.



Scheme 4.34: Synthesis of Rh(6-Me)(PPh₃)₂F

The $^{31}\text{P}\{^1\text{H}\}$ NMR spectrum of **4.48** displayed a single doublet of doublets at 23.9 ppm ($^2J_{\text{PRh}} = 174$ Hz, $^2J_{\text{PF}} = 15$ Hz) consistent with the formation of just the trans-phosphine isomer. The corresponding ^{19}F NMR spectrum displayed a broad doublet at -332.7 ppm ($^1J_{\text{FRh}} = 61$ Hz) (Figure 24).

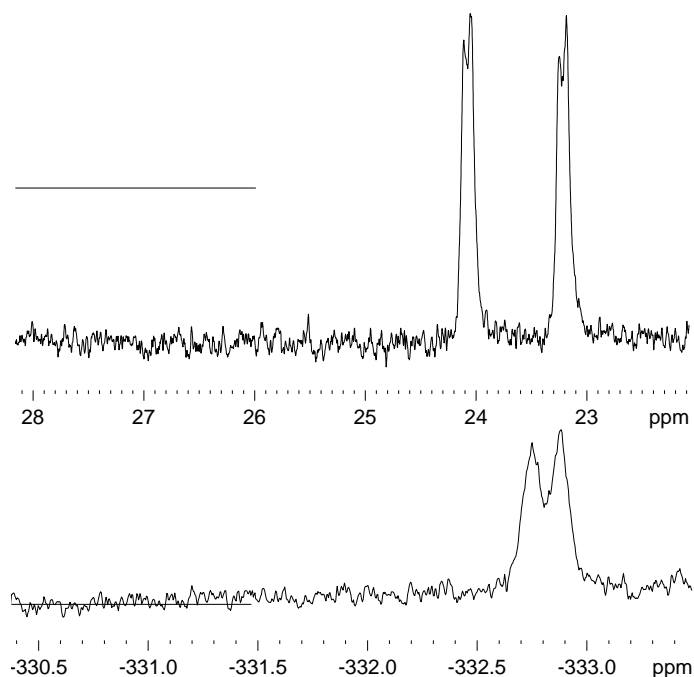
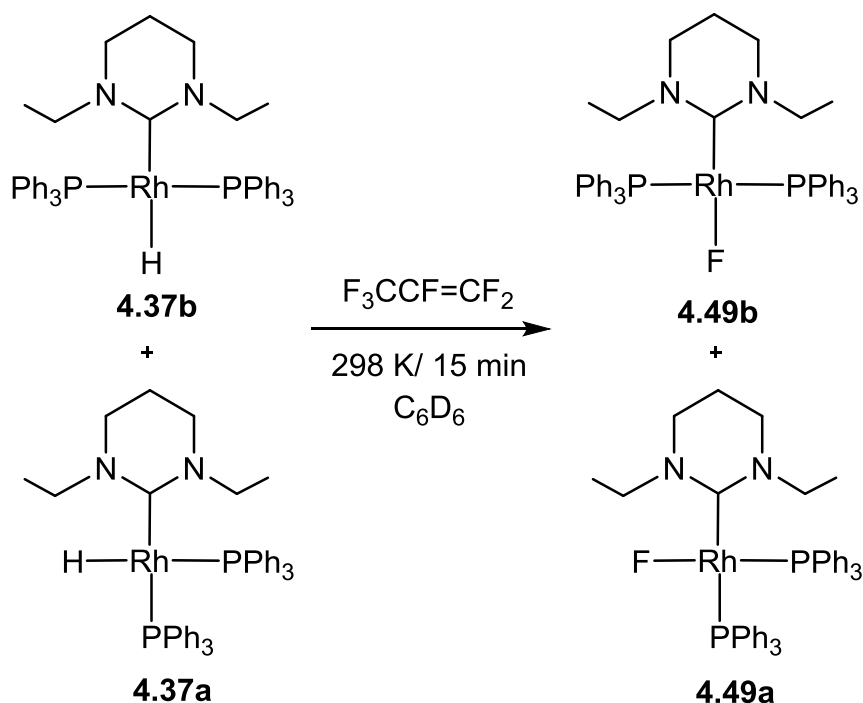


Figure 4.24 : $^{31}\text{P}\{^1\text{H}\}$ (202 MHz, top) and ^{19}F (470 MHz, bottom) NMR spectra of **4.48** (C₆D₆, 298 K)

4.18 Synthesis of Rh(6-Et)(PPh₃)₂F (4.49)

The same method was applied as above with **4.37** to afford Rh(6-Et)(PPh₃)₂F **4.49a/b** as a yellow powder (Scheme 4.35). A low yield (39%) again resulted from partial alkane solubility.⁵³



Scheme 4.35: Synthesis of cis-/trans-isomers of Rh(6-Et)(PPh₃)₂F

The ³¹P{¹H} NMR spectrum of the product showed the presence of a mixture of cis- and trans-isomers **4.49a/b** (c.f. **4.37**). A doublet of doublets was observed at 26.9 ppm (¹J_{PRh} = 174 Hz, ²J_{PF} = 19 Hz) for the trans-isomer while the cis-isomer exhibited two doublet of doublet of doublets at 60.3 and 36.6 ppm. The ¹⁹F NMR spectrum was also quite diagnostic; this displayed a broad doublet at -331.3 ppm for the trans isomer (by comparison with **4.48**), and a doublet of doublet of doublets at -285.8 ppm for the cis isomer (Figure 4.25).

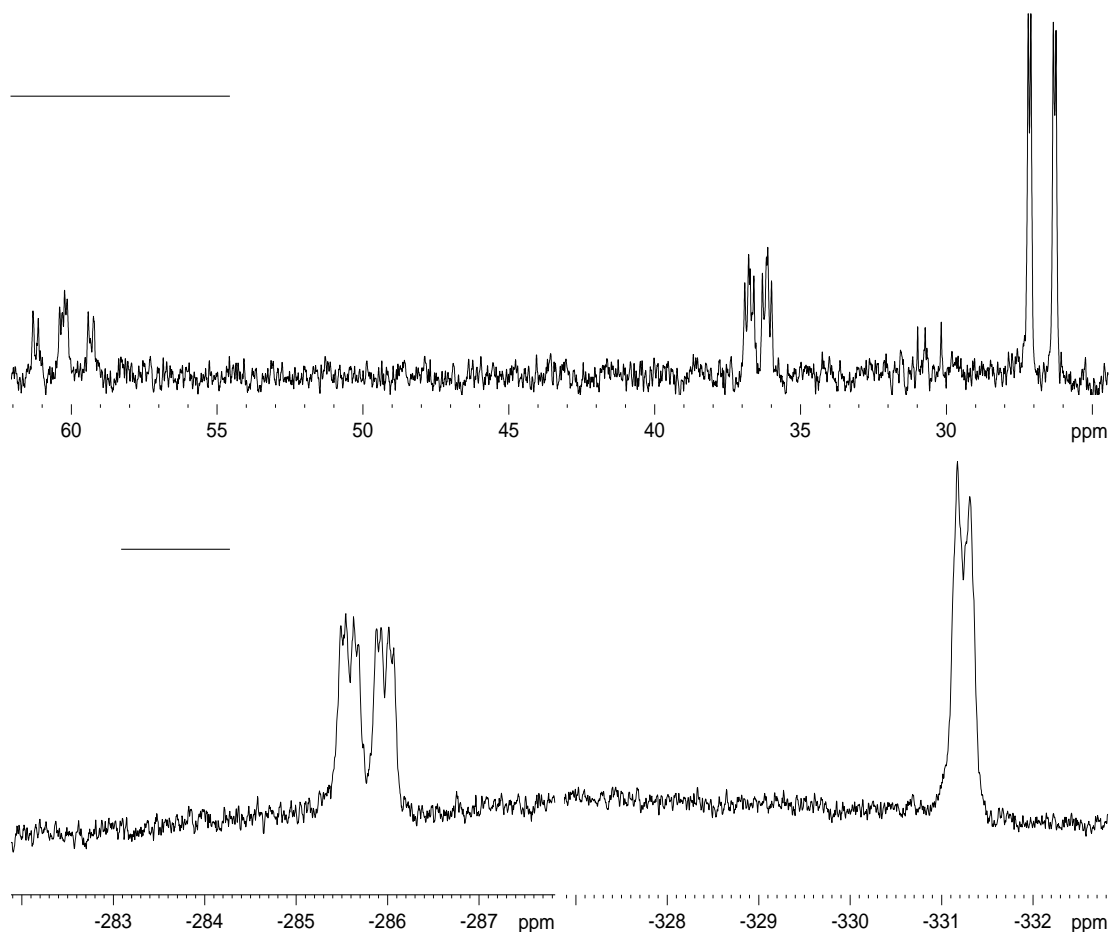
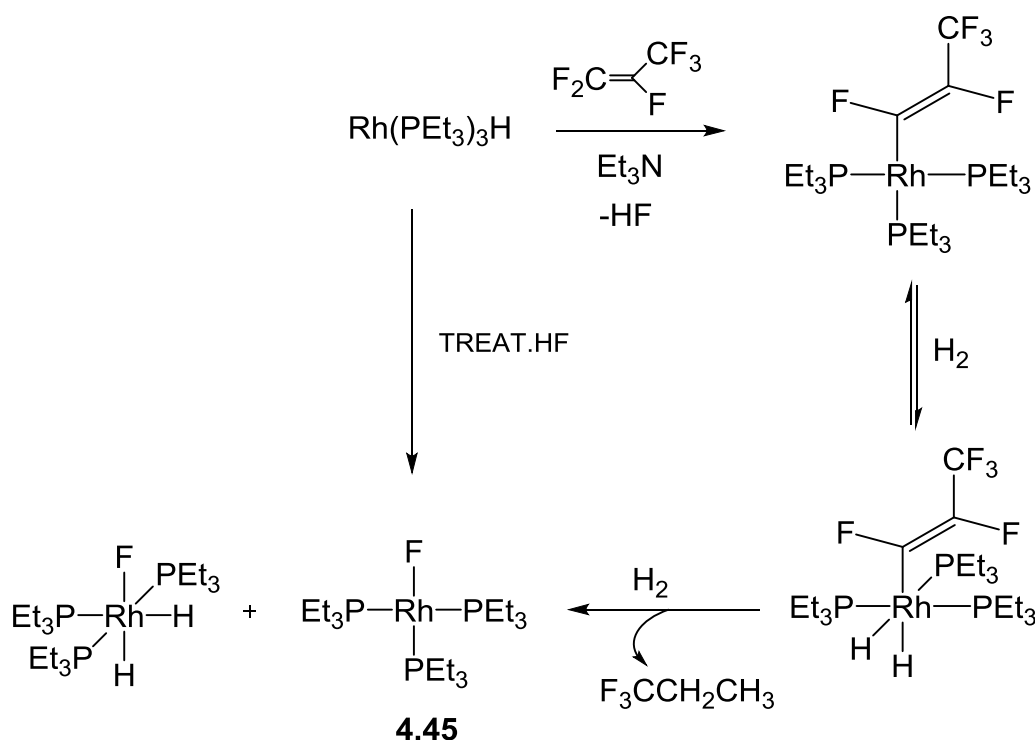


Figure 4.25: $^{31}\text{P}\{^1\text{H}\}$ (202 MHz, top) and ^{19}F (470 MHz, bottom) NMR spectra of **4.49a/b** (C_6D_6 , 298 K)

NMR spectra of the reaction volatiles obtained from both **4.48** and **4.49a/b** showed that (*E*)- $\text{F}_3\text{CCF}=\text{CFH}$ was formed as the major product, along with smaller amounts of (*Z*)- $\text{F}_3\text{CCF}=\text{CFH}$ and, more unexpectedly, $(\text{F}_3\text{C})_2\text{C}(\text{F})\text{H}$ (relative ratio 1:0.34:0.34). Assignment of the products was made by comparison of ^1H and ^{19}F NMR data to the literature.⁵⁴⁻⁵⁸ The formation of $(\text{F}_3\text{C})_2\text{C}(\text{F})\text{H}$ most likely arises as a result of attack of F^- on the fluoroalkene⁵⁹, followed by reaction of the carbanion with H^+ , abstracted from any available protic source (e.g. H_2O).

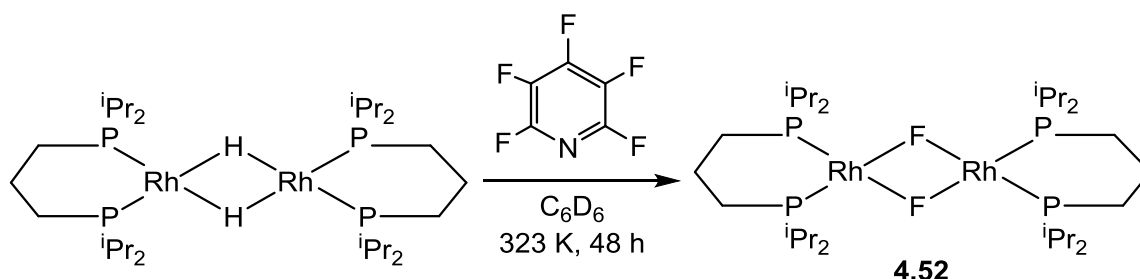
The formation of the fluorides **4.48** and **4.49a/b** contrasts with most other Rh mediated C-F bond activation reactions, which typically yield Rh-fluoroaryl or fluoroalkenyl products.⁶⁰⁻⁶³ A report by Braun discussed how $\text{F}_3\text{CCF}=\text{CF}_2$ reacted with $\text{Rh}(\text{PEt}_3)_3\text{H}/\text{base}$ to give the perfluoropropenyl complex $\text{Rh}(\text{PEt}_3)_3(\text{CF}=\text{CFCF}_3)$. Subsequent oxidative addition of hydrogen to the perfluoropropenyl complex afforded the dihydro rhodium(III) complex,

which in the presence of additional hydrogen afforded 1,1,1 trifluoropropane and two fluoride complexes, including $\text{Rh}(\text{PEt}_3)_3\text{F}$ **4.45** (Scheme 4.36).^{64,65}



Scheme 4.36: Synthesis of **4.45** via $\text{F}_3\text{CCF}=\text{CF}_2$

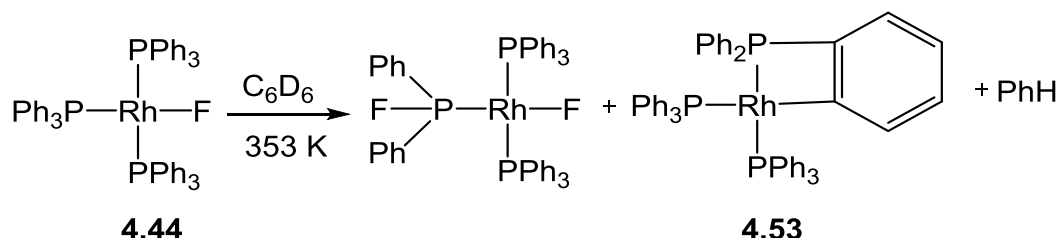
Very recently, the same group found that the bridging hydride complex $[\text{Rh}(\text{dipp})(\mu\text{-H})_2]$ cleaved aromatic C-F bonds to give the corresponding fluoride complex, $[\text{Rh}(\text{dipp})(\mu\text{-F})_2]$ **4.52** but, in this case, the formation of a dinuclear product most likely provides the driving force for Rh-F formation (Scheme 4.37).⁶⁶



Scheme 4.37: C-F activation by $[\text{Rh}(\text{dipp})(\mu\text{-H})_2]$ as a route to a dinuclear Rh-F product

4.19 Reactivity of Rh(6-NHC)(PPh₃)₂F

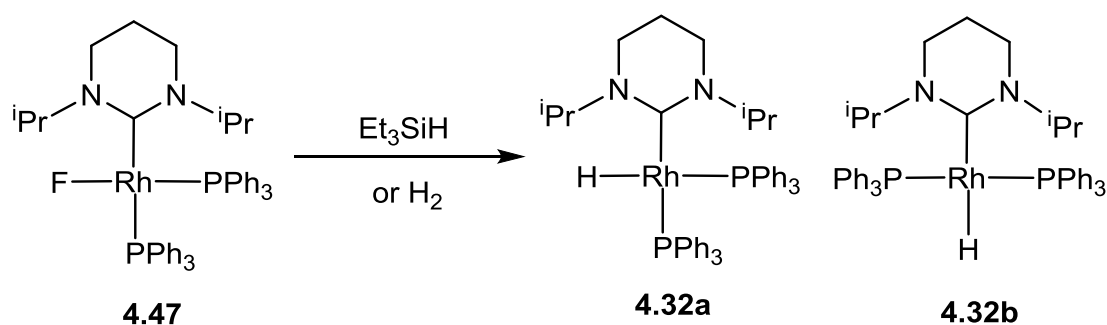
Grushin and co-workers reported the thermal decomposition of **4.44** in benzene at 353 K which took place quickly and produced two Rh products, one of which resulted from the cyclometallation of the phenyl group of Rh(PPh₃)₃F **4.44** (Scheme 4.38).⁴⁹



Scheme 4.38: Thermal decomposition of a Rh-F complex

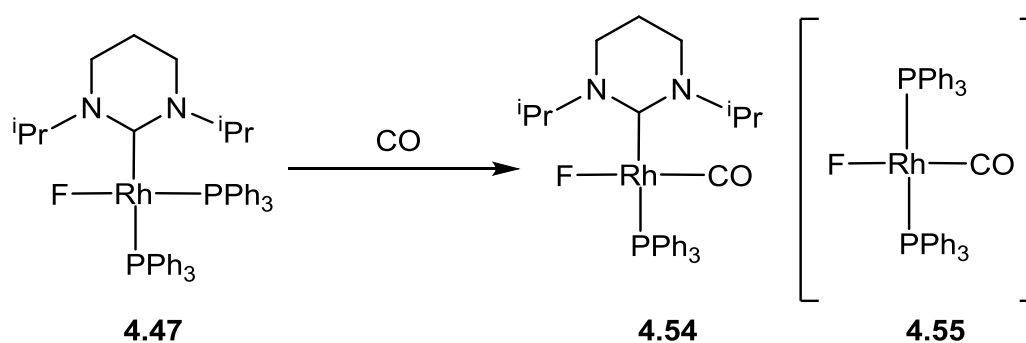
In contrast to **4.44**, Rh(6-ⁱPr)(PPh₃)₂F (**4.47**) has been reported to show higher thermal stability and no tendency to undergo any rearrangement between the Rh-F and PPh₃ ligands, although two products were generated.³⁶ Thus, heating **4.47** at 343 K for 3 h led first to the appearance of a compound assigned as the trans-phosphine isomer of Rh(6-ⁱPr)(PPh₃)₂F. A ³¹P{¹H} NMR spectrum recorded after 20 h heating still contained mostly **4.47**, but now also showed a further product that displayed two doublets of doublets at 39.4 and -40.7 ppm. The product was tentatively assigned as a cyclometalated phosphine complex principally on the basis of the characteristic very low frequency phosphorus resonance.

As low yields were obtained for **4.48** and **4.49a/b**, no further reactivity studies were really viable. However the ability to generate **4.47** in good yields via the C-F activation of perfluoropropene, led to further investigations of Rh-F reactivity. Initial work was carried out to see whether **4.47** would reverse back to the hydride derivative. Addition of H₂ or 5 equiv. of Et₃SiH to a C₆D₆ solution of **4.47** resulted in very slow conversion to the hydride complex. In the silane experiment, ca. 50% conversion to **4.32** was seen after 6 days, however heating the sample to 363 K for an additional 2 h resulted in the complete transformation to the same 1:2 mixture of cis-/trans Rh(6-ⁱPr)(PPh₃)₂H **4.32a/b** (Scheme 4.39). Interestingly, there were no NMR signals for any intermediate Rh species detectable with either reductant.



Scheme 4.39: Reversing the Rh-F complex back to hydride derivative

Exposure of a C_6D_6 solution of **4.47** to 1 atm. CO resulted in the rapid formation of the monocarbonyl complex $\text{Rh}(\text{6-}^i\text{Pr})(\text{PPh}_3)(\text{CO})\text{F}$ **4.54** within 10 min at 298 K. This displayed a doublet of doublets phosphorus signal at 30.3 ppm ($^2J_{\text{PRh}} = 122.0$ Hz, $^2J_{\text{PF}} = 23.0$ Hz), and a doublet of doublets Rh-F resonance at -282.4 ppm with $^1J_{\text{FRh}}$ and $^2J_{\text{FP}}$ splittings of 52 and 23 Hz. When the reaction was repeated with ^{13}CO , additional splittings of 16 and 76 Hz were seen in the ^{31}P and ^{19}F spectra respectively. The positioning of the ligands are shown for the product in Scheme 4.40, based on the magnitudes of these J -values. Positioning of the π -donor F trans to the π -acceptor CO, is as expected (Scheme 4.40).⁶⁷

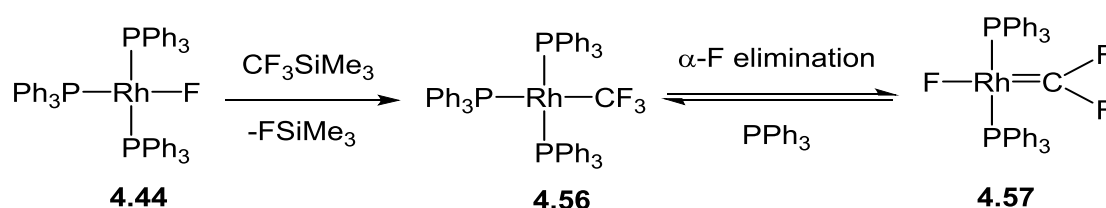


Scheme 4.40: Synthesis of the mono-CO complex

Attempts to isolate **4.54** for structural characterisation only afforded the known bis-phosphine complex $\text{Rh}(\text{PPh}_3)_2(\text{CO})\text{F}$ **4.55**.^{68,69} Further inspection showed that this was formed as soon as CO was added to **4.47** on the basis of a broad ^{19}F doublet at -271.1 ppm ($^1J_{\text{FRh}} = 54.6$ Hz), but only present in trace amounts and as a minor component with respect to **4.54**. Therefore its subsequent crystallization must simply reflect a lower solubility in C_6H_6 /hexane relative to **4.54**.

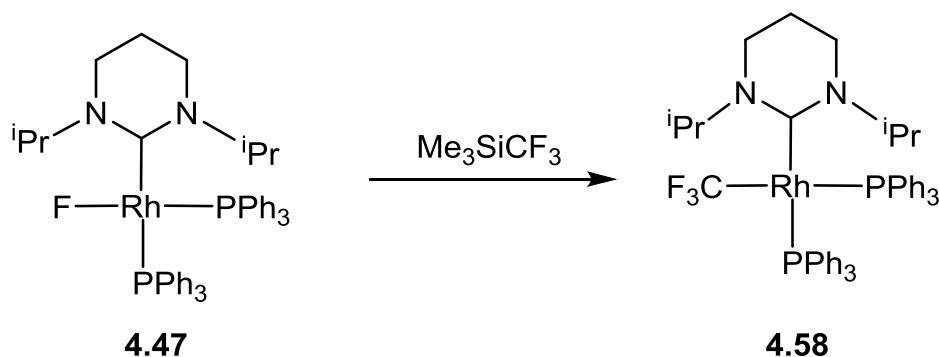
4.20 Reaction with Me₃SiCF₃

A number of groups,^{70,71} including Grushin's,^{72,73} have described the transformation of Rh-F complexes into Rh-CF₃ species through the reaction with Me₃SiCF₃. Grushin showed that treating Rh(PPh₃)₃F **4.44** with Me₃SiCF₃ in benzene resulted in the initial formation of the difluorocarbene fluoride complex Rh(PPh₃)₂(CF₂)F **4.57** presumably via the intermediate Rh(PPh₃)₃(CF₃) **4.56**, which then underwent α-F elimination upon loss of PPh₃. Addition of excess PPh₃ to a benzene solution of **4.57** afforded full conversion back to **4.56**, allowing isolation and complete characterisation (Scheme 4.41).⁷²⁻⁷⁴



Scheme 4.41: Synthesis of Rh-CF₃ complex which undergoes α-F elimination

The room temperature reaction of Me₃SiCF₃ and **4.47** rapidly generated Rh(6-ⁱPr)(PPh₃)₂(CF₃) **4.58** (Scheme 4.42). The ¹⁹F NMR spectrum showed a characteristic low frequency doublet of doublet of doublets trifluoromethyl signal at -7.2 ppm (³J_{FP} = 40 Hz, ²J_{FRh} = 23 Hz, ³J_{FP} = 13 Hz), while in the ³¹P{¹H} NMR spectrum, two partially overlapping doublet of doublet of quartets appeared at 43.0 and 41.7 ppm (Figure 4.26), consistent with a cis-phosphine geometry.



Scheme 4.42: Synthesis of Rh(6-ⁱPr)(PPh₃)₂(CF₃)

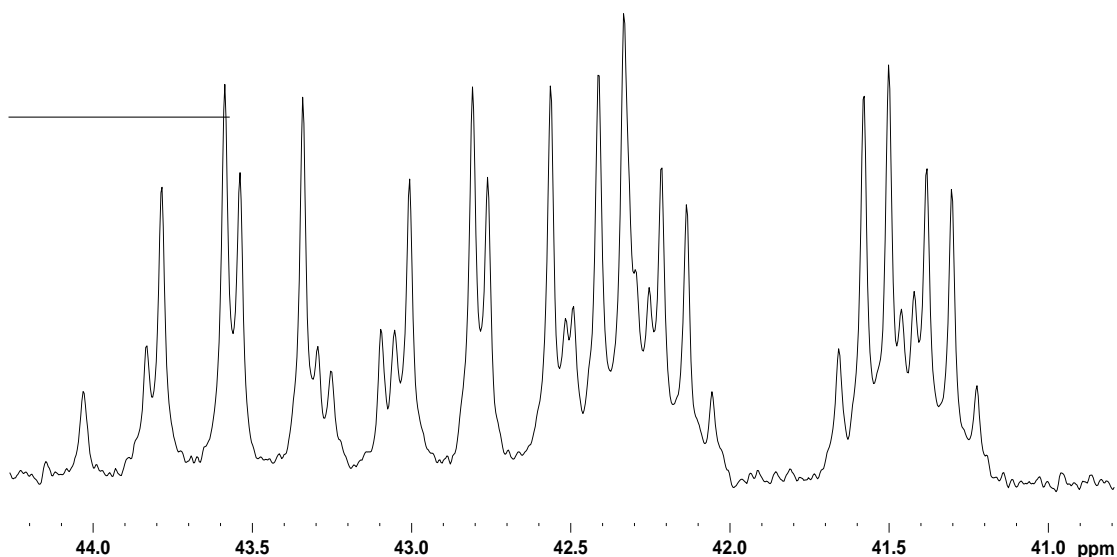


Figure 4.26: $^{31}\text{P}\{^1\text{H}\}$ NMR spectrum of **4.58** (C_6D_6 , 298 K, 162 MHz)

The most notable feature in the X-ray crystal structure of **4.58** (Figure 4.27) was the lengthening of the Rh-P bond (trans to CF_3) to 2.3020(4) Å from that trans to F in **4.47** (2.1850(7) Å), a result of the well-established high trans-influence of the trifluoromethyl ligand.^{75,76}

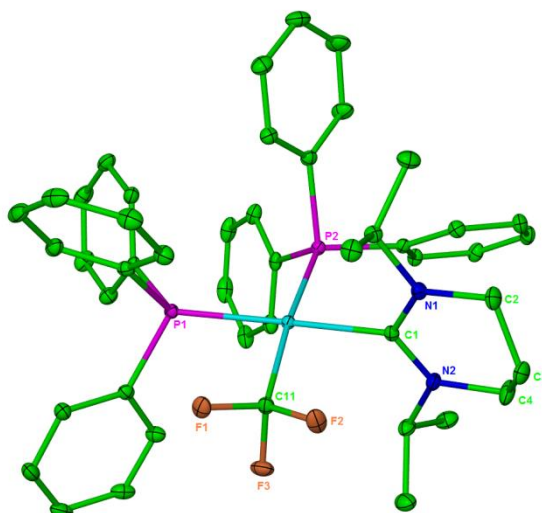


Figure 4.27: Molecular structure of $\text{Rh}(6\text{-}^i\text{Pr})(\text{PPh}_3)_2(\text{CF}_3)$ **4.58**. Ellipsoids are shown at the 30% level. Hydrogen atoms are removed for clarity. Selected bond lengths (Å) and angles ($^\circ$): Rh(1)-P(1) 2.3020(4), Rh(1)-P(2) 2.2813(4), Rh(1)-C(1) 2.0917(16), Rh(1)-C(11) 2.0993(16), P(1)-Rh(1)-C(1) 168.36(4), P(2)-Rh(1)-C(1) 92.23(4), P(1)-Rh(1)-P(1) 96.711(15), P(1)-Rh(1)-C(11) 87.07(5), P(2)-Rh(1)-C(11) 172.52(5), C(1)-Rh(1)-C(11) 84.92(6).

4.21 CHAPTER SUMMARY

The synthesis and reactivity of $\text{Ru}(\text{PPh}_3)_3(\text{CO})\text{HX}$ ($\text{X}=\text{Cl}, \text{F}$) towards 6-Me and 6-Et proved to be difficult which limited further studies, as we were unable to crystallise and fully characterise the complexes.

New hydride containing rhodium complexes of the form $\text{Rh}(6\text{-NHC})(\text{PPh}_3)_2\text{H}$ bearing 6-Me and 6-Et have been prepared from $\text{Rh}(\text{PPh}_3)_4\text{H}$. A different reactivity was observed when the Rh precursor was changed to $\text{Rh}(\text{PPh}_3)_3(\text{CO})\text{H}$. Treating with 6-Et brought about the synthesis of the dimer $[(\text{PPh}_3)_2\text{Rh}(\mu\text{-CO})_2\text{Rh}(6\text{-Et})(\text{PPh}_3)]$ **4.38**. As expected on the basis of previous studies the addition of $\text{Et}_3\text{N}\cdot 3\text{HF}$ to rhodium hydride precursors gave the corresponding bifluoride species **4.42** and **4.43a/b**.

^{19}F Magnetization transfer studies were carried out on the known $\text{Rh}(6\text{-}^i\text{Pr})(\text{PPh}_3)_2\text{FHF}$ and $\text{Rh}(6\text{-Me})(\text{PPh}_3)_2\text{FHF}$ and revealed what appears to be an intramolecular fluorine exchange process involving the F-H-F ligands. This is somewhat more facile in the **4.42** compared to **4.41**.

The Rh-F complexes **4.48** and **4.49a/b** have proven to be readily accessible through C-F activation of a perfluoroalkene by **4.36** and **4.37/b**. As low yields were obtained for **4.48** and **4.49a/b**, reactivity studies were carried out with **4.47** and revealed (i) metathesis with both H_2 and R_3SiH , (ii) 6-NHC and PPh_3 substitution by CO and (iii) Rh-F cleavage in the presence of Me_3SiCF_3 .

4.22 EXPERIMENTAL

4.22.1 General Methods

All manipulations were carried out using standard Schlenk, high vacuum and glovebox techniques using dried and degassed solvents, unless otherwise stated. NMR spectra were recorded at 298 K (unless otherwise stated) on Bruker Avance 400 and 500 MHz NMR spectrometers and referenced to residual solvent signals for ^1H and ^{13}C spectra for C_6D_6 , (δ 7.15, 128.0) and $\text{THF-}d_8$ (δ 3.58, 25.4). Unless otherwise quoted, ^1H and ^{13}C resonances for the PPh_3 ligands and non-carbenic ^{13}C signals arising from the 6-NHC ligands have been excluded. $^{31}\text{P}\{^1\text{H}\}$ and ^{19}F spectra were referenced externally to 85% H_3PO_4 (85%) and CFCl_3 respectively (both $\delta = 0.0$). Mass spectrometry was performed by the EPSRC National Mass Spectrometry Service in Swansea, UK. Elemental analyses were performed by the Elemental Analysis Service, London Metropolitan University, London, UK. IR spectra were prepared as KBr discs in an argon-filled glovebox and recorded on a Nicolet Nexus spectrometer. $\text{Rh}(\text{PPh}_3)_4\text{H}$,⁷⁷ $\text{Rh}(\text{PPh}_3)_3(\text{CO})\text{H}$,⁷⁷ $\text{Rh}(\text{6}^i\text{Pr})(\text{PPh}_3)_2\text{H}$,³⁶ $\text{Ru}(\text{PPh}_3)_3(\text{CO})\text{HCl}$,⁷⁸ $\text{Ru}(\text{PPh}_3)_3(\text{CO})\text{HF}$ ⁷⁹ were prepared according to the literature. $\text{Et}_3\text{N}\cdot 3\text{HF}$, $\text{F}_3\text{CF}=\text{CF}_2$, $\text{KN}(\text{SiMe}_3)_2$, CF_3SiMe_3 and Et_3SiH , were purchased from Sigma Aldrich and used as received. Hydrated RhCl_3 was loaned by Johnson Matthey. Hydrogen (BOC, 99.9%) and carbon monoxide (BOC, 99.9%) were used as received

Preparation of 6-NHCs

4.22.2 Synthesis of [6-MeH]PF₆.¹⁹ A 100 μL microwave vial was charged with *N,N'*-dimethyl-1,3-propanediamine (624 μL , 5.0 mmol), ammonium hexafluorophosphate (815 mg, 5.0 mmol) and triethyl orthoformate (5 mL). The vial was capped and irradiated 5 min at 418 K under stirring with a 25 W microwave power. After cooling to room temperature the reaction mixture was diluted with Et_2O (5 mL) and stirred for 10 mins to precipitate a white solid which was filtered off. Yield 856 mg (66%).

4.22.3 Synthesis of [6-EtH]PF₆.¹⁹ The same method was applied as [6-MeH]PF₆ but starting from *N,N'*-diethyl-1,3-propanediamine (795 μL , 5.0 mmol). Yield 945 mg (66%).

Preparation of a Ruthenium complex bearing 6-Me

4.22.4 Synthesis of Ru(6-Me')(PPh₃)₂(CO)H 4.35. A Schlenk flask was charged with [6-MeH]PF₆ (81.0 mg, 0.31 mmol) and KN(SiMe₃)₂ (63.0 mg, 0.31 mmol) in THF (2.5 mL) and the suspension stirred at 298 K for 1 h. The salt/base mixture was added to a J. Youngs ampoule containing Ru(PPh₃)₃(CO)HCl (100 mg, 0.11 mmol) in THF (2.5 mL). The mixture was then stirred at 298 K for 2 h and then filtered of trace amounts of a light brown solid. The filtrate was reduced to dryness and redissolved in minimum amount of benzene and the added hexane to afford a yellow powder. The solid was isolated by cannula filtration and dried under vacuum. ¹H NMR (500 MHz, C₆D₆): δ 2.7 (s, 2H, Ru-CH₂), 1.8 (s, 3H, NCH₃), 1.8 (dt, *J* = 5.9 Hz, 2H, NCH₂), 1.7 (dt, *J* = 5.9 Hz, 2H, NCH₂), 0.8 (m, 2H, NCH₂CH₂), -7.8 (t, *J* = 22.5 Hz, 1H, RuH). ³¹P {¹H} NMR: δ 60.8 (s). ¹³C{¹H} NMR: δ 47.4 (s, NCH₂CH₂), 42.2 (s, NCH₂CH₂), 40.7 (s, NCH₃), 24.1 (t, *J* = 6.9 Hz, RuCH₂), 20.7 (s, NCH₂CH₂).

Preparation of Rhodium complexes bearing 6-NHCs

4.22.5 Synthesis of Rh(6-Me)(PPh₃)₂H (4.36). A Schlenk flask was charged with [6-MeH]PF₆ (178 mg, 0.35 mmol) and KN(SiMe₃)₂ (139 mg, 0.35 mmol) in THF (5 mL) and the suspension stirred at 298 K for 1 h. The solvent was removed and the residue redissolved in benzene (5 mL) and added to a J. Youngs ampoule containing Rh(PPh₃)₄H (200 mg, 0.17 mmol) in benzene (5 mL). The mixture was then heated at 353 K for 16 h. After cooling to room temperature, the resulting deep orange-red solution was filtered by cannula, concentrated to ca. 2 mL and hexane added to afford **4.36** as an orange precipitate. The solid was isolated by cannula filtration and dried under vacuum to give a 1:20 mixture of cis- and trans-phosphine isomers of **4.36a/b**. Yield 70 mg (54%). Analysis for C₄₂H₄₃N₂P₂Rh (740.66) %; C, 68.11; H, 5.85; N, 3.78. Found, %: C, 67.98; H, 5.95; N, 3.81. ¹H NMR (500 MHz, C₆D₆) for **4.36b**: δ 8.10-8.05 (m, 11H, PC₆H₅), 7.18-7.12 (m, 13H, PC₆H₅), 7.11-7.06 (m, 6H, PC₆H₅), 3.21 (s, 6H, NCH₃), 2.00 (t, ³*J*_{HH} = 5.8 Hz, 4H, NCH₂CH₂CH₂N), 0.96 (quin, ³*J*_{HH} = 5.8 Hz, 2H, NCH₂CH₂CH₂N), -9.16 (td, ²*J*_{HP} = 23.0 Hz, ¹*J*_{HRh} = 11.0 Hz, 1H, RhH). ³¹P{¹H} NMR: δ 47.5 (d, ¹*J*_{PRh} = 180 Hz). ¹³C{¹H} NMR (C₆D₆): 223.9 (m, Rh-C_{NHC}), 141.9 ('vt', *J* = 4 Hz,

PC₆H₅), 134.6 ('vt', J = 7 Hz, PC₆H₆), 128.1 (s, PC₆H₅), 127.6 ('vt', J = 4 Hz, PC₆H₅), 45.8 (s, N-CH₃), 43.4 (s, NCH₂), 20.0 (NCH₂CH₂).

4.22.6 Synthesis of Rh(6-Et)(PPh₃)₂H (4.37). As for **4.36** but with [6-EtH]PF₆ (199 mg, 0.70 mmol) and KN(SiMe₃)₂ (139 mg, 0.70 mmol) in benzene (2 mL) and Rh(PPh₃)₄H (200 mg, 0.17 mmol) in benzene (5 mL) to give a 1:9 mixture of cis- and trans-isomers of **4.37a/b**. Yield 85 mg (64%). Analysis for C₄₄H₄₇N₂P₂Rh (768.71) %; C, 68.75; H, 6.12; N, 3.64. Found, %: C, 68.85; H, 6.06; N, 3.68. Selected ¹H NMR (500 MHz, C₆D₆) for **4.37b**: δ 4.07 (quart, ³J_{HH} = 7.2 Hz, 4H, NCH₂CH₃), 2.25 (t, ³J_{HH} = 6.0 Hz, 4H, NCH₂CH₂CH₂N), 1.19 (quint, ³J_{HH} = 6.0 Hz, 2H, NCH₂CH₂CH₂N), 0.48 (t, ³J_{HH} = 7.2 Hz, 6H, NCH₂CH₃), -9.83 (td, ²J_{HP} = 24.5 Hz, ¹J_{HRh} = 10.5 Hz, RhH). ³¹P{¹H} NMR: δ 45.8 (d, ¹J_{PRh} = 180 Hz). ¹³C{¹H} NMR: δ 222.9 (m, Rh-C_{NHC}), 142.1 ('vt', J = 17 Hz, PC₆H₆), 134.6 ('vt', J = 6 Hz, PC₆H₅), 128.5 (s, PC₆H₅), 127.6 (s, PC₆H₅), 53.1 (s, N-CH₂), 41.2 (s, NCH₂), 21.5 (s, NCH₂CH₂), 12.7 (s, NCH₂CH₃). Selected ¹H NMR (500 MHz, C₆D₆) for cis- **4.37a**: δ 5.49 (m, 2H, NCH₂CH₃), 3.19 (m, 2H, NCH₂CH₃), 2.52 (m, 2H, NCH₂CH₂CH₂N), 2.13 (m, 2H, NCH₂CH₂CH₂N), 1.25, (2H, NCH₂CH₂CH₂N), 1.13 (t, ³J_{HH} = 7.2 Hz, 3H, NCH₂CH₃), 0.88 (t, ³J_{HH} = 7.2 Hz, 3H, NCH₂CH₃), -5.39 (ddd, ²J_{HP} = 106.9 Hz, ²J_{HP} or ¹J_{HRh} = 30.5 Hz, ²J_{HP} or ¹J_{HRh} = 25.9 Hz, RhH). ³¹P{¹H} NMR: δ 51.1 (dd, ¹J_{PRh} = 144, ²J_{PP} = 25 Hz), 44.1 (dd, ¹J_{PRh} = 142, ¹J_{PP} = 25 Hz).

4.22.7 Synthesis of Rh(PPh₃)₂(CO)₂Rh(PPh₃)(6-Et) (4.38). An NMR tube was charged with [6-EtH]PF₆ (28 mg, 0.098 mmol) and KN(SiMe₃)₂ (19.6 mg, 0.098 mmol) in toluene (0.5 mL) and the suspension stirred at room temperature for 1 h. The solvent was transferred to another NMR tube containing Rh(PPh₃)₃(CO)H (30 mg, 0.033 mmol) in toluene (0.5 mL). The mixture was then stirred at 298 K for 24 h. The solvent was then concentrated down and layered with hexane to afford dark red crystals of the dinuclear compound [(PPh₃)₂Rh(μ-CO)₂Rh(6-Et)(PPh₃)] **4.38**. Yield 5 mg (12%). ³¹P{¹H} NMR (400 MHz, tol-d₈): δ 38.2 (dd, J_{PRh} = 233.5 Hz, ²J_{PRh} = 8.5 Hz), 43.0 (d, J_{PRh} = 183.0 Hz). IR (CH₂Cl₂, cm⁻¹): 1708 (ν_{CO}).

4.22.8 Synthesis of Rh(6-Me)(PPh₃)₂(FHF) (4.42). Et₃N·3HF (14.5 μL, 0.09 mmol) was added to a benzene solution (3 mL) of Rh(6-Me)(PPh₃)₂H (78 mg, 0.10 mmol) in an ampoule fitted with a J. Youngs resealable valve. After stirring at 289 K for 2 h, the solution was reduced to dryness, redissolved in a minimum amount of THF and layered with hexane to afford **4.42** as an orange-yellow solid. Yield: 41 mg (50%). Analysis for C₄₂H₄₃N₂F₂P₂Rh (778.62), %: C, 64.78; H, 5.57; N, 3.60. Found, %: C, 64.64; H, 5.72; N, 3.74. ¹H NMR (500 MHz, C₆D₆): δ 13.2 (br d, *J* ≈ 387 Hz, 1H, Rh-FHF), 3.55 (s, 6H, NCH₃), 1.59 (t, ³*J*_{HH} = 5.7 Hz, 4H, NCH₂CH₂CH₂N), 0.33 (quin, ³*J*_{HH} = 5.7 Hz, 2H, NCH₂CH₂CH₂N). ¹H NMR (500 MHz, THF-*d*₈): δ 11.7 (br, 1H, RhFHF), 7.89 (m, 13H, PC₆H₅), 7.30 (m, 17H, PC₆H₅), 3.69 (s, 6H, NCH₃), 2.08 (t, ³*J*_{HH} = 6.0 Hz, 4H, NCH₂CH₂CH₂N), 0.78 (br quin, ³*J*_{HH} = 6.0 Hz, 2H, NCH₂CH₂CH₂N). Additional selected ¹H NMR (500 MHz, THF-*d*₈): 190 K: δ 12.6 (dd, ¹*J*_{HF(distal)} ≈ 379 Hz, ¹*J*_{HF(proximal)} ≈ 42 Hz, 1H, RhFHF). ³¹P{¹H} NMR (C₆D₆): δ 26.1 (d, ¹*J*_{PRh} = 173 Hz). ¹⁹F NMR (THF-*d*₈, 300 K): δ -181.3 (br s, RhFHF), -316.4 (br s, RhFHF); 190 K: δ -176.9 (dd, ¹*J*_{FH} = 381 Hz, ²*J*_{FF} = 127 Hz, RhFHF), -312.0 (br d, ²*J*_{FF} = 125 Hz, RhFHF). ¹³C{¹H} NMR (THF-*d*₈): δ 209.1 (m, RhC_{NHC}), 137.8 ('vt', *J* = 18 Hz, PC₆H₅), 135.6 ('vt', *J* = 6 Hz, PC₆H₅), 129.8 (s, PC₆H₅), 128.6 (s, PC₆H₅), 47.1 (s, NCH₃), 45.0 (s, NCH₂), 20.5 (s, NCH₂CH₂). IR (cm⁻¹): 2506.2 (ν_{HF}), 1895.5 (ν_{HF}).

4.22.9 Synthesis of Rh(6-Et)(PPh₃)₂(FHF) (4.43). As above but with **4.37a/b**, Et₃N·3HF (21 μL, 0.13 mmol) was added by syringe to a solution of Rh(6-Et)(PPh₃)₂H (100 mg, 0.13 mmol) in toluene (3 mL) in an ampoule fitted with a J. Youngs resealable valve. After stirring at 298 K for 2 h, the solution was reduced to dryness, redissolved in a minimum amount of benzene and precipitated under vigorous stirring with addition of hexane. The yellow solid was filtered and dried. Yield: 45 mg (43%). Repeated attempts to obtain elemental analysis gave consistently low % C values. Selected ¹H NMR (500 MHz, THF-*d*₈) for **4.43b**: δ ¹H NMR (500 MHz, THF-*d*₈): δ 11.8 (br s, 1H, RhFHF), 4.64 (quart, ³*J*_{HH} = 7.2 Hz, 4H, NCH₂CH₃), 2.41 (t, ³*J*_{HH} = 6.1 Hz, 4H, NCH₂CH₂CH₂N), 1.24 (quin, ³*J*_{HH} = 6.1 Hz, 2H, NCH₂CH₂CH₂N), 0.48 (t, ³*J*_{HH} = 7.2 Hz, 6H, NCH₂CH₃). ³¹P{¹H} NMR (C₆D₆): δ 27.7 (dd, ¹*J*_{PRh} = 173 Hz, ²*J*_{PF} = 17 Hz). Selected ¹H NMR (500 MHz, THF-*d*₈) for **4.43a**: δ 11.8 (br s,

1H, RhFHF), 6.14 (m, 2H, NCH₂CH₃), 3.45 (m, 2H, NCH₂CH₃), 3.01 (m, 2H, NCH₂CH₂CH₂N), 2.37 (m, 2H, NCH₂CH₂CH₂N), 1.34 (t, ³J_{HH} = 7.1 Hz, 6H, NCH₂CH₃), 1.29 (m, 2H, NCH₂CH₂CH₂N). ³¹P{¹H} NMR: δ 60.6 (ddd, ¹J_{PRh} = 219 Hz, ²J_{PF} = 181 Hz, ²J_{PP} = 38 Hz), 36.4 (ddd, ¹J_{PRh} = 123 Hz, ²J_{PP} = 38 Hz, ²J_{PF} = 22 Hz). Additional selected ¹H NMR (400 MHz, THF-*d*₈) of 1:1 mixture of trans- and cis-P,P Rh(6-Et)(PPh₃)₂(FHF): 218 K: δ 12.27 (br m, 1H, RhFHF). ¹⁹F NMR (THF-*d*₈, 218 K): δ -177.3 (br d, *J* = 372 Hz, RhFHF), -179.4 (br d, *J* = 380 Hz, RhFHF), -273.3 (br m, RhFHF), -310.6 (br m, RhFHF). IR (cm⁻¹): 2421.7 (ν_{HF}), 2333.8 (ν_{HF}), 1883.0 (ν_{HF}).

4.22.10 Synthesis of Rh(6-Me)(PPh₃)₂F (4.48). A benzene solution (5 mL) of Rh(6-Me)(PPh₃)₂H (50 mg, 0.07 mmol) in an ampoule fitted with a J. Youngs resealable valve was freeze-pump-thaw degassed and 1 atm CF₃CF=CF₂ added. The solution was stirred at 298 K for 15 min, during which the colour changed from deep orange to pale yellow. The solution was reduced to dryness, extracted with a minimum amount of benzene and precipitated as a yellow solid upon addition of hexane under vigorous stirring. Yield: 13 mg (25%). Selected ¹H NMR (500 MHz, C₆D₆): δ 8.33-8.25 (m, 13H, PC₆H₅), 7.14-7.11 (m, 9H, PC₆H₅), 7.07-7.02 (m, 8H, PC₆H₅), 3.62 (s, 6H, NCH₃), 1.63 (t, ³J_{HH} = 6.2 Hz, 4H, NCH₂CH₂CH₂N), 0.31 (quin, ³J_{HH} = 6.2 Hz, 2H, NCH₂CH₂CH₂N). ³¹P{¹H} NMR: δ 23.9 (dd, ²J_{PRh} = 174 Hz, ²J_{PF} = 15 Hz). ¹⁹F NMR: δ -332.7 (br d, ¹J_{FRh} = 61 Hz, RhF). ¹³C{¹H} NMR: δ 210.8 (m, RhC_{NHC}), 138.2 ('vt', *J* = 17 Hz, PC₆H₅), 135.0 ('vt', *J* = 6 Hz, PC₆H₅), 128.8 (s, PC₆H₅), 46.7 (s, NCH₃), 43.8 (s, NCH₂), 19.8 (s, NCH₂CH₂). * Missing aryl C presumed to be obscured by solvent. MS (EI): *m/z* 758.1 [M]⁺, 738.1 [M-HF]⁺. HR-MS (EI): [M]⁺ calcd. *m/z* 758.2067; found 758.1848.

4.22.11 Synthesis of Rh(6-Et)(PPh₃)₂F (4.49). As above but with **4.37a/b** (50 mg, 0.065 mol). Yield: 20 mg (39%). Selected ¹H NMR (500 MHz, C₆D₆) for **4.49b**: δ 4.69 (q, ³J_{HH} = 7.2 Hz, 4H, NCH₂CH₃), 1.99 (t, *J*_{HH} = 6.0, 4H, NCH₂CH₂CH₂N), 0.76 (quin, ³J_{HH} = 6.0 Hz, 2H, NCH₂CH₂CH₂N), 0.49 (t, ³J_{HH} = 7.2 Hz, 6H, NCH₂CH₃). ³¹P{¹H} NMR: δ 26.9 (dd, ¹J_{PRh} = 174 Hz, ²J_{PP} = 19 Hz). ¹⁹F NMR: δ -331.2 (br d, ¹J_{FRh} = 65 Hz, RhF). Selected ¹H NMR (500 MHz, C₆D₆, 298 K) for **4.49a**: δ 6.51 (m, 2H, NCH₂CH₃), 3.16 (m, 2H, NCH₂CH₃), 2.53 (m, 2H, NCH₂CH₂CH₂N), 1.93 (m, 2H, NCH₂CH₂CH₂N), 1.55 (t, ³J_{HH} = 7.1 Hz, 6H, NCH₂CH₃), 1.26 (m, 2H, NCH₂CH₂CH₂N). ³¹P{¹H} NMR:

δ 60.3 (ddd, $^1J_{\text{PRh}} = 219$ Hz, $^2J_{\text{PF}} = 184$ Hz, $^2J_{\text{PP}} = 39$ Hz), 36.6 (ddd, $^1J_{\text{PRh}} = 122$ Hz, $^2J_{\text{PP}} = 36$ Hz, $^2J_{\text{PF}} = 27$ Hz). ^{19}F NMR: δ -285.8 (ddd, $^2J_{\text{FP}} = 182$ Hz, $^1J_{\text{FRh}} = 65$ Hz, $^2J_{\text{FP}} = 26$ Hz, RhF). MS (EI): m/z 768.2 $[\text{M}]^+$, 766.2 $[\text{M}-\text{HF}]^+$. HR-MS (EI): $[\text{M}]^+$ calcd. m/z 786.2402; found 786.2174.

4.22.12 Synthesis of Rh(6-ⁱPr)(PPh₃)₂Cl (4.50). An ampoule was charged with 6-ⁱPrH·PF₆ (51.0 mg, 0.16 mmol) and KN(SiMe₃)₂ (32 mg, 0.16 mmol) in THF (5 mL) and the suspension stirred at 298 K for 1 hr. The mixture was added to a J. Youngs ampoule containing Rh(PPh₃)₃Cl (50 mg, 0.05 mmol) in THF (5 mL) and the mixture stirred at 298 K for 2h. The resulting deep brown solution was filtered by cannula, concentrated to ca. 2 mL and hexane added to afford a yellow solid. The solid was isolated by cannula filtration and dried under vacuum to give **4.50**. Yield 20 mg (45%). Analysis for C₄₆H₅₀ClN₂P₂Rh (830.22), %: C, 66.47; H, 6.06; N, 3.37. Found, %: C, 66.29; H, 5.84; N, 3.42. ^1H NMR (500 MHz, C₆D₆, 298 K): δ 7.35 (sept, 2H, (CH₃)CH), 2.63 (m, 2H, NCH₂CH₂CH₂N), 2.20 (m, 2H, NCH₂CH₂CH₂N), 1.73 (d, $^3J_{\text{HH}} = 6.4$ Hz, 6H, (CH₃)₂CH), 1.33 (m, 1H, CH₂CH₂CH₂), 1.21 (m, 1H, CH₂CH₂CH₂), 0.63 (d, $^3J_{\text{HH}} = 6.4$ Hz, 6H, (CH₃)₂CH). $^{31}\text{P}\{^1\text{H}\}$ NMR: δ 51.6 (dd, $^1J_{\text{PRh}} = 212$ Hz, $^2J_{\text{PP}} = 37$ Hz), 39.9 (dd, $^1J_{\text{ClRh}} = 121$ Hz, $^2J_{\text{PP}} = 36$ Hz)

4.22.13 Synthesis of Rh(6-Et)(PPh₃)₂Cl (4.51). An ampoule was charged with 6-EtH·PF₆ (18.5 mg, 0.06 mmol) and KN(SiMe₃)₂ (13 mg, 0.06 mmol) in THF (5 mL) and the suspension stirred at 298 K for 1 hr. The mixture was added to a J. Youngs ampoule containing Rh(PPh₃)₃Cl (50 mg, 0.05 mmol) in THF (5 mL) and the mixture stirred at 298 K for 2h. After cooling to room temperature, the resulting deep orange-red solution was filtered by cannula, concentrated to ca. 2 mL and hexane added to afford an orange precipitate. The solid was isolated by cannula filtration and dried under vacuum to give a **4.51** as a mixture of isomers. Yield 25 mg (57%). Selected ^1H NMR (500 MHz, C₆D₆) for trans-Rh(6-Et)(PPh₃)₂Cl: δ 4.70 (q, $^3J_{\text{HH}} = 7.16$ Hz, 4H, NCH₂CH₃), 1.98 (t, $^3J_{\text{HH}} = 6.03$ Hz, 4H, NCH₂CH₂CH₂N), 0.71 (m, $^3J_{\text{HH}} = 6.03$ Hz, 2H, NCH₂CH₂CH₂N), 0.50 (t, $^3J_{\text{HH}} = 7.16$ Hz, 6H, NCH₂CH₃). $^{31}\text{P}\{^1\text{H}\}$ NMR: δ 30.8 (d, $^1J_{\text{PRh}} = 164.3$ Hz). Selected ^1H NMR (500 MHz, C₆D₆) for cis-Rh(6-Et)(PPh₃)₂Cl: δ 6.34 (m, 2H, NCH₂CH₃), 3.22 (m, 2H, NCH₂CH₃), 2.52 (m, 2H, NCH₂CH₂CH₂N), 1.89 (m, 2H, NCH₂CH₂CH₂N),

1.02, (1H, NCH₂CH₂CH₂N), 0.70, (1H, NCH₂CH₂CH₂N), 1.52 (t, ³J_{HH} = 7.10 Hz, 6H, NCH₂CH₃). ³¹P{¹H} NMR: δ 52.2 (dd, ¹J_{PRh} = 212 Hz, ²J_{PP} = 37 Hz), 39.1 (dd, ¹J_{CIRh} = 117 Hz, ²J_{PP} = 36 Hz)

4.22.14 Synthesis of Rh(6-ⁱPr)(PPh₃)(CO)F (4.54). CO (1 atm) was admitted to a J. Youngs NMR tube containing a C₆D₆ solution (0.5 mL) of Rh(6-ⁱPr)(PPh₃)₂F (10 mg, 0.01 mmol) and the solution interrogated by multinuclear NMR spectroscopy. Selected ¹H NMR (400 MHz, C₆D₆): δ 6.82 (sept, ³J_{HH} = 6.7 Hz, 2H, NCH(CH₃)₂), 2.52 (m, 2H, NCH₂CH₂CH₂N), 2.38 (m, NCH₂CH₂CH₂N), 1.30 (d, ³J_{HH} = 6.7 Hz, 6H, NCH(CH₃)₂), 1.17 (br m, 2H, NCH₂CH₂CH₂N), 1.04 (d, ³J_{HH} = 6.8 Hz, 6H, NCH(CH₃)₂). ³¹P{¹H} NMR: δ 30.3 (dd, ¹J_{PRh} = 122 Hz, ²J_{PF} = 23 Hz; additional ²J_{PC} splitting (16 Hz) in ¹³CO labelled sample). ¹⁹F NMR: δ -282.4 (dd, ¹J_{FRh} = 52 Hz, ²J_{FP} = 23 Hz; additional ²J_{FC} splitting (76 Hz) in ¹³CO labelled sample, RhF). Selected ¹³C{¹H} NMR of ¹³CO-labelled sample (C₆D₆): δ 191.9 (ddd, ²J_{CF} = 76 Hz, ²J_{CRh} = 72 Hz, ²J_{CP} = 16 Hz, RhCO).

4.22.15 Synthesis of Rh(6-ⁱPr)(PPh₃)₂(CF₃) (4.58). To a benzene (5 mL) solution of Rh(6-ⁱPr)(PPh₃)₂F (70 mg, 0.09 mmol) was added Me₃SiCF₃ (55 μL, 0.37 mmol). The reaction mixture was stirred for 10 min at 298 K before the solvent was removed and the residue redissolved in THF/Et₂O to afford orange-yellow crystals of the product. Yield: 25 mg (34%). Analysis for C₄₇H₅₀N₂F₃P₂Rh (864.73), %: C, 65.28; H, 5.83; N, 3.24. Found, %: C, 65.00; H, 5.72; N, 3.36. ¹H NMR (500 MHz, C₆D₆): δ 7.94-7.66 (m, 10H, PC₆H₅), 7.23 (sept, ³J_{HH} = 6.6 Hz, 2H, NCH(CH₃)₂), 7.05-6.72 (m, 20H, PC₆H₅), 2.67 (m, 2H, NCH₂CH₂CH₂N), 2.28 (m, NCH₂CH₂CH₂N), 1.54 (d, ³J_{HH} = 6.6 Hz, 6H, NCH(CH₃)₂), 1.33 (m, 2H, NCH₂CH₂CH₂N), 0.65 (d, ³J_{HH} = 6.6 Hz, 6H, NCH(CH₃)₂). ³¹P{¹H} NMR: δ 43.0 (ddq, ¹J_{PRh} = 136 Hz, ²J_{PP} = 32 Hz, ³J_{PF} = 13 Hz), 41.7 (dq, ¹J_{PRh} = 126 Hz, ³J_{PF} = 40 Hz, ²J_{PP} = 32 Hz). ¹⁹F NMR: δ -7.2 (ddd, ³J_{FP} = 40 Hz, ²J_{FRh} = 23 Hz, ³J_{FP} = 13 Hz, RhCF₃).

References

- (1) Herrmann, W. A.; Köcher, C. *Angew. Chem., Int. Ed.* **1997**, *36*, 2162.
- (2) Hahn, F. E.; Jahnke, M. C. *Angew. Chem., Int. Ed.* **2008**, *47*, 3122.
- (3) Iglesias, M.; Beetstra, D. J.; Kariuki, B.; Cavell, K. J.; Dervisi, A.; Fallis, I. A. *Eur. J. Inorg. Chem.* **2009**, 1913.
- (4) Armstrong, R.; Ecott, C.; Mas-Marzá, E.; Page, M. J.; Mahon, M. F.; Whittlesey, M. K. *Organometallics* **2010**, *29*, 991.
- (5) Özdemir, I.; Gürbüz, N.; Gök, Y.; Çetinkaya, B. *Heteroat. Chem.* **2008**, *19*, 82.
- (6) Dunsford, J. J.; Tromp, D. S.; Cavell, K. J.; Elsevier, C. J.; Kariuki, B. M. *Dalton Trans.* **2013**, *42*, 7318.
- (7) Yun, J.; Marinez, E. R.; Grubbs, R. H. *Organometallics* **2004**, *23*, 4172.
- (8) Schneider, S. K.; Rentzsch, C. F.; Krüger, A.; Raubenheimer, H. G.; Herrmann, W. A. *J. Mol. Catal. A: Chem.* **2007**, *265*, 50.
- (9) Bortenschlager, M.; Mayr, M.; Nuyken, O.; Buchmeiser, M. R. *J. Mol. Catal. A: Chem.* **2005**, *233*, 67.
- (10) Kremzow, D.; Seidel, G.; Lehmann, C. W.; Fürstner, A. *Chem. Eur. J.* **2005**, *11*, 1833.
- (11) Bazinet, P.; Yap, G. P. A.; Richeson, D. S. *J. Am. Chem. Soc.* **2003**, *125*, 13314.
- (12) Alder, R. W.; Blake, M. E.; Bortolotti, C.; Bufali, S.; Butts, C. P.; Linehan, E.; Oliva, J. M.; Orpen, A. G.; Quayle, M. J. *Chem. Commun.* **1999**, 241.
- (13) Moerdyk, J. P.; Bielawski, C. W. *Organometallics* **2011**, *30*, 2278.
- (14) Magill, A. M.; Cavell, K. J.; Yates, B. F. *J. Am. Chem. Soc.* **2004**, *126*, 8717.
- (15) Saba, S.; Brescia, A. M.; Kaloustian, M. K. *Tetrahedron Lett.* **1991**, *32*, 5031.
- (16) Jazzar, R.; Liang, H.; Donnadiou, B.; Bertrand, G. *J. Organomet. Chem.* **2006**, *691*, 3201.
- (17) Iglesias, M.; Beetstra, D. J.; Knight, J. C.; Ooi, L.-L.; Stasch, A.; Coles, S.; Male, L.; Hursthouse, M. B.; Cavell, K. J.; Dervisi, A.; Fallis, I. A. *Organometallics* **2008**, *27*, 3279.

- (18) Arduengo, A. J.; Krafczyk, R.; Schmutzler, R.; Craig, H. A.; Goerlich, J. R.; Marshall, W. J.; Unverzagt, M. *Tetrahedron* **1999**, *55*, 14523.
- (19) Aidouni, A.; Bendahou, S.; Demonceau, A.; Delaude, L. *J. Comb. Chem.* **2008**, *10*, 886.
- (20) Scarborough, C. C.; Guzei, I. A.; Stahl, S. S. *Dalton Trans.* **2009**, 2284.
- (21) Iglesias, M.; Beetstra, D. J.; Stasch, A.; Horton, P. N.; Hursthouse, M. B.; Coles, S. J.; Cavell, K. J.; Dervisi, A.; Fallis, I. A. *Organometallics* **2007**, *26*, 4800.
- (22) Binobaid, A.; Iglesias, M.; Beetstra, D. J.; Kariuki, B.; Dervisi, A.; Fallis, I. A.; Cavell, K. J. *Dalton Trans.* **2009**, 7099.
- (23) Davies, C. J. E.; Page, M. J.; Ellul, C. E.; Mahon, M. F.; Whittlesey, M. K. *Chem. Commun.* **2010**, *46*, 5151.
- (24) Tekavec, T. N.; Zuo, G.; Simon, K.; Louie, J. *J. Org. Chem.* **2006**, *71*, 5834.
- (25) Xi, Z.; Liu, B.; Chen, W. *J. Org. Chem.* **2008**, *73*, 3954.
- (26) Gu, S.; Ni, P.; Chen, W. *Chinese Journal of Catalysis* **2010**, *31*, 875.
- (27) Hatakeyama, T.; Hashimoto, S.; Ishizuka, K.; Nakamura, M. *J. Am. Chem. Soc.* **2009**, *131*, 11949.
- (28) Shimasaki, T.; Tobisu, M.; Chatani, N. *Angew. Chem., Int. Ed.* **2010**, *49*, 2929.
- (29) Page, M. J.; Lu, W. Y.; Poulten, R. C.; Carter, E.; Algarra, A. G.; Kariuki, B. M.; Macgregor, S. A.; Mahon, M. F.; Cavell, K. J.; Murphy, D. M.; Whittlesey, M. K. *Chem. Eur. J.* **2013**, *19*, 2158.
- (30) Scarborough, C. C.; Grady, M. J. W.; Guzei, I. A.; Gandhi, B. A.; Bunel, E. E.; Stahl, S. S. *Angew. Chem., Int. Ed.* **2005**, *44*, 5269.
- (31) Scarborough, C. C.; Popp, B. V.; Guzei, I. A.; Stahl, S. S. *J. Organomet. Chem.* **2005**, *690*, 6143.
- (32) Mayr, M.; Wurst, K.; Ongania, K. H.; Buchmeiser, M. R. *Chem. Eur. J.* **2004**, *10*, 1256.
- (33) Dunsford, J. J.; Cavell, K. J.; Kariuki, B. M. *Organometallics* **2012**, *31*, 4118.
- (34) Park, J. K.; McQuade, D. T. *Synthesis* **2012**, *44*, 1485.
- (35) Herrmann, W. A.; Elison, M.; Fischer, J.; Köcher, C.; Artus, G. R. J. *Chem. Eur. J.* **1996**, *2*, 772.

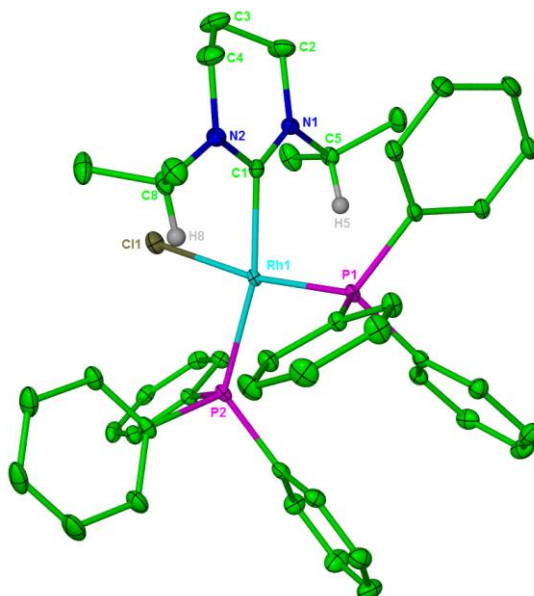
- (36) Segarra, C.; Mas-Marzá, E.; Lowe, J. P.; Mahon, M. F.; Poulten, R. C.; Whittlesey, M. K. *Organometallics* **2012**, *31*, 8584.
- (37) Alder, R. W.; Chaker, L.; Paolini, F. P. V. *Chem. Commun.* **2004**, 2172.
- (38) Otto, M.; Conejero, S.; Canac, Y.; Romanenko, V. D.; Rudzevitch, V.; Bertrand, G. *J. Am. Chem. Soc.* **2004**, *126*, 1016.
- (39) Amani, J.; Musavi, S. M. *Tetrahedron* **2011**, *67*, 749.
- (40) Tang, C. Y.; Phillips, N.; Bates, J. I.; Thompson, A. L.; Gutmann, M. J.; Aldridge, S. *Chem. Commun.* **2012**, *48*, 8096.
- (41) Scott, N. M.; Dorta, R.; Stevens, E. D.; Correa, A.; Cavallo, L.; Nolan, S. P. *J. Am. Chem. Soc.* **2005**, *127*, 3516.
- (42) Douglas, S.; Lowe, J. P.; Mahon, M. F.; Warren, J. E.; Whittlesey, M. K. *J. Organomet. Chem.* **2005**, *690*, 5027.
- (43) Freeman, M. A.; Young, D. A. *Inorg. Chem.* **1986**, *25*, 1556.
- (44) Lee, D. H.; Kwon, H. J.; Patel, P. P.; Liable-Sands, L. M.; Rheingold, A. L.; Crabtree, R. H. *Organometallics* **1999**, *18*, 1615.
- (45) Murphy, V. J.; Hascall, T.; Chen, J. Y.; Parkin, G. *J. Am. Chem. Soc.* **1996**, *118*, 7428.
- (46) Jasim, N. A.; Perutz, R. N. *J. Am. Chem. Soc.* **2000**, *122*, 8685.
- (47) Whittlesey, M. K.; Perutz, R. N.; Greener, B.; Moore, M. H. *Chem. Commun.* **1997**, 187.
- (48) Roe, D. C.; Marshall, W. J.; Davidson, F.; Soper, P. D.; Grushin, V. V. *Organometallics* **2000**, *19*, 4575.
- (49) Grushin, V. V.; Marshall, W. J. *J. Am. Chem. Soc.* **2004**, *126*, 3068.
- (50) Grushin, V. V. *Acc. Chem. Res.* **2010**, *43*, 160.
- (51) Noveski, D.; Braun, T.; Krückemeier, S. *J. Fluorine Chem.* **2004**, *125*, 959.
- (52) Coulson, D. R. *J. Am. Chem. Soc.* **1976**, *98*, 3111.
- (53) Due to low yields of **4.48** and **4.49** we turned to a different precursor and studied the reactivity of Wilkinson's catalyst towards 6-NHCs. We successfully synthesised Rh(6-ⁱPr)(PPh₃)₂Cl **4.50** and Rh(6-Et)(PPh₃)₂Cl **4.51**, which were isolated and spectroscopically structurally characterised (Appendix 1-4). However repeating the reaction with 6-Me failed to generate the analogous chloride complex, and only produced a mixture of unknown products.

- (54) Burton, D. J.; Spawn, T. D.; Heinze, P. L.; Bailey, A. R.; Shinya, S. *J. Fluorine Chem.* **1989**, *44*, 167.
- (55) Koroniak, H.; Palmer, K. W.; Dolbier, W. R.; Zhang, H. Q. *Magn. Reson. Chem.* **1993**, *31*, 748.
- (56) Clot, E.; Megret, C.; Kraft, B. M.; Eisenstein, O.; Jones, W. D. *J. Am. Chem. Soc.* **2004**, *126*, 5647.
- (57) Toscano, P. J.; Brand, H.; Liu, S. C.; Zubieta, J. *Inorg. Chem.* **1990**, *29*, 2101.
- (58) Foris, A. *Magn. Reson. Chem.* **2004**, *42*, 534.
- (59) Miller, W. T.; Fried, J. H.; Goldwhite, H. *J. Am. Chem. Soc.* **1960**, *82*, 3091.
- (60) Braun, T.; Wehmeier, F. *Eur. J. Inorg. Chem.* **2011**, 613.
- (61) Noveski, D.; Braun, T.; Neumann, B.; Stammler, A.; Stammler, H. G. *Dalton Trans.* **2004**, 4106.
- (62) Kuehnel, M. F.; Lentz, D.; Braun, T. *Angew. Chem., Int. Ed.* **2013**, *52*, 3328.
- (63) Amii, H.; Uneyama, K. *Chem. Rev.* **2009**, *109*, 2119.
- (64) Noveski, D.; Braun, T.; Schulte, M.; Neumann, B.; Stammler, H. G. *Dalton Trans.* **2003**, 4075.
- (65) Braun, T.; Noveski, D.; Neumann, B.; Stammler, H. G. *Angew. Chem., Int. Ed.* **2002**, *41*, 2745.
- (66) Zámotná, L.; Ahrens, M.; Braun, T. *J. Fluorine Chem.* **2013**, *155*, 132.
- (67) Cairns, M. A.; Dixon, K. R.; McFarland, J. J. *J. Chem. Soc., Dalton Trans.* **1975**, 1159.
- (68) Vaska, L.; Peone, J. J. *Inorg. Synth.* **1974**, *15*, 65.
- (69) Colquhoun, I. J.; McFarlane, W. *J. Magn. Reson.* **1982**, *46*, 525.
- (70) Vicente, J.; Gil-Rubio, J.; Bautista, D. *Inorg. Chem.* **2001**, *40*, 2636.
- (71) Vicente, J.; Gil-Rubio, J.; Guerrero-Leal, J.; Bautista, D. *Organometallics* **2004**, *23*, 4871.
- (72) Goodman, J.; Grushin, V. V.; Larichev, R. B.; Macgregor, S. A.; Marshall, W. J.; Roe, D. C. *J. Am. Chem. Soc.* **2009**, *131*, 4236.
- (73) Goodman, J.; Grushin, V. V.; Larichev, R. B.; Macgregor, S. A.; Marshall, W. J.; Roe, D. C. *J. Am. Chem. Soc.* **2010**, *132*, 12013.

- (74) Macgregor, S. A.; Roe, D. C.; Marshall, W. J.; Bloch, K. M.; Bakhmutov, V. I.; Grushin, V. V. *J. Am. Chem. Soc.* **2005**, *127*, 15304.
- (75) Tomashenko, O. A.; Grushin, V. V. *Chem. Rev.* **2011**, *111*, 4475.
- (76) Hughes, R. P. *Adv. Organomet. Chem.* **1990**, *31*, 183.
- (77) Ahmad, N.; Levison, J. J.; Robinson, S. D.; Uttley, M. F. *Inorg. Synth.* **1990**, *28*, 81.
- (78) Ahmad, N.; Levison, J. J.; Robinson, S. D.; Uttley, M. F. *Inorg. Synth.* **1974**, *15*, 45.
- (79) Reade, S. P.; Nama, D.; Mahon, M. F.; Pregosin, P. S.; Whittlesey, M. K. *Organometallics* **2007**, *26*, 3484.

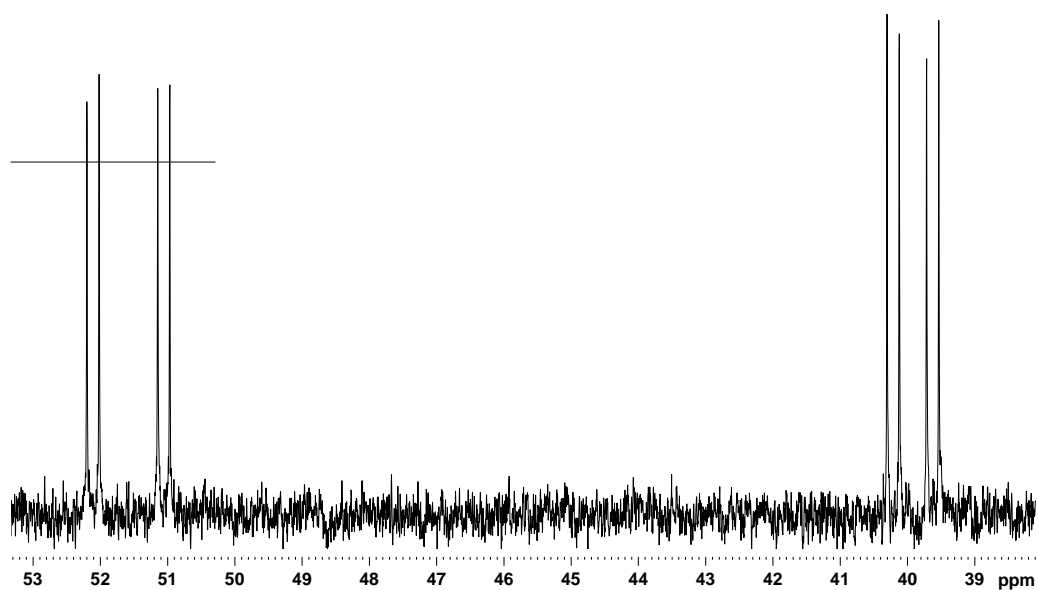
Appendices

Appendix 1: X-ray crystal structure of Rh(6-ⁱPr)(PPh₃)₂Cl (4.50)



Bond lengths [Å] and angles [°] for Rh(6- ⁱ Pr)(PPh ₃) ₂ Cl	
Rh(1)-C(1)	2.057(2)
Rh(1)-P(1)	2.2088(6)
Rh(1)-P(2)	2.3301(6)
Rh(1)-Cl(1)	2.4248(7)
C(1)-Rh(1)-P(1)	90.42(6)
P(1)-Rh(1)-P(2)	101.52
C(1)-Rh(1)-P(2)	166.49(7)
C(1)-Rh(1)-Cl(1)	80.56(6)
P(1)-Rh(1)-Cl(1)	170.98(2)
P(1)-Rh(1)-Cl	87.41(2)

Appendix 2: $^{31}\text{P}\{^1\text{H}\}$ NMR spectrum of $\text{Rh}(6\text{-}^i\text{Pr})(\text{PPh}_3)_2\text{Cl}$ (**4.50**)



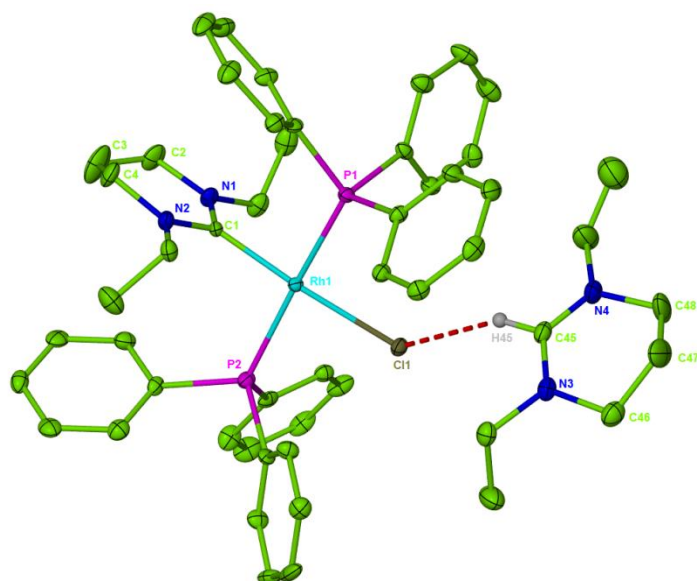
$^{31}\text{P}\{^1\text{H}\}$ NMR spectrum of **4.50** in C_6D_6 at 298 K

Cis phosphine isomer:

δ 51.6 (dd, $^1J_{\text{PRh}} = 212$ Hz, $^2J_{\text{PP}} = 37$ Hz),

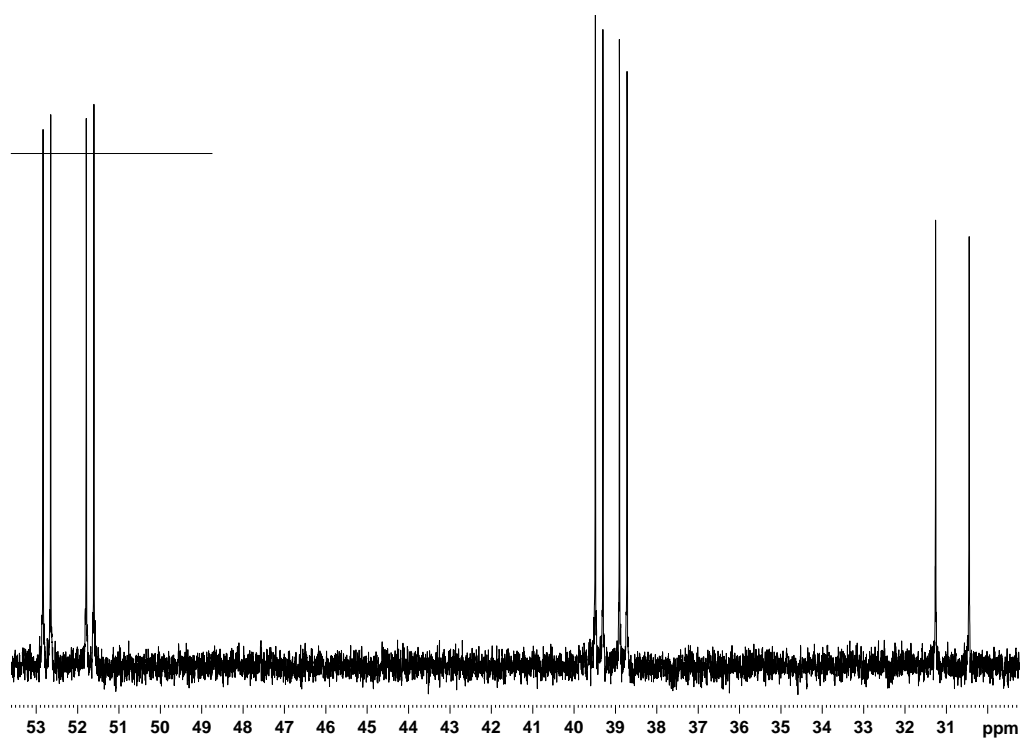
δ 39.9 (dd, $^1J_{\text{ClRh}} = 121$ Hz, $^2J_{\text{PP}} = 36$ Hz)

Appendix 3: X-ray crystal structure of Rh(6-Et)(PPh₃)₂Cl (4.51)



Bond lengths [Å] and angles [°] for Rh(6-Et)(PPh ₃) ₂ Cl	
Rh(1)-C(1)	1.989(5)
Rh(1)-P(1)	2.2886(15)
Rh(1)-P(2)	2.315(12)
Rh(1)-Cl(1)	2.4413
C(1)-Rh(1)-P(1)	89.82(16)
C(1)-Rh(1)-P(2)	93.4(3)
P(1)-Rh(1)-P(2)	173.0(2)

Appendix 4: $^{31}\text{P}\{^1\text{H}\}$ NMR spectrum of $\text{Rh}(\text{6-Et})(\text{PPh}_3)_2\text{Cl}$ (**4.51**)



$^{31}\text{P}\{^1\text{H}\}$ NMR spectrum of **4.51** in C_6D_6 at 298 K

Cis phosphine isomer:	δ 52.2 (dd, $^1J_{\text{PRh}} = 212$ Hz, $^2J_{\text{PP}} = 37$ Hz), δ 39.1 (dd, $^1J_{\text{ClRh}} = 117$ Hz, $^2J_{\text{PP}} = 36$ Hz)
Trans phosphine isomer:	δ 30.8 (d, $^1J_{\text{PRh}} = 164.3$ Hz)